UNIVERSITY OF CAMBRIDGE

Department of Chemistry

Studies Towards the Total Synthesis of Hemicalide

A dissertation submitted for the degree of
Doctor of Philosophy
at the University of Cambridge

Bing Yuan Han

Trinity Hall

September 2018

Supervisor: Prof. Ian Paterson

Author: Bing Yuan Han

ABSTRACT

The discovery of a novel marine natural product hemicalide **(1)**, with promising anticancer activity, has sparked interest in elucidating its full three-dimensional structure. Studies into the total synthesis and stereochemical assignment of the complex polyketide structure of hemicalide are described in this dissertation. Overall, this synthesis-enabled stereochemical assignment has established the relative configuration of 11 stereocentres out of a total of 21. All the requisite stereocentres have been configured with excellent diastereoselectivity and this work establishes a solid foundation for ongoing efforts towards the total synthesis of hemicalide.

In the first chapter, previous synthetic efforts by the Ardisson-Cossy team are outlined, including their initial proposed assignment for the C1-C28 region of hemicalide. This is followed by a discussion of the computational studies undertaken in our group which casts doubt on the suggested 3D structure. Chapter two describes the synthesis of three key hemicalide fragments corresponding to the C1-C6 **(A)**, C7-C15 **(B)** and C16-C28 **(C)** regions. Modifications from previous work have been made where appropriate to enable an expedient gram-scale synthesis of these fragments. The experimental results in this chapter support earlier computational DP4 NMR predictions about the most probable C18-19 relative stereochemistry.

The next chapter investigates fragment coupling strategies to furnish two possible diastereomeric candidates for a C1-C28 truncate **(D)** in conjunction with work carried out in parallel by Lam. Further elaboration enabled detailed NMR chemical shift comparisons to conclude the relative stereochemistry between the C7-C15 and the C16-C28 regions. These experiments also gave further insight on the nature of the C1 carboxyl group. Unlike the earlier fragments, the C26-C35 region has no assigned stereochemistry. The flexible conformational nature of this section has frustrated computational studies so synthetic studies have been undertaken. In the final chapter of this dissertation, a library of fragments **(E)** was synthesised to help assign the configuration of this section.

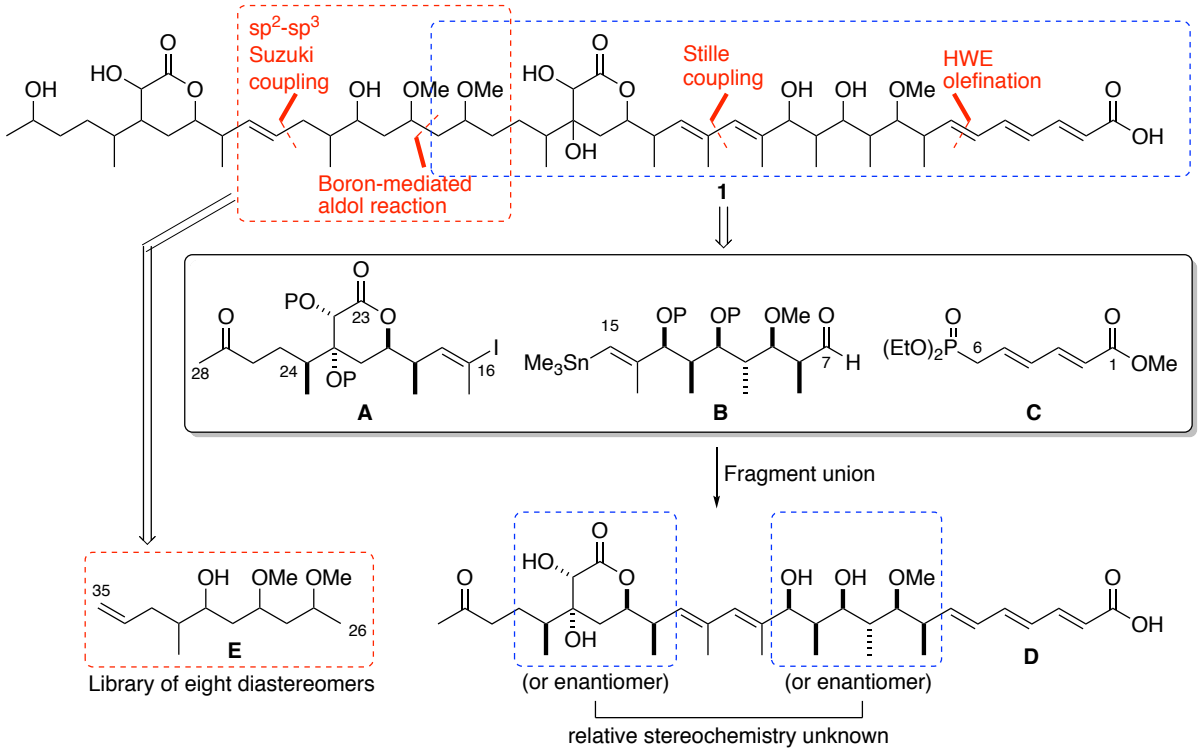
sp2-sp3
Suzuki
coupling
Boron-mediated
aldol reaction
Stille
coupling
HWE
olefination
1
A
B
C
Fragment union
E
Library of eight diastereomers
D
(or enantiomer)
(or enantiomer)
relative stereochemistry unknown

DECLARATION

I hereby declare that my thesis/dissertation entitled is the result of my own work and includes nothing which is the outcome of work done in collaboration except as declared in the Preface and specified in the text. It is not substantially the same as any that I have submitted, or, is being concurrently submitted for a degree or diploma or other qualification at the University of Cambridge or any other University or similar institution except as declared in the Preface and specified in the text. I further state that no substantial part of my dissertation has already been submitted, or, is being concurrently submitted for any such degree, diploma or other qualification at the University of Cambridge or any other University of similar institution except as declared in the Preface and specified in the text. It does not exceed the prescribed word limit of 60,000 words.

_____

Bing Yuan Han
30 September 2018

ACKNOWLEDGEMENTS

First and foremost, I would like to thank Prof. Ian Paterson for the opportunity to work in his group for my PhD. His guidance and advice have been indispensable while embarking on such a challenging and stimulating project. I am also grateful to Prof. Jonathan Goodman for offering helpful insight and a fresh perspective on the project.

This PhD project would also not be possible without my fellow Team Hemicalide members, Dr. Callum MacGregor and Nelson Lam, who also proofread this thesis. I had a smooth start on the project with Callum laying down most the groundwork. I am also glad to have Nelson working by my side during the darkest days of the project. I will remember fondly our late evenings together salvaging our latest blunders in the lab, discussing the future direction of the project and rating various Asian restaurants.

I would also like to thank all past and present members of Lab 122 from 2013-2018 with whom I have had the pleasure to overlap with. In particular, Dr. Mike Housden, Dr. Simon Williams and Matthew Anketell deserve mention for their help on a day-to-day basis and the engaging discussions about organic chemistry. I am deeply grateful for the running of NMR spectra, the generous sharing of chemicals and the excellent tastes in music in every bay I have worked in, especially Talia Pettigrew, Rachel Porter, Nika Anzicek. Above all, I would like to thank Andrew Phillips and Adam Yip, my fellow dwellers at Sunrise Land, who have to put up with me both in the lab and at home.

My lab work has been greatly expedited with the speedy hands of the first floor technicians Nic Davies and Naomi Hobbs. I am also grateful to the NMR service technicians Dr. Peter Grice and Duncan Howe for enduring my unending requests for high quality NMR spectra on miniscule amounts of material.

This is the conclusion of an eight-year-long journey in Cambridge. I am blessed to have had the love and support from my family and well wishes from the extended Han family to allow me to pursue my dreams. Thank you Pa, Ma and Meimei; this time I really am leaving university and will get a ‘real job’ now.

TABLE OF CONTENTS

NOMENCLATURE

For compounds related to hemicalide **1** (**Figure 1**), the carbon skeleton numbering is based on the numbering scheme as assigned in the original isolation literature.[1]

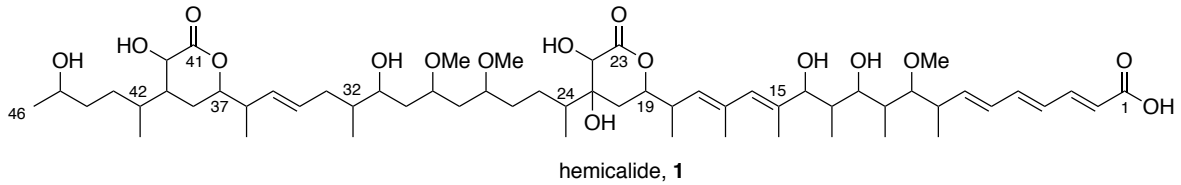

hemicalide, **1**

Figure 1: Numbering scheme of Hemicalide

The *syn* and *anti* convention for assigning relative stereochemistry is used throughout, as first defined by Masamune[2] (**Figure 2**). A *syn* relationship is defined by any two substituents both pointing to the same side of the plane of the paper when the main chain is drawn in a zig-zag conformation as demonstrated with A and C. If the two substituents are on opposite sides of the plane of the paper, then they are defined as *anti* as demonstrated with B and D.

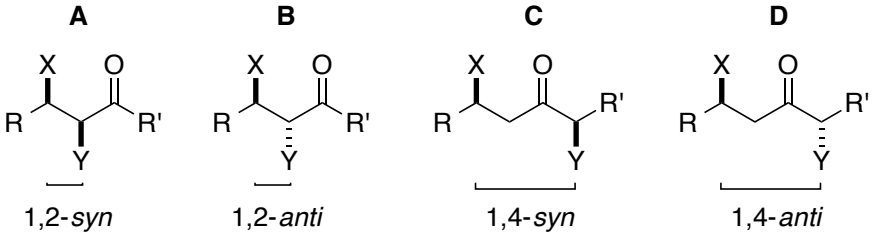

Figure 2: *syn* and *anti* relationships

The two metal enolates P and Q are referred to as the *Z*- and *E*-enolates respectively, according to the accepted IUPAC conventions. The metal-oxygen substituent is designated in all cases as having the highest priority (**Figure 3**).

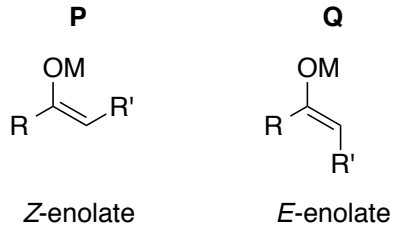

Figure 3: *Z*- and *E*- enolate geometries

ABBREVIATIONS

Å	Ångstrom
Ac	Acetyl
Ar	Aromatic
aq.	Aqueous
BAIB	(Diacetoxyiodo)benzene
bipy	Bipyridyl
Bn	Benzyl
Bz	Benzoyl
brsm	Based on recovered starting material
Bu	n-butyl
cat.	Catalytic
Cp	Cyclopentadienyl
COSY	^{1}H–^{1}H correlation spectroscopy
CuTC	Copper thiophenecarboxylate
CSA	Camphorsulfonic acid
Cy	Cyclohexyl
DCC	*N*,*N*'-Dicyclohexylcarbodiimide
DDQ	2,3-Dichloro-5,6-dicyano-1,4-benzoquinone
DIAD	Diisopropyl azodicarboxylate
DIBAL	Diisobutylaluminium hydride
DIPCl	*B*-chlorodiisopinocamphenylborane
DIPEA	Diisopropylethylamine or Hünig's base
DMAP	4-dimethylaminopyridine
DMB	2,3-Dimethoxybenzyl
DME	1,2-Dimethoxyethane
DMF	*N*,*N*'-Dimethylformamide
DMP	Dess–Martin periodinane
DMSO	Dimethyl sulfoxide
DNA	Deoxyribonucleic acid
dppf	1,1'-Bis(diphenylphosphino)ferrocene
d.r.	Diastereomeric ratio
DTBMP	2,6-Di-tert-butyl-4-methylpyridine
e.e.	Enantiomeric excess

eq.	Equivalents
Et	Ethyl
FT-IR	Fourier Transform-Infrared spectroscopy
g	Gram(s)
HMBC	Heteronuclear Multiple Bond Correlation spectroscopy
HMDS	Hexamethyldisilazine
HSQC	Heteronuclear Single Quantum Coherence spectroscopy
HPLC	High Performance Liquid Chromatography
HWE	Horner–Wadsworth–Emmons
h	Hour(s)
Hz	Hertz
i-	Iso
IC_{50}	Half maximal inhibitory concentration
Ipc	Isopinocamphenyl
J	$^{1}H–^{1}H$ coupling constant
L	Unspecified ligand
LDA	Lithium diisopropylamide
M	Unspecified metal; Molar
Me	Methyl
min	Minute(s)
mg	Milligram(s)
mmol	Millimole(s)
mL	Millilitre(s)
mol	Mole(s)
MS	Molecular sieves
Ms	Mesyl (methanesulfonyl)
MTPA	α-Methoxy-α-(trifluoromethyl)phenylacetate
n-	Normal
NBS	*N*-Bromosuccinimide
NIS	*N*-Iodosuccinimide
nM	Nanomolar
NMO	*N*-Methylmorpholine *N*-oxide
NMP	*N*-Methyl-2-pyrrolidone
NMR	Nuclear Magnetic Resonance spectroscopy
NOESY	Nuclear Overhauser Effect spectroscopy

P	Unspecified protecting group
PE 30-40	Petroleum Ether, bp 30-40 °C or pentanes
PE 40-60	Petroleum Ether, bp 40-60 °C or hexanes
Ph	Phenyl
pin	Pinacolate
PMB	Para-methoxybenzyl
PMBTCA	Para-methoxybenzyl trichloroacetamide
PT	1-Phenyl-1*H*-tetrazol-5-yl
py	Pyridine
R	Unspecified substituent
RCM	Ring Closing Metathesis
R_f	Retention factor
ROESY	Rotating-frame Nuclear Overhauser Effect spectroscopy
rt	Room temperature
t-	Tert-
TASF	Tris(dimethylamino)sulfonium difluorotrimethylsilicate
TBS	Tert-butyldimethylsilyl
TEMPO	(2,2,6,6-Tetramethylpiperidin-1-yl)oxy
TES	Triethylsilyl
THF	Tetrahydrofuran
TLC	Thin layer chromatography
TMDS	Tetramethyldisiloxane
TMS	Tetramethylsilane or trimethylsilyl
TMSE	(Trimethylsilyl)ethyl
Tf	Triflyl (trifluoromethanesulfonyl)
Ts	Tosyl (para-toluenesulfonyl)
µl	Microlitre(s)
µmol	Micromolar(s)

CHAPTER ONE: INTRODUCTION

1.1 Introduction to Marine Natural Products as Anticancer Therapeutics

Natural products are a rich source of bioactive molecules that can be investigated in the search for new drugs and therapies. Historical examples are well exemplified by the extraction of morphine from *Papaver somniferum* poppies in 1803 and the isolation of the first antibiotic penicillin from the fungus *Penicillium notatum* by Fleming in 1929.[3] Currently, more than half of the drugs on the market are of natural origin. This reflects the advantages of using natural products as a lead structure, namely their high biological target specificity and binding efficiency.[4]

Alternative drug discovery programs commonly utilise high throughput screening in conjunction with combinatorial chemistry to accelerate the screening of synthetic compounds. Nonetheless, such approaches have not been as successful as natural product discovery in identifying bioactive compounds for further studies.[5] Advancements in analytical and spectroscopic techniques have also enabled the elucidation of multiple novel compounds even in complex mixtures such as crude extracts from natural sources.[6] In the cases of natural products that are derived from microbial origins, a better understanding of the genomic composition of the source organism has also opened up the possibility of manipulating the relevant gene clusters to obtain new compounds.[5] This has led to a renaissance of natural products discovery in the search for new drug candidates.

For many years, pharmacognosy has been focused on natural products derived from terrestrial environments. However, attention has more recently turned towards studying marine organisms as a rich, unexplored reservoir for discovering new chemical leads in medicine.[7] As many as 10 million unique species inhabit these aquatic environments, making the deep sea one of the most biodiverse habitats on Earth, rivaling other species-rich colonies like rainforests.[8]

Several hundred metres below the surface, deep sea organisms have to survive under extreme conditions such as low light intensity, low temperatures, low oxygen levels and intensely high pressures.[8] The marine organisms that produce the most promising and potent lead compounds tend to be sessile organisms with no apparent physical defence mechanisms as they are believed to have evolved chemical defences instead.[9] There is often debate as to whether it is the marine organism themselves or their symbiotic microorganisms that produce the bioactive natural

products in question.[10] These compounds are usually highly potent as they would be greatly diluted by seawater once discharged by the organism and this potency makes them valuable targets for further clinical studies, particularly as anticancer agents for chemotherapy.[9] In particular, marine sponges, where microbes may constitute up to 60% of the biomass, are popular targets for harvesting secondary metabolites to study. Most of these bioactive compounds are only produced in tiny amounts as secondary metabolites and this fact places a limit on their usefulness for mass harvesting.[11] Total synthesis could provide a sustainable, alternative supply source within practical limits and would also allow access to novel structural analogues of the original compound.[12]

The first commercial success story of a marine natural product reaching Food and Drug Administration (FDA) approval is cytarabine (Cytosar-U®)[13] **2** (**Figure 4**), now an anticancer drug. Metabolites from the marine sponge *Tethya crypta* were used as lead compounds from which the synthetic analogue cytarabine was developed. More recent examples can be found in trabectedin (Yondelis®)[13] **3**, isolated from the tunicate *Ecteinascidia turbinata*, and eribulin mesylate (Halaven®)[13] **4**, a synthetic analogue of halichondrin B produced by the sponge *Halichodria okadai*. Of particular note is that trabectedin **3** is the original natural product without any modifications during any phase of its development.[5] Despite the success of these natural products, the vast majority does not pass clinical trials as they do not outperform an industry standard or might exhibit toxic side effects.[5]

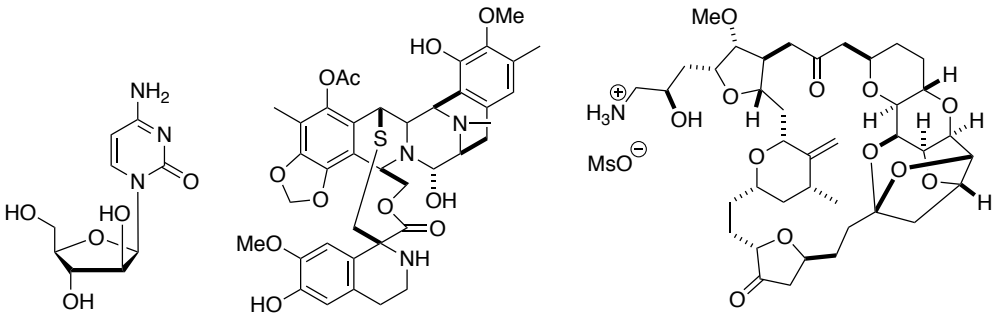

Figure 4: Examples of marine natural products that have obtained FDA approval

While marine natural products with therapeutic uses include treatments for pain management, antivirals and hypertriglyceridemia, the overwhelming majority of them have been selected for their anticancer properties.[5] This reflects the commercial value of anticancer treatments as cancer represents one of the leading causes of death in developed nations. In addition, several anticancer drugs have shown synergistic interactions when administered together.[5] This opens up further possibilities of 'cocktail' treatments to enhance the efficacy of the individual components.

The events in the cell cycle are highly regulated and many anomalies can cause the cell cycle to arrest, eventually signaling the cell for programmed cell death, or apoptosis.[14] Anticancer compounds take advantage of the high rate of cellular division in cancerous cells compared to normal cells, killing them at a faster rate than healthy cells.[14] Common biological targets of anticancer drugs include DNA and topoisomerases but most importantly microtubules, formed of α- and β-tubulin polymers. All known antimitotic compounds specifically bind to β-tubulin in the microtubule polymer but not α-tubulin.[15]

Microtubules are important to cell division by forming the mitotic spindle where chromosomes attach themselves in preparation for migration towards the new daughter cell nuclei.[15] Movement of the microtubules arises from its dynamic behavior of polymerisation, leading to growth, and depolymerisation, resulting in shortening. Well-established antimitotic compounds are known to interfere with microtubule dynamics by either inhibiting tubulin polymerisation or depolymerisation. Drugs that bind to the vinca domain, named after the *Vinca* alkaloids such as vinblastine **5** and vincristine **6** (**Figure 5**), destabilise tubulin growth.[15] Another well-characterised binding site is the taxoid domain, a target for taxanes derived from the *Taxus* yew trees most prominently featuring paclitaxel **7** and docetaxel **8**.[15] It has been shown that epothilone A **9** and discodermolide **10** operate through a similar microtubule-stabilising mechanism as the taxanes.[15]

While many successful antimitotic drugs have been developed based on the *Vinca* alkaloid or taxane scaffold, an emerging threat in the form of cancer cell resistance renders many of these compounds ineffective during treatment.[16] Resistant cancer cells overexpress the MDR1 gene responsible for the production of P-gp, an efflux pump that removes hydrophobic compounds from the cell, a common characteristic of the *Vinca* alkaloids and the taxanes. Alternatively, some malignant cells overexpress βIII-tubulin, an isotype of β-tubulin, which inherently enhances dynamic instability of microtubules and counteracts the stabilising action of taxanes. Solutions to these problems have included designing second- and third-generation taxanes to escape recognition by P-gp. Additionally, new drug candidates such as peluroside A **11** and laulimalide **12** have been identified as drugs that target βIII-tubulin and are awaiting clinical trials (**Figure 5**).[16]

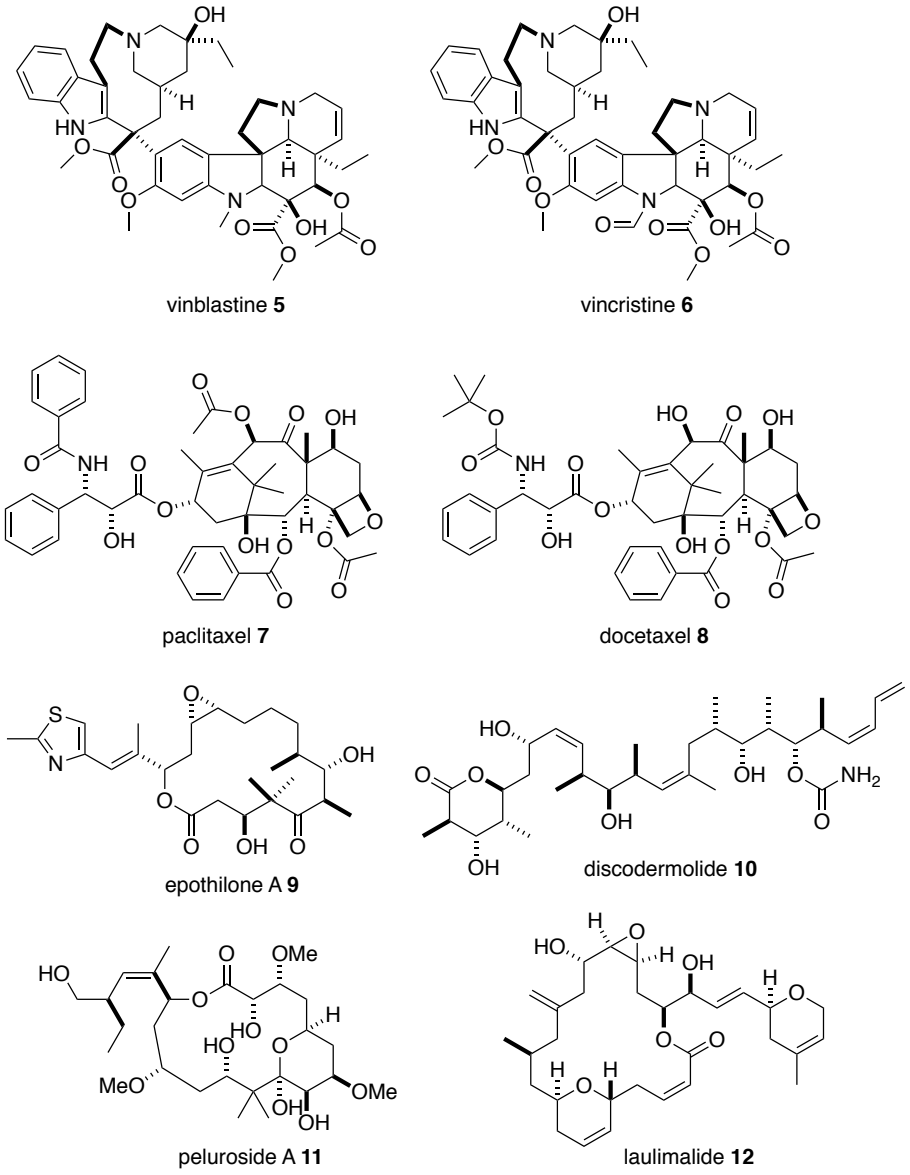

Figure 5: Examples of anticancer natural products

1.2 Methods for Structural Elucidation

1.2.1 The Role of Total Synthesis in Structural Determination

Advancements in purification and analytical techniques, in particular NMR spectroscopy, have enabled detailed structural determination on microgram quantities of novel compounds. Despite this, more than 300 structural revisions to natural products have been made since 1990.[17] Ultimately, total synthesis remains a powerful tool in providing incontrovertible proof of the true structure of a compound.

For example, while the relative and absolute stereochemistry of spongosoritin A[18] **13** was not assigned during isolation, it was assumed that it would have a (6*R*, 8*R*) configuration by analogy with *des*-hydroxygracilioether C **14**, gracilioether B **15** and gracilioether C **16**, all isolated from relatives of the same *Plakortis* genus of marine sponges (**Figure 6**). However, the recent discovery of other secondary metabolites such as **17** and **18** have cast doubt on the assumption that the family of natural products share a common biosynthetic pathway. Perkins' synthesis of both diastereomers **13** and **19** and subsequent NMR comparison made it clear for the first time that the true structure was indeed (6*R*, 8*R*) as suspected.[18]

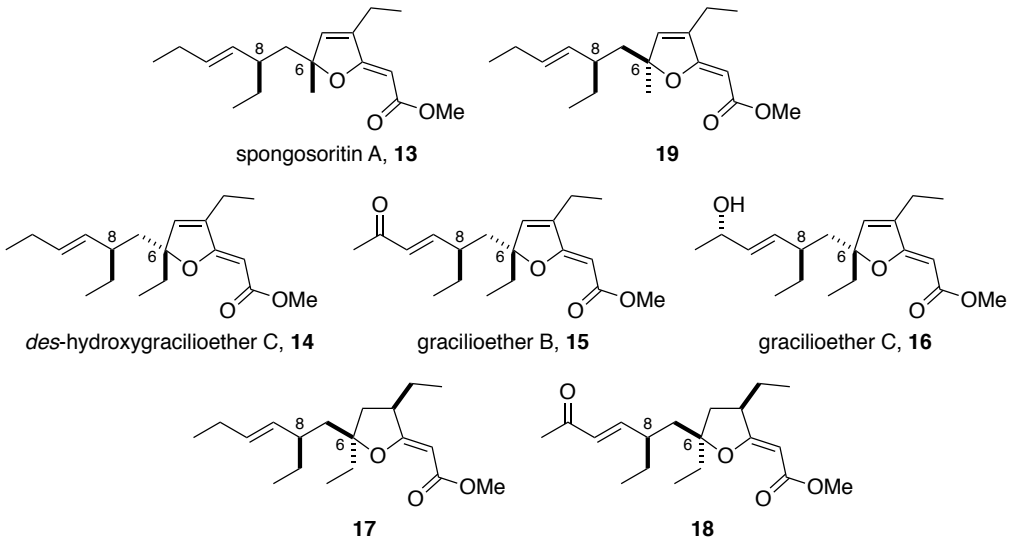

Figure 6: Proposed structure of spongosoritin A and other related compounds

In the case of callipeltoside A **20**, the relative stereochemistry of the *trans* cyclopropane ring with respect to the rest of the molecule could be not be determined initially. Synthetic efforts towards the two possible diastereomers by Paterson[19] and Trost[20] indicated that both putative structures **20** and **21** correlated equally well with the natural product (**Figure 7**). Examination of the optical

rotation and the circular dichroism spectrum provided the final proof for the relative and absolute configuration of the compound. This problem would eventually be revisited in the form of phorbaside A **22**, bearing significant structural similarity to callipeltoside A. Intriguingly, the proposed structure featured the antipodal cyclopropane moiety on the basis of semiquantitative circular dichroism studies. The Paterson[21] approach to synthesise the two possible diastereomers **22** and **23** was once again met with inconclusive results from NMR correlations. Validation of the proposed structure **22** was obtained from correlation of circular dichroism and optical rotation data.

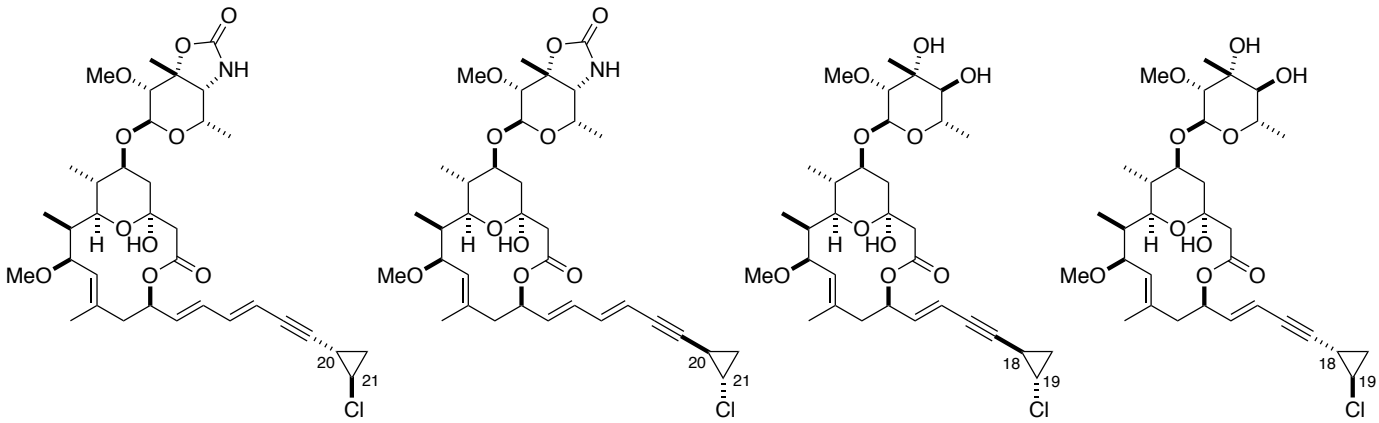

Figure 7: Proposed structures of callipeltoside A and phorbaside A and their *epi*- counterparts

1.2.2 NMR-based Prediction Methods for Structural Determination

Although total synthesis is a powerful tool for validating the proposed structure for complex organic molecules, it is a time-consuming and resource-intensive process. Consequently, the use of *ab initio* NMR calculations for virtual molecules has attracted much attention in recent years. Pioneered by Bifulco[22], this approach has led to the structural reassignment of several natural products such as hexacyclinol[23,24] and maitotoxin.[25]

By comparing the predicted chemical shifts against the experimental values, one candidate structure, if not a handful, should emerge as a good match with the natural product. This will greatly reduce the number of structures under consideration to expedite further synthetic efforts if required. The quantification of the fit for each possible structure is best characterised by the DP4 probability, developed by Smith and Goodman.[26] The level of success of DP4 has been shown to be significantly better than other statistical parameters such as correlation coefficients.

The DP4 probability is an extension of the earlier CP3 parameter[27], also developed by Smith and Goodman. This is useful for assigning two sets of experimental data to two possible structures, typically found when performing a stereoselective reaction that yields a major and minor product. DP4 is used when there is only one set of experimental values to be matched against multiple putative structures. This method was applied to the structural determination of leiodermatolide **24** where the DP4 results identified partial fragments **25** and **26** with the same relative stereochemistry as proposed by the isolation team (**Figure 8**).[28] This marked the first time the structure of a complex polyketide was analysed with the DP4 protocol.

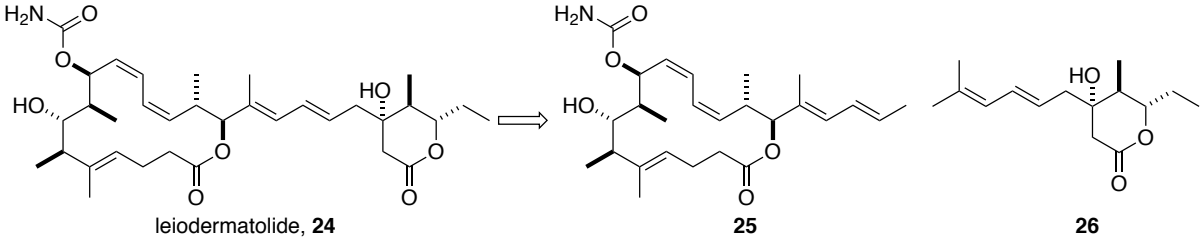

Figure 8: Proposed structure of leiodermatolide and the virtual fragments used in DP4 analysis

A standard NMR-based prediction process begins with a conformational search on all the candidate molecules under examination and identifying all low-energy conformers, typically within 10 kJ mol^{-1} of the global minina. Density Functional Theory (DFT) Gauge Including Atomic Orbital (GIAO) calculations are then performed on these conformers and weighted according to a Boltzmann distribution to yield a combined calculated chemical shift for each atom. Linear regression may be applied at this stage to remove any systematic errors by applying an appropriate scaling factor. The error associated with each resonance is then computed.[26]

DP4 analysis assumes that the errors between the calculated and experimental data obey a t-distribution. The probability of encountering each error in a given structure can be computed accordingly and the product of these probabilities represents the overall absolute probability. Bayes' theorem can be used to convert the absolute probabilities into relative probabilities to identify the most likely candidate. Taking into account both ^{1}H and ^{13}C data provides an even more accurate prediction with DP4 analysis.[26] Since enantiomers display identical NMR spectra, DP4 cannot be used to assign absolute stereochemistry but only relative stereochemistry.

The synergy between computational and synthetic efforts towards structural determination is best showcased by baulamycin A **27** (**Figure 9**). Attempts to reach a total synthesis of this natural product by Goswami[29] and Aggarwal[30] were frustrated by the discovery that spectroscopic data for their synthetic compound did not match the reported values for the natural product. Having

concluded that the initial stereochemical assignment was incorrect, Aggarwal set out to determine the correct configuration of baulamycin out of 128 possible stereoisomers.[30] The flexible nature of the carbon backbone greatly complicated computational efforts in studying baulamycin as the experimental NMR parameters are derived from a weighted average of multiple low-energy conformers of the molecule. However, restricting the analysis to just four possible diastereomers in the C11-C1' region made the calculations more feasible. By comparing the ^{1}H–^{1}H coupling constants and ROESY measurements, the relative stereochemistry in this region was reassigned to *anti–anti–syn*. Unfortunately, this approach did not lead to any conclusive result when applied to the C4-C8 region. An expedient synthesis of the remaining four possible diastereomers was enabled by the assembly-line synthesis methodology[31] developed in the Aggarwal group. This was achieved by using chiral building blocks with predetermined *e.e.* to produce the four diastereomers as a mixture with carefully chosen ratios. Analysis of the signal intensities in the ^{13}C NMR then allowed identification of each diastereomer. Standard NMR correlation parameters revealed an unambiguous reassignment of this region to *syn–syn*. Having corrected the relative stereochemistry of baulamycin, the absolute configuration was determined by comparing optical rotation data. The revised structure **28** reveals a correction of five out of seven misassigned stereocentres.[30]

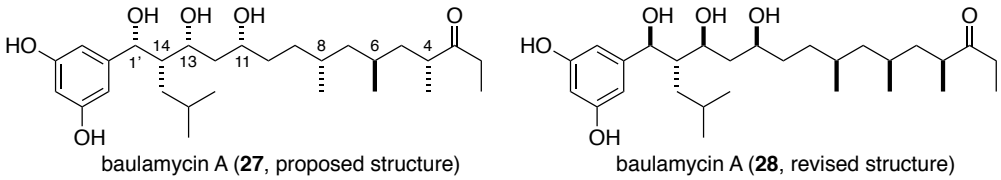

Figure 9: Proposed and revised structures for baulamycin A

1.3 Introduction to Hemicalide: Isolation, Characterisation and Biological Activity

Found in the deep waters around the Torres Islands of Vanuatu, hemicalide was isolated from the marine sponge *Hemimycale sp.* by the CNRS-Pierre Fabre Laboratories working together with the Institut de Recherche pour le Dévelopment (IRD).[1] A fresh sample of *Hemimycale sp.* (5 kg) was lyophilised (650 g) and sequentially macerated with $CHCl_3$ and twice with aqueous EtOH. The combined filtrates were concentrated *in vacuo* to obtain an aqueous syrup, which was washed with CH_2Cl_2 and EtOAc to eliminate inorganic salts. The desalinated extract was concentrated *in vacuo*, taken up in aqueous MeOH and partitioned with hexane; only the methanolic extract displayed the desired pharmacological activity. This extract was further purified with flash column chromatography (EtOAc and MeOH) and HPLC (H_2O and MeCN) to afford the active molecule hemicalide (0.5 mg, 0.000077% with respect to lyophilisate).[1]

High resolution electrospray ionisation time of flight mass spectrometry (HRESITOFMS) identified a $(M–H)^-$ component with *m/z* = 1061.6780 which corresponded to a molecular formula of $C_{59}H_{97}O_{16}$.[1] The two-dimensional structure (**Figure 8**) of hemicalide was assigned as **1** by extensive NMR spectroscopic studies which indicated a 46-carbon atom skeleton comprising a conjugated trienic acid (C1-C7), a polyproprionate stereohexad (C8-C13), a conjugated diene (C14-C17), an α,β-dihydroxylactone (C19-C23) and an α-hydroxylactone (C37-C41).[1] Although the methyl ester analogue of hemicalide was described by the isolation team, its characterization was not reported. Due to the low isolated yield, no further chemical derivatisation nor degradation experiments could be carried out to help assign the absolute configuration of the 21 stereocentres in hemicalide.

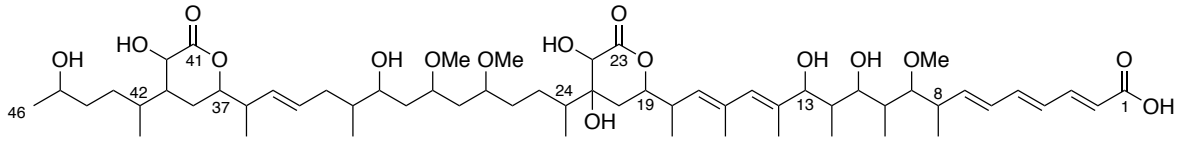

hemicalide, **1**

Figure 10: The two-dimensional structure of hemicalide

Hemicalide has demonstrated potent antiproliferative activity against a panel of various human cancer cell lines with a mean IC_{50} in the subnanomolar concentrations (**Table 1**).[1] This makes it an attractive target for further biological studies in addition to its structurally complexity.

Cell Line	Disease	IC_{50} (nM)
A549	Non small cell lung cancer	0.82
BxPC3	Pancreatic cancer	0.47
LoVo	Colon cancer	0.081
MCF7	Breast cancer	0.011
Namalwa	Burkitt's lymphoma	1.1
SK-OV-3	Ovarian cancer	0.33

Table 1: Antiproliferative activity of hemicalide against various cancer cell lines

Attempts to define hemicalide's mechanism of action on cellular activity have been probed by using HeLa tumor cells in immunocytochemistry assays. Within a dosage range of 5-50 nM, cells in interphase were found to be devoid of their microtubular cytoskeleton, as labeled by α-tubulin, while centrosomes were present and separated, as labeled by γ-tubulin. On the other hand, mitotic cells were found to be arrested in prometaphase without microtubules, while the centrosomes were also present and separated.[1] This evidence suggested that hemicalide destabilises the α/β-microtubule network through a novel, unexplored mechanism that differs from other well-known antimitotic natural products.[15] Due to the low isolation yield, further biological studies were not possible.

1.4 Stereochemical Assignment of Hemicalide

1.4.1 C1-C15 Polypropionate Stereohexad

When studying the ^{13}C NMR spectrum of hemicalide, Ardisson noticed that the chemical shift due to Me12 was unusually low at 7.6 ppm, indicating that C12 belonged to a *syn-syn* C11-C13 stereotriad.[32] The same phenomenon was not observed for Me10, which suggested that the C9-C11 stereotriad was *anti-anti*, *syn-anti* or *anti-syn* in its relative relationship. These observations reduced the possible number of diastereomers for this region from 32 to six. To assist the stereochemical assignments, synthetic efforts towards diastereomers **29A-29F** were undertaken to compare their NMR spectral data with hemicalide (**Figure 11**).[32]

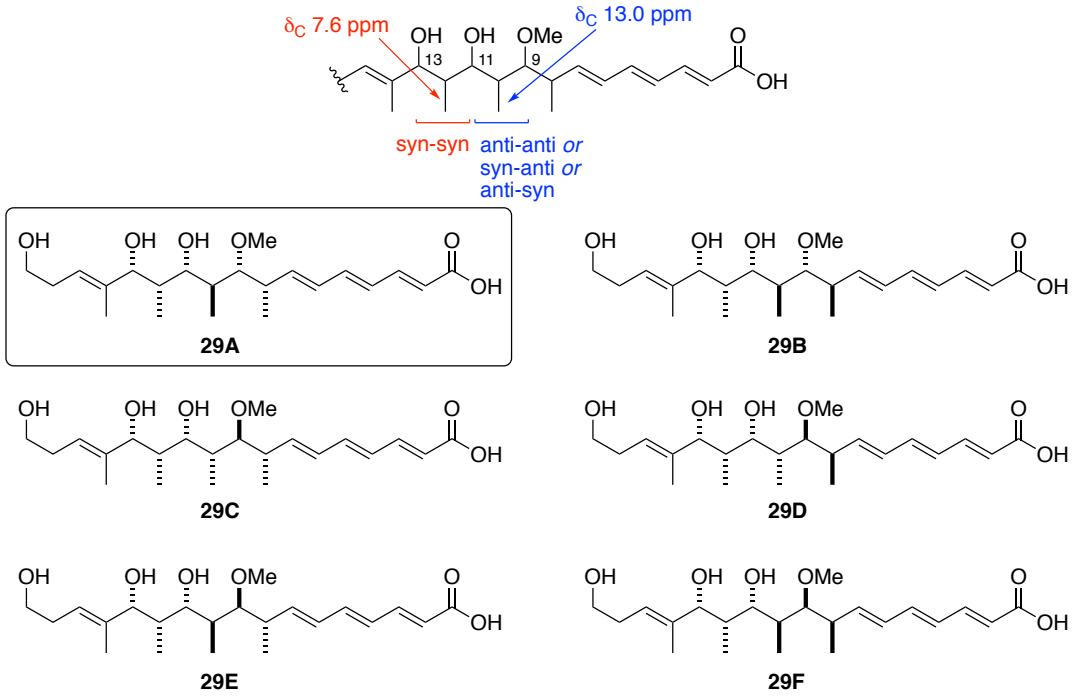

Figure 11: Diastereomers used for Ardisson's NMR-based comparison studies on the C1-C15 region of hemicalide

Initial studies of the ^{13}C NMR signals related to the C1-C7 region for all these diastereomers showed substantial differences in chemical shifts which was attributed to the natural product being isolated as a carboxylate salt instead of the carboxylic acid. The use of a model system **30** confirmed that a similar deviation profile in the ^{13}C NMR was observed upon deprotonation to afford the sodium salt **31** (**Scheme 1**). Notably, this salt effect did not affect the aliphatic region beyond the trienic acid and enabled comparison of the C8-C13 region in diastereomers **29A-29F** with hemicalide.[32]

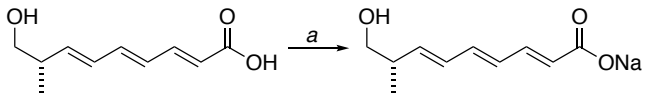

30 **31**

Reagents and conditions: (a) NaH, THF, 0 °C

Scheme 1: Ardisson's synthesis of a model carboxylate salt to examine a possible 'salt effect'

Closer examination of the C8-C13 region in the ^{13}C NMR spectrum then eliminated diastereomers **29C-29F** as potential candidates due to the large differences in chemical shifts ($|\Delta\delta_C| > 1$ ppm) (**Figure 11**). To further identify a better correlation with hemicalide, the ^{1}H NMR spectrum of diastereomers **29A** and **29B** were compared and this study suggested that diastereomer **29A** was the better match to hemicalide ($|\Delta\delta_H| < 0.1$ ppm).[32]

Independently, DP4 analysis was undertaken by Smith[26] in the Goodman group based on all 32 possible diastereomers **32A-32AF** (**Figure 12**). The results concur that diastereomer **32A** has the highest probability (85.2%) of having the same relative stereochemistry as the corresponding region of hemicalide with the next most likely structure **32J** being assigned a 13.4% probability. However, **32J** does not exhibit the expected *syn*/*anti* stereotriad pattern, thus increasing the confidence level of **32A** being the correct diastereomer.

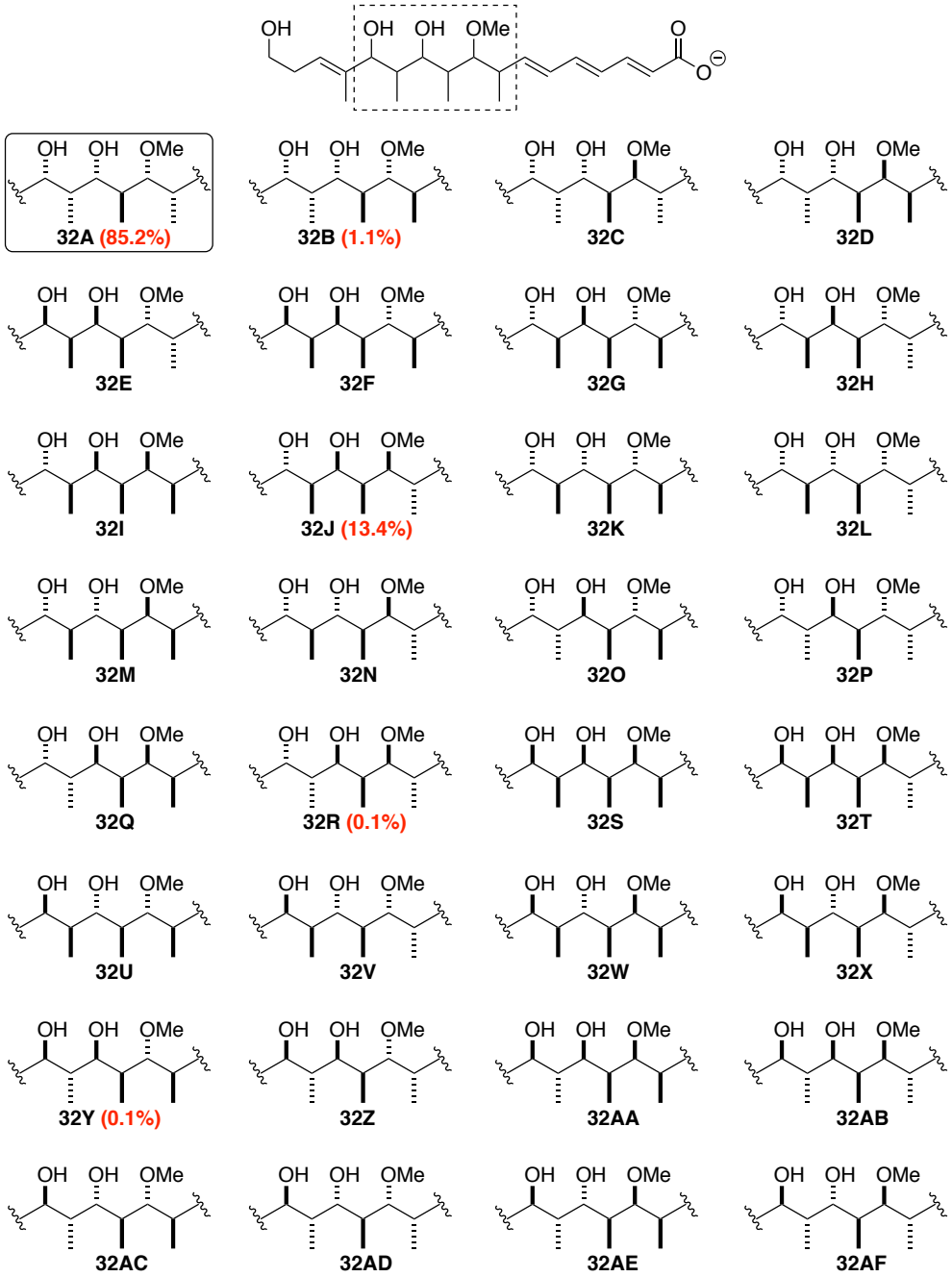

Figure 12: Diastereomers used for Smith's DP4 analysis on the C1-C15 region of hemicalide and their calculated probabilities for matching hemicalide; only values above 0.1% are listed.

1.4.2 C17-C25 α,β-Dihydroxy-δ-lactone

Investigations into elucidating the relative stereochemistry for the C17-C25 region of hemicalide were also carried out by Ardisson (**Figure 13**).[33] NOESY analysis established correlations between H22 and H24, Me24 as well as to one H20 proton. The latter H20 proton also showed a $^{3}J_{19,20}$ coupling constant of 11.5 Hz with H19, indicating a *trans* relationship. These results indicated that both C21 and C22 hydroxyl groups were *cis* to each other but *trans* to the C19 chain. These observations reduced the possible number of diastereomers for this region from 16 to four. As with previous work on the C1-C15 fragment, all four diastereomers of model fragments with hemicalide **33A** to **33D** were synthesised to compare their NMR data with hemicalide (**Figure 13**).[33]

Comparison studies of the ^{13}C NMR spectra for the four diastereomers proved, unfortunately, to be inconclusive as all four had similar deviation profiles. On inspection of the ^{1}H NMR spectra instead, the signals corresponding to H20, H24 and H25 of hemicalide were observed as part of a broad 22H methylene multiplet and the H18 signal was a broad multiplet that did not lead to meaningful conclusions.[1] Ardisson asserted that any signal due to H22 would be less sensitive to structural changes in the lactone than H19 so a comparison of the chemical shift of this signal eliminated diastereomers **33C** and **33D** (**Figure 13**) as suitable candidates bearing the natural stereochemistry. Indeed, the chemical shifts for H19 in the spectra of all four diastereomers were very different from that in hemicalide, presumably due to the presence of an ether oxygen at C17 as opposed to an olefin. Closer inspection of the multiplicity of the H19 signal being a ddd suggested that 18,19-*anti* diastereomer **33B** was a closer match to hemicalide than the corresponding 18,19-*syn* **33A**.[33]

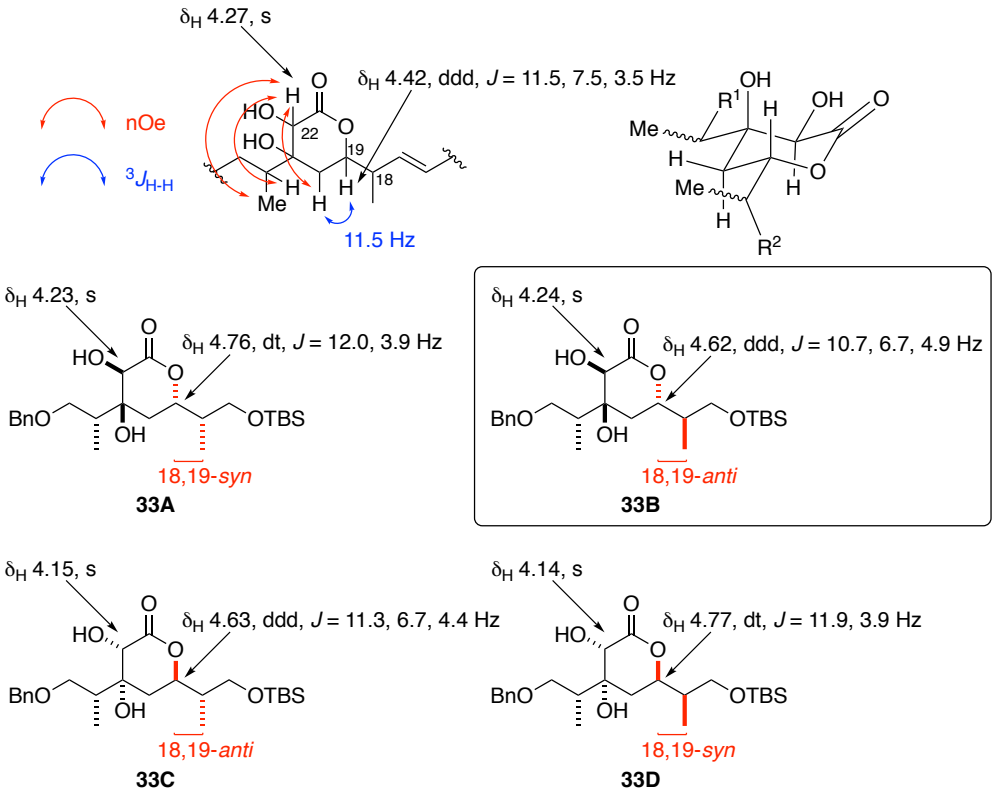

Figure 13: Diastereomers used for Ardisson's NMR-based comparison studies on the C17-C25 region of hemicalide

On closer inspection, however, this interpretation was considered by us to be inconclusive. Notably, the corresponding H37 signal of hemicalide in a similar δ-lactone ring appears as a ddd (J = 11.0, 7.5, 3.9 Hz) where a 36,37-*syn* relationship has been determined (*vide infra*). Likewise, a similar system in a rhizoxin D intermediate **34** (**Figure 14**) developed by the Leahy group[34] also shows a ddd multiplicity (J = 12.1, 3.6, 2.9 Hz) for the oxymethine proton in a *syn* relationship. More importantly, later work by the Ardisson group[35] during the synthesis of the C18-C24 δ-lactone yielded intermediate **35** where the multiplicity had now changed to a dt (J = 11.3 Hz, 3.9 Hz), casting doubt on the validity of the initial stereochemical assignment.

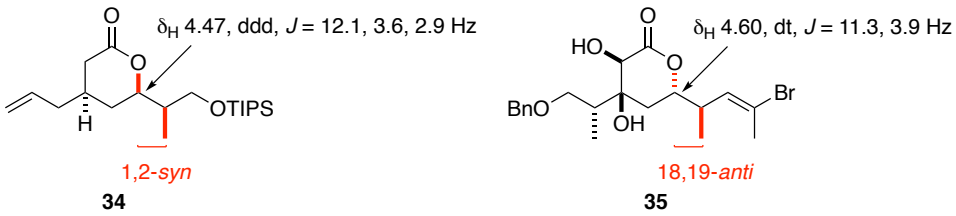

Figure 14: Comparison of other similar δ-lactone systems to **12**

DP4 calculations were also performed by MacGregor[36] for this region with all 16 possible diastereomers (**Figure 15**) to independently assign the stereochemistry of a C16-C27 virtual fragment. However, this analysis identified the 18,19-*syn* diastereomer **36M** as having the highest

probability (99.0%) of matching the stereochemistry of hemicalide. Diastereomer **36N**, corresponding to the structure proposed by Ardisson, was assigned a 1.0% probability with the DP4 analysis. We reason that having the olefin group at C17 renders model systems **36A-36P** structurally more similar to hemicalide and enables a more realistic comparison.

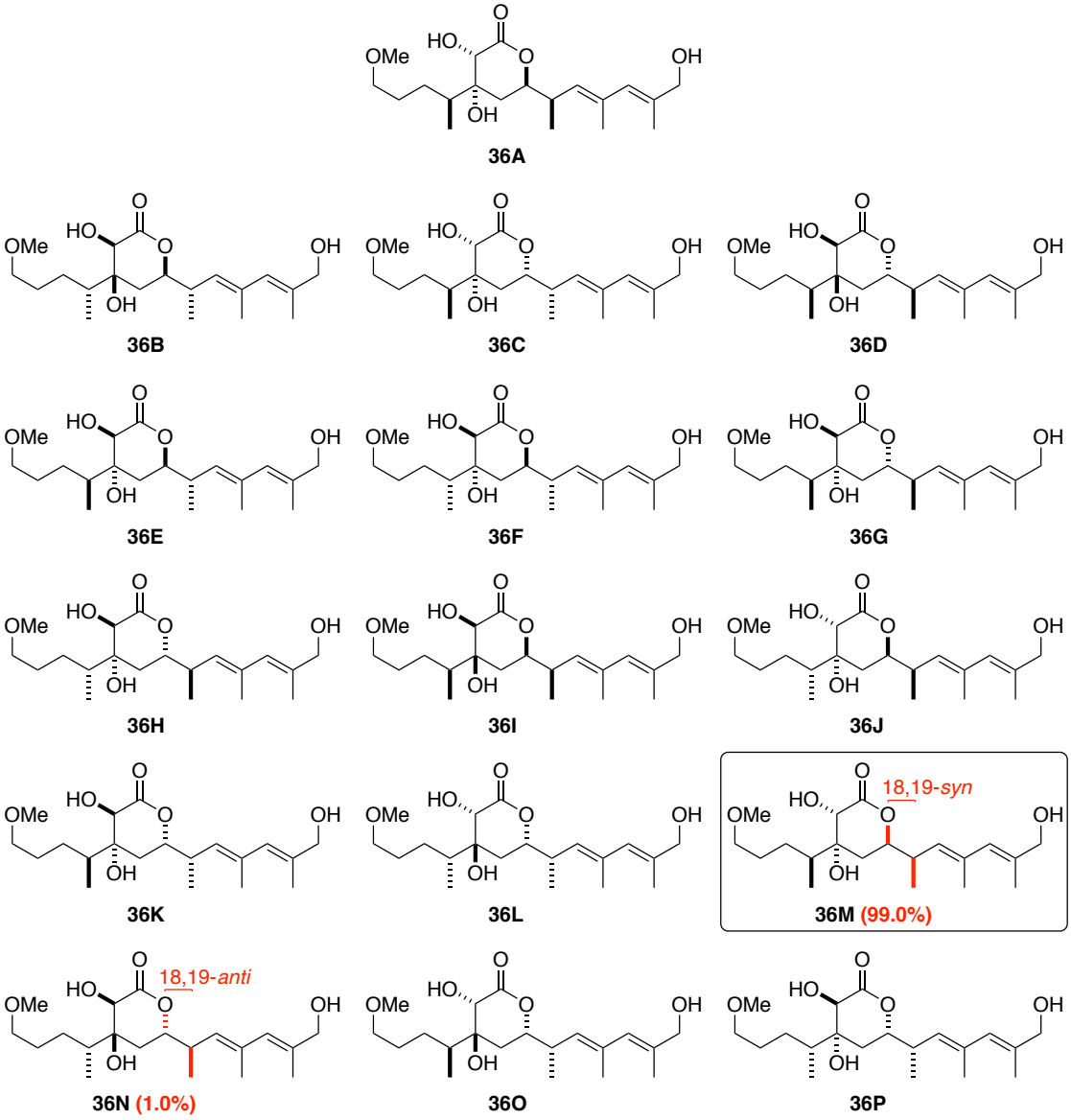

Figure 15: Diastereomers used for MacGregor's DP4-based comparison studies on the C18-C25 region of hemicalide and their calculated probabilities for matching hemicalide; only values above 0.1% are listed.

1.4.3 C25-C34 Polyacetate Stereotriad

To date, there has been no published research on elucidating the stereochemistry within the C25-C34 region, neither synthetic efforts nor modeling. The reported ^{1}H NMR spectrum listing signals for this region is of little use as most signals (H25, H26, H28, H30, H32, H33) are within a broad 22H methylene multiplet (δ_H 2.02-1.02 ppm) and the remaining key signals (H27, H29, H31) are broad multiplets without resolved coupling information.[1] Likewise, there are no particular ^{13}C NMR signals of interest, with the exception of the unusual upfield shift of C30 (δ_C 32.2 ppm).[1]

DP4 calculations carried out by MacGregor in this region of hemicalide on diastereomers **37A-37H** (**Figure 11**) have yet to propose any particular stereoisomer with high confidence.[37] The conformationally flexible nature of this region has made the computational modelling more challenging.

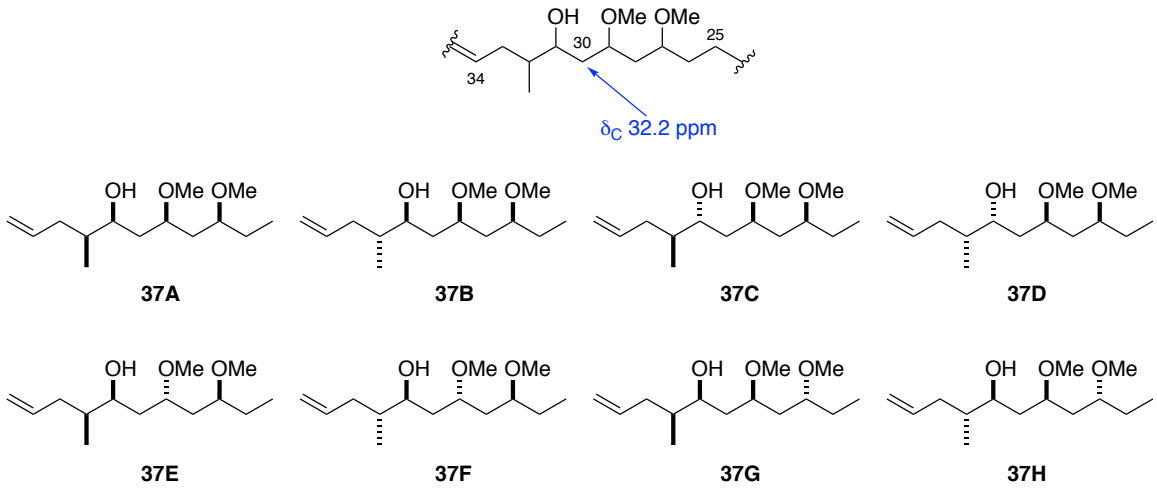

Figure 16: Diastereomers used for MacGregor's DP4-based comparison studies on the C25-C34 region of hemicalide

1.4.4 C35-C46 α-Hydroxy-δ-lactone

As with the C18-C24 α,β-dihydroxylactone, Ardisson used NOESY analysis to help assign the stereochemistry within the C35-C46 α-hydroxylactone.[38] Correlations were found between H37, H40 and Me42, implying a *cis* relationship between H37 and H40 but a *trans* relationship between H37 and H42. This study reduced the number of possible diastereomers from 32 to eight. While synthetic efforts towards all eight diastereomers were ongoing, it soon became apparent that epimers at C45 displayed almost identical NMR data, rendering it impossible to confidently assign the configuration at this remote stereocentre. For the purposes of preliminary structure determination, the absolute configuration at C45 was arbitrarily assigned as (45*R*) and the number of diastereomers to be considered was further reduced to four (**Figure 17**).[38]

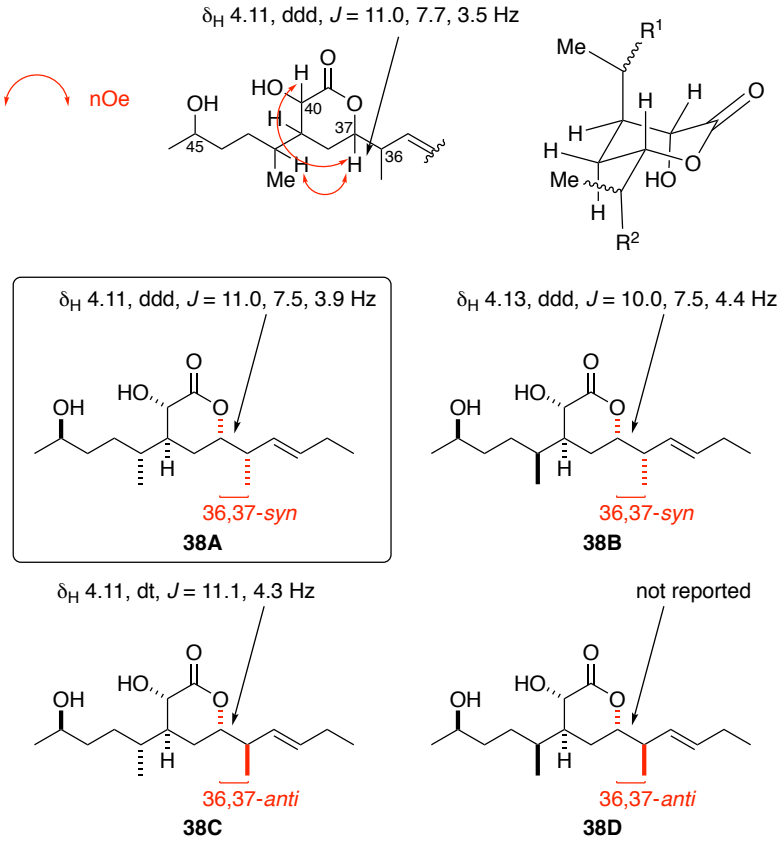

Figure 17: Diastereomers used for Ardisson's NMR-based comparison studies on the C35-C46 region of hemicalide

Comparisons with the corresponding region of hemicalide were made between diastereomers **38A**, **38B** and **38C**, but not with **38D** (**Figure 9**), presumably because the deviations in its NMR spectrum were too significant. For selected representative carbons (C36, Me36, C37, C38, C39, C42, Me42, C43), diastereomer **38A** showed the best agreement ($|\Delta\delta_C| < 0.5$ ppm) with the corresponding ^{13}C NMR signals in hemicalide. It was noted that the spectra of diastereomers **38A**

and **38B** showed similar chemical shifts for C36, Me36 and C37, while those for diastereomers **38A** and **38C** showed similar chemical shifts for C39, C42, Me42 and C43.[38] This observation indicated that an epimeric centre at C36 or C42 did not affect the chemical shifts of the opposite chain on the lactone, explaining why diastereomer **38D** was no longer considered a plausible candidate for comparison.

To further support the stereochemical assignment, the ^{1}H NMR spectral data of diastereomers **38A**, **38B** and **38C** (**Figure 17**) were also re-examined. Once again, the 36,37-*syn* diastereomer **38A** emerged as the best fit for hemicalide. The multiplicity of the oxymethine H37 signal was also a good match with hemicalide, suggesting that a configurational change at C36 could induce significant conformational changes in the lactone.[38]

Without access to the NOESY data at the time, the ^{1}H NMR spectral data for hemicalide was examined where a $^{3}J_{39,40}$ coupling constant of 11.3 Hz between H39 and H40 suggested a *trans* relationship and in agreement with Ardisson's studies. DP4 calculations undertaken by MacGregor[36] for this region used all 32 possible diastereomers **39A-39AF** (**Figure 13**) of the C35-C46 region. While these calculations are not yet complete, it appears that the 36,37-*syn* diastereomer **39A** is predicted with confidence and in agreement with Cossy and Ardisson.

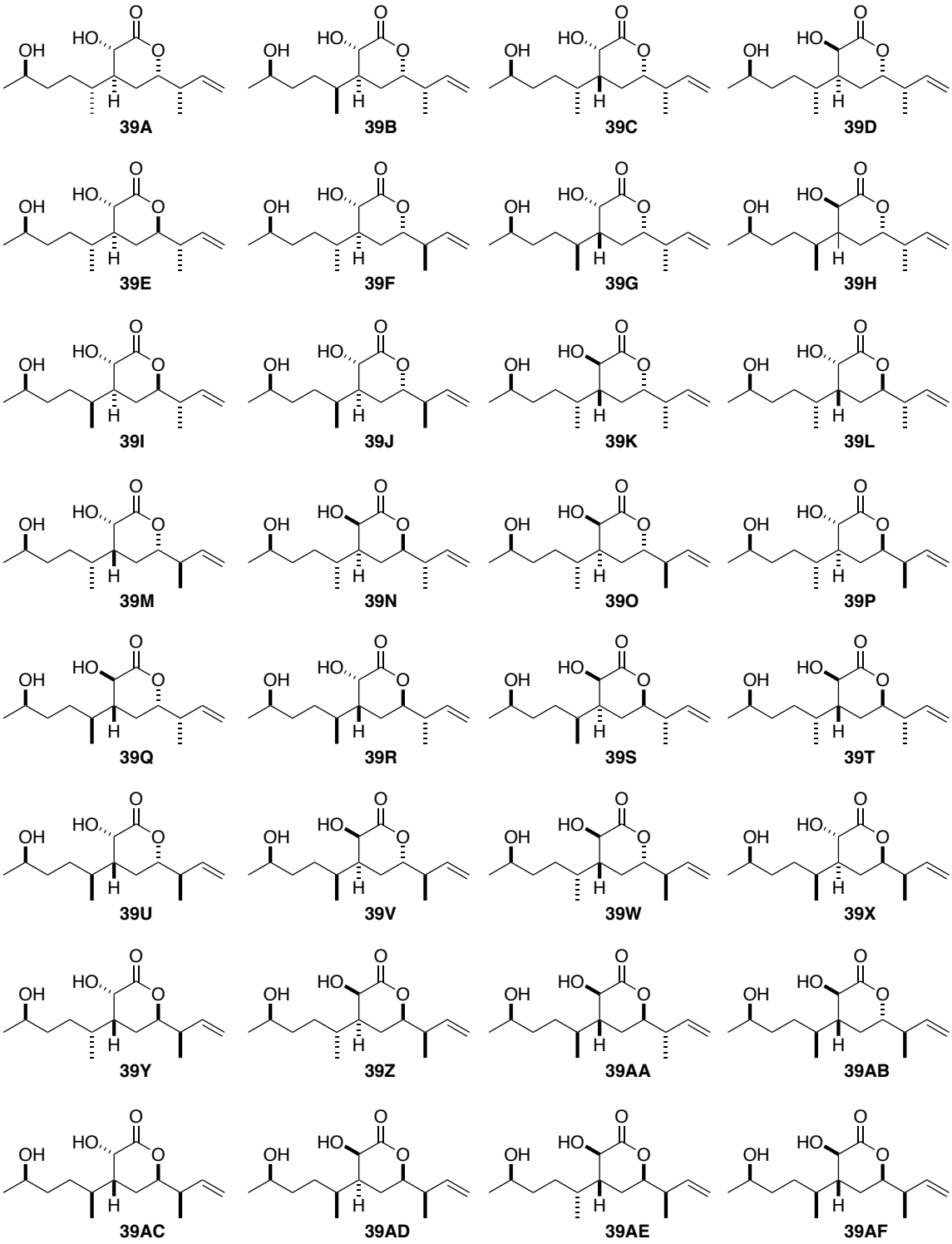

Figure 18: Diastereomers used for MacGregor's DP4-based comparison studies on the C35-C46 region of hemicalide

1.5 Previous Synthetic Work on Hemicalide

1.5.1 C1-C15 Polypropionate Stereohexad

The Ardisson and Cossy groups are working together towards the synthesis of hemicalide and have reported their results in a series of papers.

Ardisson's synthesis[32,35] of the C1-C17 stereohexad-containing fragment began from (*S*)-Roche ester (*S*)-**40** which was transformed into aldehyde **41** via TBS protection of the alcohol, DIBAL reduction of the ester moiety and then oxidised to aldehyde **21** under Swern conditions.[39] This was engaged with lactate-derived ketone **42**[40] in a Paterson boron-mediated aldol reaction to afford the 1,2-*anti* aldol adduct **43**[41] with high diastereoselectivity (*d.r.* >20:1). Methylation of the aldol adduct **43** was carried out (MeOTf, DTBMP), followed by reduction with $LiBH_4$ and oxidative cleavage of the nascent diol with $NaIO_4$ to afford aldehyde **44**. This was submitted to an Evans aldol reaction[42] with oxazolidinone **45** to obtain the 1,2-*syn* aldol adduct **46** (**Scheme 2**).

Cleavage of the oxazolidinone auxiliary from product **46** (**Scheme 1**) occurred smoothly *via* a Weinreb amide[43] and the free alcohol was protected as TMS ether **47**. Nucleophilic addition of the lithiated derivative of vinyl iodide **48** into Weinreb amide[44] **47** followed by deprotection of the TMS ether with Amberlyst-15 resin gave ketone **49**. A 1,3-*syn* reduction of the ketone with $Zn(BH_4)_2$ *via* chelation control[45] and protection of the resultant diol as a siloxane ($t\text{-}Bu_2Si(OTf)_2$, 2,6-lutidine) afforded intermediate **50**. Exchange of the vinyl silane for a vinyl iodide (NIS) and cleavage of the TBS ether (CSA) afforded alcohol **51**.

To complete the fragment synthesis, alcohol **51** was first oxidised to the aldehyde with DMP[46] (**Scheme 2**) where it was treated with phosphonate **52** in a HWE olefination[47] to arrive at the fully elaborated C1-C15 fragment **53**. Phosphonate **52** was obtained from 2,4-hexadienoic acid **54** in a sequential Mitsunobu reaction[48] ($TMSCH_2CH_2OH$, PPh_3, DIAD), cross metathesis with allyl bromide and the Hoveyda-Grubbs II catalyst[49] and an Arbuzov reaction[50] ($P(OEt)_3$).

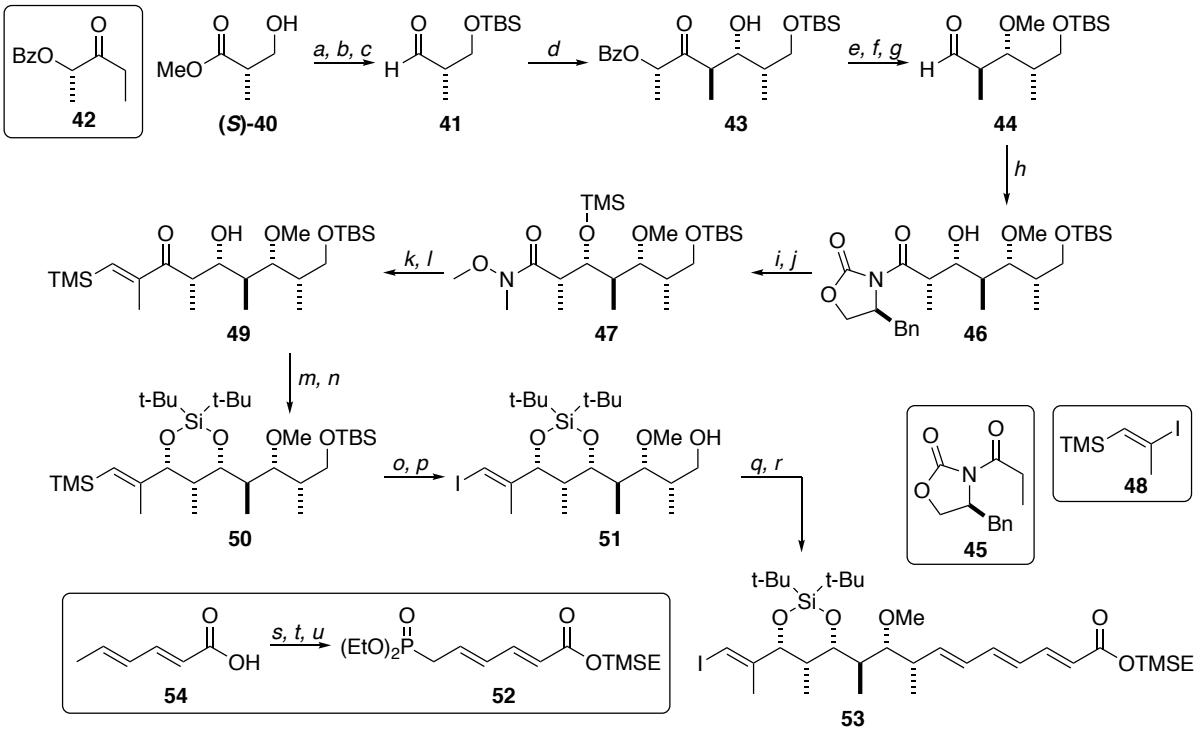

Reagents and conditions: (a) TBSCl, imidazole, DMF, rt; (b) DIBAL, CH_2Cl_2, –40 °C → –20 °C, 98% over two steps; (c) $(COCl)_2$, DMSO, Et_3N, CH_2Cl_2, –55 °C → rt, 100% (d) Cy_2BCl, Me_2NEt, **42**, Et_2O, –0 °C, *then* **41**, –78 °C → –25 °C, 98%; (e) MeOTf, DTBMP, CH_2Cl_2, 45 °C, 76%; (f) $LiBH_4$, THF, –78 °C → rt; (g) $NaIO_4$, MeOH, rt, 84% over two steps; (h) Bu_2BOTf, Et_3N, **45**, CH_2Cl_2, 0 °C, *then* **44** –78 °C → 0 °C; (i) MeONHMe•HCl, $AlMe_3$, CH_2Cl_2, –20 °C → rt, 75%; (j) TMSOTf, 2,6-lutidine, CH_2Cl_2, –30 °C, 93%; (k) **48**, t-BuLi, Et_2O, –90 °C, *then* **47**, –78 °C → –50 °C, 99%; (l) Amberlyst-15, MeOH, rt, 99%; (m) $Zn(BH_4)_2$, Et_2O, CH_2Cl_2, –78 °C → –50 °C, 87%, *d.r.* 9:1; (n) $t\text{-}Bu_2Si(OTf)_2$, 2,6-lutidine, DMF, rt, 76%; (o), NIS, THF, 0 °C, 87%; (p) CSA, MeOH, 0 °C, 87%; (q), DMP, CH_2Cl_2, rt; (r) LDA, **52**, THF, –78 °C, *then* **51**, –78 °C → 0 °C, 92% over two steps; (s) $TMSCH_2CH_2OH$, PPh_3, DIAD, THF, 0 °C → rt, 83%; (t) $CH_2{=}CHCH_2Br$, Hoveyda–Grubbs II catalyst (3 mol%), CH_2Cl_2, rt, 62%; (u) $P(OEt)_3$, 120 °C, 96%

Scheme 2: Synthesis of intermediate **53** in Ardisson's route to the C1-C15 fragment

1.5.2 C16-C25 α,β-Dihydroxy-δ-lactone and Fragment Assembly of a C1-C25 Subunit

Synthetic efforts directed towards the C16-C25 fragment of hemicalide by the Ardisson group[14] employed a Dias allylation[51] as the first step (**Scheme 3**). Allylsilane **55** was prepared from (*R*)-Roche ester **(*R*)-40** by benzyl protection, Grignard addition into the ester moiety[52] and a Peterson olefination[53] with Amberlyst-15. Exposure of allylsilane **55** to $SnCl_4$ and the known aldehyde **56** led to alcohol **57** in high diastereoselectivity (*d.r.* 19:1). Subsequent acylation with 2-bromoacetyl bromide and ozonolysis afforded ketone **58**. An alternative, higher-yielding route developed by the Cossy group first used methyl ketone **59**, which was also prepared from **(*R*)-40**, with

aldehyde **56** in a titanium-mediated aldol reaction[54] to form aldol adduct **60** (*d.r.* 9:1) which was acylated with 2-bromoacetyl bromide to give ketone **58** (**Scheme 3**).

To form the lactone core **61** (**Scheme 3**), a SmI_2-mediated intramolecular Reformatsky reaction[55] was performed on ketone **58** followed by dehydration with $SOCl_2$. Dihydroxylation of enoate **61** with $K_2OsO_4•2H_2O$ and NMO furnished diol **62** with high chemoselectivity and diastereoselectivity. Protection of diol **62** as *bis*-TES ethers (TESOTf, 2,6-lutidine) and exchange of the vinyl bromide for a vinyl boronic ester afforded product **63**.

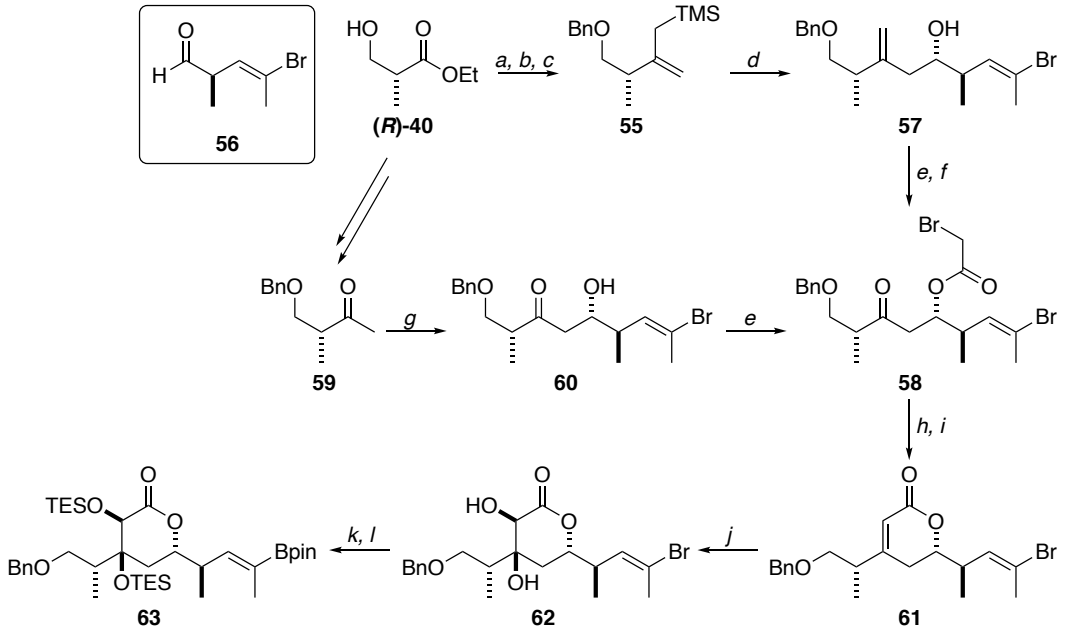

Reagents and conditions: (a) BnTCA, TfOH, cyclohexane/CH_2Cl_2, rt, 85%; (b) $TMSCH_2MgCl$, $CeCl_3$, THF, –78 °C → rt, 67%; (c) Amberlyst-15, n-hexane, rt, 90%; (d) $SnCl_4$, **55**, CH_2Cl_2, –78 °C, *then* **56**, –78 °C, 62%; (e) $BrCH_2COBr$, py, CH_2Cl_2, 0 °C, 100%, (f) O_3, Sudan red III, CH_2Cl_2, –78 °C, *then* PPh_3, 50%; (g) $TiCl_4$, DIPEA, **59**, CH_2Cl_2, –78 °C, *then* **56**, –78 °C, 73%; (h) SmI_2, THF, –78 °C → rt, (i) $SOCl_2$, py, CH_2Cl_2, 0 °C, 79% over two steps; (j) $K_2OsO_4•2H_2O$ (5 mol%), NMO, acetone/H_2O, rt, 100% (*d.r.* >95:5), (k) TESOTf, 2,6-lutidine, CH_2Cl_2, rt, 77%; (l) $PdCl_2(PPh_3)_2$ (2.4 mol%), PPh_3, PhOK, B_2pin_2, THF, 50 °C, 82%

Scheme 3: Synthesis of intermediate **63** in Ardisson's route to the C16-C25 fragment

With both the C1-C15 and C16-C25 fragments **53** and **63** in hand, the Cossy and Ardisson groups[35] employed a Suzuki coupling[56] (**Scheme 4**) using catalytic $Pd(PPh_3)_4$ and TlOEt to afford the C1-C25 fragment **64**. Cleavage of the TES ethers and the TMSE ester (TASF) and the siloxane (HF•py/py) gave the benzyl-protected C1-C25 fragment **65**.

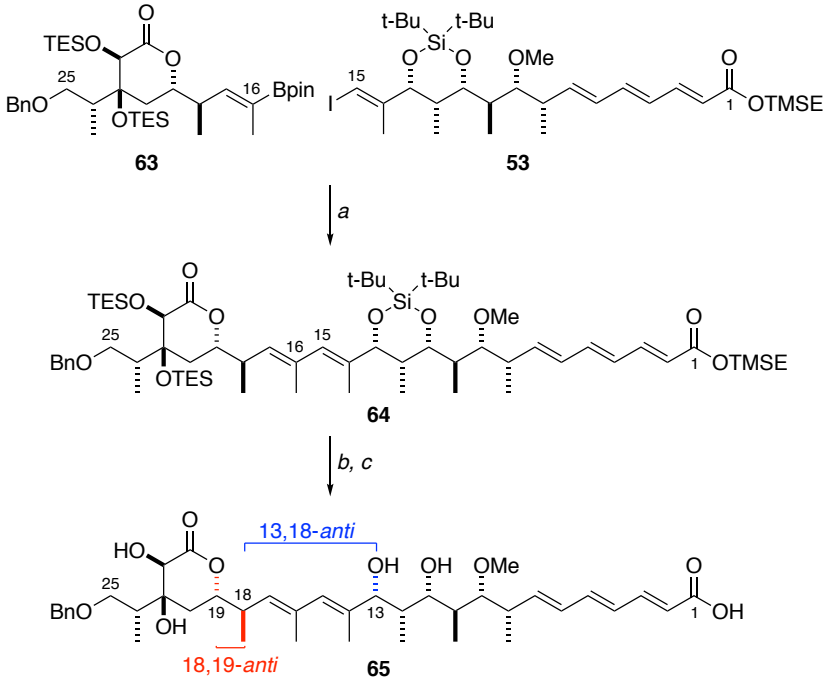

Reagents and conditions: (a) $Pd(PPh_3)_4$ (1 mol%), TlOEt, THF/H_2O, rt, 97%; (b) TASF, DMF, rt; (c) HF•py, THF, 0 °C, 40% over two steps

Scheme 4: Cossy and Ardisson's Suzuki coupling and global deprotection of the C1-C25 fragment **65**

Comparisons between the ^{1}H and ^{13}C NMR spectral data of fragment **65** and hemicalide have also been made (**Figure 19**).[35] Due to the salt effect observed in previous correlation studies (See Chapter 1.4.1), the C1-C7 region was not considered for the analysis. Overall, there was good agreement with the natural product ($|\Delta\delta_H| < 0.1$ ppm and $|\Delta\delta_C| < 1.5$ ppm) for the C8-C24 region. However, upon closer inspection, the C18-C24 δ-lactone region is clearly not as good a match for the corresponding region in hemicalide than the C8-C13 stereohexad region. Of particular note are the resonances for H18 and H19 with Δδ of –0.08 and +0.08 ppm respectively. This raises concerns over the stereochemical assignment of the C18-C24 δ-lactone, in particular the 18,19-*anti* relationship, which the Paterson group believes should be 18,19-*syn* instead.

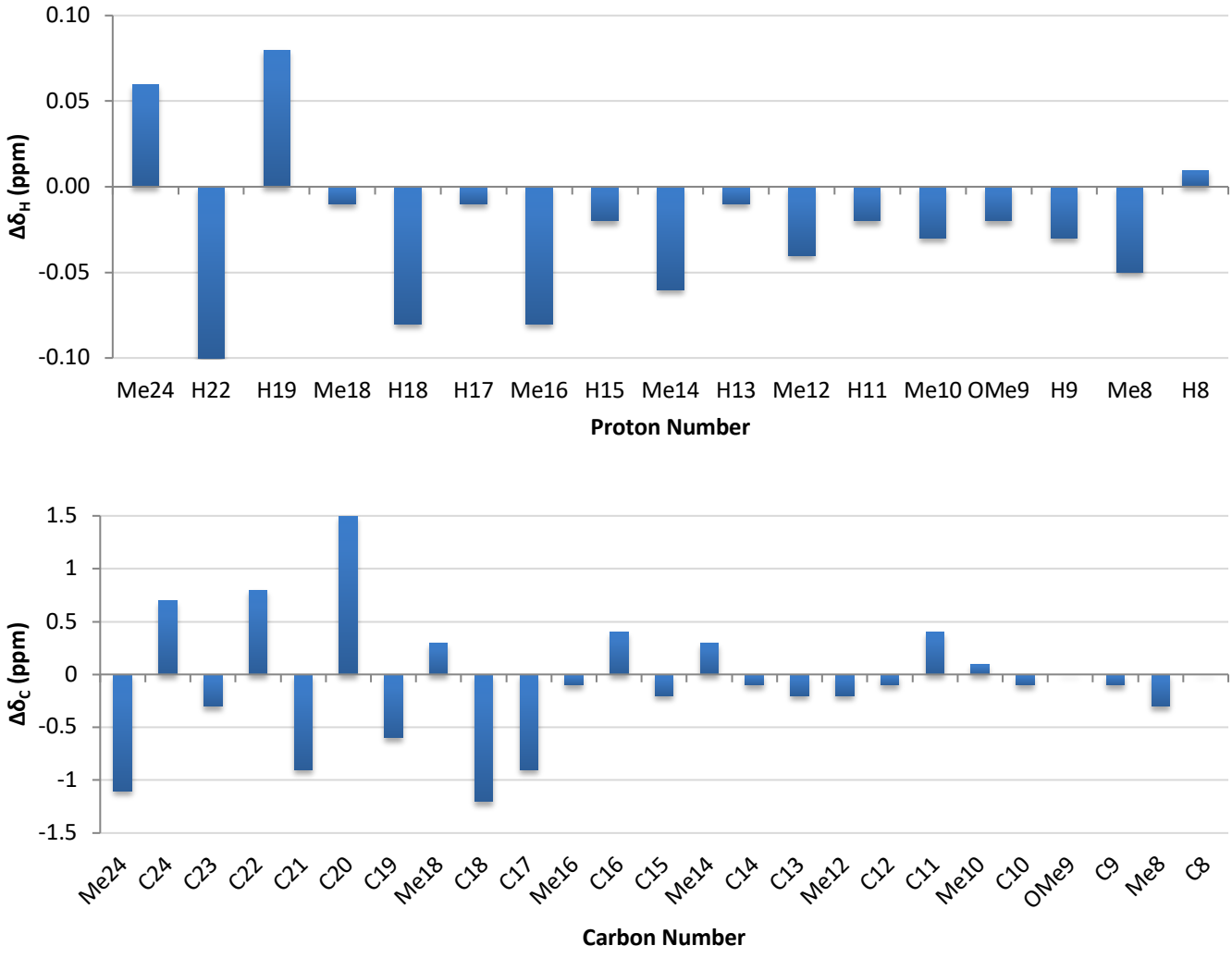

Figure 19: NMR correlations of subunit **65** against natural hemicalide

1.5.3 C35-C46 α-Hydroxy-δ-lactone

The reported synthesis of the remaining C35-C46 fragment by the Cossy and Ardisson groups[18] returned to (*S*)-Roche ester **(*S*)-40** as the chiral building block (**Scheme 5**). The hydroxyl group in ester **(*S*)-40** was protected with as a PMB ether and transaminated to the Weinreb amide **66**. Reduction of Weinreb amide **66** using DIBAL afforded an aldehyde which was treated with Hafner–Duthaler's allyltitanium complex **67**[57] to afford homoallylic alchohol **68**. The product **68** was acylated with acryloyl chloride and ring-closing metathesis took place in the presence of Grubbs II catalyst[58] to give unsaturated δ-lactone **69**. The boronic ester **70** (**Scheme 6**) was obtained from optically pure alcohol **71** *via* TBS protection (TBSCl, imidazole) and cross metathesis catalysed by the Grubbs II catalyst.

To join intermediates **69** and **70**, a rhodium-catalysed conjugate addition[59] was employed to afford product **72** (d.r. 5:1) (**Scheme 5**). α-Oxidation of the lactone was achieved by enolisation with NaHMDS and treatment with Davis' oxaziridine **73**[60], leading to alcohol **74** as a single diastereomer. The final stereocentre in intermediate **75** was installed *via* a hydroxyl-directed hydrogenation with Crabtree's catalyst[61] with poor diastereoselectivity (d.r. 2:1). The absolute configuration of this new methyl-bearing stereocentre was assigned by Vibrational Circular Dichroism (VCD) analysis[62] as (42*R*).

Further chain extension to intermediate **76** (**Scheme 5**) was enabled by sequential TBS protection (TBSOTf, 2,6-lutidine) of the free alcohol **75** and oxidative cleavage of the PMB ether (DDQ, pH 7 buffer). Oxidation of alcohol **76** with DMP[46] afforded an aldehyde which was engaged in a Julia–Kocienski olefination[43] with PT sulfone **77** to give olefin **78** where exposure to HF•py/py completed the synthesis of the unprotected C35-C46 model fragment **79**.

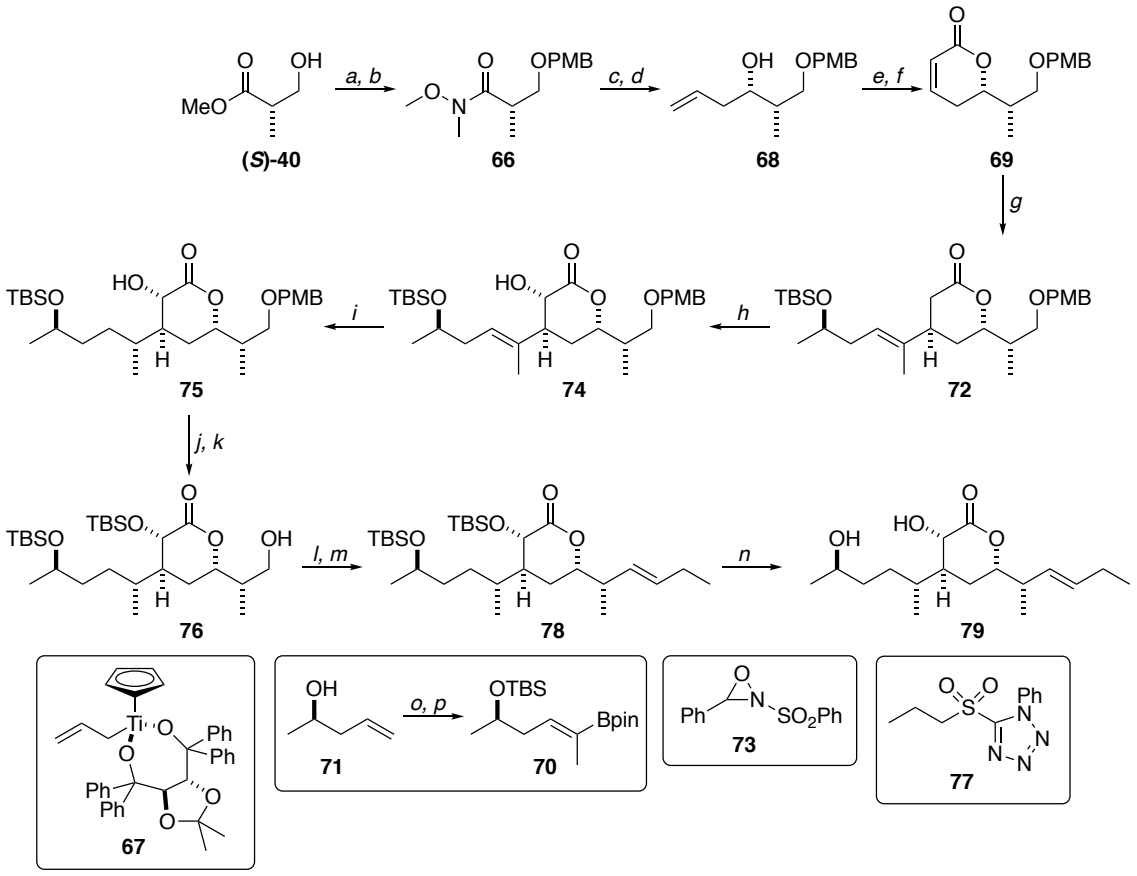

Reagents and conditions: (a) PMBTCA, CSA, CH_2Cl_2, rt; (b) MeONHMe•HCl, i-PrMgCl, THF, –40 °C → –10 °C, 87% over two steps; (c) DIBAL, THF, –78 °C → –40 °C; (d) **67**, Et_2O, –78 °C, 92% over two steps; (e) CH_2=CHCOCl, DIPEA, CH_2Cl_2, –78 °C; (f) Grubbs II catalyst (5 mol%), CH_2Cl_2, reflux, 72% over two steps; (g) **70**, $[Rh(COD)Cl]_2$ (3 mol%), LiOH, dioxane/H_2O, 40 °C, 74%; (h) NaHMDS, THF, –78 °C, *then* **73**, –78 °C, 72%; (i) Crabtree's catalyst (8 mol%), H_2, CH_2Cl_2, rt, 72%; (j) TBSOTf, 2,6-lutidine, CH_2Cl_2, 0 °C, 92%; (k) DDQ, CH_2Cl_2/H_2O, rt, 99%; (l) DMP, $NaHCO_3$, CH_2Cl_2, rt; (m) **77**, KHMDS, THF, –78 °C → rt, 70% over two steps; (n) HF•py, THF, rt, 95%; (o) TBSCl, imidazole, DMF, rt, 96% (p) isopropenyl pinacol boronate, Grubs II catalyst (4 mol%), CH_2Cl_2, reflux, 55%

Scheme 5: Cossy's synthesis of a C32-C46 fragment **79** of hemicalide

We note that **79** is only a model fragment for the C35-C46 region of hemicalide which cannot be used for further fragment coupling. However, Cossy and Ardisson do intend to use the Julia–Kocienski olefination on an earlier intermediate which allows fragment coupling to the remainder of the molecule. For selected representative atoms, the ^1H and ^{13}C NMR spectral data of **79** is in good agreement with hemicalide ($|\Delta\delta_H| < 0.1$ ppm and $|\Delta\delta_C| < 0.5$ ppm).

1.5.4 Correction of the 18,19-*syn* Relationship

Following the Paterson group's disclosure of the 18,19-*syn* relationship, the Cossy group[63] re-examined their initial stereochemical assignment by synthesising subunit **80** (**Figure 20**) in an analogous fashion to intermediate **37** (See Chapter 1.5.2). The erroneous 18,19-*anti* relationship was then corrected to 18,19-*syn* in agreement with our results based on the improved correlations of **80** with hemicalide compared to **37**.

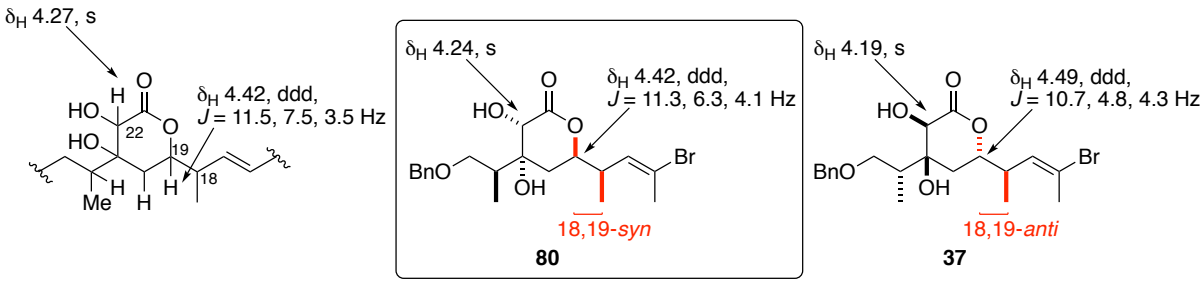

Figure 20: Diastereomers used for Cossy's re-examination of the C17-C25 region of hemicalide

Unexpectedly, the change in stereochemistry at C19 led to a diminished performance of the $SOCl_2$-mediated dehydration and the subsequent Upjohn dihydroxylation during the synthesis of intermediate **80**. These were key reactions used to construct the lactone ring and to set the diol stereocentres.[33] Meanwhile, ongoing synthetic efforts to extend the C1-C25 subunit beyond C25 were met with disappointing results. The Cossy group took this opportunity to change their retrosynthetic plan leading to a C1-C27 subunit instead.[63]

The revised synthesis began from (*S*)-citronellol **81** as a chiral building block (**Scheme 6**). Following a TES protection, the olefin was subjected to an ozonolysis with a reductive workup to afford alcohol **82**. The crude **82** could be telescoped through five more steps *via* aldehyde **83**, involving benzyl protection, a Swern oxidation, a Pihko methylenation[64], aldehyde reduction and benzoylation leading to benzoate **84** in a 64% yield over six steps.

Allylstannane **85** was obtained *via* a palladium-mediated stannylation with Trost's conditions (**Scheme 6**).[65] This set the stage for an asymmetric allylation of known aldehyde **56** under the reagent control of Corey's bromoborane complex **86**.[66] Although the adduct **87** was obtained as a 88:12 mixture of *syn* and *anti* epimers, the desired 18,19-*syn* diastereomer could be isolated in 69% yield. A simple esterification then delivered acrylate **88** smoothly as an RCM precursor. The use of Nolan's catalyst[67] **89** led to enoate **90** in 83% yield after extensive screening.

The Cossy group found that Upjohn conditions were not optimal for the dihydroxylation when the enoate features an 18,19-*syn* relationship instead of 18,19-*anti*. Like the Paterson group, the use of citric acid[68] as an additive provided a marked improvement for this reaction (*vide infra*) leading to diol **91** in 70% yield. Following a *bis*-TES protection, the vinyl bromide was exchanged for a vinyl boronate under palladium catalysis to afford intermediate **92** (**Scheme 6**).

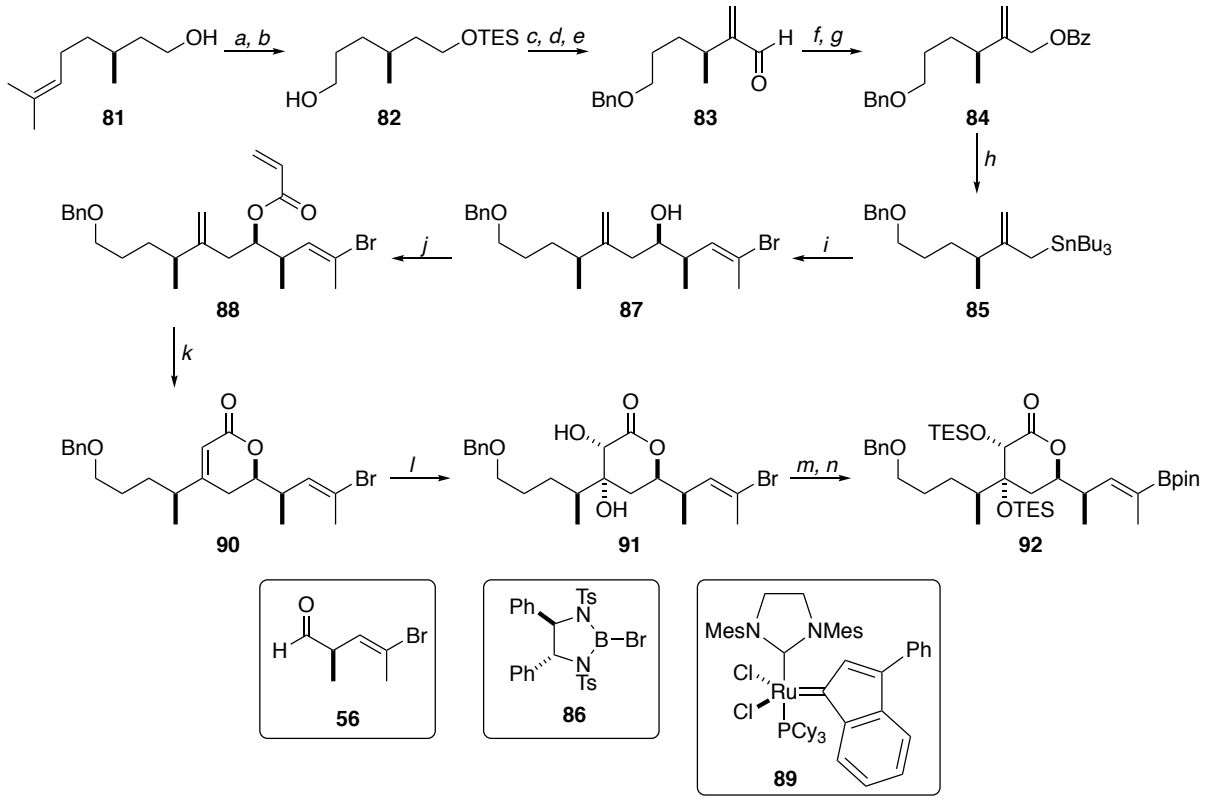

Reagents and conditions: (a) TESCl, Et_3N, CH_2Cl_2, 0 °C → rt, 100%; (b) O_3, CH_2Cl_2, –78 °C, *then* $NaBH_4$, MeOH, rt; (c) NaH, THF, 0 °C, *then* BnBr, TBAI, 0 °C → rt; (d) $(COCl)_2$, DMSO, CH_2Cl_2, –78 °C → –45 °C, *then* Et_3N, –78 °C → rt; (e) HCHO (35 wt. % in H_2O), pyrrolidine, $CH_3CH_2CO_2H$, i-PrOH, 45 °C; (f) $LiAlH_4$, THF, 0 °C; (g) PhCOCl, Et_3N, rt, 64% over six steps; (h) $Pd(PPh_3)_4$ (5 mol%), $(Bu_3Sn)_2$, Et_2AlCl, n-BuLi, THF, –78 °C → rt, 100%; (i) **86**, CH_2Cl_2, rt, *then* **56**, –78 °C, 78% (*d.r.* 88:12); (j) CH_2=CHCOCl, DIPEA, CH_2Cl_2, –78 °C, 91%; (k) **89** (10 mol%), PhMe, 100 °C, 83%; (l) K_2OsO_4•$2H_2O$ (2 mol%), NMO, citric acid, THF/H_2O, rt, 70%; (m) TESOTf, 2,6-lutidine, CH_2Cl_2, 0 °C, 96%; (n) $PdCl_2(PPh_3)_2$, PPh_3, PhOK, B_2pin_2, THF, 50 °C, 66%

Scheme 6: Cossy's revised approach to fragment **92** featuring the corrected 18,19-*syn* relationship

To assemble the full C1-C27 subunit, vinyl boronate **92** was coupled with vinyl iodide **53** in a palladium-catalysed Suzuki reaction[56] in the presence of aqueous TlOEt (**Scheme 7**). This afforded the product diene **93** in good yield (82%). As with previous deprotection attempts, the desilylation was carried out in two steps. The TES ethers at C21 and C22 as well as the TMSE ester were removed with TASF, followed by the C11 and C13 TES ethers upon exposure to

buffered HF•py. Carboxylic acid **94** was thus obtained in 90% yield, representing one of two possible diastereomers for this subunit, featuring a 13,18-*anti* relationship. To date, the Cossy and Ardisson groups have not reported an attempt to synthesise the other 13,18-*syn* diastereomer.

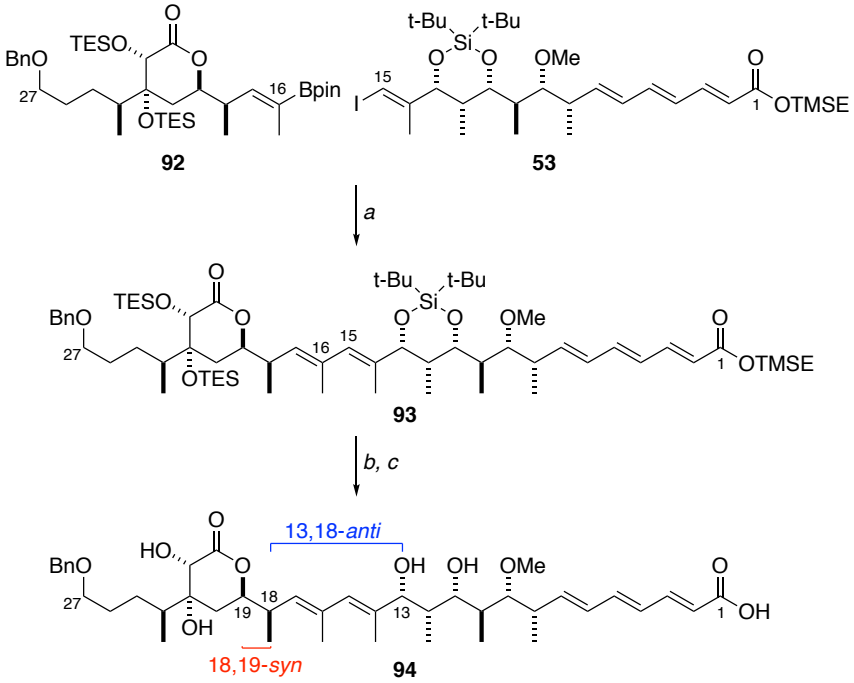

Reagents and conditions: (a) $Pd(PPh_3)_4$ (1 mol%), TlOEt, THF, rt, 82%; (b) TASF, DMF, rt; (c) HF•py/py, THF, 0 °C, 90% over two steps

Scheme 7: Cossy and Ardisson's Suzuki coupling and global deprotection of the C1-C25 fragment **94**

The change from an 18,19-*anti* to 18,19-*syn* relationship has a marked effect on the NMR correlations of subunit **65** and **94** (**Figure 21**). This is particularly evident in the δ-lactone section spanning C17-C24 where 18,19-*syn* subunit **94** is a much better fit for the natural product than the initially proposed 18,19-*anti* subunit **65**. Previously, the largest errors for 18,19-anti subunit **65** were $|\Delta\delta_H| < 0.1$ ppm and $|\Delta\delta_C| < 1.5$ ppm; with the 18,19-*syn* subunit **94**, these errors were now reduced to $|\Delta\delta_H| < 0.04$ ppm and $|\Delta\delta_C| < 0.5$ ppm.

Despite the improved correlations, the chemical shift deviations in subunit **94** are relatively large given that this molecule constitutes just over half of the entire carbon backbone. With no rationalisation for the Cossy group synthesising only one of two possible diastereomers of **94**, this leads us to speculate that the 13,18-*anti* relationship, as featured in **94**, is not present in natural hemicalide.

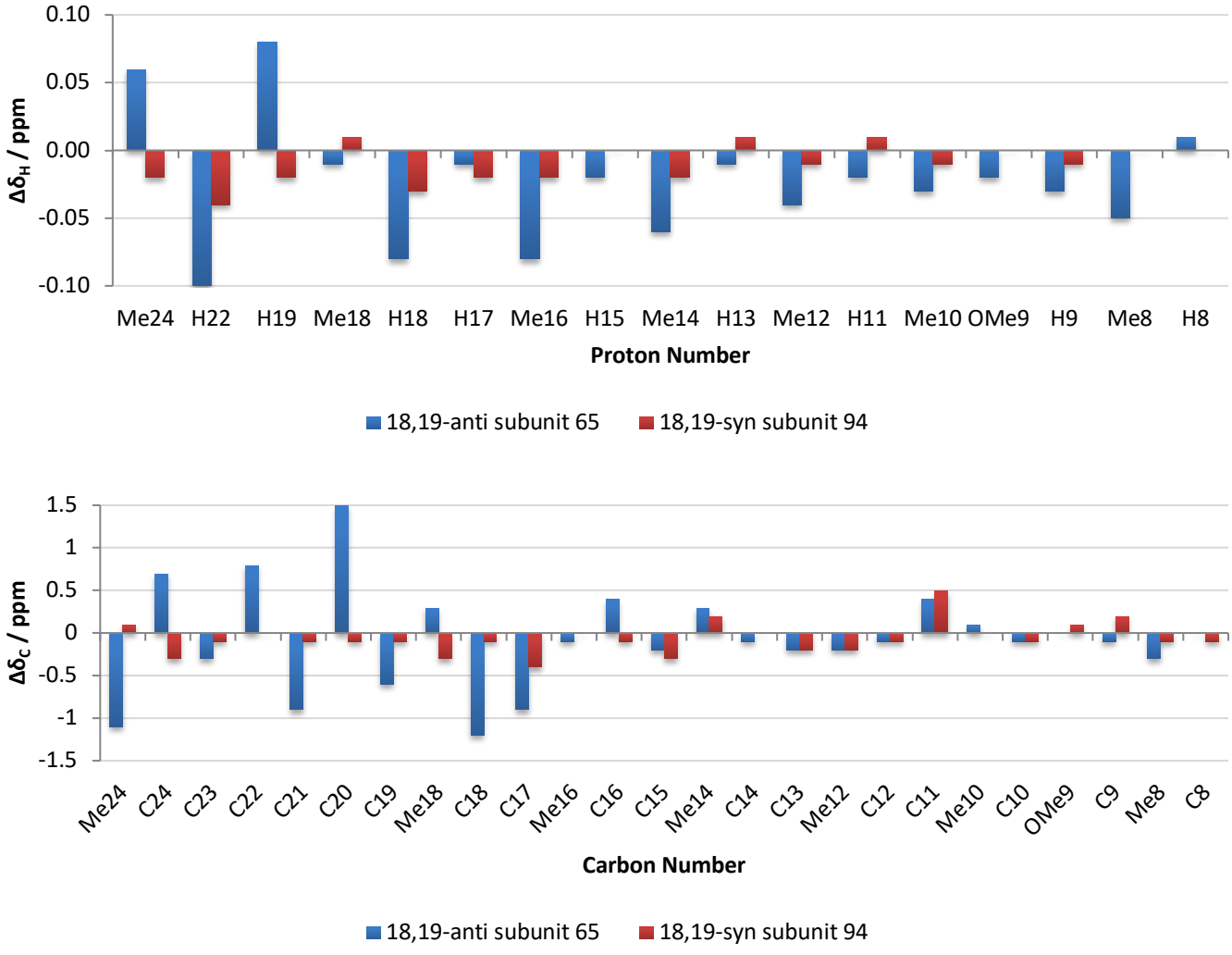

Figure 21: NMR correlations of the 18,19-*anti* fragment **65** and the 18,19-*syn* fragment **94**

1.5.5 Summary

To date, the Ardisson and Cossy groups have proposed the relative configurational assignment of most stereocentres in hemicalide **1** through NMR-based comparison studies of the relevant diastereomeric model fragments. These results have identified **29A**,[32] **33B**[33] and **38A**[38] as bearing the same relative stereochemistry in the corresponding C1-C17, C17-C25 and C32-C46 regions of hemicalide (**Figure 22**). Independently, the Paterson group has also carried out DP4 analysis to predict the most probable structure for each fragment.[36] The DP4 analysis also identifies model fragments with the same stereochemistry as **29A** and **38A** for the C1-C17 and the C34-C46 regions, but suggests **36M** as a more likely structure than **33B** for the C17-C25 fragment instead. We are confident of our assignment in **36M** as it is structurally more similar to the natural product than **33B**, making the analysis more reliable. The Cossy group ultimately conceded that the C17-C25 fragment **80** should bear a 18,19-*syn* relationship rather than 18,19-*anti*.

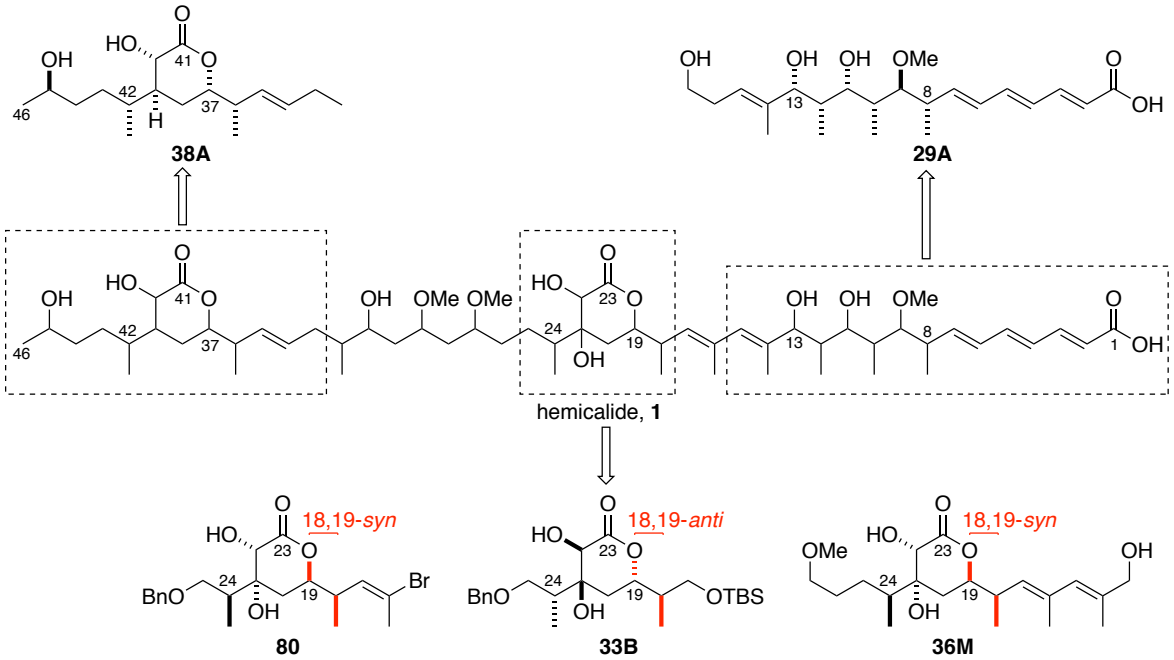

Figure 22: Summary of the stereochemical assignment for the C1-C17, C17-C25 and C32-C46 regions of hemicalide as determined by the Ardisson, Cossy and Paterson groups

The Cossy and Ardisson groups have undertaken synthetic efforts towards the assembly of a C1-C25 unit[35] **65** (**Scheme 4**) as well as a revised C1-C27 unit[63] **93** of hemicalide (**Scheme 7**) by utilizing a Suzuki coupling for fragment coupling. Comparison studies of the C1-C25 fragment **65** with hemicalide have revealed potential stereochemical assignment issues in the C18-C24 δ-lactone region, especially the C18-C19 *anti* relationship. Further examination of the revised subunit **94** have then raised questions about the veracity of the 13,18-*anti* assignment. A route to

a model fragment of the C32-C46 region **79** has also been described[38] (**Scheme 5**) but further modifications are required to make it useful for fragment coupling.

CHAPTER TWO: SYNTHESIS OF THE C1-C15 AND C16-C28 FRAGMENTS

2.1 Initial Objectives and Synthetic Plan

Hemicalide **1** is a synthetic target of interest as it features several polypropionate and polyacetate motifs which can be readily assembled with the use of asymmetric boron aldol reaction protocols developed in our group. As outlined in Scheme **8**, three key disconnection sites have been identified as suitable fragment union strategies. It was envisioned to use a late stage boron aldol reaction to form the C28-C29 bond. This gives rise to two key fragments of equal complexity, namely a C1-C28 subunit **95** where the relationship between the two stereoclusters still needs to be rigorously established. The remaining C29-C46 subunit **96** can be further disconnected with an sp^2-sp^3 Suzuki coupling[56] to construct the C33-C34 bond to give the C29-C33 and C34-C46 subunits **97** and **98** respectively.

Although the assignment of the relative stereochemistry of hemicalide within the C1-C17 region and the C18-C24 region has been independently proposed by the DP4 method and synthesis of model systems, the relationship between the two stereoclusters is currently unknown. Hence, it was desirable to selectively synthesise both diastereomers **99** and **100** in order to compare all NMR spectral data against that reported[1] for hemicalide to determine which is more likely to represent the natural stereochemistry of the full polyketide. This approach has been successfully employed by our group during the total synthesis of spirastrellolide A.[69]

Compounds **99** and **100** bear a methyl ketone at C28 which provides a handle for a diastereoselective boron aldol coupling to allow for future extension towards the full natural product. A Stille coupling[70] would be used to join the C1-C15 fragment **101** to the C16-C28 dihydroxylactone fragment **102** with the flexibility for a late-stage iodine-tin exchange on either fragment as required. Both enantiomers **101** and *ent*-**101** would be synthesised separately and individually coupled to intermediate **102** in order to generate the two diastereomers **99** and **100** respectively. The work discussed in this chapter describes the synthesis of **101**, *ent*-**101** and **102** while coworker Nelson Lam[71] synthesised *ent*-**102** concurrently. This work builds on the route which was previously developed by Callum MacGregor[37] with the aim of further optimising the synthesis of the key building blocks.

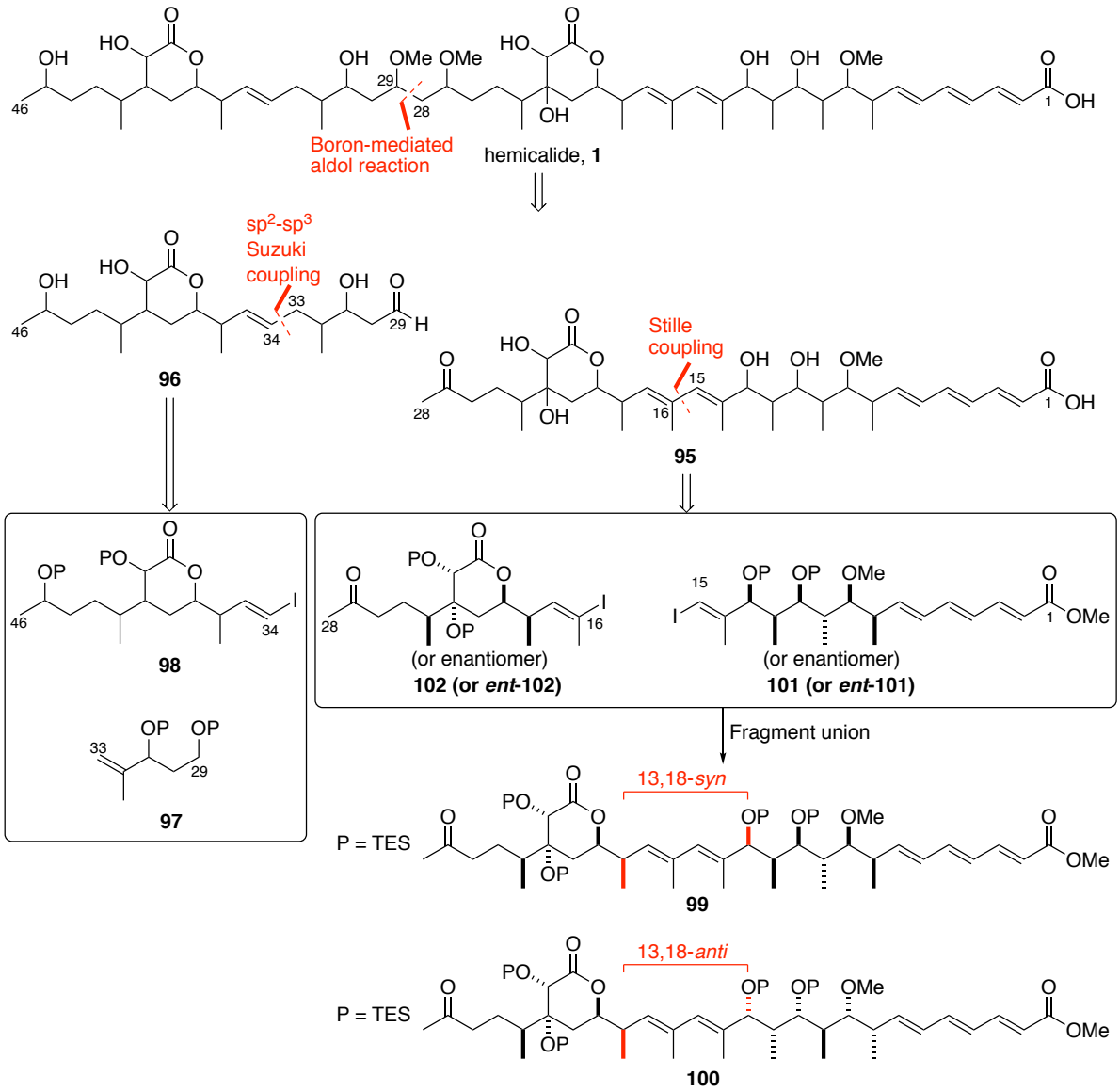

Scheme 8: Key disconnections and coupling strategy for the diastereomeric C1-C28 fragments **99** and **100**

2.2 Synthesis of the C1-C15 Fragment 101

2.2.1 Retrosynthesis and Strategy

Intermediate **101** features several functionalities and stereochemical relationships that are useful in planning a synthesis (**Scheme 9**). The triene region could be made *via* a HWE olefination[47] between aldehyde **103** and phosphonate **104** in order to achieve the requisite (*E*)-geometry. The 1,4-*syn* relationship between C8 and C11 could be constructed by a boron-mediated aldol reaction[72] between aldehyde **105** and ethyl ketone **106**. Ketone **106** itself is obtained from the commercially available (*R*)-Roche ester **(*R*)-40**.[73] The 1,2-*syn* relationship between C12 and C13

in aldehyde **105** could be installed *via* an Evans aldol reaction[42] between aldehyde **107** and oxazolidinone **108**.

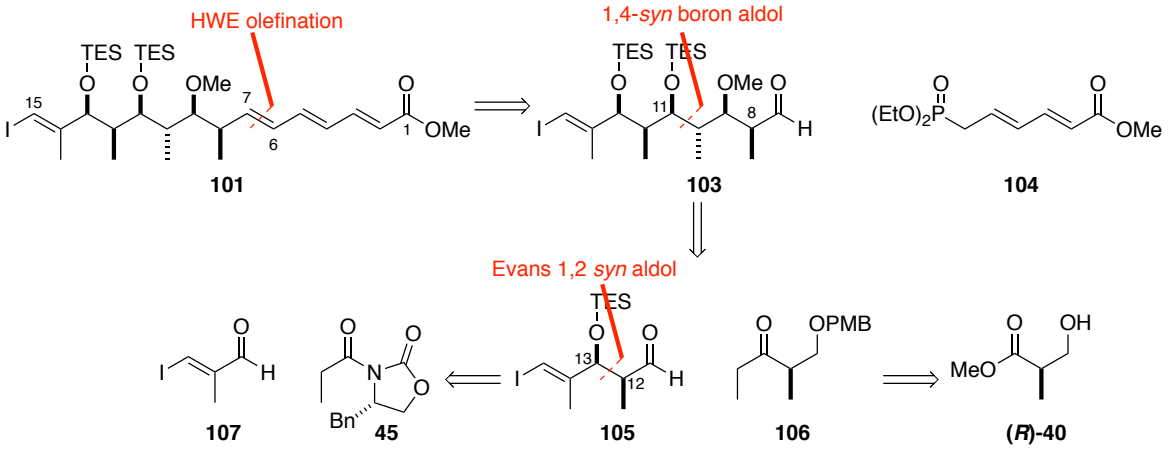

Scheme 9: Retrosynthetic analysis of the C1-C15 fragment **101**

2.2.2 Synthesis of the C11-C15 Aldehyde 105

Oxazolidinone **45** could be prepared following Evans' protocol[74] (**Scheme 10**). Reduction of L-phenylalanine **108** with $LiAlH_4$ gave aminoalcohol **109** which was cyclised with diethyl carbonate under basic conditions to give auxiliary **110**. Acylation of the auxiliary was achieved by deprotonating with n-BuLi followed by trapping with propionyl chloride to give oxazolidinone **45** in 50% over three steps.

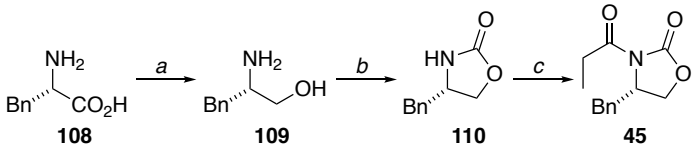

Reagents and conditions: (a) $LiAlH_4$, Et_2O, 0 °C → rt, 75%; (b) $CO(OEt)_2$, 100 °C, 78%; (c) n-BuLi, THF, –78 °C; CH_3CH_2COCl, 85%

Scheme 10: Synthesis of Evans auxiliary derivative **108**

The known aldehyde **107** was prepared in a four step sequence from diethyl methylmalonate **111** (**Scheme 11**). This had also previously been employed in our group's total synthesis of leiodermatolide.[75] Malonate ester was alkylated (NaH, CHI_3) to give intermediate **112**, which upon treatment with KOH in EtOH at elevated temperatures was converted into carboxylic acid **113** *via* the intermediate dicarboxylate.[76] This hydrolysis-decarboxylation-elimination sequence occurred in good yield (71%) and with excellent control of olefin geometry.

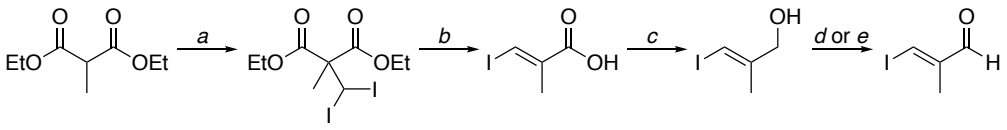

111 **112** **113** **114** **107**

Reagents and conditions: (a) NaH, THF, rt → reflux; CHI_3; (b) KOH, EtOH, reflux, 58% over two steps; (c) $LiAlH_4$, Et_2O, 0 °C → rt, 79% (d) MnO_2, CH_2Cl_2, rt, 88% (e) CuBr, bipy, DMAP, TEMPO, O_2 balloon, MeCN, rt, 91%

Scheme 11: Synthesis of aldehyde **107** from diethyl methylmalonate **111**

Carboxylic acid **113** was reduced to alcohol **114** ($LiAlH_4$, 77%) which was oxidised to aldehyde **107** (**Scheme 10**).[76] On a small scale, this oxidation was possible by using MnO_2 as the oxidant. However, as the scale of reaction was increased (>20 mmol), this procedure became operationally unfeasible as the reaction was still sluggish despite the use of superstoichiometric equivalents (10-20 eq.) of MnO_2. A more practical alternative for this transformation was to use a catalytic copper-TEMPO system[77] where molecular oxygen was employed as the terminal oxidant. While the original optimised conditions called for Cu(OTf) and NMI, these could be substituted with CuBr and DMAP respectively and the reaction proceeded cleanly with good yield (91%) in just under 5 h.

A mechanism for the copper-TEMPO mediated oxidation has been proposed by Stahl (**Scheme 12**).[78] The catalyst **115** is activated by O_2 to form **116** which dimerises to the peroxo-bridged binuclear Cu(II) species **117**. This is sequentially reduced to complex **118** followed by the active mononuclear Cu(II) species **119**. Following ligand exchange of the substrate for hydroxide in intermediate **120**, hydride abstraction by TEMPO then generates the aldehyde product together with turnover of the catalytic system. Notably, H_2O_2 is generated as a by-product that disproportionates into H_2O and O_2 under the reaction conditions. This proposal is consistent with Stahl's observation that the stoichiometry of O_2 consumed to alcohol substrate is 1:2.[78]

Due to its volatility and instability, aldehyde **107** was always freshly prepared and subjected to further reaction immediately without storage or further purification. While the presence of TEMPO could be detected by ^1H NMR spectroscopy in the crude **107**, this did not appear to have any detrimental effect on the subsequent aldol reaction.

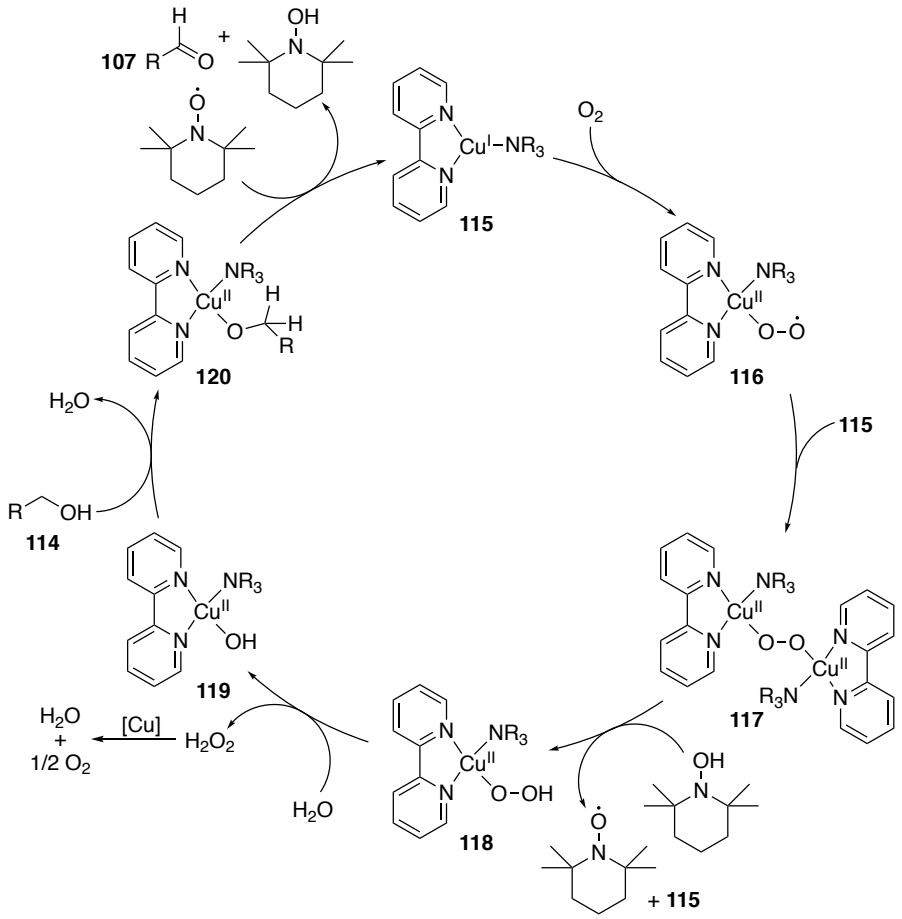

Scheme 12: Proposed mechanism for the oxidation of **114** to **107**

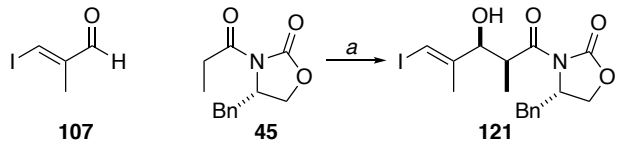

Reagents and conditions: (a) **45**, Bu_2BOTf, DIPEA, CH_2Cl_2, –78 °C, *then* **107**, –78 °C → –20 °C, 80% (*d.r.* >20:1)

Scheme 13: Evans aldol reaction of **107** and **108** to form aldol adduct **121**

Aldehyde **107** was treated with the boron enolate of propionyl-oxazolidinone **45** under the conditions developed by Evans (**Scheme 13**).[42] Enolisation of ketone **45** was conducted at –78 °C with Bu_2BOTf and DIPEA. To ensure complete enolisation, the reaction mixture was briefly warmed to –10 °C but cooled back to –78 °C before introducing aldehyde **107**. The reaction mixture was then transferred to a freezer overnight. Cleavage of any residual boronate ester from the aldol adduct could be achieved by repeatedly azeotroping the crude material with MeOH to generate the volatile $B(OMe)_3$ species.

Chelation of the boron Lewis acid between the carbonyl and the oxazolidinone presents two competing transition states, **TS-I** and **TS-II**, in which the methyl group on the propionyl arm of the oxazolidinone is either pointing away or towards the bulky auxiliary (**Scheme 14**). The preferred transition state for deprotonation minimises developing allylic ($A_{1,3}$) strain, thus **TS-I** leads to the favoured (*Z*)-enolate **122**. The excellent stereocontrol in the aldol reaction can be attributed to the clean generation of the (*Z*)-enolate **122** in >100:1 selectivity.

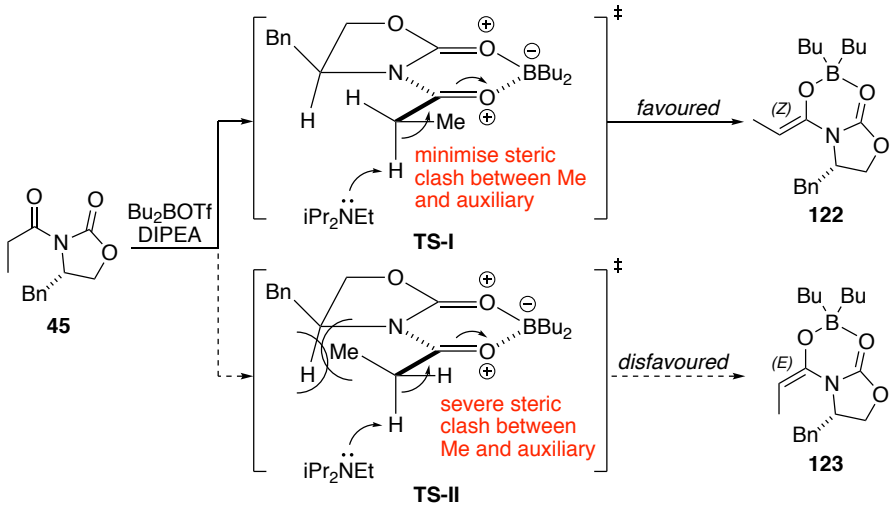

Scheme 14: Selective (*Z*)-enolization of oxazolidinone **45**

Reaction of the (*Z*)-enolate **122** with aldehyde **107** would be expected to occur *via* the highly ordered, six-membered chair-like transition state (**Scheme 15**).[79] To minimse 1,3-diaxial interactions, the main chain of the aldehyde would adopt a pseudo-equatorial position. The high levels of diastereoselectivity of this aldol reaction is determined by the chiral auxiliary adopting a low energy conformation within the transition state that opposes the enolate C–O dipole. Thus, two possible transition states, **TS-III** and **TS-IV**, are in competition where the benzyl group either points away from or into the other substituents on the chair. In practice, this steric interaction is minimised in transition state **TS-III** and leads to aldol adduct **121** as the major product with excellent diastereoselectivity (80%, *d.r.* >20:1) (**Scheme 13**).

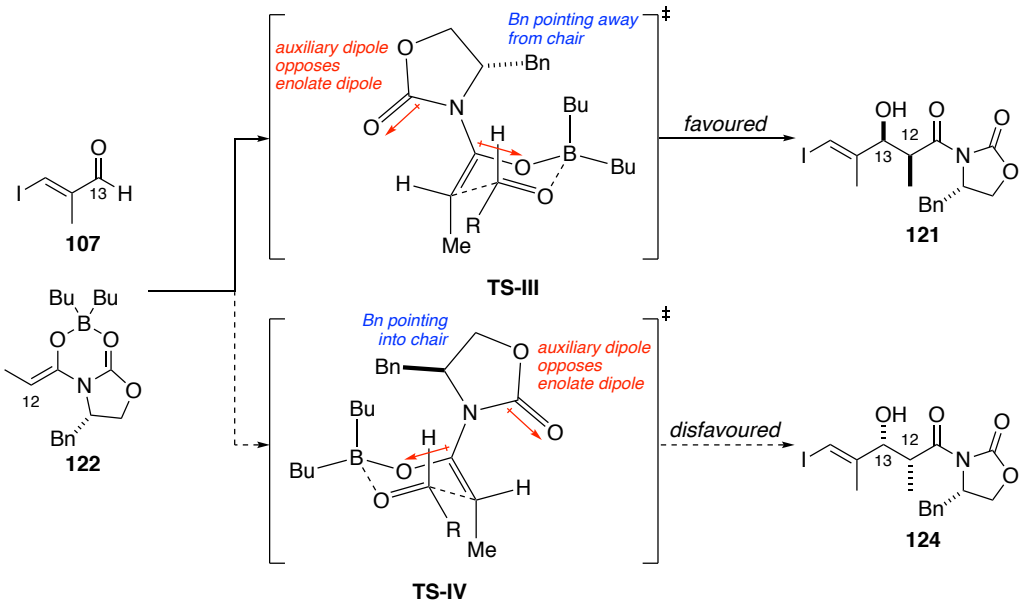

Scheme 15: Diastereoselective transition states for the aldol reaction of **107** and **122**

The expected *syn* relative stereochemistry in product **121** was confirmed by ^{1}H NMR spectroscopic analysis. β-hydroxyketones are known to adopt a chair-like conformation due to a stabilising intramolecular hydrogen bonding interaction between the carbonyl lone pair and the β-hydroxyl group (**Figure 23**).[80] The measured vicinal coupling constant between H12 and H13 ($^{3}J_{12,13}$ = 3 Hz) in **121** is highly indicative of a 1,2-*syn* relationship due to the gauche arrangement of the protons.

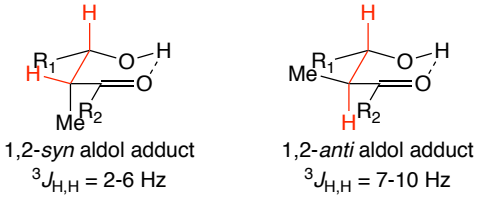

Figure 23: Comparison of chair-like conformers of 1,2-*syn* and 1,2-*anti* aldol adducts

A comparison of all NMR spectroscopic data was in full agreement with the previously synthesised[37] enantiomeric aldol adduct ***ent*-121**, where the absolute configuration at C13 was assigned *via* Mosher ester analysis.[81–83]

Further elaboration of aldol adduct **121** into aldehyde **105** was first explored with the route developed by MacGregor. Intermediate **121** was treated with $AlMe_3$ and MeN(H)OMe•HCl to cleave and recover the oxazolidinone auxiliary **110** (83% recovery) together with formation of Weinreb amide[43] **125** (93%) (**Scheme 16**). Here, it was crucial that the β-hydroxyl group was free to allow coordination of the Lewis acid to the proximal carbonyl alone instead of forming a

chelated complex between the two carbonyls, thus selectively activating it towards nucleophilic substitution. The hydroxyl group of Weinreb amide **125** was then later protected as a TES ether **126** (TESCl, imidazole) in good yield (94%). Intermediate **126** was reduced using DIBAL[44] (70%) to ensure that no over-reduction occurred. This reaction was found to be somewhat capricious as some degree of epimerisation at C12 was sometimes observed (20:1 to 6:1) in this work. Efforts to control the stoichiometry of DIBAL employed and to lower the reaction temperature were met with no improvement.

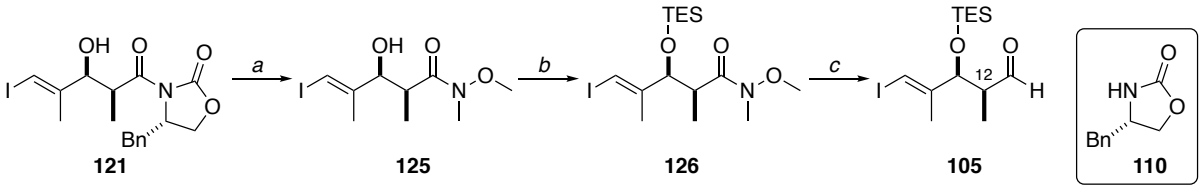

Reagents and conditions: (a) MeN(H)OMe•HCl, $AlMe_3$, THF, 0 °C → rt, *then* **121**, 0 °C → rt, 93%; (b) TESCl, imidazole, CH_2Cl_2, 94%; (c) DIBAL, PhMe, –78 °C → –30 °C, 70%

Scheme 16: First synthetic route towards aldehyde **105** from intermediate **121**

To overcome the problem associated with epimerisation of aldehyde **105**, an alternative synthetic pathway was proposed (**Scheme 17**). In this sequence, aldol adduct **121** was first protected as the TES ether **127** (TESCl, imidazole, 92%) and the product reduced to alcohol **128** with $LiBH_4$ (80%). The reduction step occurred predominantly at the imide carbonyl and not the oxazolidinone to allow for recovery of the auxiliary **110** (78%). Alcohol **129** was oxidised to aldehyde **105** by a Swern oxidation[39] cleanly in excellent yield (99%) without any loss of stereochemical purity. In addition to an improvement in yield (61% and 73% over three steps respectively), the latter was preferred because it was essential to deliver aldehyde **105** as a single stereoisomer for the subsequent boron-mediated aldol reaction.

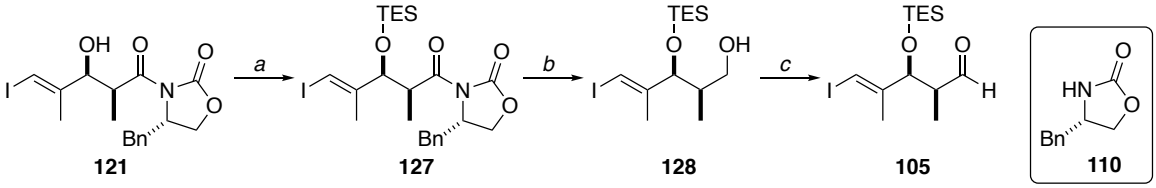

Reagents and conditions; (a) TESCl, imidazole, CH_2Cl_2, 92%; (b) $LiBH_4$, Et_2O, –78 °C → 0 °C, 80%; (c) $(COCl)_2$, DMSO, Et_3N, CH_2Cl_2, –78 °C → –20 °C, 99%

Scheme 17: Alternative synthetic route towards aldehyde **105** from intermediate **121**

Before moving on to examining the next step, it is worth highlighting that while the Evans aldol reaction delivered intermediate **121** in good yield and *d.r.*, the success of the reaction was inextricably dependent on the quality of Bu_2BOTf used. As such, an alternative protocol

developed by Crimmins was investigated as an alternative for this reaction.[84] The original conditions employed by Crimmins require the use of $TiCl_4$ and two equivalents of (–)-sparteine, where the amine is functioning as both a base and a ligand for titanium. However, this protocol was restricted to chiral auxiliaries containing oxazolidinethiones and thiazolidinethiones. In addition, cost considerations due to (–)-sparteine have limited the utility of this protocol. Further work by Crimmins showed that a mixture of DIPEA and NMP was an effective substitute for (–)-sparteine in their capacity as a base and ligand respectively.[85] This improved protocol also expanded its substrate scope to include oxazolidinones. Crimmins reported a range of aldehydes that engaged successfully with propionyl-oxazolidinone **45** with mostly excellent yields and *d.r.* (**Scheme 18**).[85]

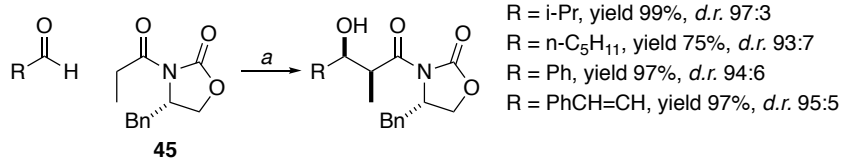

Reagents and conditions; (a) **45**, $TiCl_4$, DIPEA, NMP, CH_2Cl_2, 0 °C, *then* RCHO, various yields

Scheme 18: Examples of Evans aldol reactions performed by Crimmins with the modified protocol

Applying these conditions to substrates **107** and **45** gave aldol adduct **121** with an improved yield of 88% but poorer stereoselectivity of *d.r.* 10:1 (**Scheme 19**). Unlike the Evans conditions, an appreciable quantity of the diastereomer **124** was detected in the crude product. While **121** and **124** were initially inseparable, they were readily separated following protection as their TES ethers (TESCl, imidazole). It was critical that clean separation was achieved at this stage, or else **128** and ***ent*-128** would be obtained upon reductive cleavage of the auxiliary ($LiBH_4$), thus eroding the *e.e.* of **128**.

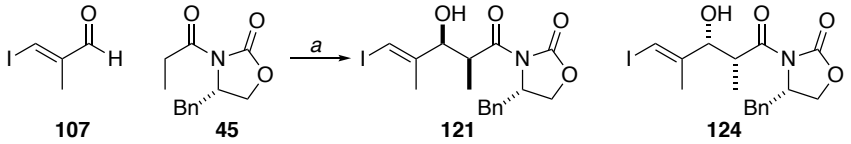

Reagents and conditions; (a) **45**, $TiCl_4$, DIPEA, NMP, CH_2Cl_2, 0 °C, *then* **107**, 88% (*d.r.* 10:1)

Scheme 19: Evans aldol reaction of **107** and **45** to form aldol adduct **121** with Crimmins' conditions

Arguments for rationalising the selective (*Z*)-enolisation of **45** with $TiCl_4$ to form titanium enolate **129** are analogous to the case with Bu_2BOTf. The proposed transition states that account for the Crimmins reaction also bear resemblance to the Evans ones (**Scheme 20**). In the preferred transition state **TS-V**, NMP has coordinated to titanium. This allows the auxiliary to adopt a conformation that opposes the enolate C–O dipole and minimises steric clash by placing the bulky benzyl group out of the chair. The formation of the unwanted isomer **124** can be attributed

to a competing transition state **TS-VI** where the auxiliary binds to the titanium metal. This represents a failure of NMP to completely coordinate to titanium.

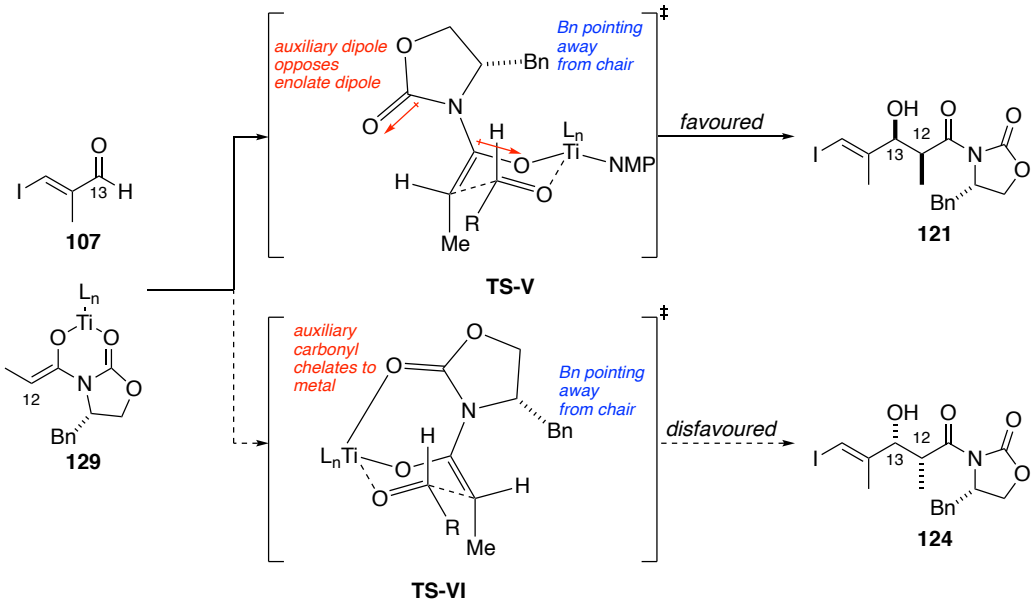

Scheme 20: Diastereoselective transition states for the aldol reaction of **107** and **129** under Crimmins' conditions

2.2.3 Synthesis of the C7-C15 Stereohexad

Following standard group protocols, the ethyl ketone **106** was readily synthesised from commercially available Roche ester **(*R*)-40** in three steps (**Scheme 21**) as precedented in our work for aplyronine A.[73] The hydroxyl group of Roche ester **(*R*)-40** was protected with PMBTCA under acid catalysis to afford PMB ether **130** in 85% yield. Ester **130** was transformed into Weinreb amide **131** under standard conditions (MeON(H)Me•HCl, i-PrMgCl, 88%) and the product was reacted with EtMgBr to afford ethyl ketone **106** in 94% yield.

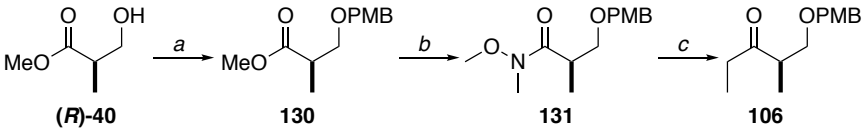

Reagents and conditions: (a) PMBTCA, PPTS, CH_2Cl_2, 0 °C → rt, 85%; (b) MeN(H)OMe•HCl, i-PrMgCl, THF, –20 °C, 88%; (c) EtMgBr, Et_2O, –78 °C → –10 °C, 94%

Scheme 21: Synthesis of ethyl ketone **106** from (*R*)-Roche ester **(*R*)-40**

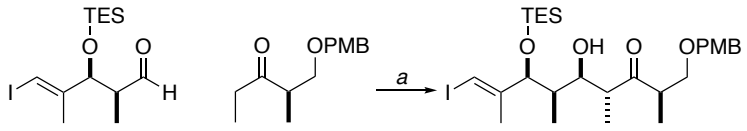

Reagents and conditions: (a) **106**, Cy_2BCl, Et_3N, Et_2O, 0 °C, *then* **105**, –78 °C → –20 °C, 70% (*d.r.* >20:1)

Scheme 22: Boron-mediated aldol reaction of **105** and **106** to form aldol adduct **132**

A boron-mediated aldol reaction (**Scheme 22**) between ketone **106** and aldehyde **105** could now be carried out. This would require the generation of the (*E*)-enolate of ketone **106** which could be achieved by using Cy_2BCl and Et_3N. By binding to either of the carbonyl lone pairs in ketone **106**, two competing transition states, **TS-VII** and **TS-VIII**, may arise (**Scheme 23**). It has been proposed by Goodman using molecular orbital calculations[86] that **TS-VIII** is favoured due to a minimisation of steric clash between the bulky boron groups and the large group of the ketone and activation of the acidic C–H proton by hydrogen-bonding from the Cl atom. Using a small base like Et_3N enables facile deprotonation despite the crowded reactive centre. The computational methods support the observation that (*E*)-enolate **134** is formed in excellent selectivity.

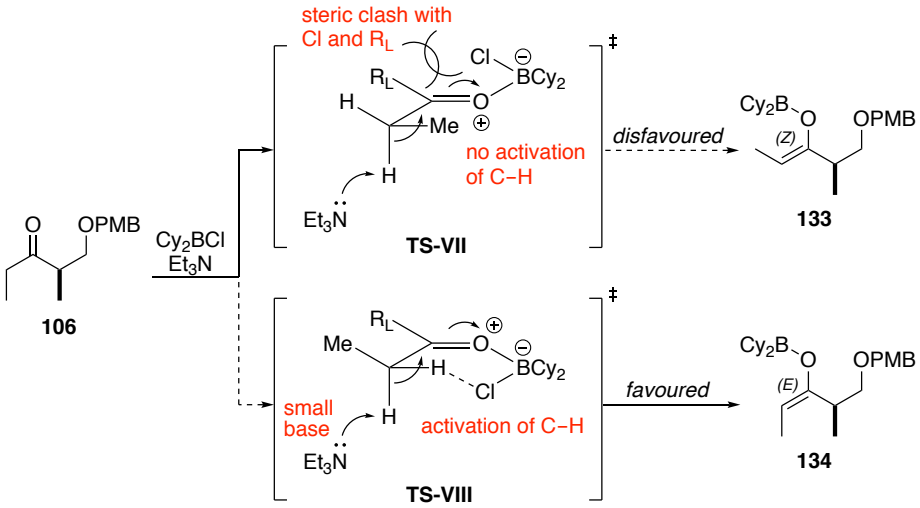

Scheme 23: Selective (*E*)-enolisation of ketone **106**

The six-membered transition state to account for the diastereoselectivity in the aldol reaction itself is calculated to be boat-like in conformation, allowing for a stabilising formyl hydrogen bond interaction between the electron rich oxygen atom of the PMB ether and the activated aldehyde formyl proton in the axial position (**Scheme 24**).[46] The preferred transition state for the reaction is that which minimises allylic ($A_{1,3}$) strain along C8-C10 as well as observing Felkin–Anh control from the α-chiral aldehyde.[87] In this case, the Felkin product also minimises *syn*-pentane interactions[88] along C10-C12 and **TS-IX** is therefore fully matched. In practice, reaction

of ketone **106** and aldehyde **105** led to aldol adduct **132** as the major product featuring a 1,2-*anti*-1,4-*syn* relationship in high diastereoselectivty (>20:1) and in good yield (70%) (**Scheme 24**).

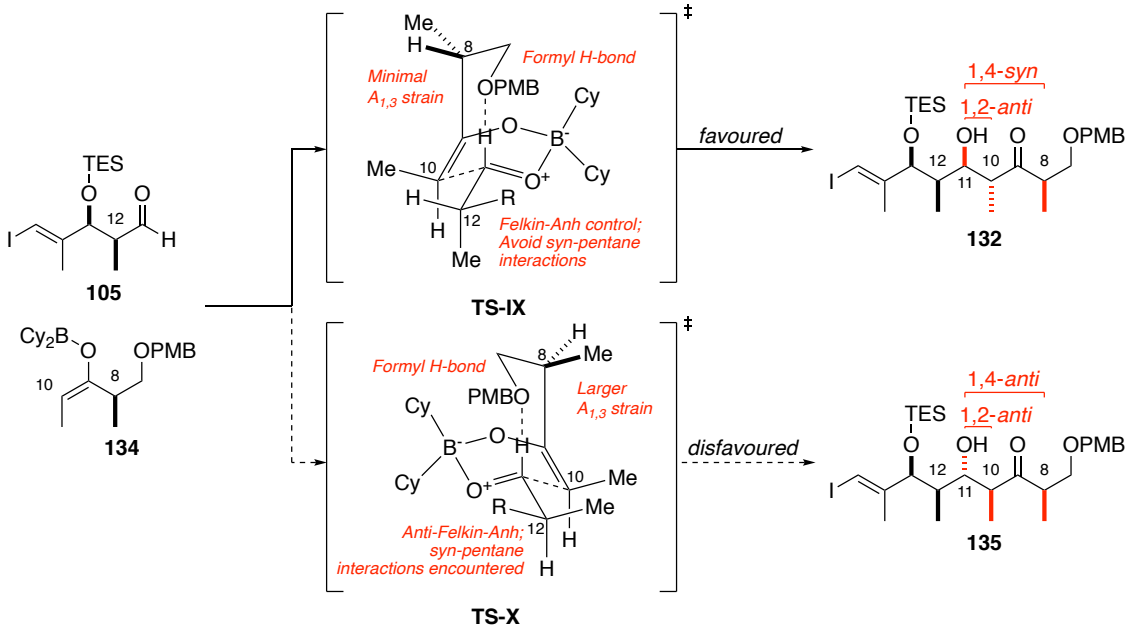

Scheme 24: Diastereomeric transition states for the aldol reaction of **105** and **134**

As before, the relative stereochemistry between C10 and C11 in aldol product **132** was confirmed by inspection of the vicinal coupling constant in the ^{1}H NMR spectrum.[80] In this instance, the large $^{3}J_{10,11}$ value of 9 Hz confirmed the 1,2-*anti* relationship. All spectroscopic data was in full agreement with the data previously reported by MacGregor[37] of the enantiomeric aldol adduct ***ent*-132** where the absolute configuration at C11 was assigned by Mosher ester analysis,[81–83] thus confirming the expected stereochemistry of **132** as drawn.

Next, the hydroxyl group of aldol product **132** was protected as the TES ether **136** with TESOTf and 2,6-lutidine in good yield (82%) (**Scheme 25**). To install the final stereocentre in the stereohexad, the ketone moiety at C9 of intermediate **136** was reduced with DIBAL at low temperature (–40 °C) to give the (9*S*) configuration of alcohol **137** (80%). Pleasingly, this reduction occurred with high diastereoselectivity (*d.r.* >20:1).

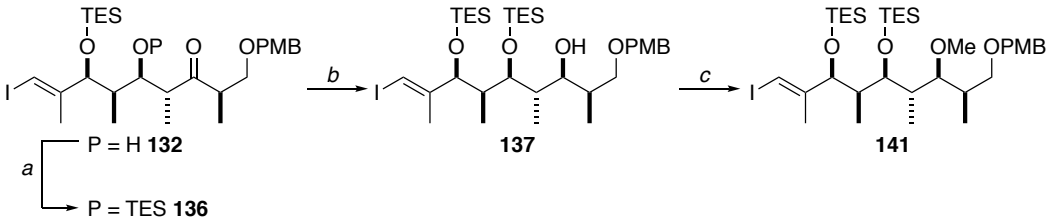

Reagents and conditions: (a) TESOTf, 2,6-lutidine, CH_2Cl_2, –78 °C, 91%; (b) DIBAL, CH_2Cl_2, –78 °C → –40 °C, 84% (*d.r.* >20:1); (c) Me_3OBF_4, Proton Sponge®, 4Å MS, CH_2Cl_2, rt, 71%.

Scheme 25: Synthesis of methyl ether **141** from aldol adduct **132**

The high level of diastereoselectivity of the reduction of ketone **136** was proposed to proceed *via* a chelated transition state (**Scheme 26**).[89] Hydride delivery would occur by axial attack going through a chair-like transition state rather than a twist-boat-like one. **TS-XI** is the lower energy transition state by avoiding steric hindrance from the methyl group and the incoming nucleophile, leading to alcohol **137** as the product rather than **138**.

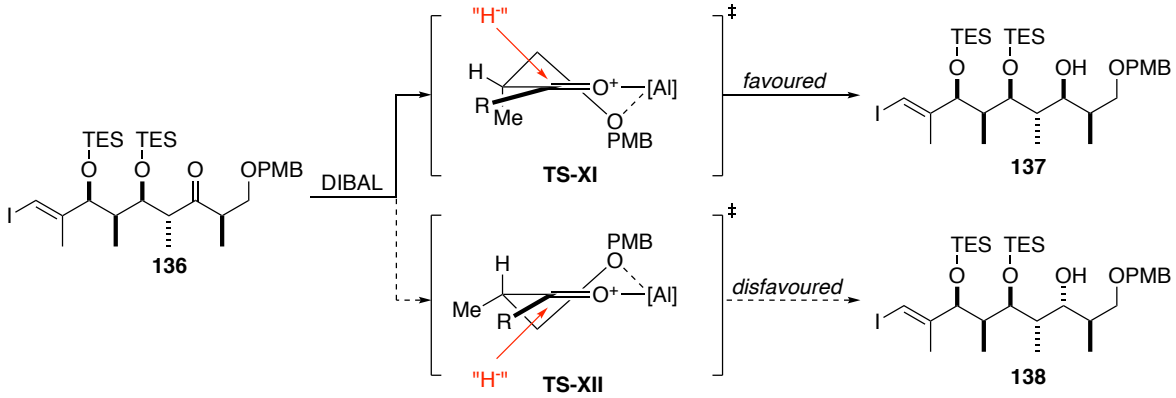

Scheme 26: Diastereomeric transition states for the reduction of **136**

To confirm the stereochemical outcome of the reduction step, both (*S*) and (*R*)-MTPA ester derivatives **139** and **140** were prepared from the corresponding MTPA acids under Steglich conditions (DCC, DMAP) (**Scheme 27**).[90]

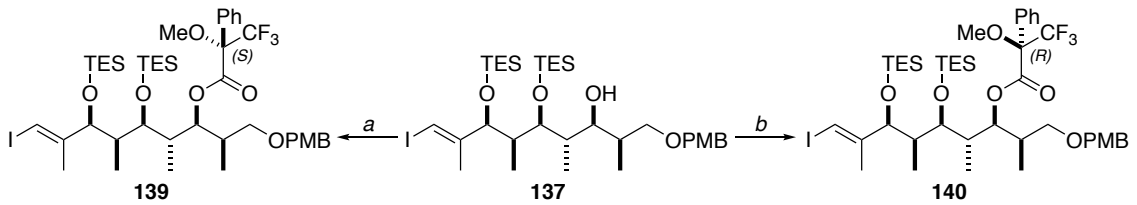

Reagents and conditions: (a) (*S*)-MTPA, DCC, DMAP, CH_2Cl_2, rt, 60%; (b) (*R*)-MTPA, DCC, DMAP, CH_2Cl_2, rt, 84%

Scheme 27: Formation of (*R*) and (*S*) MTPA esters **139** and **140**

MTPA derivatives of secondary alcohols adopt a preferred conformation in which the carbinyl proton, MTPA ester carbonyl and MTPA trifluoromethyl group lie in the same plane (**Figure 24(a)**). As a result, the protons of the (*R*)-MTPA ester that lie on the same side of the plane as the phenyl group (H_a, H_b, H_c) are diamagnetically shielded, resulting in upfield chemical shifts relative to the same proton signals in the corresponding (*S*)-MTPA ester (H_a, H_b, H_c), which are on the same side of the plane as the methoxy group. Thus, unambiguous assignments of proton signals with $\Delta\delta > 0$ ($\Delta\delta = \delta_S - \delta_R$) belong to protons on the right-hand side of the MTPA plane from the perspective of the MTPA trifluromethyl group (**Figure 24(b)**); by contrast, protons with $\Delta\delta < 0$ belong to protons on the left-hand side of the plane.[81–83] Following this model, the configuration at C9 was unambiguously determined to be (9*S*).

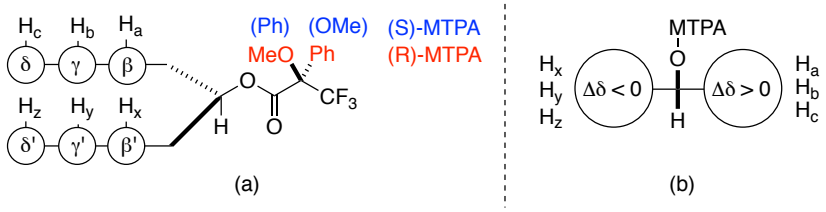

Figure 24: Mosher ester analysis

Proton	δ_H (*S*)-MTPA **139**	δ_H (*R*)-MTPA **140**	$\Delta\delta = \delta_S - \delta_R$
H12	1.94	1.92	+0.02
Me12	0.81	0.76	+0.05
H11	3.65	3.61	+0.04
H10	2.20	2.18	+0.02
Me10	1.06	0.89	+0.17
H8	2.56	2.58	–0.02
Me8	0.82	0.85	–0.03
H7a	3.10	3.14	–0.04
H7b	3.07	3.14	–0.07
$ArCH_{2a}$	4.37	4.40	–0.03
$ArCH_{2b}$	4.34	4.35	–0.01

Table 2: List of chemical shifts in MTPA esters **139** and **140** for Mosher ester analysis of **137**

The planned intermediate **141** was completed by methylation of the newly formed hydroxyl group of alcohol **137** using Meerwein's salt (72%). The use of Proton Sponge® and activated ground 4Å MS was critical to the success of this reaction, otherwise TES ether cleavage was

observed (**Scheme 25**). This side reaction was also reported by MacGregor[37] during preliminary investigations into this transformation.

2.2.4 Synthesis of the C1-C15 Fragment *via* HWE Olefination

At this point, attention was turned towards synthesising the C1-C6 phosphonate **104** in preparation for the eventual HWE reaction.[47] Treating sorbic acid **54** with thionyl chloride in methanol furnished methyl sorbate **142** in essentially quantitative yield. The allylic carbon was then brominated with NBS in refluxing benzene (**Scheme 28**). The previously reported route towards **143** gave a low yield of 24% for this reaction so further investigations were carried out to optimise this step. The primary cause for the low yield was the presence of multiple by-products that could not be removed by chromatography. It was assumed that some of the by-products might be geometric isomers of **143**, but any attempt at isomerisation *via* conjugate addition-elimination (DMAP) or radical-assisted π-bond rotation (I_2) did not lead to any changes in the product composition. Other possible by-products include further bromination of **143** although this was not thoroughly examined. By quenching the reaction before the onset of by-product formation (2 h), the yield of **143** could be increased to 37% with the option for recovering unreacted methyl sorbate **142**. Although the bromination step gave a modest yield, the low cost of the starting material and reagents enabled multi-gram quantities of **143** to be routinely synthesised. Gratifyingly, the subsequent Arbuzov reaction[50] where bromide **143** was heated in excess triethyl phosphite gave phosphonate **104** in excellent yield (94%).

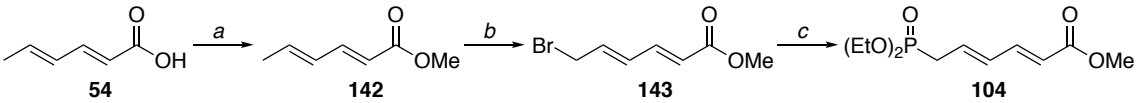

54 **142** **143** **104**

Reagents and conditions: $SOCl_2$, MeOH, reflux, 95%; (b) NBS, $(BzO)_2$, PhH, reflux, 37%; (c) $P(OEt)_3$, 120 °C, 94%

Scheme 28: Synthesis of phosphonate **104**

With the methyl ether **141** in hand, the stage was set to access a single enantiomer of the C1-C15 fragment **101**. This involved oxidative deprotection of the PMB ether to give primary alcohol **144** (DDQ, pH 7 buffer) and oxidation to aldehyde **103** (DMP)[46] in 99% yield. The crucial HWE olefination was conducted by treating aldehyde **103** with the lithium anion of phosphonate **104** to yield the full C1-C15 fragment **101** as single (*E*, *E*, *E*) geometric isomer in 65% yield (**Scheme 29**).

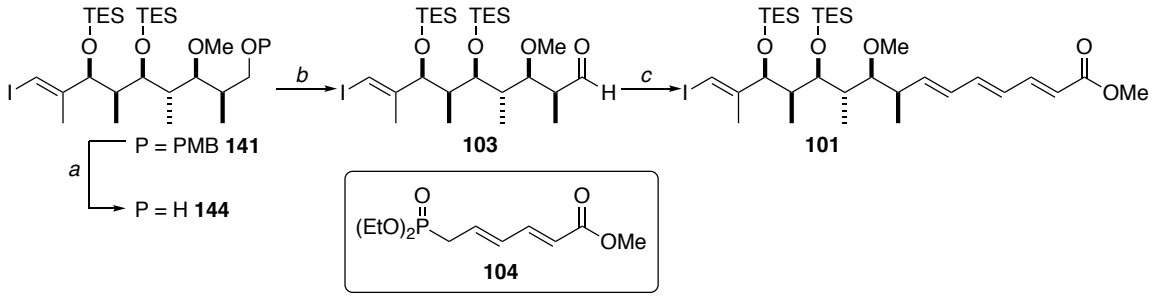

Reagents and conditions: (a) DDQ, pH 7 buffer, CH_2Cl_2, rt, 77%; (b) DMP, $NaHCO_3$, CH_2Cl_2, rt, 95%; (c) **104**, LDA, THF, –78 °C, *then* **103**, –78 °C, 70%

Scheme 29: The final three steps to the C1-C15 fragment **101**

The high selectivity for the (*E*) geometric isomer in the HWE olefination can be understood by examining the relative rates of the elementary steps in the reaction mechanism (**Figure 25**).[47] Initially, the phosphonate anion **145** forms either a *syn* or *anti* adduct with the aldehyde rapidly and reversibly, where $k_{syn} > k_{anti}$, thus **146** is the major intermediate. However, the subsequent cyclisation to give a four-membered oxaphosphatane is slower. In this case, $k_{trans} > k_{cis}$, so **147** smoothly transforms into **148** where its only fate is to collapse into the desired (*E*) product **101**. Any remaining intermediate **146** equilibrates back to **145** and **147** instead of undergoing cyclisation to **149** due to the slow kinetics of this step, hence delivering the desired product **101** instead of the (*Z*, *E*, *E*) olefin **150**.

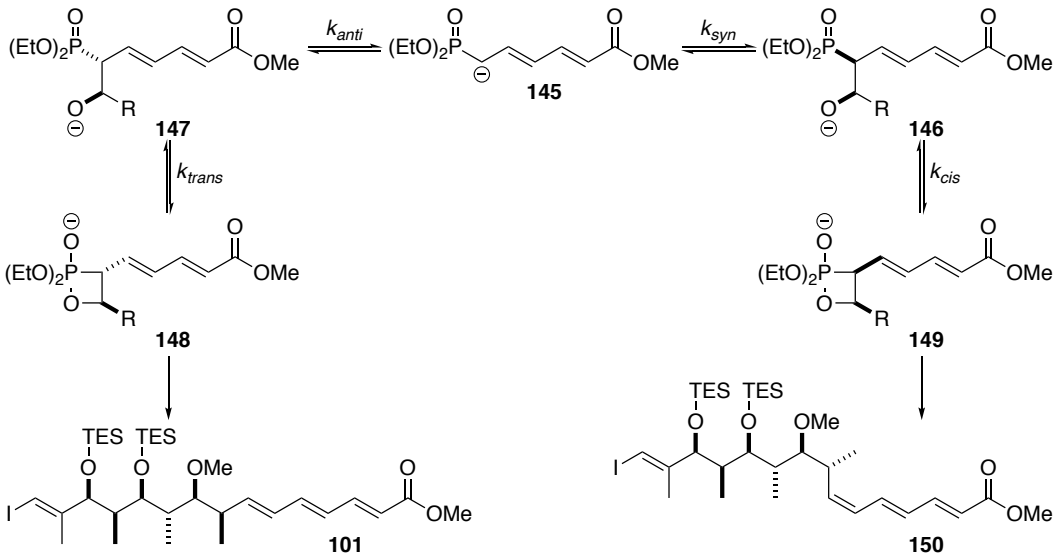

Figure 25: Mechanism of the HWE olefination

At this point, the synthesis of **101** has been achieved in 11 steps in the longest linear sequence with an overall yield of 11.3% (**Scheme 30)**. By using oxazolidinone ***ent*-45** (derived from L-phenylalanine) and ketone ***ent*-106** (derived from Roche ester **(*S*)-40**), the analogous route (**Scheme 31**) could be undertaken to deliver ***ent*-101** in 14.0 yield over 11 steps.

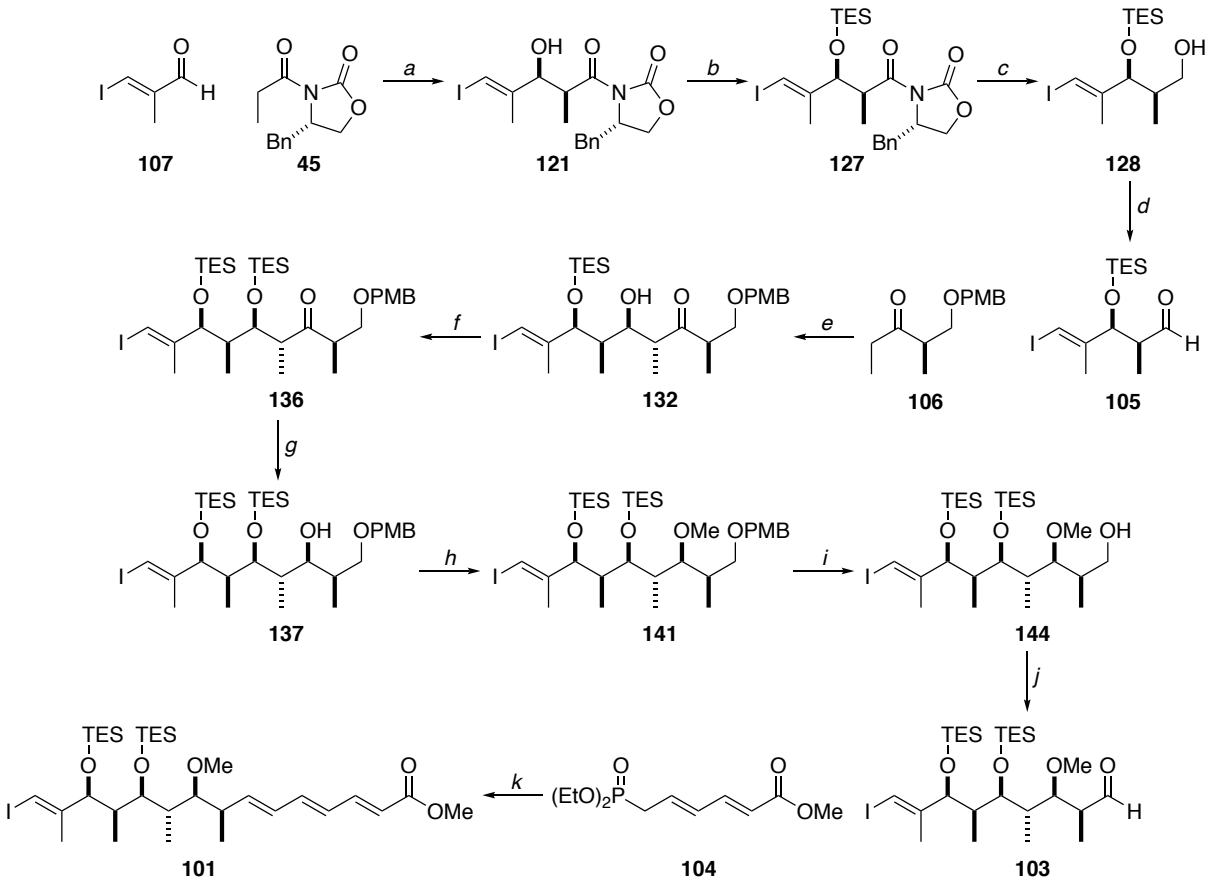

Reagents and conditions; (a) **45**, Bu_2BOTf, DIPEA, CH_2Cl_2, –78 °C → –10 °C, *then* **107**, –78 °C, 80% (*d.r.* >20:1); (b) TESCl, imidazole, CH_2Cl_2, 92%; (c) $LiBH_4$, Et_2O, –78 °C → 0 °C, 80%; (d) $(COCl)_2$, DMSO, Et_3N, CH_2Cl_2, –78 °C → –20 °C, 99%; (e) **106**, Cy_2BCl, Et_3N, Et_2O, –78 °C → 0 °C, *then* **105**, –78 °C, 70% (*d.r.* >20:1) ;(f) TESOTf, 2,6-lutidine, CH_2Cl_2, –78 °C, 91%; (g) DIBAL, CH_2Cl_2, –78 °C → –40 °C, 84% (*d.r.* >20:1); (h) Me_3OBF_4, Proton Sponge®, 4Å MS, CH_2Cl_2, rt, 71%; (i) DDQ, pH 7 buffer, CH_2Cl_2, rt, 77%; (j) DMP, $NaHCO_3$, CH_2Cl_2, rt, 95%; (k) **104**, LDA, THF, –78 °C, *then* **103** –78 °C, 70%.

Scheme 30: Synthesis of the C1-C15 fragment **101** from **45**, **107** and **106**

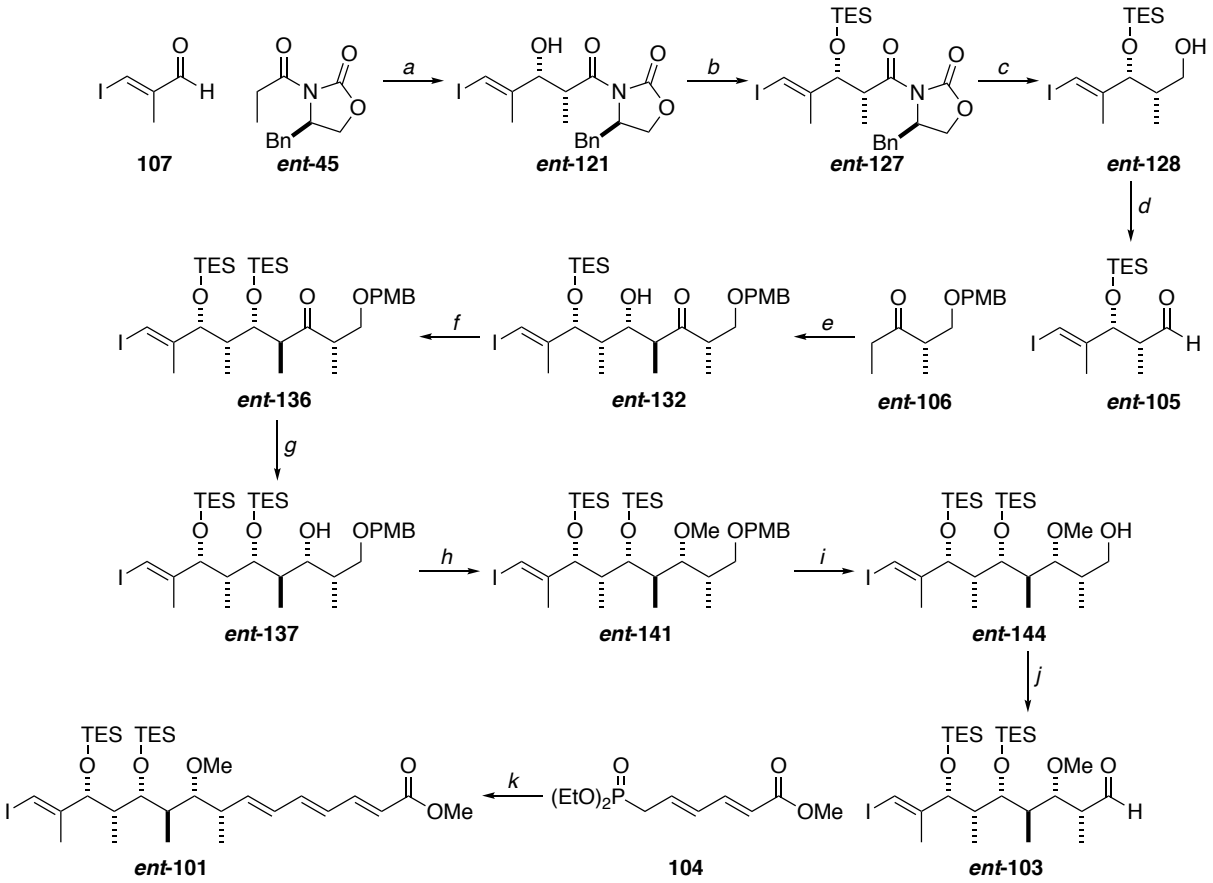

Reagents and conditions; (a) ***ent*-45**, Bu_2BOTf, DIPEA, CH_2Cl_2, –78 °C → –10 °C, *then* **107**, –78 °C, 79% (*d.r.* >20:1); (b) TESCl, imidazole, CH_2Cl_2, 97%; (c) $LiBH_4$, Et_2O, –78 °C → 0 °C, 82%; (d) $(COCl)_2$, DMSO, Et_3N, CH_2Cl_2, –78 °C → –20 °C, 95%; (e) ***ent*-106**, Cy_2BCl, Et_3N, Et_2O, –78 °C → 0 °C, *then* ***ent*-105**, –78 °C, 74% (*d.r.* >20:1) ;(f) TESOTf, 2,6-lutidine, CH_2Cl_2, –78 °C, 97%; (g) DIBAL, CH_2Cl_2, –78 °C → –40 °C, 82% (*d.r.* >20:1); (h) Me_3OBF_4, Proton Sponge®, 4Å MS, CH_2Cl_2, rt, 72%; (i) DDQ, pH 7 buffer, CH_2Cl_2, rt, 80%; (j) DMP, $NaHCO_3$, CH_2Cl_2, rt, 99%; (k) **104**, LDA, THF, –78 °C, *then* ***ent*-103** –78 °C, 70%

Scheme 31: Synthesis of the C1-C15 fragment ***ent*-102** from ***ent*-45**, **107** and ***ent*-106**

2.3 Synthesis of the C16-C28 Fragment 102

2.3.1 Retrosynthesis and Strategy

The proposed C16-C28 fragment **102** incorporates the α,β-dihydroxy-δ-lactone of hemicalide and terminates in a methyl ketone and vinyl iodide (**Scheme 32**). The methyl ketone functionality would be installed by a $Ba(OH)_2$-mediated HWE olefination[91] of a C25 aldehyde followed by conjugate reduction of the intermediate enone. The 1,2-diol functionality would be installed by a *syn*-dihydroxylation of the corresponding α,β-unsaturated lactone and would come from vinyl iodide **151**.

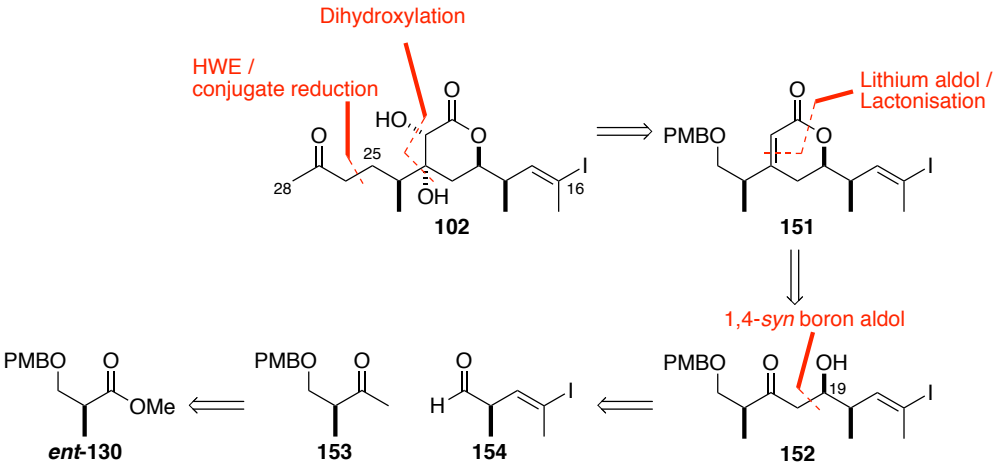

Scheme 32: Retrosynthetic analysis of the C16-C28 fragment **102**

The α,β-unsaturated lactone of intermediate **151** could be assembled by an aldol addition of **152** with ethyl acetate followed by dehydration. Using group methodology, a diastereoselective 1,4-*syn* aldol reaction between ketone **153** and aldehyde **154** could be used to install the correct configuration at C19 (**Scheme 32**). Both ketone **153** and aldehyde **154** can be obtained from the same enantiomer of Roche ester derivative ***ent*-130**.

2.3.2 Synthesis of the Aldol Adduct 152

Following MacGregor's work, the ester ***ent*-130** was reduced with $LiAlH_4$ to give the primary alcohol **155** (90%) which was oxidised to the aldehyde **156** under Swern conditions[39] ($(COCl)_2$, DMSO; Et_3N) (**Scheme 33**). To avoid the risk of racemisation of aldehyde **156** on storage, it was immediately submitted to the Corey–Fuchs reaction[92] (CBr_4, PPh_3) to obtain 1,1-dibromo olefin **157** in 77% yield over two steps. Treament of olefin **157** with n-BuLi to effect a Fristch–Buttenberg–Wiechell rearrangement followed by trapping with MeI afforded alkyne **158** (92%).[92]

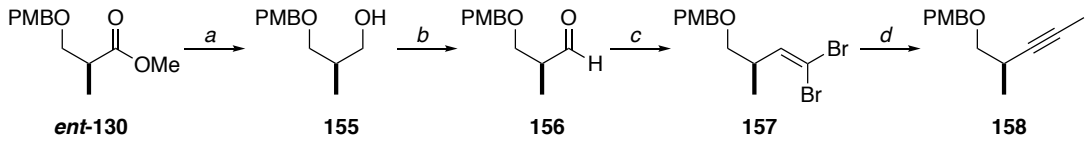

***ent*-130** **155** **156** **157** **158**

Reagents and conditions: (a) $LiAlH_4$, Et_2O, 0 °C → rt, 90%; (b) $(COCl)_2$, DMSO, Et_3N, CH_2Cl_2, –78 °C → –20 °C; (c) PPh_3, CBr_4, CH_2Cl_2, 0 °C, *then* **156**, –78 °C → 0 °C, 77% over two steps; (d) n-BuLi, THF, –78 °C; MeI, –78 °C, 92%

Scheme 33: Synthesis of alkyne **158** from ester ***ent*-130**

The regio- and stereocontrolled transformation of alkyne **158** into vinyl iodide **159** was achieved *via* hydrozirconation with *in situ* preparation of the Schwartz reagent ($Cp_2Zr(H)Cl$),[93] followed by trapping of the organozirconium species with I_2 in 78% yield (**Scheme 34**). While the Schwartz reagent is commercially available, it is known to be sensitive to light, air and moisture upon long-term storage so an *in situ* generation of this reagent is helpful in addressing these issues. Addition of the Schwartz reagent across the alkyne occurs in a *syn*-stereospecific fashion where the zirconium adds to the least hindered end of the alkyne to minimise steric interactions.[94] Using an excess (2 eq.) of the Schwartz reagent has been shown to improve the regioselectivity *via* a reversible second addition to both regioisomers which undergoes free bond rotation and β-hydride eliminates to form the major (*E*) regioisomer under thermodynamic control (**Figure 26**).[94]

The vinyl iodide **159** was converted into the sensitive aldehyde **154** by sequential DDQ-mediated PMB ether cleavage to give the alcohol **160** in 90% yield and oxidation with DMP[46] (**Scheme 34**). Aldehyde **154** was found to be very sensitive and best prepared fresh and used in the subsequent aldol reaction with minimal purification. As the vinyl iodide was suspected to contribute to the instability of aldehyde **154**, it was proposed as an alternative to employ alkyne **158** and install the vinyl iodide at a later stage. This was inspired by precedent from Nicolaou's synthesis of apoptolidin[95] for a late-stage hydroiodination of an advanced intermediate. Disappointingly, intermediates **161** and **162** proved to be extremely volatile and did not lead to any useful results.

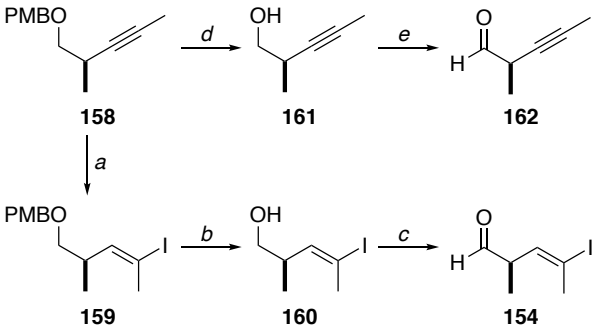

Reagents and conditions: (a) Cp_2ZrCl_2, DIBAL, THF, 0 °C, *then* **158**, 0 °C → rt, *then* I_2, –78 °C, 76%; (b) DDQ, pH 7 buffer, CH_2Cl_2, rt, 90%; (c) DMP, $NaHCO_3$, CH_2Cl_2, rt, 80%; (d) DDQ, pH 7 buffer, CH_2Cl_2, rt, 52%; (e) DMP, $NaHCO_3$, CH_2Cl_2, rt, yield N.C.

Scheme 34: Synthesis of aldehyde **154** from alkyne **158**

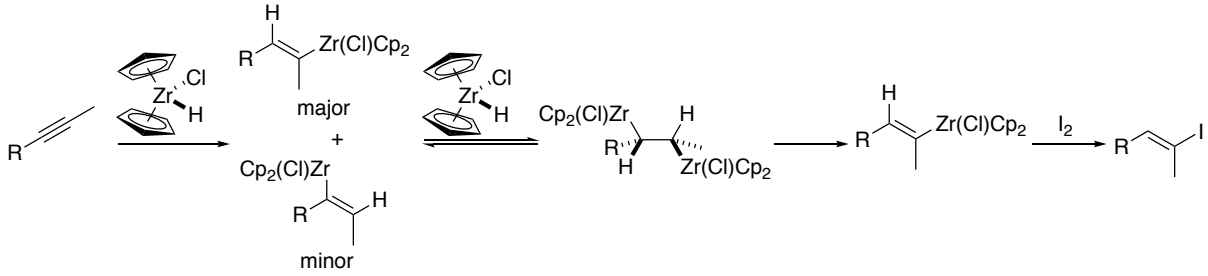

Figure 26: Mechanism of hydrozirconation of alkyne **158**

The 1,4-*syn* aldol reaction between the methyl ketone **153** and the aldehyde **154** afforded the aldol adduct **152** in 68% yield and with the same *d.r.* of 9:1 in the DMB ether series carried out by MacGregor[37] (**Scheme 35**). The initial choice of the DMB analogue of **153** was to facilitate a facile, late-stage deprotection due to concerns about the sensitivity of the vinyl iodide functional group. However, later work in the PMB ether series confirmed that these precautions were unfounded. In addition, the use of the methyl ketone **153** simplified production of this intermediate as it could be obtained from a common intermediate in the C1-C15 fragment, Weinreb amide ***ent*-131**, by reacting with MeMgBr (92%).

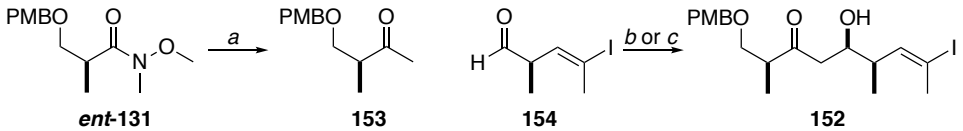

Reagents and conditions: (a) MeMgBr, –78 °C → –10 °C, Et_2O, 92%; (b) **153**, Cy_2BCl, Et_3N, Et_2O, 0 °C, *then* **154**, –78 °C → –20 °C, 68% (*d.r.* 9:1); (c) **153**, (–)-DIPCl, Et_3N, Et_2O, 0 °C, *then* **154**, –78 °C → –20 °C, 64% (*d.r.* >20:1)

Scheme 35: Boron-mediated aldol reaction of **153** and **154** to form aldol adduct **152**

Compared to the analogous aldol reaction using **106**, the use of a methyl ketone instead of an ethyl ketone has led to an erosion of *d.r.* in the product. As with aldol adduct **132**, the six-membered transition state invoked in the aldol reaction of enolate **163** and aldehyde **154** is thought to be boat-like in conformation, allowing for a stabilizing formyl hydrogen bond interaction between the electron rich oxygen atom of the PMB ether and the activated aldehyde formyl proton in the axial position (**Scheme 36**).[72] Two competing transition states, **TS-XIII** and **TS-XIV**, can arise but their difference in energy is significantly reduced as they have similar amounts of allylic strain along C20-C24 due to C20 only bearing H atoms. The absence of a Me group at C20 also precludes *syn*-pentane interactions as a stereocontrol element. Moderate diastereoselectivity may be imparted by Felkin–Anh control from the α-chiral aldehyde, leading to aldol adduct **152** as the major product (**Scheme 36**).[87]

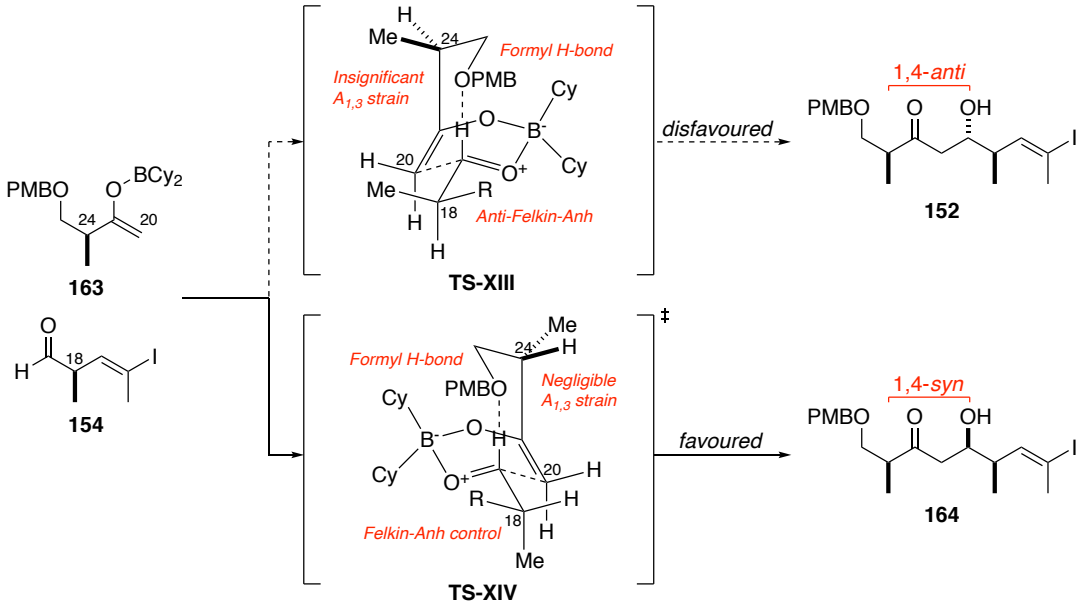

Scheme 36: Diastereomeric transition states for the aldol reaction of **154** and **163**

In light of the moderate level of stereocontrol, the use of chiral (–)-Ipc ligands to further reinforce the diastereoselectivity was explored in order to improve the *d.r.* of the aldol reaction. This has been precedented in our group's synthesis of the chivosazoles.[96] Gratifyingly, this change in conditions to enolisation with (–)-DIPCl and Et_3N delivered aldol adduct **152** as a single diastereomer with only a slight decrease in yield (**Scheme 35**).

These results reflect the steric influence of the chiral (–)-Ipc ligands in the aldol reaction as analysed by DFT calculations.[97] For **TS-XV**, the axial ligand has a Me group that clashes with the highly ordered boat transition state but points away in the preferred transition state **TS-XVI**.

Together with the Felkin–Anh control[87] discussed earlier, the pathway leading to major product **152** is now significantly lower in energy than the alternative (**Scheme 37**).

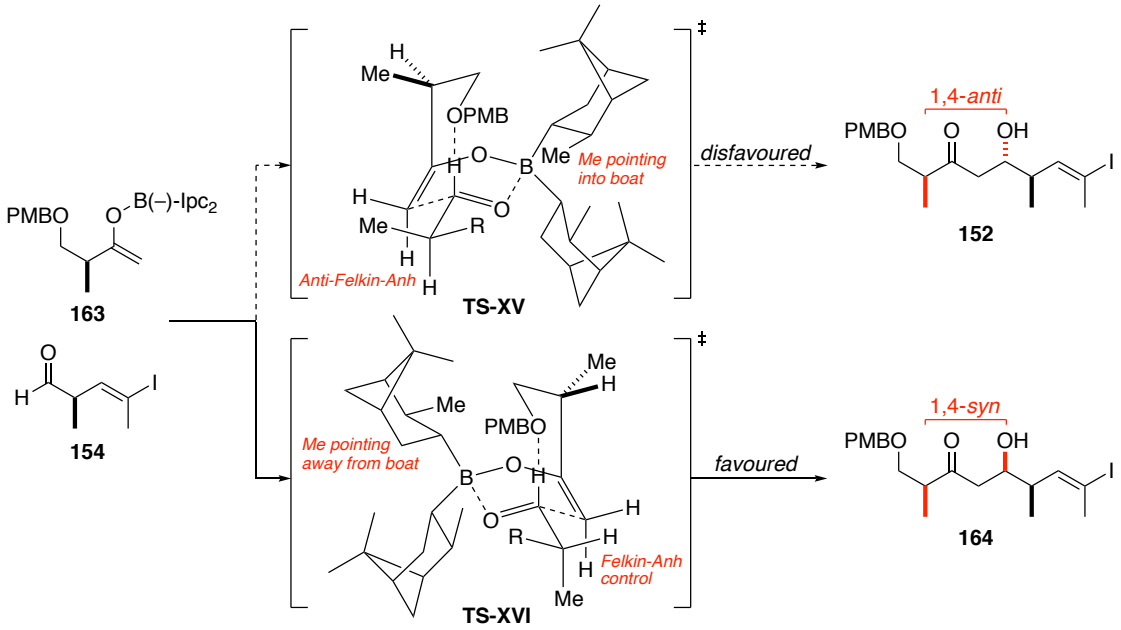

Scheme 37: Diastereomeric transition states for the aldol reaction of **154** and **163** with chiral ligands

The absolute configuration of the aldol adduct **152** was confirmed by Mosher ester analysis.[81–83] Both (*S*) and (*R*)-MTPA ester derivatives **165** and **166** were prepared from the corresponding MTPA acids under Steglich conditions (DCC, DMAP) (**Scheme 38**).[90] Despite being unable to fully assign the proton signals in MTPA ester **165**, there were sufficient signals on both sides of the carbinyl proton to allow for the anticipated (19*R*) assignment (**Table 3**).

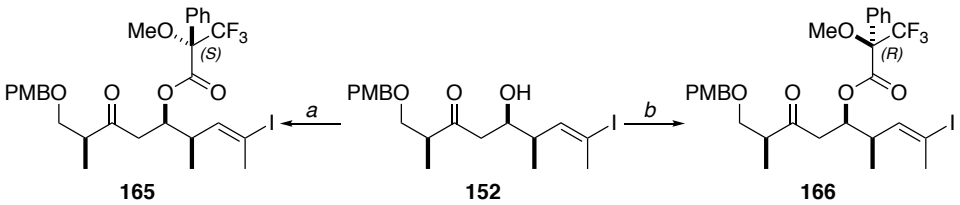

Reagents and conditions: (a) (*S*)-MTPA, DCC, DMAP, CH_2Cl_2, rt, 63%; (e) (*R*)-MTPA, DCC, DMAP, CH_2Cl_2, rt, 76%

Scheme 38: Formation of (*S*)- and (*R*)-MTPA esters **165** and **166**

Proton	δ_H (*S*)-MTPA **165**	δ_H (*R*)-MTPA **166**	$\Delta\delta = \delta_S - \delta_R$
H25a	3.55	3.49	+0.06
H25b	3.46	3.41	+0.05
H24	N.A.[a]	2.88	N.A.
Me24	0.99	0.94	+0.05
H20a	N.A.[a]	2.85	N.A.
H20b	N.A.[a]	2.75	N.A.
H18	N.A.[a]	2.76	N.A.
Me18	0.87	0.92	–0.05
H17	5.87	5.98	–0.11
Me16	2.32	2.40	–0.08

[a] obscured in a 4H multiplet

Table 3: List of chemical shifts in MTPA esters **165** and **166** for Mosher ester analysis of **152**

2.3.3 Synthesis of Diol 174

The resulting aldol product **152** was protected as the TBS ether **167** in good yield (TBSOTf, 2.6-lutidine, 88%) and used in the subsequent acetate aldol reaction (**Scheme 39**). The ketone **167** was successfully reacted with the lithium enolate of ethyl acetate to afford aldol adduct **168** as a 5:1 mixture of inseparable diastereomers. Exposure of **168** to HF•py effected deprotection of the TBS ether and *in situ* lactonisation to give intermediate **169**. When working on a large scale, the use of HF•py could be substituted with TsOH in methanol. Lactone **169** remained an inseparable mixture of epimers in the same 5:1 ratio.

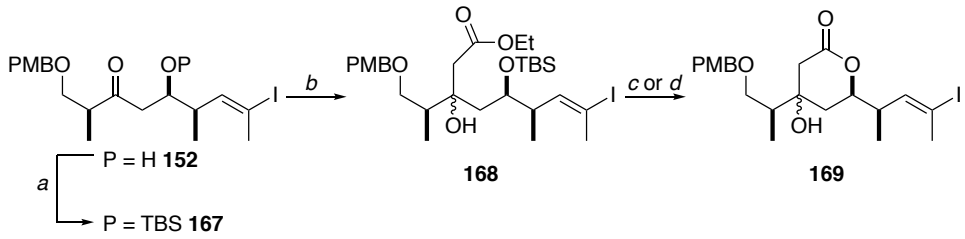

Reagents and conditions: (a) TBSOTf, 2,6-lutidine, CH_2Cl_2, –78 °C, 95%; (b) LDA, EtOAc, THF, –78 °C, *then* **167**, 97%; (c) HF•py, THF, 0 °C → rt, 85%; (d) TsOH, MeOH, rt, 83%

Scheme 39: Synthesis of lactone **169** from aldol adduct **152**

Although the two epimers of lactone **169** could not be cleanly separated, the minor isomer was isolated with sufficient purity to conduct nOe studies. Key correlations between Me24 and $H20_{ax}$ as well as $H22_{ax}$ indicate that the minor component is **169B** with a (21*S*) configuration.

Accordingly, the major epimer had to be **169A**. The major and minor epimers of aldol adduct **168** can therefore be assigned as **168A** and **168B** respectively. Further investigation into the stereoinduction was not pursued as the C21 stereocentre would be destroyed in the next step *via* a dehydration reaction. However, the configuration of C21 did in fact appear to have consequences for this step (*vide infra*).

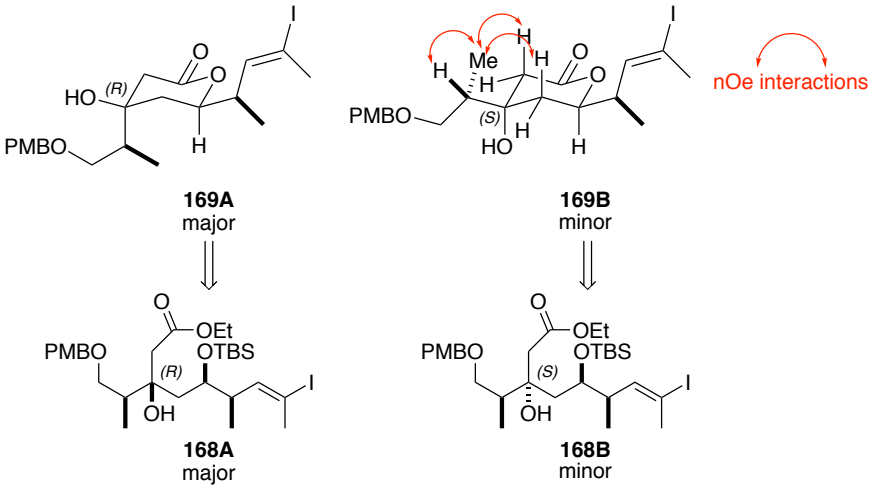

Figure 27: Identification of the major and minor epimers of **168** and **169**

In the event, the dehydration reaction was first carried out using conditions employed by MacGregor[37] (MsCl, Et_3N) (**Table 4, Entry 1**). However, the desired elimination product **151** was consistently obtained along with significant quantities of an inseparable product-like impurity. While the impurity could not be fully characterised, an inspection of its ^1H NMR spectrum suggested the presence of a tri-substituted olefin so **170** was proposed as the putative structure. Attempts to isomerise **170** to the desired product **151** with acid (TsOH, MeOH) or base (LDA) did not alter the ratio of **151** to **170**.

Various other dehydration conditions were examined in order to minimise the formation of this by-product. Turning to Ardisson's choice of $SOCl_2$ and pyridine[33] (**Entry 2**) did not lead to any improvement, nor did other conventional methods such as the Burgess reagent[98] (**Entries 3-5**). Pleasingly, mixing lactone **169** with Ac_2O and DMAP[99] (**Entry 6**) in refluxing benzene and pyridine led to clean formation of the α,β-unsaturated δ-lactone **151**.

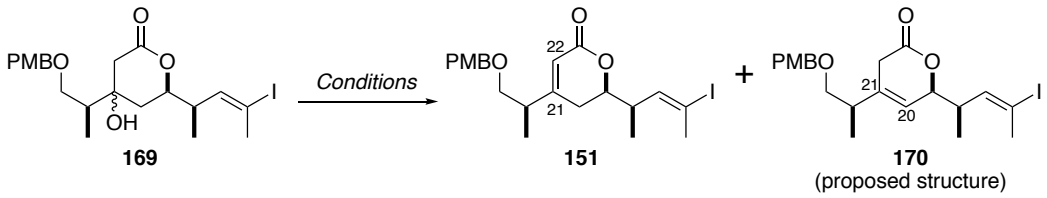

Entry	Conditions	Result
1	MsCl, Et_3N, CH_2Cl_2, 0 °C → rt, 5 h	83% yield, 5:1 **151**:**170**
2	$SOCl_2$, py, 0 °C → rt, 5 h	81% yield, 5:1 **151**:**170**
3	TsCl, py, CH_2Cl_2, rt → rt, 18 h	Recovered **169**
4	Burgess reagent, THF, rt, 2 h	Complex mixture
5	Ac_2O, DBU, CH_2Cl_2, rt, 5 h	Complex mixture
6	Ac_2O, DMAP, py/PhH, reflux, 16 h	88% yield, only **151**

Table 4: Conditions examined for the dehydration of **169** to **151**

Although the dehydration problem had been resolved, the origin of by-product **170** had yet to be understood. A similar impurity was also identified in the work of MacGregor[37] who worked with the DMB analogue of **169**. The combined results of this investigation and MacGregor's results suggested that the amount of impurity **170** in the dehydration reaction correlated positively with the *d.r.* of lactone **169**. A closer inspection of the supporting NMR spectra in Ardisson's work[33] once again revealed the presence of this evasive impurity. This is despite the fact that Ardisson's intermediate **171** was synthesised as a single diastereomer *via* a highly stereoselective Reformatsky reaction involving the chelated transition state **TS-XVII** (**Scheme 40**). The idea that the dehydration mechanism was stereospecific was thus ruled out with this finding.

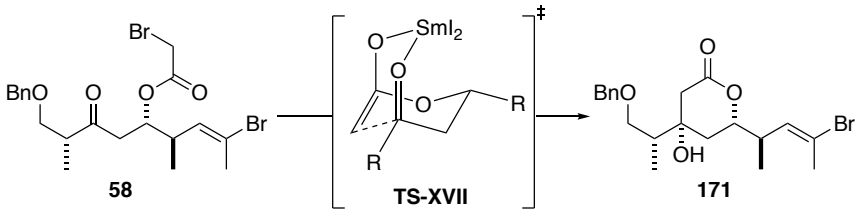

Reagents and conditions: (a) SmI_2, THF, –78 °C → rt, yield N.C.

Scheme 40: Synthesis of Ardisson's intermediate **171** *via* a Reformatksy reaction

Various modes of elimination were considered next to shed light on the reaction. Epimer **172**, with an axially positioned OR leaving group, is well set-up for an E2-like pathway (or $E1_{cb}$) with a greater preference for deprotonation at H22 than H20 due to its lower pK_a (**Figure 28**). This is also true for conformer **173A** of the corresponding epimer but not for conformer **173B** with an equatorial OR group. Instead, it reacts via an E1-like mechanism with less discrimination for H22

or H20, resulting in a mixture of products. In order to encourage an E2-like elimination instead of E1-like for both epimers, a poorer leaving group, such as OAc, would be better suited than an excellent one like OMs or OSO_2Cl.

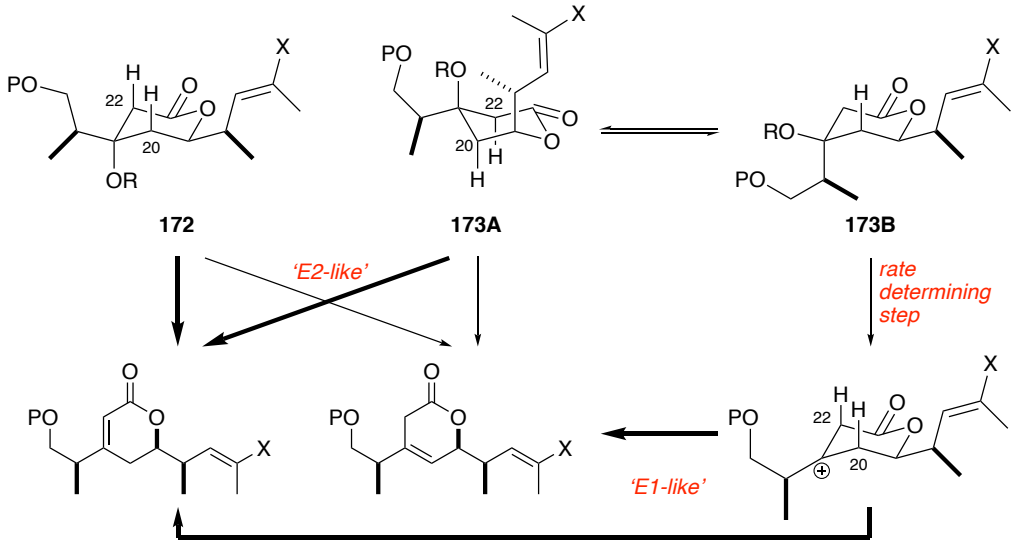

Figure 28: Proposed rationalisation of the stereochemical dependence of C21 for the dehydration

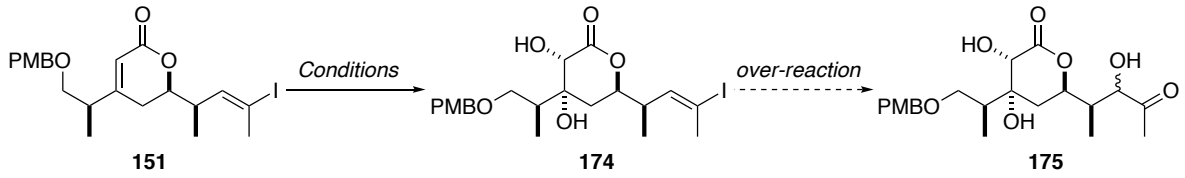

Entry	Conditions	Result
1	10 mol% K_2OsO_4•$2H_2O$, 6 eq. NMO, t-BuOH/H_2O/THF, 0 °C, variable times	25-50% **174**
2	5 mol% K_2OsO_4•$2H_2O$, 6 eq. NMO, 2 eq. citric acid, t-BuOH/H_2O/THF, 0 °C, 18 h	25% conversion
3	5 mol% K_2OsO_4•$2H_2O$, 1.2 eq. NMO, 2 eq. citric acid, t-BuOH/H_2O/THF, rt, 3 h	50% conversion
4	5 mol% K_2OsO_4•$2H_2O$, 1.2 eq. NMO, 2 eq. citric acid, t-BuOH/H_2O/THF, rt, 18 h	48% **174**, 34% **175**
5	2 mol% K_2OsO_4•$2H_2O$, 0.6 eq. NMO, 2 eq. citric acid, t-BuOH/H_2O/THF, rt, 5 h	55% **174**, 30% **151**
6	$KMnO_4$, Me_2CO/H_2O, 0 °C → rt, 5 h	Complex mixture
7	$KMnO_4$, TBAB, CH_2Cl_2/H_2O, 0 °C → rt, 5 h	Complex mixture

Table 5: Conditions examined for the dihydroxylation of **151** to **174**

With the pure α,β-unsaturated δ-lactone **151** at hand, the stage was set for a dihydroxylation to install the final two stereocentres in this fragment (**Table 5**). Under standard Upjohn conditions (K_2OsO_4•$2H_2O$, NMO), the desired diol **174** was obtained along with significant amounts of triol **175**. This result was also reported by MacGregor.[37] Clearly, the conjugated alkene has similar

electronic properties with the vinyl iodide, thus compromising the chemoselectivity. In contrast, Ardisson did not observe this problem with a vinyl bromide as it is more electron deficient than the lactone alkene.[33]

Modifications to the Upjohn conditions were explored to improve on the existing results. Sharpless found that the use of citric acid as an additive can greatly accelerate the dihydroxylation of electron deficient alkenes and improve their yield.[68] Initially, it appeared that adding citric acid to the reaction at 0 °C offered no improvement (**Table 5, Entry 2**) but repeating the reaction at room temperature enabled us to reproduce the maximum conversion of 50% in a shorter time while using less osmium and NMO (**Entry 3**). Citric acid did not entirely solve the chemoselectivity problem as complete consumption of NMO still led to significant quantites of triol **175** (**Entry 4**). By employing a substoichiometric amount of NMO (**Entry 5**), diol **174** could be reliably obtained in 55% yield while the starting material **151** could also be recovered and resubmitted twice more to increase the throughput of the reaction. This result could also be reproduced on a gram scale.

Mechanistically, dihydroxylation begins with a [3+2] cycloaddition of OsO_4 with the olefin to form an osmate ester **176** (**Figure 29**). Under homogenous Upjohn conditions, oxidation of this Os(VI) complex outcompetes hydrolysis, thus interrupting the first catalytic cycle and shunting the process towards a second catalytic cycle via intermediates **177** and **178**.[68] A deleterious pathway deactivates the catalyst in the form of dianion **180**, arising from deprotonation of *bis*-osmate ester **179**. This 18-electron complex is remarkably stable and resistant to hydrolysis, thus inhibiting product release and lowering catalyst turnover. Electron withdrawing groups on the substrate lower the pKa of complex **179**, making it more susceptible to deprotonation even in the presence of a weak base such as *N*-methylmorpholine, the by-product of NMO re-oxidation. Acidic conditions thus suppress this unwanted side reaction and maintain the turnover of the catalyst.[68]

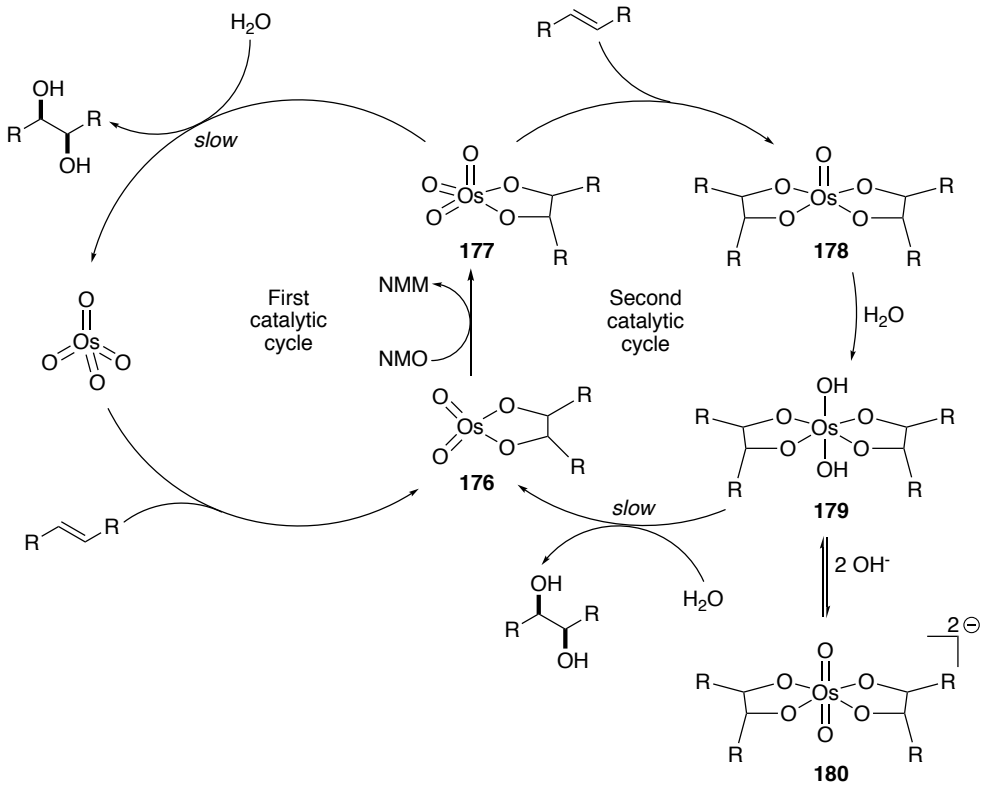

Figure 29: Mechanism of dihydroxylation under homogenous Upjohn conditions

In addition to its role as an acid buffer, citric acid can also chelate to osmium. In particular, this protects Os(VI) complexes from disproportionation to Os(VIII) and insoluble Os(IV) species which can occur under acidic conditions. The free carboxylic acids on the citrate also create a hydrophilic environment around osmium which accelerates the rate limiting hydrolysis of the osmate ester **182**, thus avoiding the undesired secondary cycle. Under these conditions, the catalytic cycle can be further simplified (**Figure 30**).[68]

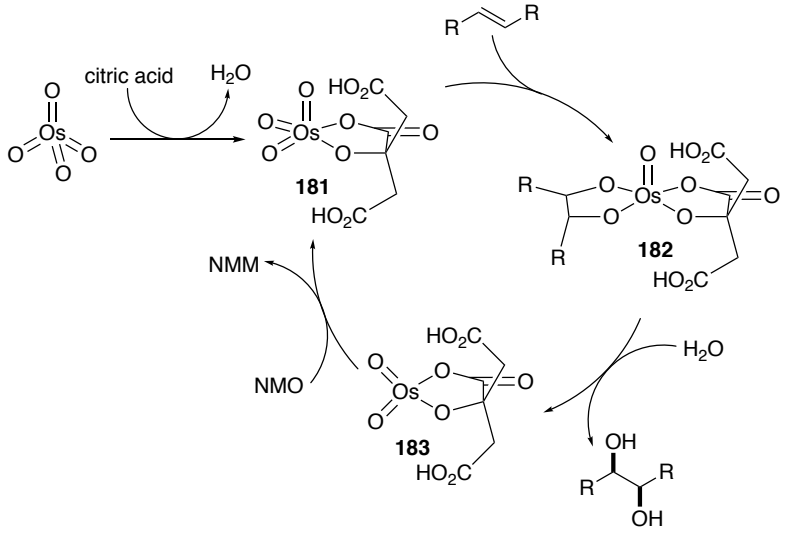

Figure 30: Revised mechanism of dihydroxylation with citric acid additives

Other attempts at addressing the chemoselectivity issue included exploring reagents that were selective for electron deficient olefins. $KMnO_4$ was identified as a suitable reagent due to its nucleophilic character. There have been several examples[100] in the literature that demonstrate the chemoselective nature of $KMnO_4$ and may even have marked improvement in yield compared to OsO_4 (**Scheme 41**). Unfortunately, the use of $KMnO_4$ with enoate **151** led to complex mixtures (**Table 5, Entries 6-7**).

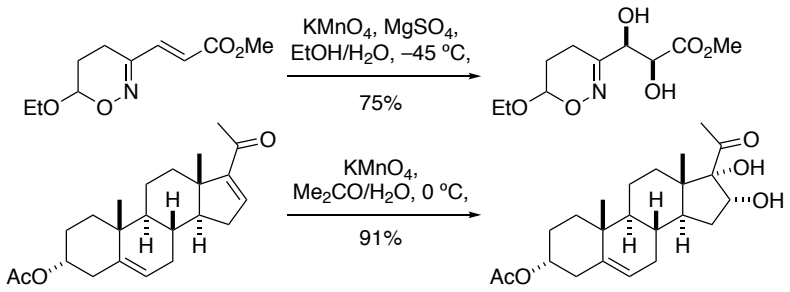

Scheme 41: Examples of permanganate-mediated dihydroxylations showing chemoselectivity for electron deficient olefins

An alternative route for achieving enhanced chemoselectivity was to deprotect the PMB group (DDQ) and use the free OH group in **151** to direct the osmium reagent to the nearest olefin. Disappointingly, this approach did not lead to any improved selectivity for the lactone alkene over the vinyl iodide (**Scheme 42**).

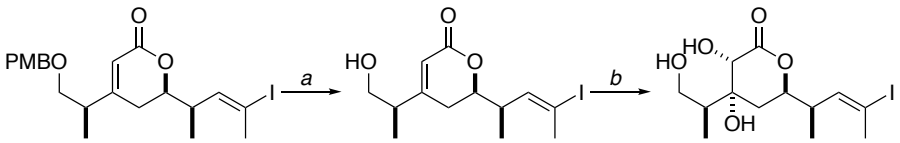

151 **184** **185**

Reagents and conditions: (a) DDQ, pH 7 buffer, CH_2Cl_2, rt, 85%; (b) $K_2OsO_4 \bullet 2H_2O$, NMO, citric acid, THF, rt, 30%

Scheme 42: Exploring the possibility of a hydroxyl-directed dihydroxylation of **151**

The π-face selectivity of the Upjohn dihydroxylation was accounted for with a model developed by Datta (**Figure 31(a)**).[101] The lactone ring adopts a half-chair conformation **186** where the C15-C18 sidechain shields the top face, hence favouring approach of the osmium reagent from below the ring. As the olefin has (*E*)-geometry, and hence two low energy conformers, the Houk model[102] predicts that the allylic chiral centre at C24 does not exert any significant stereocontrol for the dihydroxylation.[103] Through nOe studies, the relative configuration of C21 and C22 was established as *syn* in accordance with the predictions (**Figure 31(b)**)

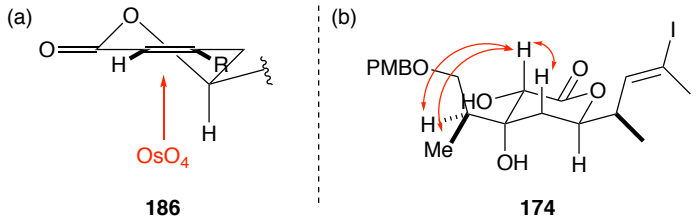

Figure 31: Stereochemical rationalisation and proof of diol **174**

With all the requisite stereocentres installed for this fragment, greater attention was paid to the H19 resonance henceforth as this was one of the key signals used by Ardisson in their stereochemical assignment of this fragment. For example, H19 was observed to display a ddd splitting pattern (J = 11.5, 6.6, 3.7 Hz) in diol **174** that is more similar to natural hemicalide[1] **1** (J = 11.3, 7.5, 3.5 Hz) than Ardisson's proposed fragment **33B** (J = 13.2, 6.1, 3.9 Hz).[33] This result was also consistent for all downstream intermediates, lending further support for the proposed reassignment of the 18,19-*anti* relationship by Ardisson-Cossy to 18,19-*syn* (*vide infra*).

2.3.4 Completion of the C16-C28 Fragment

To complete the C16-C28 fragment synthesis (**Scheme 43**) diol **174** was protected as a *bis*-TES ether **187** (TESOTf, imidazole) and the PMB group removed under mild oxidative conditions (DDQ). Alcohol **188** was then subjected to a Dess–Martin oxidation[46] to prepare aldehyde **189** and used immediately in a HWE reaction[91] with β-ketophosphonate **190** using $Ba(OH)_2$ to minimise the risk of epimerisation at C24.

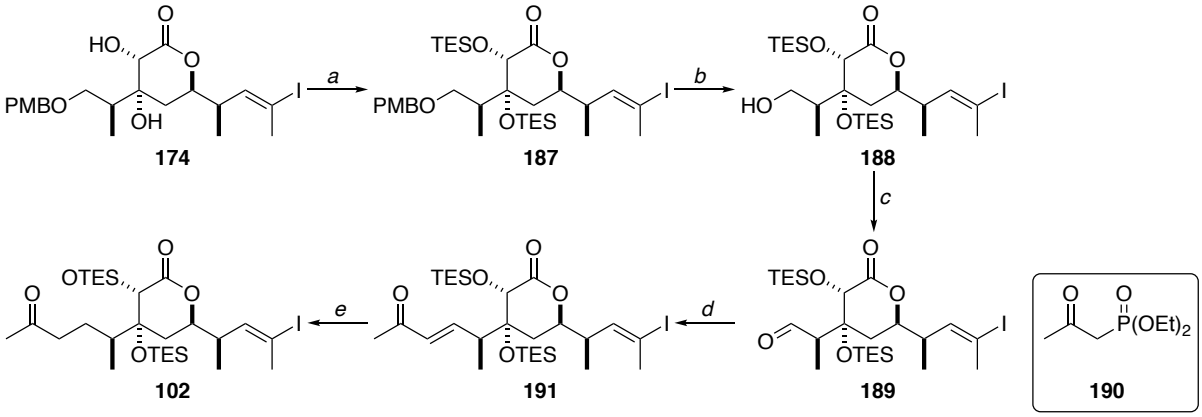

Reagents and conditions: (a) TESOTf, 2,6-lutidine, CH_2Cl_2, 0 °C, 88%; (b) DDQ, pH 7 buffer, CH_2Cl_2, rt, 80%; (c) DMP, $NaHCO_3$, CH_2Cl_2, rt; (d) **190**, $Ba(OH)_2$, THF, rt, *then* **189**, THF/H_2O, 0 °C → rt, 80% over two steps; (e) $Cu(OAc)_2 \bullet H_2O$, PPh_3, TMDS, PhMe, rt, 67%

Scheme 43: Completion of the C16-C28 fragment **102**

In this manner, **191** was delivered as a single geometric (*E*) isomer from the HWE reaction. The choice of mild conditions ($Ba(OH)_2$) in this case is particularly suited for the deprotonation of a β-ketophosphonate such as **190**. Chelation of the metal ion to both the carbonyl and phosphonate oxygen atoms lowers the pK_a of the methylene protons, thus facilitating anion formation.[91] The mechanism of the HWE reaction is then analogous to the reaction described for triene **101**, thus accounting for the high selectivity for the (*E*) isomer.

Moving forward, the enone **191** was submitted to a Stryker's reduction[104] in order to furnish the full C16-C28 fragment **102**. The reaction was investigated with several variations on how the copper-hydride complex is prepared. Using solid hexameric $[PPh_3CuH]_6$ gave the lowest yield, ostensibly due to the difficulty in preparing this reagent with the rigorous exclusion of air. An *in situ* formulation of the reagent as a solution[105] ($Cu(OAc)_2$, PPh_3, TMDS) proved more robust and the copper species could be employed catalytically. Under these conditions, turnover of the catalytic cycle is achieved by reduction of the cuprate enolate **192** with TMDS to silyl enol ether **193**, thus regenerating the active copper (I) hydride species (**Figure 32**).

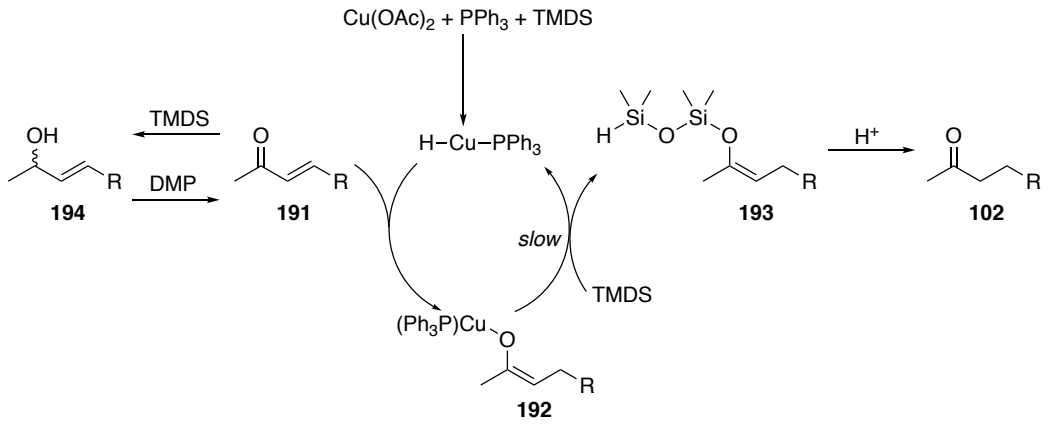

Figure 32: Mechanism of the conjugate reduction of **191** to **102**

The conjugate reduction had been shown to proceed with modest yields (53%) and required further optimisation as ^1H NMR analysis of the crude reaction mixture revealed several by-products. Purification revealed at least one of the by-products to be **194** as a mixture of epimers at C27. This was further verified by showing that both isomers of **194** converged onto a single product upon oxidation (DMP[46], $NaHCO_3$). This suggests that TMDS is undergoing a competing 1,2-reduction of enone **191**, presumably occurring during the rate limiting catalyst turnover step. Employing stoichiometric amounts of copper alongside careful monitoring of the reaction improved the yield of ketone **102** to 67%. It is also possible that product **102** has undergone a similar 1,2-reduction, thus diminishing its yield, although this reduced product could not be identified after chromatography.

With these results, the synthesis of **102** (**Scheme 44**) has been achieved in 18 steps in the longest linear sequence with an overall yield of 4.4%. By using ketone ***ent*-153** and aldehyde ***ent*-154** (both derived from Roche ester **(*R*)-40**), an analogous route (**Scheme 45**) was undertaken by Lam to deliver ***ent*-102** in a similar yield.[71]

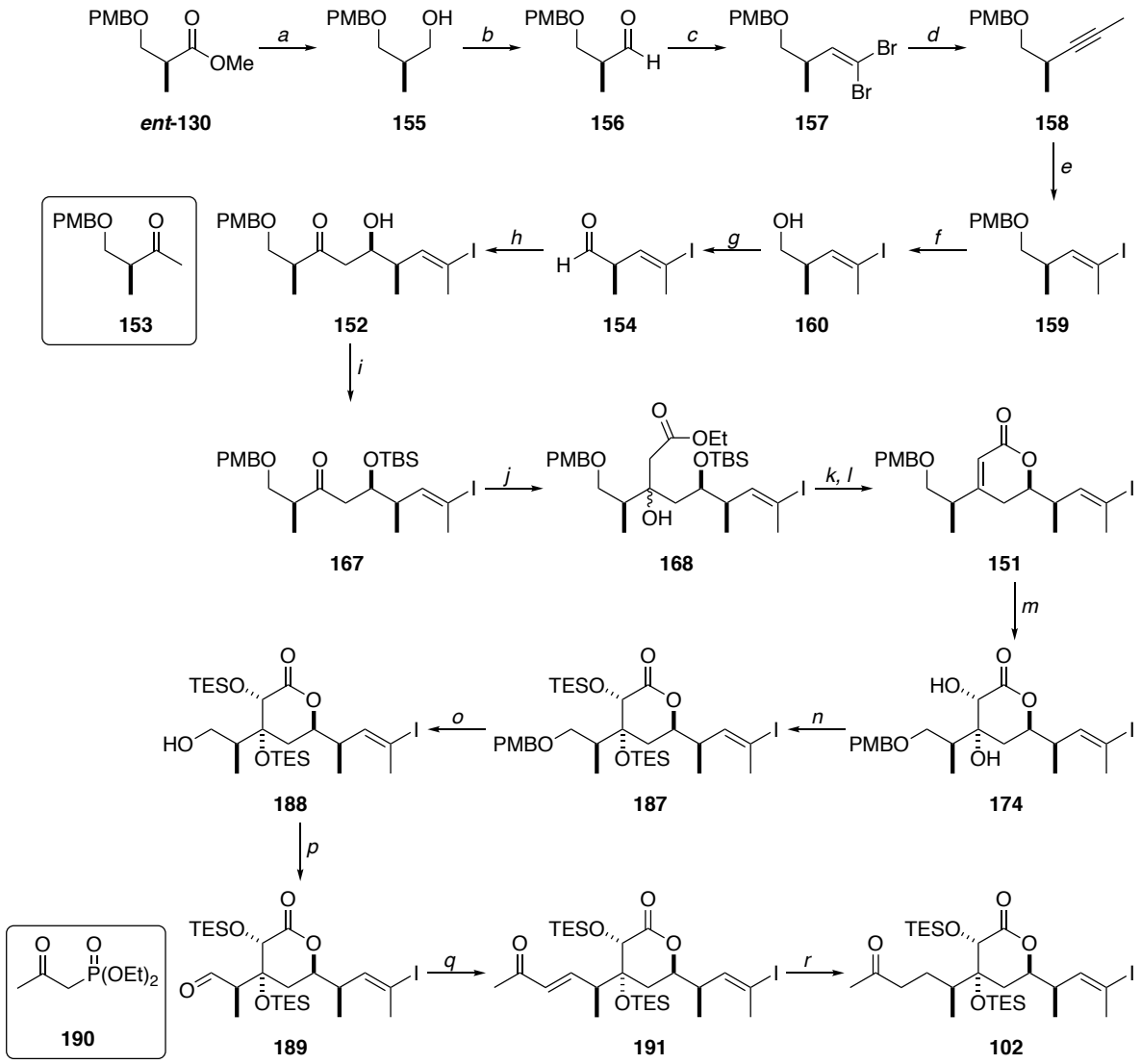

Reagents and conditions: (a) $LiAlH_4$, Et_2O, 0 °C → rt, 90%; (b) $(COCl)_2$, DMSO, Et_3N, CH_2Cl_2, –78 °C → –20 °C; (c) PPh_3, CBr_4, CH_2Cl_2, 0 °C, *then* **156**, –78 °C → 0 °C, 77% over two steps; (d) n-BuLi, THF, –78 °C; MeI, –78 °C, 92%; (e) Cp_2ZrCl_2, DIBAL, THF, 0 °C, *then* **158**, 0 °C → rt, *then* I_2, –78 °C, 76%; (f) DDQ, pH 7 buffer, CH_2Cl_2, rt, 90%; (g) DMP, $NaHCO_3$, CH_2Cl_2, rt, (h) **153**, (–)-DIPCl, Et_3N, Et_2O, –78 °C → 0 °C, *then* **154**, –78 °C, 70% over two steps; (i) TBSOTf, 2,6-lutidine, CH_2Cl_2, –78 °C, 95%; (j) LDA, EtOAc, THF, –78 °C, 97%; (k) HF•py, THF, 0 °C → rt, 85%; (l) Ac_2O, DMAP, PhH/py, reflux, 88%; (m) K_2OsO_4•$2H_2O$ (2 mol%), NMO, citric acid, t-BuOH/H_2O/THF, rt, 5 h, 55%; (n) TESOTf, 2,6-lutidine, CH_2Cl_2, 0 °C, 88%; (o) DDQ, pH 7 buffer, CH_2Cl_2, rt, 80%; (p) DMP, $NaHCO_3$, CH_2Cl_2, rt; (q) **190**, $Ba(OH)_2$, THF, rt, *then* **189**, THF/H_2O, 0 °C → rt, 80% over two steps; (r) $Cu(OAc)_2$•H_2O, PPh_3, TMDS, PhMe, rt, 67%

Scheme 44: Completion of the C16-C28 fragment **102**

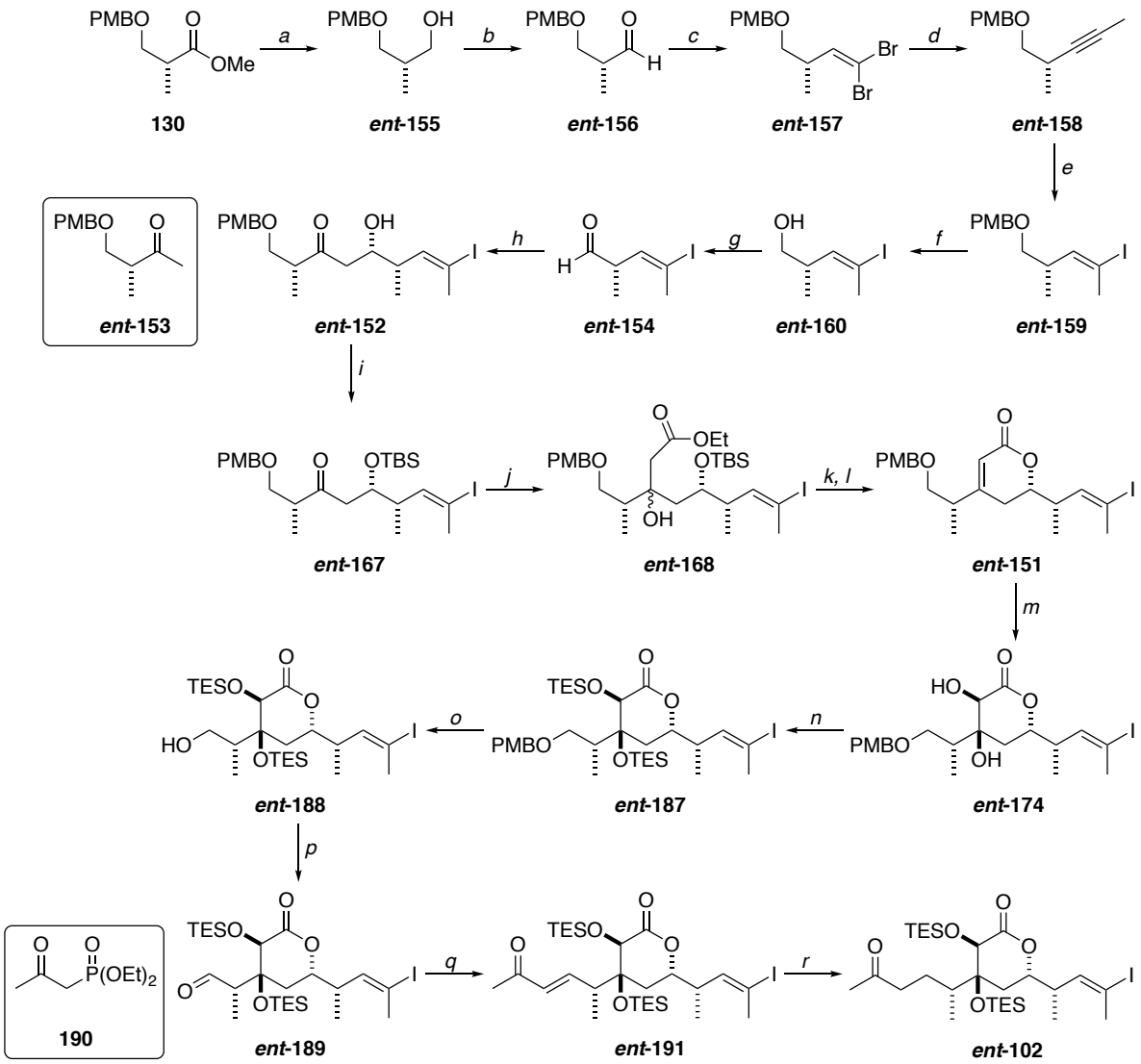

Reagents and conditions: (a) $LiAlH_4$, Et_2O, 0 °C → rt, 76%; (b) $(COCl)_2$, DMSO, Et_3N, CH_2Cl_2, –78 °C → –20 °C; (c) PPh_3, CBr_4, CH_2Cl_2, 0 °C, *then* ***ent*-156**, –78 °C → 0 °C, 80% over two steps; (d) n-BuLi, THF, –78 °C; MeI, –78 °C, 91%; (e) Cp_2ZrCl_2, DIBAL, THF, 0 °C, *then* ***ent*-158**, 0 °C → rt, *then* I_2, –78 °C, 78%; (f) DDQ, pH 7 buffer, CH_2Cl_2, rt, 84%; (g) DMP, $NaHCO_3$, CH_2Cl_2, rt, (h) ***ent*-153**, (–)-DIPCl, Et_3N, Et_2O, –78 °C → 0 °C, *then* ***ent*-154**, –78 °C, 62% over two steps; (i) TBSOTf, 2,6-lutidine, CH_2Cl_2, –78 °C, 97%; (j) LDA, EtOAc, THF, –78 °C, 97%; (k) HF•py, THF, 0 °C → rt, 89%; (l) Ac_2O, DMAP, PhH/py, reflux, 89%; (m) K_2OsO_4•$2H_2O$ (2 mol%), NMO, citric acid, t-BuOH/H_2O/THF, rt, 5 h, 40%; (n) TESOTf, 2,6-lutidine, CH_2Cl_2, 0 °C, 88%; (o) DDQ, pH 7 buffer, CH_2Cl_2, rt, 80%; (p) DMP, $NaHCO_3$, CH_2Cl_2, rt; (q) **190**, $Ba(OH)_2$, THF, rt, *then* ***ent*-189**, THF/H_2O, 0 °C → rt, 80% over two steps; (r) $Cu(OAc)_2$•H_2O, PPh_3, TMDS, PhMe, rt, 70%

Scheme 45: Completion of the C16-C28 fragment ***ent*-102** by Lam

CHAPTER THREE: FRAGMENT UNION AND NMR CORRELATIONS

3.1 Stereochemical Studies of the C1-C15 Fragment

Although the synthesis of the C1-C15 fragment **101** had been carried out with excellent diastereoselectivity at every step, we wished to investigate how well the spectroscopic data for this truncate might fit with the natural product. To this end, the *bis*-TES protecting groups were removed with HF•py/py to give diol **195** in 75% yield for NMR correlation studies (**Scheme 46**). This reaction also served as a model study for the global deprotection later.

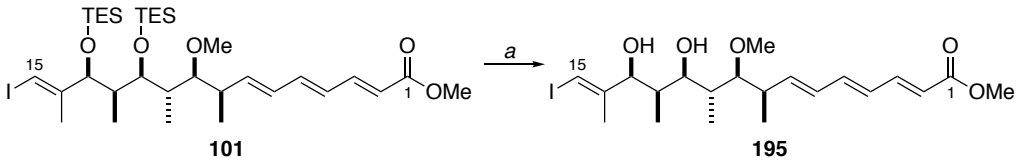

101 **195**

Reagents and conditions: (a) HF•py/py, THF, 0 °C → rt, 75%

Scheme 46: Deprotection of the C1-C15 fragment **101**

Although natural hemicalide contains a carboxylic acid at C1, previous work by Ardisson cast doubt on this. A possible 'salt effect' was proposed which was responsible for distorting the chemical shifts of the C1-C7 trienic signals.[32] Ardisson also showed that this perturbation did not extend into the aliphatic region hence the C1 methyl ester in diol **195** was not hydrolysed and the entire C1-C7 region was also excluded from spectroscopic comparison with natural hemicalide. In addition, resonances arising from C14 and C15 were ignored due to their proximity to the truncated end as the vinyl iodide functionality bears little resemblance with the natural product.

A comparison of the ^{13}C NMR spectrum of the C1-C15 fragment **195** (**Figure 32**) was inconclusive as most resonances had relatively large deviations and it appeared to have worse homology with hemicalide than the Ardisson fragment **65**.[35] Fortunately, in the ^{1}H NMR spectrum, fragment **195** correlated closely with hemicalide and also the Ardisson fragment **65** though notable exceptions were observed at H11 and H13. The difference at H13 could be attributed to the proximity to vinyl iodide in fragment **195**, a major structural difference compared to the diene present in hemicalide. The deviation in chemical shift at H11 was concerning initially, but there was strong confidence in the assigned configuration at this centre because of the Mosher ester analysis performed earlier. In addition, the multiplicity of H11 in fragment **195** (dd, J = 9.3, 2.2 Hz) is very similar to hemicalide (dd, J = 9.6, 2.0 Hz).

As the spectra are recorded in d_4-MeOD, we can likely rule out an internal hydrogen-bonding network enabling hemicalide to fold upon itself. This leaves a conformational effect as the most plausible reason for the chemical shift deviation of H11. The presence of the α,β-dihydroxylactone must affect the overall conformation of the molecule even without any hydrogen-bonding interactions.

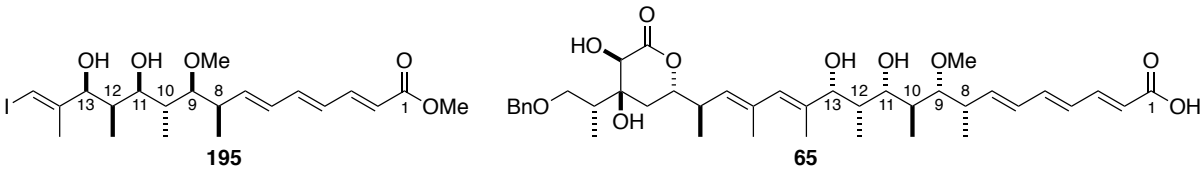

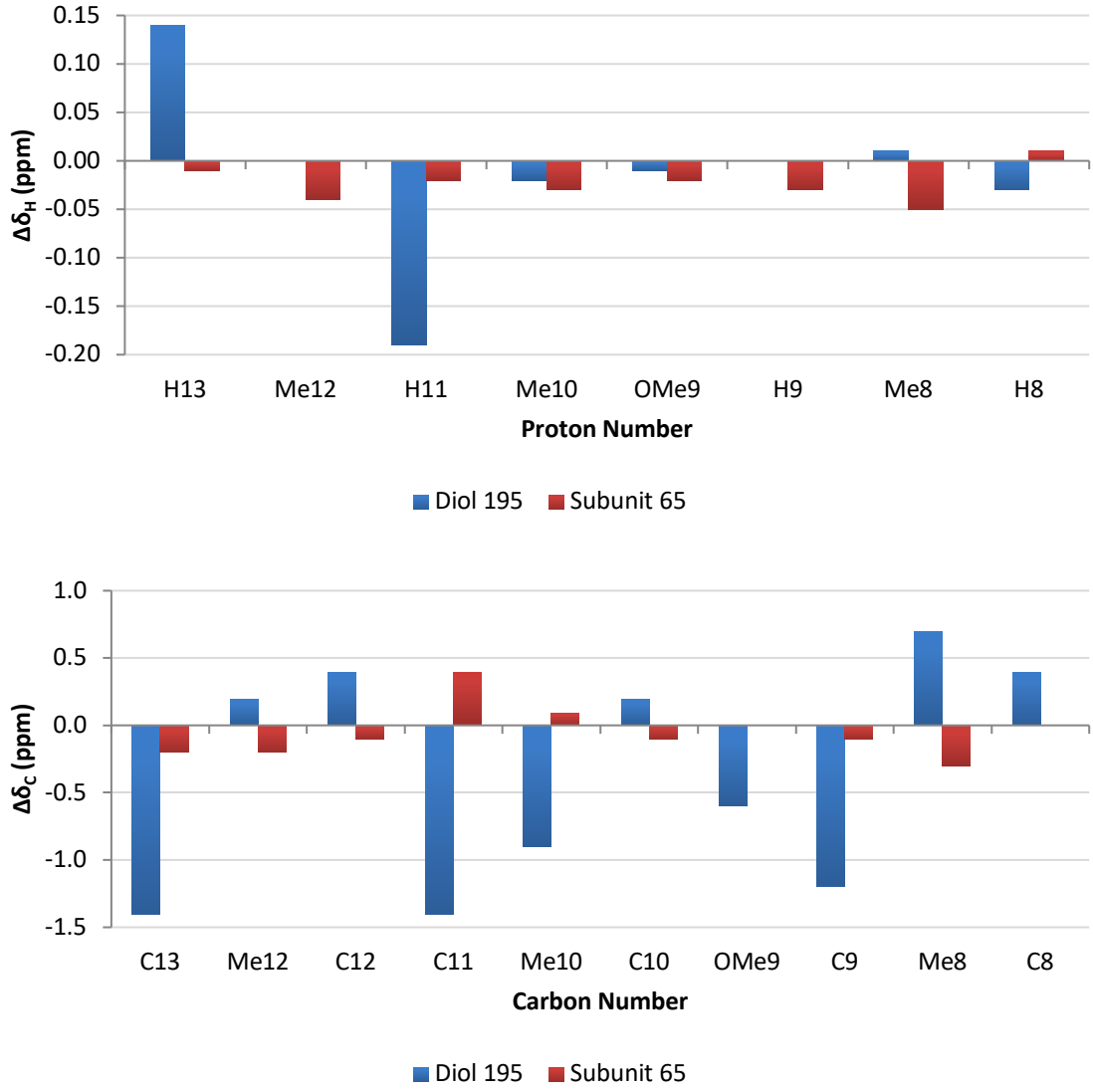

Figure 33: NMR correlations of the C1-C15 fragment **195** compared against the Ardisson fragment **65**

The availability of intermediates **101** and **195** provided an opportunity to carry out model studies on the methyl ester hydrolysis at the C1 carboxyl terminus (**Scheme 47**). The use of KOTMS was pursued initially as a mild alternative to an alkali metal hydroxide-mediated hydrolysis but complex reaction profiles were produced with both **196** and **197**. Pleasingly, $Ba(OH)_2 \bullet 8H_2O$-mediated hydrolysis delivered clean conversion of the methyl esters **101** and **197** to carboxylic acids **198** and **199** respectively as judged by ^1H NMR spectroscopic analysis of the crude products.

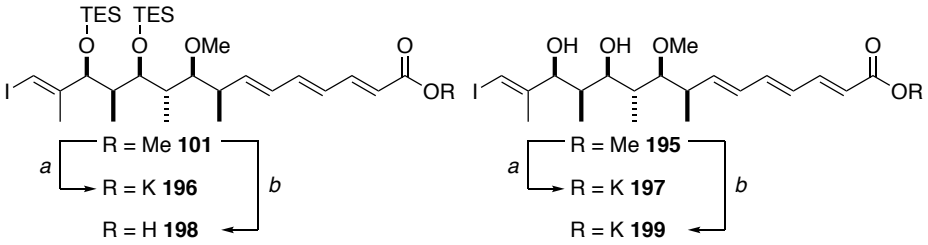

Reagents and conditions: (a) KOTMS, THF, rt; (b) $Ba(OH)_2 \bullet 8H_2O$, MeOH, rt

Scheme 47: Model studies of methyl ester hydrolysis in intermediates **101** and **195**

3.2 Stereochemical reassignment of the C16-C28 fragment

The stereochemical reassignment of the C16-C28 region of hemicalide was investigated by using **174** (**Scheme 48**) as a branchpoint in the synthesis. This also allowed vinyl iodide **174** to be used as a model system for studying the Stille coupling[70] in our planned synthesis. Earlier work by MacGregor[37] demonstrated that although vinyl trimethylstannane **200** was accessible *via* a Wulff-Stille reaction[106] with a 67% yield, it was highly unstable and would decompose faster than it could be used in the Stille coupling. As such, vinyl stannane **201** was selected as the coupling partner instead. This was prepared from **114** via a lithium-halogen exchange (NaH, t-BuLi) followed by trapping with $SnBu_3Cl$ (60%). To ensure the hydroxyl group does not quench any lithiated species under the reaction conditions, **114** was first deprotonated with NaH.

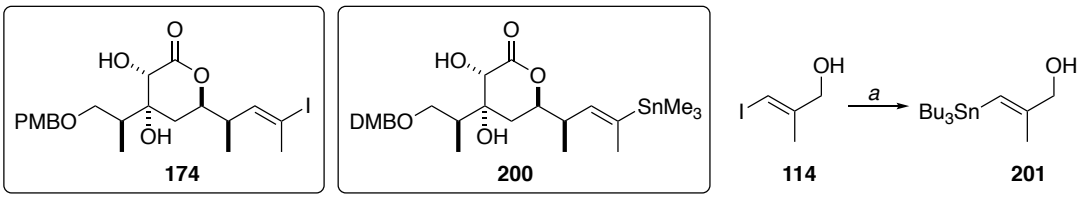

Reagents and conditions: (a) NaH, **114**, THF 0 °C, *then* t-BuLi, $SnBu_3Cl$, –78 °C, 60%

Scheme 48: Generating a suitable vinyl stannane partner for the model Stille coupling

The Stille coupling represents a reliable method of joining two fragments because organostannanes exhibit wide functional group tolerance and good reactivity with electrophiles. Further advancements to this protocol have been developed over the years, particularly to address the rate limiting transmetallation step in the catalytic cycle (**Figure 34**). The rate acceleration observed when copper (I) salts are added is well documented and is attributed to a tin-copper exchange to generate a more nucleophilic organocuprate species. However, the positive influence of copper is limited by the reversible nature of the tin-copper exchange so a tin scavenger is required to drive the equilibrium to completion. Fluoride sources have been proposed as a tin scavenger by Baldwin but face severe restrictions in their utility due to their incompatibility with silyl protecting groups.[107] Fürstner reported that $[NBu_4][Ph_2PO_2]$ was an effective substitute for fluoride, enabling the Stille coupling to be conducted under essentially neutral conditions.[108] This modified protocol was successfully employed in late stage fragment couplings of several natural products such as leiodermatolide,[75] iejimalide B[109] and ouabagenin.[110] Pleasingly, these conditions were also successful in the cross coupling of vinyl iodide **174** and vinyl stannane **201** in a 1:1 ratio to give the (*E*, *E*) diene **202** in 74% yield (**Scheme 49**). The stoichiometry in the model reaction boded well for the fragment coupling in the full system as it enabled both late-stage intermediates to be used efficiently without wastage.

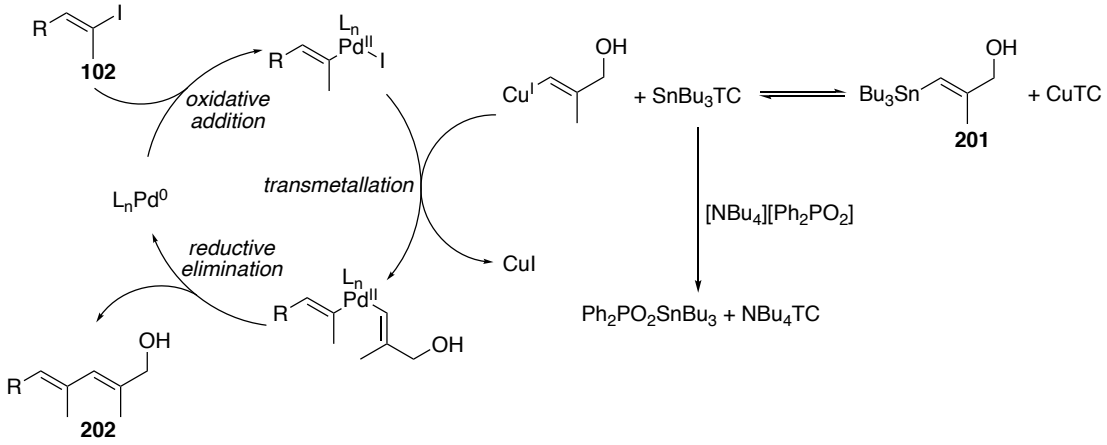

Figure 34: Mechanism of the Stille coupling with modifications by Fürstner

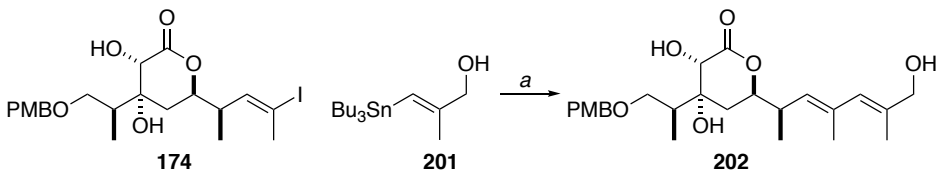

Reagents and conditions: (a) $Pd(PPh_3)_4$, CuTC, $[NBu_4][Ph_2PO_2]$, DMF, 0 °C, 74%

Scheme 49: Sucessful Stille coupling of **174** and **201** to give truncate **202**

Initial NMR studies of diene **202** were hampered by the fact that the H19 signal was obscured by the methylene protons of the PMB protecting group in d_4-MeOD. Over concerns that allylic oxidation at C13 will outcompete the deprotection at C24, as observed during the Paterson group's total synthesis of the aplyronines, we decided not to remove the PMB group with standard DDQ conditions. Pleasingly, by irradiating H20 in an nOe experiment, the enhanced H19 resonance could be clearly seen as a ddd (**Figure 35**).

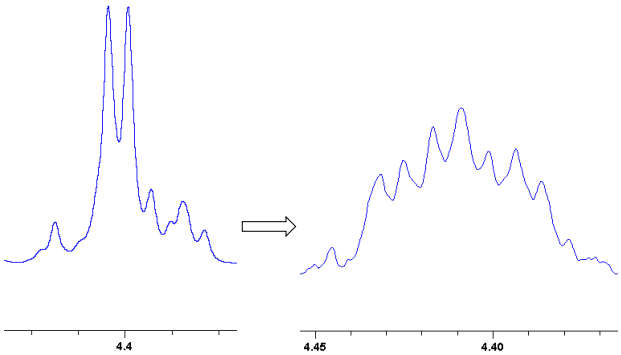

Figure 35: Revealing the shape of the H19 resonance in an nOe experiment by irradiating H20

The NMR spectra of diene **202** were compared against hemicalide[1] and the Ardisson fragment[35] **65** as well (**Figure 36**). As diene **202** lacked the C1-C15 region of the natural product, it was not surprising that the molecule appeared to be a poorer fit with hemicalide compared to the Ardisson fragment **65** at positions C14-C18. Within the lactone ring, diene **202** exhibited an improved correlation in ^{1}H NMR chemical shifts for H19 and H22 against Ardisson's intermediate **65**. These were considered diagnostic signals in their stereochemical assignment. With Ardisson's truncate **65**, H19 and H22 showed chemical shift deviations of 0.12 and –0.10 ppm respectively while the corresponding resonances in diene **202** had much smaller differences of –0.01 and –0.04 ppm.

In addition, the peak shape and *J* values of H19 (ddd, *J* = 11.6, 7.7, 3.7 Hz) in diene **202** strongly agree with the reported values for natural hemicalide (ddd, *J* = 11.3, 7.5, 3.5 Hz), unlike the Ardisson fragment **65** (ddd, *J* = 13.2, 6.1, 3.9 Hz). Based on these observations, the stereochemical relationship between C18 and C19 was thus confidently reassigned from *anti* to *syn* in support of the earlier computational work.[36]

Ardisson's pursuit of an 18,19-*anti* relationship can be understood as a result of the misleading studies conducted on fragments that were structurally different from the natural product. These model candidates terminated in an oxy-methylene carbon at C17 instead of a diene which is present in hemicalide (See Chapter 1.4.2).[33] Following our group's published reassignment of the

18,19-*syn* relationship,[36] the Ardisson–Cossy team acknowledged that their 18,19-*anti* intermediates did not correlate well with hemicalide and updated their synthetic route to reflect the revised 18,19-*syn* relationship.[63]

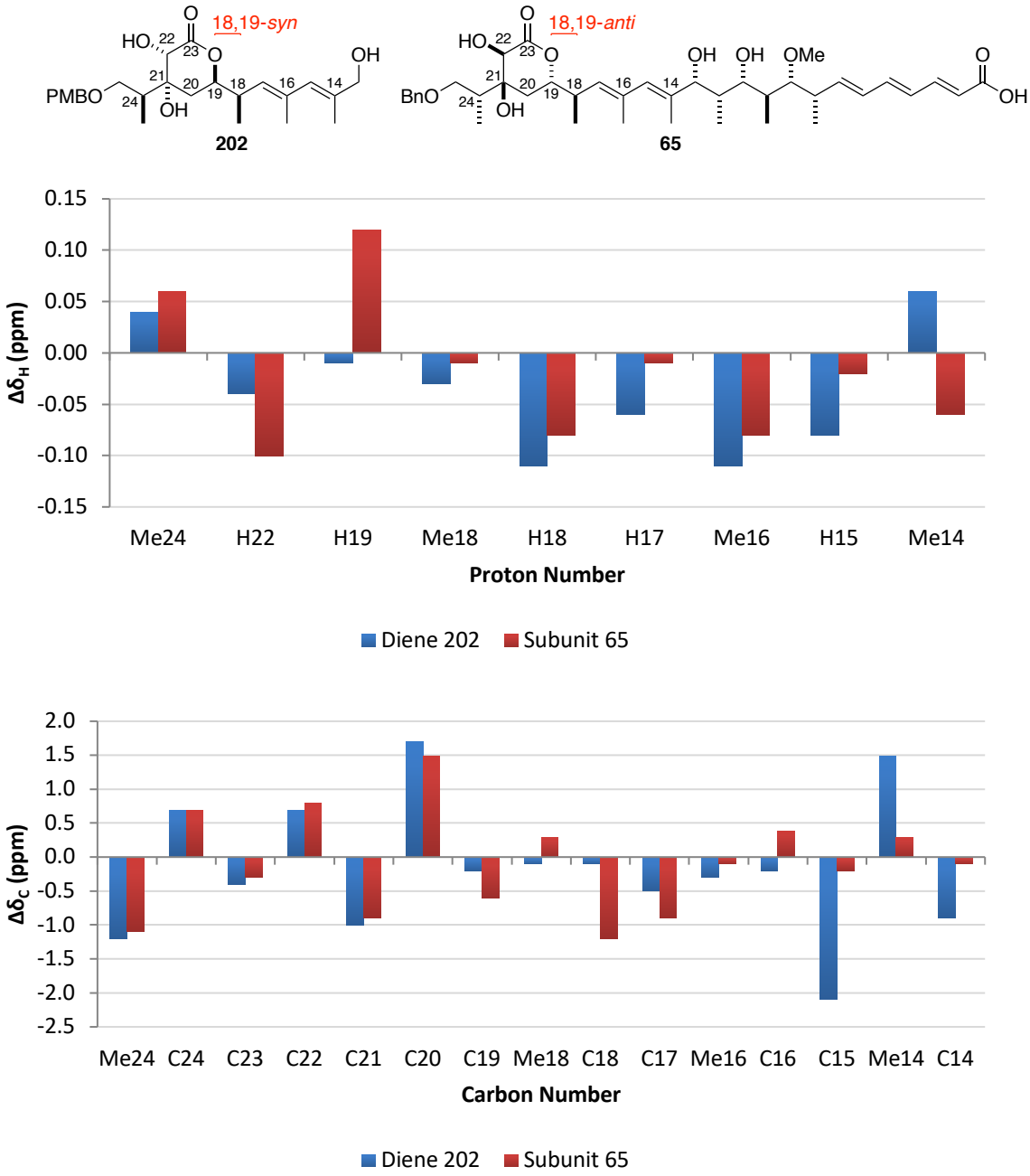

Figure 36: NMR correlations of the C14-24 fragment **202** compared against the Ardisson fragment **65**

3.3 Fragment Union

3.3.1 Access to Vinyl Stannanes *via* Lithium-Halogen Exchange

The failure to install an organotin handle on the C16-C28 fragment reliably by MacGregor, together with the success of synthesising vinyl stannane **201** *via* a lithium-halogen exchange, prompted a change in our fragment coupling strategy.

To avoid chemoselectivity issues arising from a lithium-halogen exchange approach in the C1-C15 fragment, the vinyl stannane would have to be installed before the C1 methyl ester is appended *via* the HWE reaction.[47] Using the conditions employed previously, vinyl iodide **144** was transformed into vinyl stannane **203** by first deprotonating with NaH, then carrying out a lithium-halogen exchange with a $SnBu_3Cl$ trap. This step suffered greatly from the formation of olefin **204** as an inseparable by-product (**Scheme 50**). The amount of olefin **204** formed was inconsistent and confounded attempts to diagnose the problem as arising from proto-destannylation of the product or quenching of the *in situ* generated vinyl lithium species.

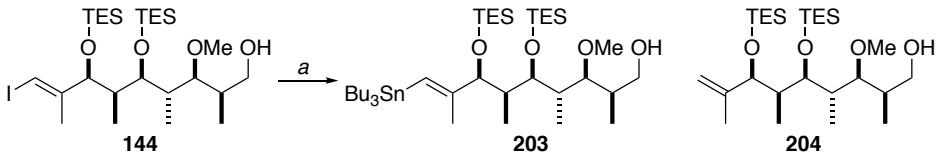

Reagents and conditions: (a) NaH, **144**, THF 0 °C, *then* t-BuLi, $SnBu_3Cl$, –78 °C, 59%

Scheme 50: Preparing vinyl stannanes **203** *via* lithium-halogen exchange

The next step in oxidising alcohol **203** to aldehyde **205** also proved to be more problematic than expected. The various conditions screened (**Table 6**) either led to poor conversion, further proto-destannylation leading to aldehyde **206** or epimerisation at C8. Due to these disappointing results, the idea of advancing intermediates bearing the vinyl stannane functional group towards the HWE reaction was not pursued further.

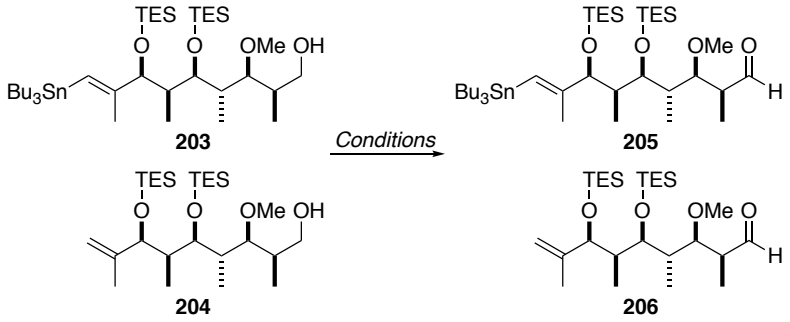

Entry	Conditions	Result
1	DMP, $NaHCO_3$	Full conversion; extensive proto-destannylation; no epimerisation
2	DMSO, Et_3N, SO_3•py	Incomplete conversion; some proto-destannylation; no epimerisation
3	TEMPO, BAIB	Incomplete conversion; moderate proto-destannylation; some epimerisation

Table 6: Conditions examined for the oxidation **203** to **205**

Given the apparent sensitivity of the vinyl stannane functional group, intermediate **203** was then submitted to a Stille coupling[108] with the C16-C28 fragment **102** immediately. Gratifingly, this cross coupling proceeded smoothly to give 13,18-*syn* diene **207** with 78% yield (**Scheme 51**). Any proto-destannylated by-product **204** from the lithium-halogen exchange step did not interfere in the Stille coupling. It was envisaged that by-product **204** could be recycled by subjecting it to a Heck reaction[111] with vinyl iodide **102** to generate the desired 13,18-*syn* diene **207**. However, this idea was not explored further due to the scarcity of **204**.

The C7 alcohol was then oxidised with Dess–Martin periodinane[46] (99%) and used immediately in a HWE reaction[47] with phosphonate **104** to yield the complete 13,18-*syn* diastereomer of the C1-C28 truncate **99** with a yield of 54% (**Scheme 51**). Despite employing an excess of the phosphonate, no reaction was observed at the C27 ketone under the reaction conditions. By repeating the process with ***ent*-203**, the 13,18-*anti* series of intermediates could be obtained in an analogous fashion, culminating in the 13,18-*anti* diastereomer of the C1-C28 truncate **100**.

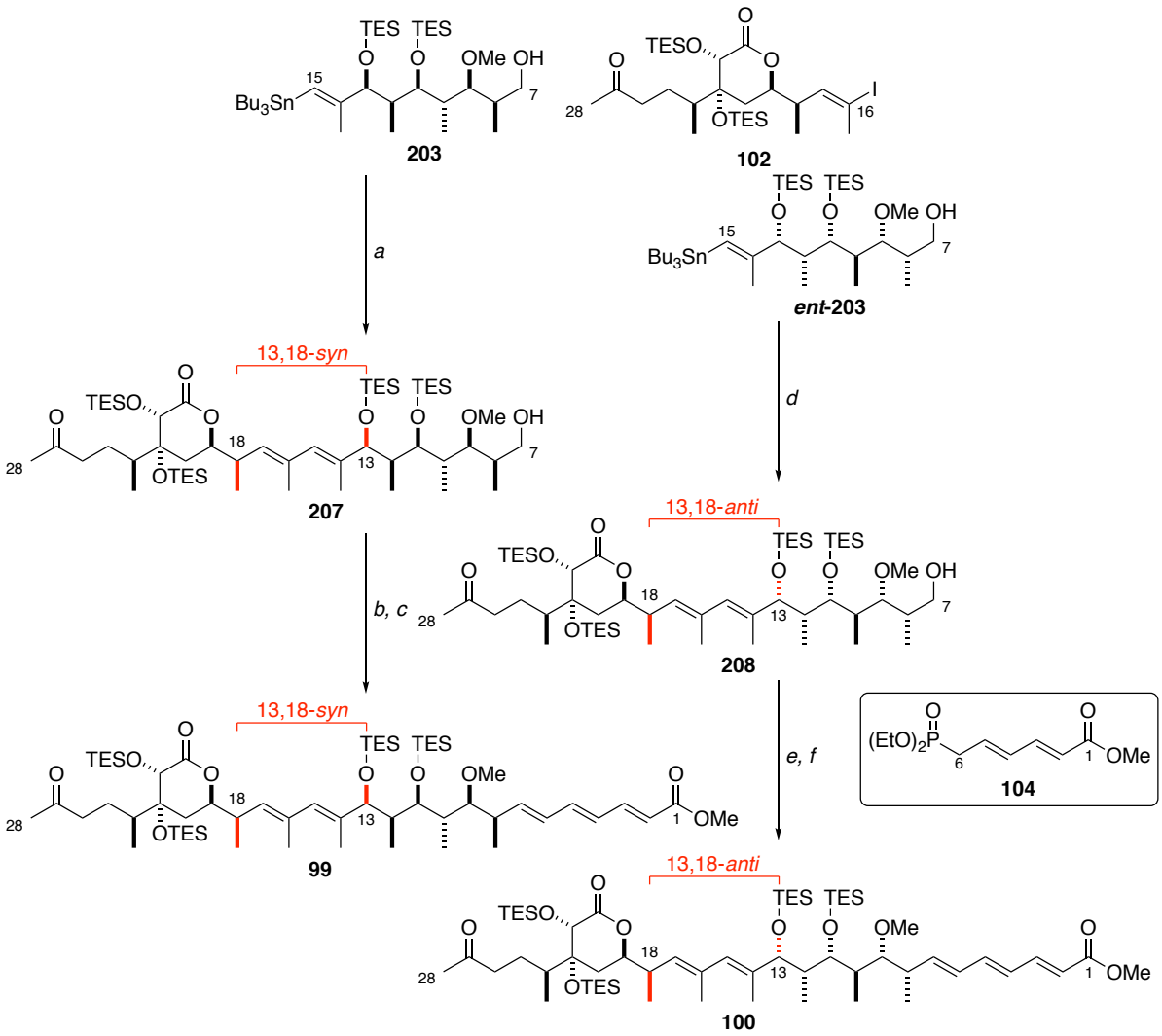

Reagents and conditions: (a) $Pd(PPh_3)_4$, CuTC, $[NBu_4][Ph_2PO_2]$, DMF, 0 °C, 78%; (b) DMP, $NaHCO_3$, CH_2Cl_2, rt, 99%; (c) **104**, LDA, THF, –78 °C → –40 °C, 52%; (d) $Pd(PPh_3)_4$, CuTC, $[NBu_4][Ph_2PO_2]$, DMF, 0 °C, 74%; (e) DMP, $NaHCO_3$, CH_2Cl_2, rt, 99%; (f) **104**, LDA, THF, –78 °C → –40 °C, 55%

Scheme 51: Successful Stille coupling and HWE olefination to produce C1-C28 truncates **99** and **100**

This represents the first successful attempt at synthesising the two possible diastereomers, 13,18-*syn* **99** and 13,18-*anti* **100**, of the full C1-C28 region of hemicalide. However, this was not the most efficient method of fulfilling this objective. As the longest linear sequence involves the C16-C28 fragment **102**, stepwise elaboration of the C7-C28 fragments **207** and **208** makes the synthesis less convergent.

3.3.2 Access to Vinyl Stannanes *via* Wulff–Stille Reactions

To maximise convergency, the Stille coupling should be performed last in the fragment coupling sequence. This requires the vinyl stannane to be installed on the C1-C15 fragment **101** in the presence of the C1 methyl ester. Alternatively, a more robust replacement for trimethylstannane **209** had to be synthesised. As such, the Wulff–Stille reaction[106] was re-examined in both cases to see if this was possible.

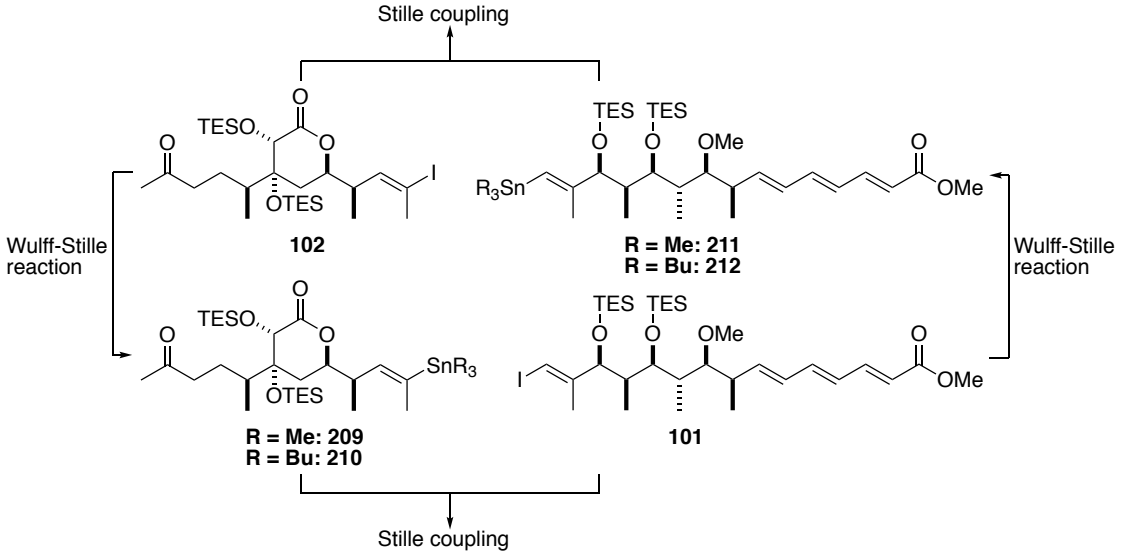

Entry	Transformation	Conditions	Result
1	**102 → 210**	$Pd(PPh_3)_4$, LiCl, $(Bu_3Sn)_2$	No reaction
2	**102 → 210**	$Pd(PPh_3)_2Cl_2$, Li_2CO_3, $(Bu_3Sn)_2$	No reaction
3	**101 → 212**	$Pd(PPh_3)_2Cl_2$, Li_2CO_3, $(Bu_3Sn)_2$	No reaction
4	**101 → 211**	$Pd(PPh_3)_2Cl_2$, Li_2CO_3, $(Me_3Sn)_2$	Full conversion, 70% yield

Table 7: Exploring different vinyl iodide substrates and conditions for the Wulff–Stille reaction

Tributylstannane derivatives were considered as a replacement for trimethylstannes due to their increased stability. The success of intermediates **201** and **203** in their respective Stille couplings showed that they were reactive enough to be viable coupling partners. Unfortunately, the use of $(Bu_3Sn)_2$ instead of $(Me_3Sn)_2$ in the Wulff–Stille reaction[106] of **101** or **102** simply returned the starting material unchanged (**Table 7, Entries 1-3**). Examples in the literature for this type of reaction invariably used 1,2-disubstituted olefins. Ostensibly, the Me group at C14 presents significant steric hindrance that disfavours the C–Sn bond formation.

Having exhausted various methods of accessing the vinyl tributylstannane **212**, the only recourse left was installing a vinyl trimethylstannane on the C1-C15 fragment **101**. Gratifingly, trimethylstannane **211** was synthesised in good yield (**Table 7, Entry 4**) and could be stored in the freezer for a reasonable length of time without degradation.

Due to insufficient quantities of the C16-C28 fragment **102**, the remainder of the fragment union was continued with the enantiomeric fragment ***ent*-102** prepared by Lam. This did not affect any subsequent conclusions as we are only investigating the relative configuration between the C8-C13 and C18-C24 stereoclusters.

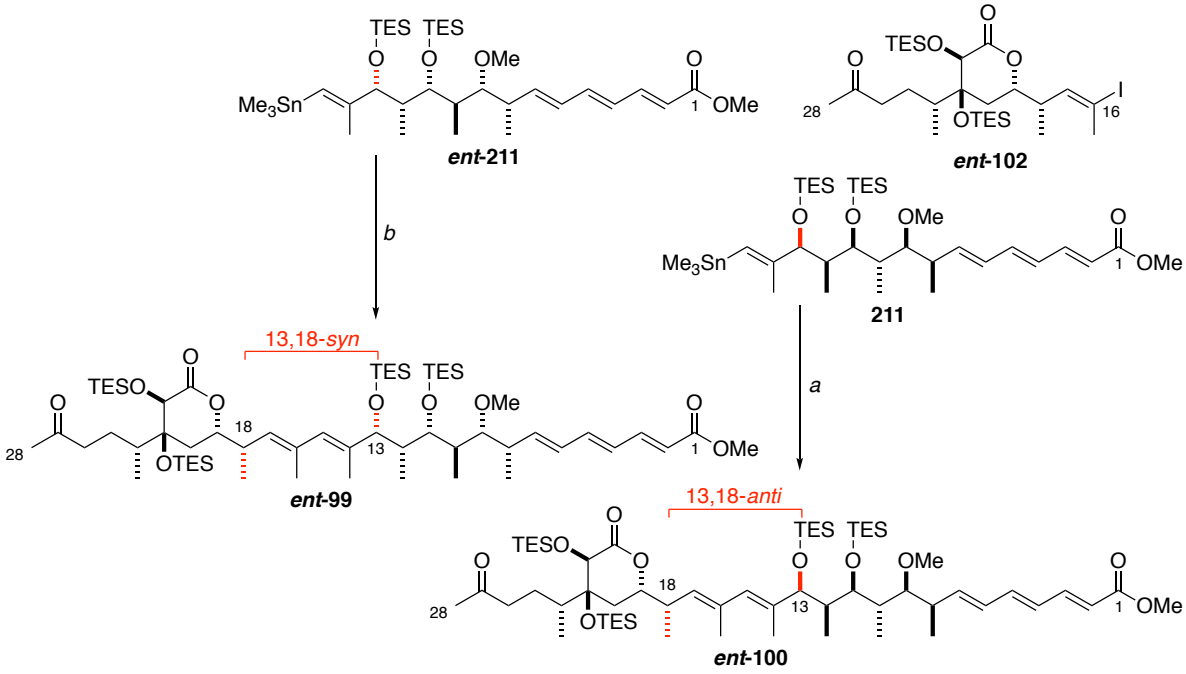

Reagents and conditions: (a) $Pd(PPh_3)_4$, CuTC, $[NBu_4][PhPO_2]$, DMF, 0 °C, 70%; (b) $Pd(PPh_3)_4$, CuTC, $[NBu_4][PhPO_2]$, DMF, 0 °C, 72%

Scheme 52: Final revised fragment union to produce C1-C28 truncates ***ent*-99** and ***ent*-100**

The critical Stille coupling of vinyl iodide ***ent*-102** and vinyl stannane **211** was carried out under Fürstner conditions[108] previously used to synthesise dienes **207** and **208**. This delivered the 13,18-*anti* diastereomer ***ent*-100** of the C1-C28 truncate in good yield (72%). This result was highly reproducible and worked well on various scales (up to 0.150 mmol). By selecting the appropriate enantiomer of vinyl stannane **211**, both the 13,18-*syn* and 13,18-*anti* diastereomers of the C1-C28 truncate, ***ent*-99** and ***ent*-100** respectively, were successfully prepared by Lam[71] and the author respectively (**Scheme 52**).

At this point, it was noted that the 13,18-*syn* and 13,18-*anti* diastereomers did exhibit notable differences in their ^{1}H and ^{13}C NMR spectra when recorded in $CDCl_3$ despite the distal 1,6-related nature of the two stereoclusters. Obviously, a meaningful comparison can only be made with the protecting groups removed and with the appropriate solvent (d_4-MeOD) but, at the time, it strengthened our confidence in this synthesis-enabled stereochemical assignment *via* NMR studies.

3.4 Derivatisation and NMR Studies

At this point, the revised fragment union using an elaborate Stille coupling[108] had now reliably delivered the full carbon chain in the C1-C28 region of hemicalide. While it appeared tempting to subject ***ent*-99** and ***ent*-100** to a global deprotection, this was not done for two reasons. Firstly, the natural product does not feature a ketone at C27 so these truncates would not be suitable for NMR correlation studies.[1] More importantly, MacGregor had demonstrated that without a protecting group, the C21 hydroxyl group would spontaneously hemiketalise[37] with the C27 ketone, leading to a completely unrelated structure **213** that would complicate our spectroscopic studies (**Scheme 53**).

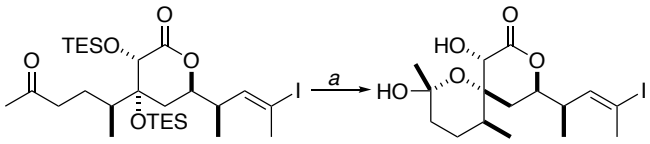

102 **213**

Reagents and conditions: (a) HF•py, THF, 0 °C → rt, 50%

Scheme 53: Hemiketalisation during MacGregor's attempt to deprotect C16-C28 fragment **102**

To overcome these issues, the C27 ketone in ***ent*-100** was first reduced to **214** ($NaBH_4$). In the absence of any significant stereocontrol elements, a 2:1 mixture of epimers was obtained. To simplify NMR interpretation, a CBS reduction[112] was also attempted on the C16-C28 fragment **102** as a model reaction but a similar *d.r.* was observed, indicating that reagent control is not possible due to poor steric differentiation in the ketone. Methylation of **214** (Meerwein salt, Proton Sponge®, 4A MS) occurred uneventfully to give **215** in good yield. A similar set of reactions was also carried out by Lam[71] in the 13,18-*syn* series beginning with ***ent*-99** to give **216** and **217** (**Scheme 54**).

Cossy noted that in a system such as **38A** (**Figure 17**), epimers at this distal stereocentre were expected to display quasi-identical NMR spectra.[38] Indeed, the C27 epimers of **215** and **217** exhibited signals that were indistinguishable in the C1-C24 region. While there were differences within the C25-C28 region due to their proximity to the epimeric C27 stereocentre, this region of the molecule was deemed less diagnostic due to its proximity to the truncated end and thus excluded from any NMR correlation studies.

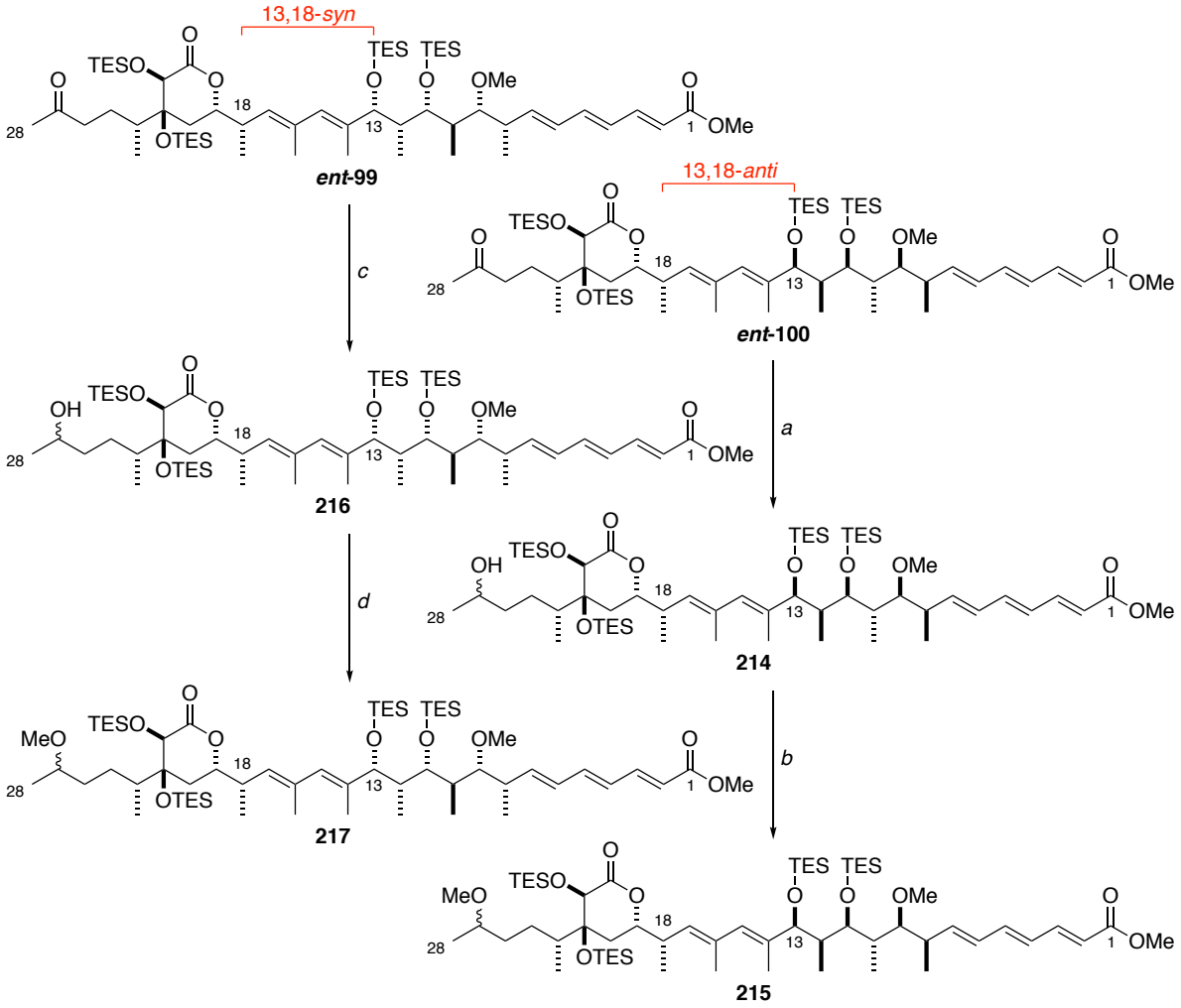

Reagents and conditions: (a) $NaBH_4$, MeOH, rt, 92%; (b) Me_3OBF_4, Proton Sponge®, 4Å MS, CH_2Cl_2, rt, 68%; (c) $NaBH_4$, MeOH, rt, 95%; (d) Me_3OBF_4, Proton Sponge®, 4Å MS, CH_2Cl_2, rt, 87%

Scheme 54: Transforming the C27 ketone into a methyl ether in **215** and for **217** for further studies

Henceforth, the stage was set for examining the global deprotection. Previously, model studies for the deprotection had been conducted on the C1-C15 fragment **101** and the C16-C28 fragment **102** by the author (**Scheme 46**) and MacGregor[37] (**Scheme 53**) respectively. These results suggested that HF•py was a suitable reagent to remove all four TES groups from the C1-C28 truncate **215**. While these conditions led to facile removal of the C11 and C13 TES groups in

diastereomer **215**, no further conversion could be achieved by extending the reaction time. Disappointingly, increasing the concentration of HF•py only led to degradation of the whole molecule.

Further investigation by Lam revealed an interesting observation that the C11 and C13 TES groups were orthogonal to the C21 and C22 TES groups.[71] Various conditions (HF•py, HF/MeCN, TsOH, PPTS, TBAF, TASF) were screened on the constituent fragments ***ent*-211** and ***ent*-102**. The results showed that when one reagent was successful at deprotecting one pair of the TES groups, it was either inert to the other or would cause degradation. After extensive trials, a two-step sequence was established where the C21 and C22 TES groups were first removed with TASF and the crude mixture submitted directly to HF•py/py to furnish the 13,18-*syn* tetraol **218**. Pleasingly, this newly developed protocol also worked for the 13,18-*anti* series to yield the 13,18-*anti* tetraol **219**. Finally, both methyl esters **218** and **219** were subjected to a basic hydrolysis with $Ba(OH)_2$•$8H_2O$ (**Scheme 55**). A low yield was noted for both the 13,18-*syn* and 13,18-*anti* acids **220** and **221** respectively; this was most likely due to their increased hydrophilic character leading to material losses during the aqueous work-up.

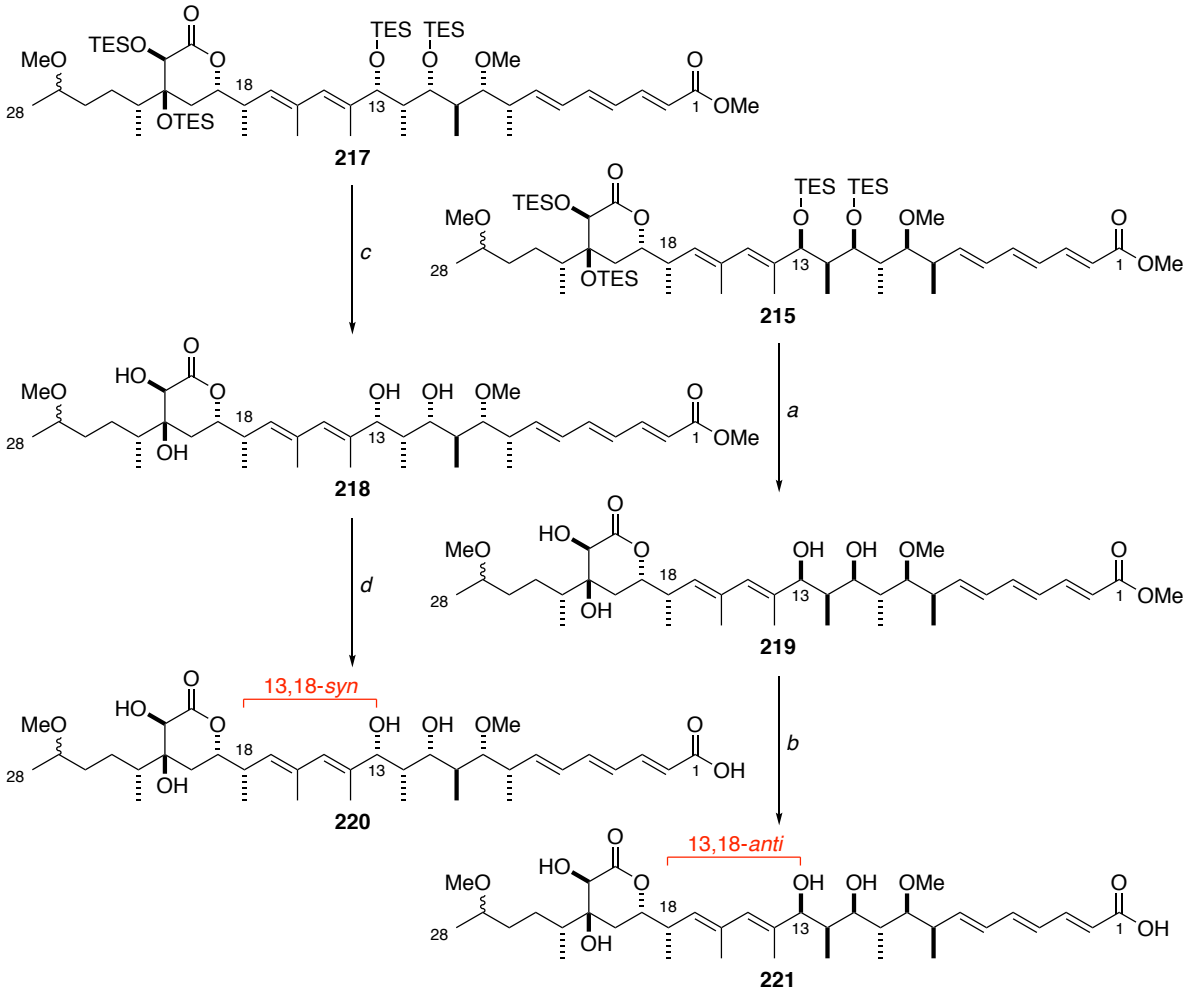

Reagents and conditions: (a) TASF, THF/DMF, 0 °C → rt, *then* HF•py/py, THF, 0 °C → rt, 67%; (b) $Ba(OH)_2$•$8H_2O$, MeOH, rt, 50%; (c) TASF, THF/DMF, 0 °C → rt, *then* HF•py/py, THF, 0 °C → rt, 95%; (d) $Ba(OH)_2$•$8H_2O$, MeOH, rt, 50%

Scheme 55: Global deprotection of C1-C28 truncates arriving at free acids **220** and **221**

Although diastereomers ***ent*-99** and ***ent*-100** exhibited clear NMR chemical shift differences in $CDCl_3$, the target compounds **220** and **221** showed more subtle differences in d_4-MeOD, with the largest differences not exceeding 0.04 ppm in ^1H NMR or 0.6 ppm in ^{13}C NMR. Overall, the 13,18-*syn* acid **220** displayed a remarkably good fit with 0 ppm deviations in the majority of its ^1H and ^{13}C resonances. Resonances that displayed poor correlations in the constituent C1-C15 fragment **101** or C16-C28 fragment **102** now showed significant improvements. This was particularly evident for H11 ($\Delta\delta_H$ –0.19 → 0 ppm, $\Delta\delta_C$ –1.4 → 0 ppm), H15 ($\Delta\delta_H$ –0.08 → 0 ppm, $\Delta\delta_C$ –2.1 → 0 ppm) and C20 ($\Delta\delta_C$ 1.7 → 0.1 ppm) amongst other examples. The extraordinarily good NMR correlations of diastereomer **220**, particular in the ^1H NMR spectrum, strongly supports a 13,18-*syn* relationship in natural hemicalide.[113]

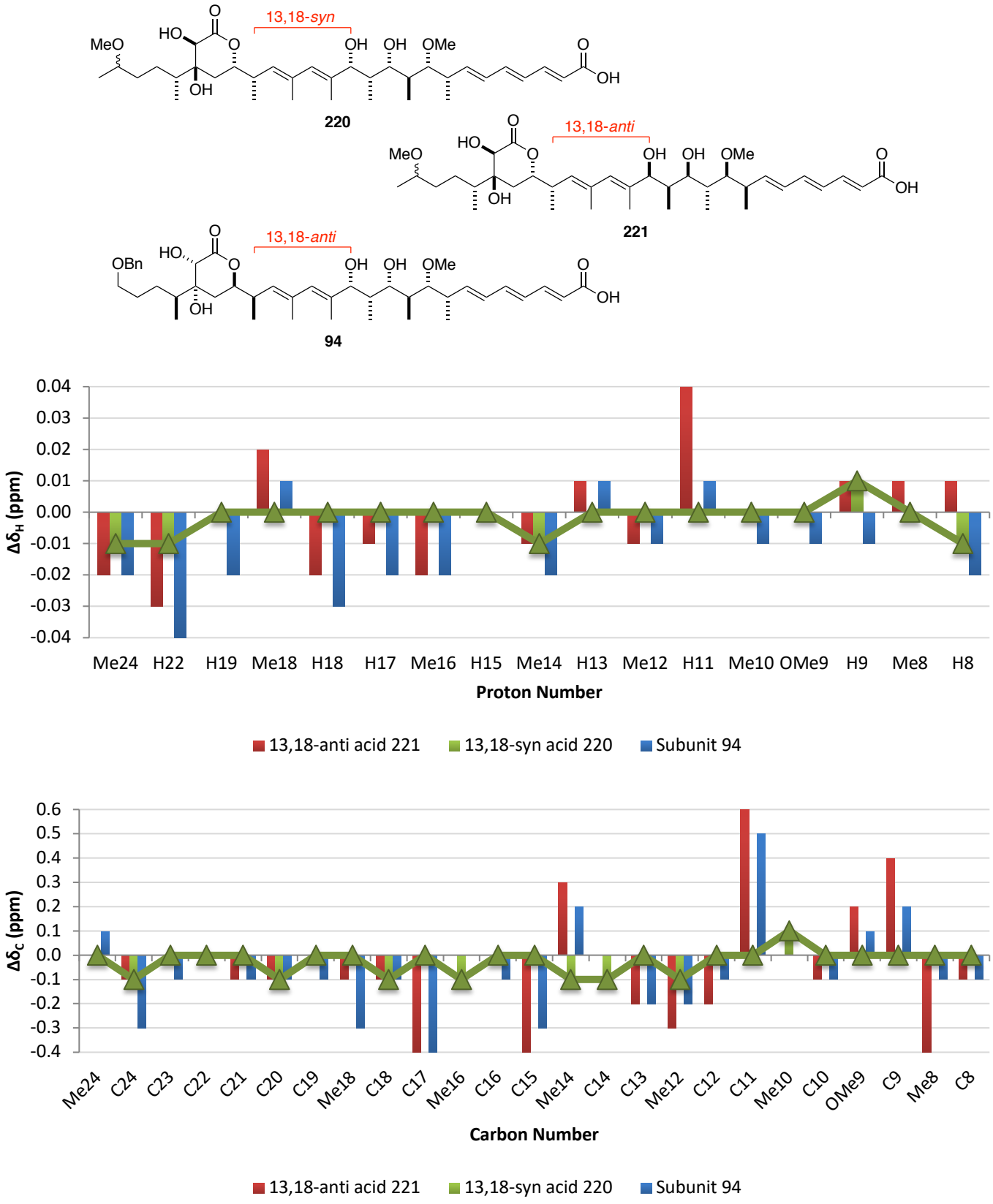

Figure 37: NMR correlations of the 13,18-*syn* truncate **220** and 13,18-*anti* truncate **221** compared against the Ardisson fragment **94** in the aliphatic region

While the 13,18-*anti* diastereomer **221** was not as good a fit as its *syn* counterpart, the chemical shift differences for each resonance were still much smaller than the corresponding signal in the uncoupled fragments. This lends further support to the idea that the overall conformation of hemicalide is dependent on the presence of certain structural features. In addition, the 13,18-*anti* diastereomers **221** also correlates well with the Ardisson–Cossy fragment[63] **94**, featuring the revised 18,19-*syn* relationship, an indirect verification of the *anti* relationship between C13 and C18 in both compounds.

As mentioned in Chapter 1.4.1, Ardisson raised the prospect that natural hemicalide was isolated as a carboxylate salt with an unknown counterion instead of a free acid.[32] This was based on the finding that carboxylate **31** and carboxylic acid **30** have a similar ^{1}H NMR deviation profile as fragment **29A** and hemicalide in the C1-C7 trienic region. To investigate this claim, carboxylates **222** and **223** were also studied by deprotonating carboxylic acids **220** and **221** with Na_2CO_3 (**Scheme 56**).

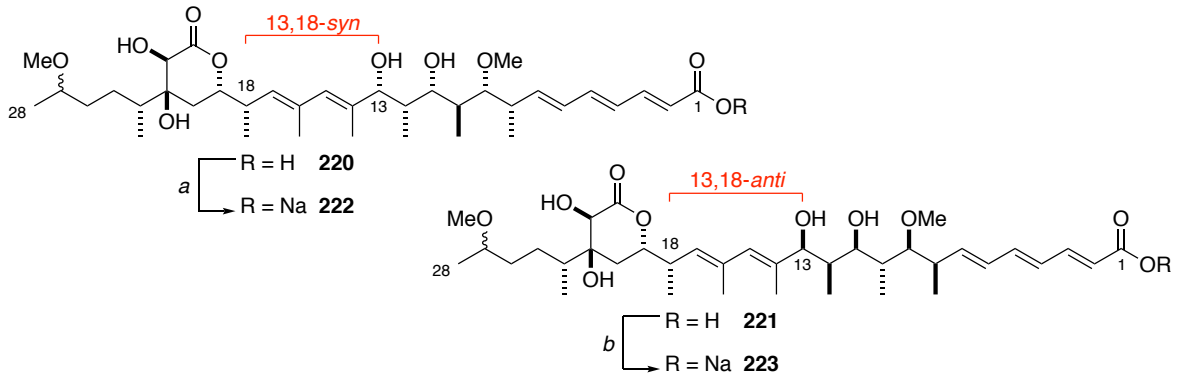

Reagents and conditions: (a) Na_2CO_3, d_4-MeOD, rt, 99%; (b) Na_2CO_3, d_4-MeOD, rt, 99%

Scheme 56: Deprotonation of C1-C28 truncates **220** and **221**

Like the carboxylic acids **220** and **221**, the C8-C24 region was first studied in the carboxylate salts **222** and **223**. The sum of errors, as well as the maximum error, for the ^{1}H and ^{13}C NMR spectra of carboxylates **222** and **223** were tabulated (**Table 8**) and compared against the known acids **220**, **221** and **94**. Once again, the 13,18-*syn* carboxylate **222** emerged as the better match to natural hemicalide compared to the 13,18-*anti* carboxylate **223** (**Entry 2 vs. 4**). However, it was also clear that the anion had a worse correlation than the free acid for both the 13,18-*syn* and 13,18-*anti* series (**Entries 1 vs. 2, 3 vs. 4**), thus contradicting Ardisson's results.

Entry	Compound	Sum $\|\Delta\delta_H\|$	Max $\|\Delta\delta_H\|$	Sum $\|\Delta\delta_C\|$	Max $\|\Delta\delta_C\|$
1	**13,18-*syn* acid 220**	**0.05**	**0.01**	**0.8**	**0.1**
2	13,18-*syn* salt **222**	0.08	0.02	1.7	0.2
3	13,18-*anti* acid **221**	0.22	0.04	4.1	0.6
4	13,18-*anti* salt **223**	0.22	0.04	4.3	0.7
5	Cossy acid **94**	0.26	0.04	3.8	0.5

Table 8: Tabulated values for the sum of errors and maximum errors in the ^{1}H and ^{13}C NMR spectra of 13,18-*syn* acid **220**, 13,18-*syn* salt **222**, 13,18-*anti* acid **221** and 13,18-*anti* salt **223** as well as Cossy's subunit **94**

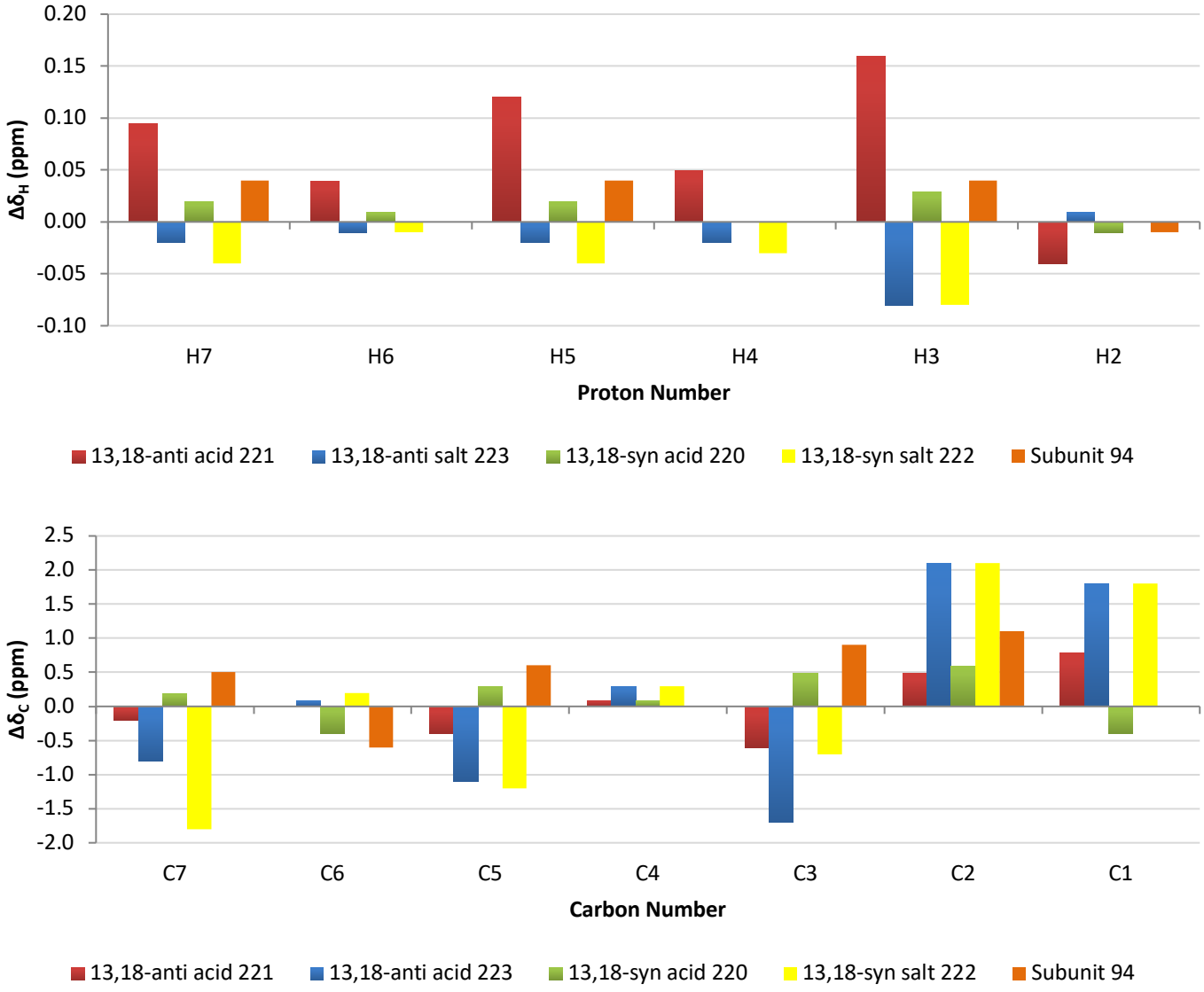

Figure 38: NMR correlations of the 13,18-*syn* acid **220**, 13,18-*syn* salt **222**, 13,18-*anti* acid **221** and 13,18-*anti* salt **223** compared against the Ardisson fragment **94** in the C1-C7 trienic region

The electronic properties of the C1 carboxyl group had a substantial influence on the chemical shifts of C1-C7 but otherwise did not significantly affect the resonances from C8 onwards. If only considering the C1-7 region, it would appear that neither 13,18-*syn* carboxylate **222** nor 13,18-*anti* carboxylate **223** correlate well with natural hemicalide, with both compounds performing worse than the carboxylic acids **220** and **221** again (**Figure 38**).

Lam proposed that the precise chemical shifts of the C1-C7 region depended on the protonation state of the free acid.[71] Even the slightest trace of acetic acid, which was used as an eluent additive during chromatographic purification of the free acid, could cause the ^{1}H NMR resonances to drift in an irreproducible fashion.

When free acids **220** and **221** were in a strongly acidic environment, such as post-HCl workup, or fully deprotonated with Na_2CO_3, all resonances appeared sharp. When the spectra were recorded post-chromatography, the signals were sometimes observed to broaden, particularly in the ^{13}C NMR spectra for C1, C2 and C3 in acid **220**.[71] This was attributed to the rapid auto-ionisation equilibrium of the free acid.

These results suggest that the NMR spectra of natural hemicalide were in fact acquired as a carboxylic acid rather than the carboxylate salt as suggested by Ardisson. However, the sensitivity of the resonances relating to C1-C7 towards the pH of the NMR sample makes this region unreliable for any future NMR correlation study.

3.5 Conclusions

The revised fragment coupling strategy now features a convergent synthetic route to the C1-C28 intermediate ***ent*-99** spanning 19 steps in the longest linear sequence with an overall yield of 2.9% (**Scheme 52**).[113] This is a productive intermediate that can be used in a planned boron-mediated aldol reaction to forge the C28-C29 bond to assemble the full carbon and oxygen skeleton of hemicalide.

Various stereochemical and structural corrections have also been made in this region of hemicalide with the aid of NMR spectroscopic analysis. Most notably, the 18,19-*anti* relationship has been reassigned to 18,19-*syn* and the 13,18-*anti* relationship also reassigned to 13,18-*syn* as indicated in structure **220**. Furthermore, the C1 carboxyl group has also been reassigned from a carboxylate salt to a carboxylic acid (**Figure 39**).[113]

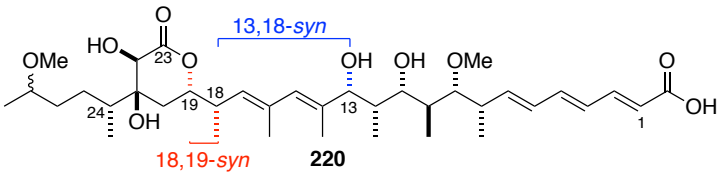

Figure 39: Final revised relative stereochemistry in the C1-C28 region of hemicalide

CHAPTER FOUR: BEYOND THE C1-C28 REGION

4.1 DP4 Analysis and Application to the C26-C35 Region

The use of *ab initio* calculations of NMR chemical shifts has been central to the Paterson group's approach towards the total synthesis of hemicalide. In particular, it was instrumental in identifying the misassigned 18,19-*anti* stereochemistry in the absence of any further experimental evidence at the time.[36]

Previous attempts by MacGregor to study the C26-C35 region of hemicalide were met with inconclusive results.[37] The low quality of the experimental NMR data has been suggested as one possible reason. In the ^{1}H NMR spectrum of natural hemicalide, there is a broad 22H multiplet spanning 2.02-1.22 ppm, encompassing H26, H28, H30, H32, H33.[1] All of these signals were recorded as 1.62 ppm, the midpoint of the multiplet, as the experimental value. Without access to various 2D NMR spectra of hemicalide, it is not possible to refine their chemical shifts further. This has consequences for the scaling factor employed to arrive at the corrected predicted chemical shift values.[26] The inadequacies of the experimental data can be mitigated by synthesising a library of fragments (**Figure 40**) alongside their virtual counterparts. While it still may not be possible to completely resolve the afflicted resonances, we expect to be able to find more accurate values for their chemical shifts, hence improving the scaling factor used in the computational work to refine the DP4 predictions for this region.

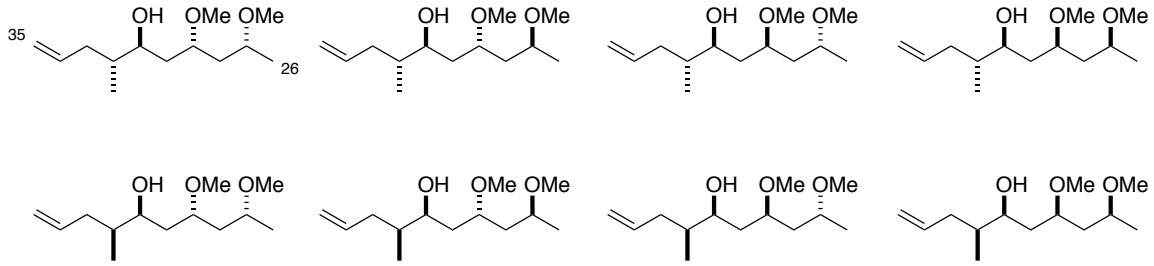

Figure 40: Library of fragments for the C26-C35 region of hemicalide

Synthesising a library of fragments in this region of hemicalide also provides an opportunity to study the planned aldol reaction that will be used to couple the C1-C28 fragment ***ent*-99** to the remainder of the molecule, along with relevant functional group manipulations.

4.2 Towards the synthesis of a library of fragments for the C26-C35 region

The synthesis of the library fragments commenced with the lithium aldol reaction of ethyl acetate and methacrolein to give racemic aldol adduct **224** (**Scheme 57**). The allylic alcohol functionality in **224** enables a kinetic resolution[114] *via* a Sharpless asymmetric epoxidation[115] to obtain enantioenriched **224** if required. However, this was not pursued as the DP4 analysis only distinguishes between diastereomers but not enantiomers. Following a silyl protection of the C31 hydroxyl group (TBSCl, imidazole), a controlled reduction of ester **225** to aldehyde **226** with DIBAL was carried out at –78 °C (84% over two steps).

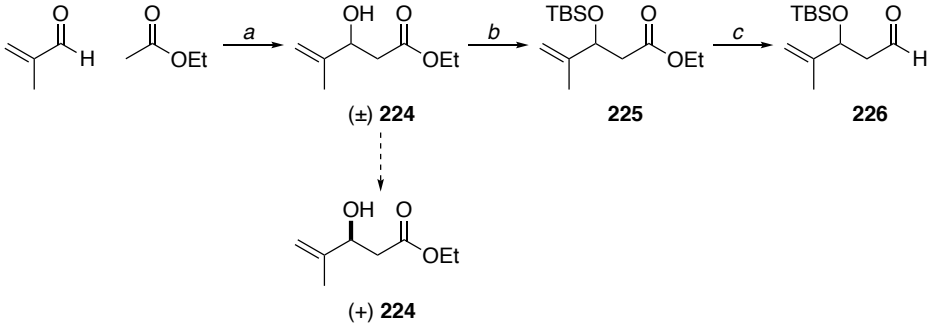

Reagents and conditions: (a) LDA, EtOAc, THF, –78 °C, *then* methacrolein, –78 °C, 93%; (b) TBSCl, imidazole, CH_2Cl_2, rt, 88%; (c) DIBAL, CH_2Cl_2, –78 °C, 95%

Scheme 57: Synthesis of aldol adduct **226** from aldol adduct **224**

By using the silyl enol ether derived from acetone as a surrogate for the C1-C28 truncates, a Mukaiyama aldol reaction[116] with aldehyde **226** was investigated. The use of BF_3•Et_2O delivered the presumed 1,3-*anti* product **227** (*vide infra*) with a *d.r.* of 5:1 in 78% yield (**Table 9, Entry 1**). Lowering the temperature to –100 °C did not improve the diastereoselectivity (**Entry 2**). Other Lewis acids were also screened for the Mukaiyama aldol reaction but none were superior to BF_3•Et_2O in terms of stereoselectivity (**Entries 3-5**).

Non-Mukaiyama aldol conditions were also investigated in parallel. The use of LDA gave a poorer *d.r.* than BF_3•Et_2O, while a boron-mediated aldol had the lowest *d.r.* and in the opposite sense as well (**Table 9, Entries 6-7**). The epimeric products **227** and **228** could not be separated at this stage nor any point further downstream. With this in mind, the use of chiral Ipc ligands for the aldol reaction may be required when incorporating this fragment coupling strategy into the planned synthesis of hemicalide to ensure a synthetically useful level of stereocontrol.

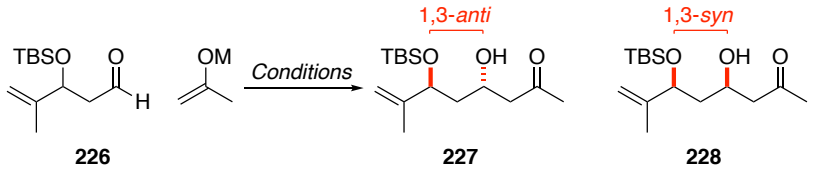

Entry	M	Conditions	Temperature	Result (**227**:**228**)
1	$SiMe_3$	BF_3•Et_2O,	–78 °C	*d.r.* 5:1
2	$SiMe_3$	BF_3•Et_2O	–100 °C	*d.r.* 5:1
3	$SiMe_3$	$TiCl_4$	–78 °C	*d.r.* 3:1
4	$SiMe_3$	Me_2AlCl	–78 °C	*d.r.* 2:1
5	$SiMe_3$	$MeAlCl_2$	–78 °C	*d.r.* 2:1
6	Li	LDA	–78 °C	*d.r.* 4:1
7	BCy_2	Cy_2BCl, Et_3N	–78 °C	*d.r.* 1:2

Table 9: Conditions examined for the aldol reaction with aldehyde **226**

As aldol adduct **227** was formed as a racemate, the Mosher ester analysis[81–83] could not be used to verify the configuration of C29. Instead, the stereochemistry of the aldol adduct **227** was probed by deprotecting the TBS group to trigger *in situ* cyclisation (**Scheme 58**). The configuration at C29 could then be studied through the relevant ^1H–^1H coupling constants and nOe interactions in the expected hemiacetals **229** and **230**. Disappointingly, various attempts to do so either led to complex mixtures (aq. HCl or HF•py/py) or the formation of acetal **231** as a single diastereomer ($HC(OMe)_3$, CSA, MeOH). The stereoconvergence can be rationalised by a rapid and reversible $E1_{cb}$/conjugate addition of MeOH prior to acetal formation, leading to **231** as the thermodynamic product.

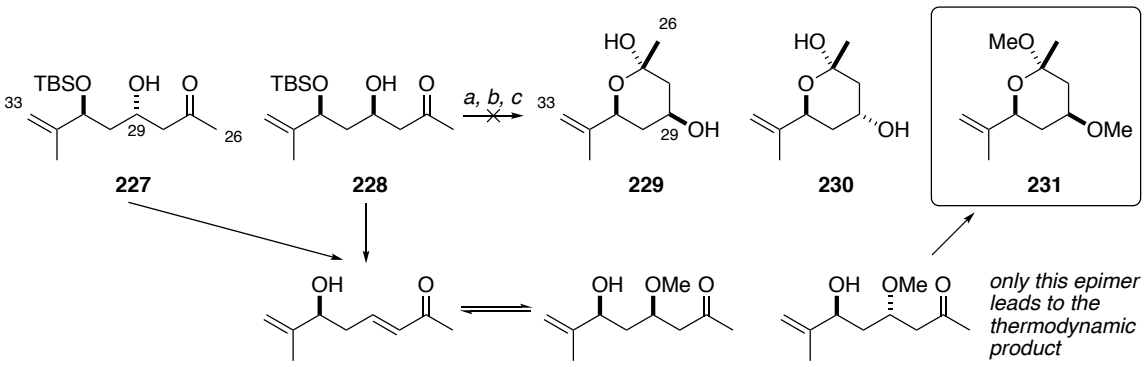

Reagents and conditions: (a) $HC(OMe)_3$, CSA, MeOH, rt; (b) HCl (aq.), THF, rt; (c) HF•py/py, THF, rt

Scheme 58: Attempted formation of hemiacetal **229** to probe the stereochemistry of aldol adduct **227**

The results of the aldol reaction screening indicate that an open transition state, by employing Mukaiyama conditions, offers the best diastereoselectivity. Despite a failure to secure definitive proof of the C29 stereochemistry, it was assumed that the 1,3-*anti* stereoinduction was in accordance with the Evans polar model (**Scheme 59**).[117] The reactive conformer for the aldehyde has the OTBS group pointing away from the carbonyl to oppose its dipoles, where **TS-XVIII** is the lower energy transition state by having the small H group at the β position point into the carbonyl, leading to **227** as the major product. The expected *anti* diastereoselectivity is in agreement with various examples in the literature, such as Evans' stereochemical studies[117] on **232** and **233** as well as Hsung's synthesis[118] of intermediates **234** and **235** while investigating spirastrellolide A (**Scheme 60**).

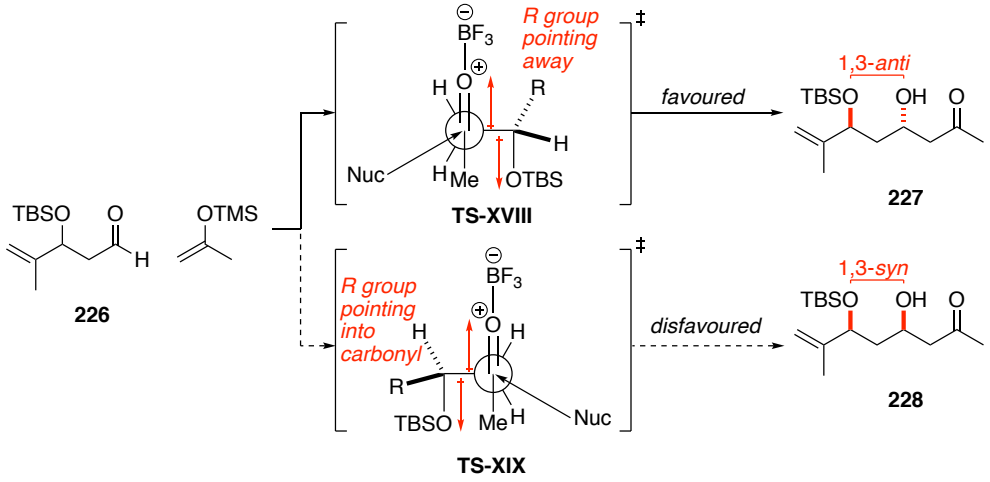

Scheme 59: Evans polar model for the Mukaiyama aldol reaction of aldehyde **226**

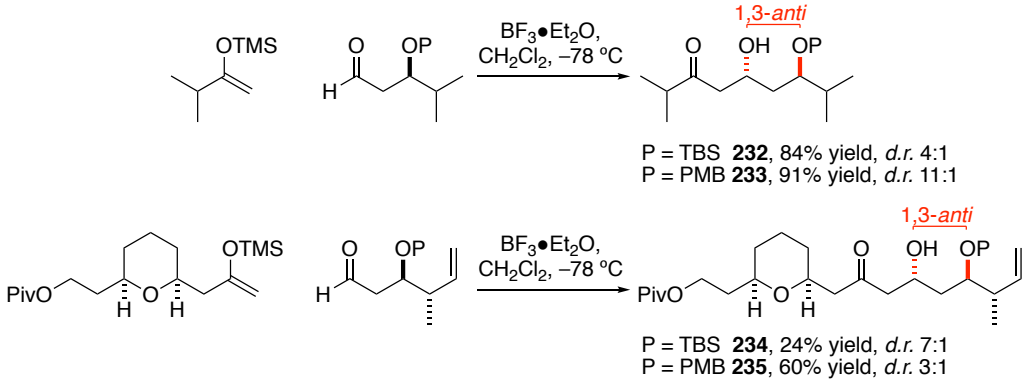

Scheme 60: Examples of diastereoselective Mukaiyama aldols operating solely under 1,3-stereoinduction

Aldol adduct **227** could be elaborated in two complementary ways to obtain either a 1,3-*syn* diol or 1,3-*anti* diol. By performing a Narasaka reduction[119] (Cy_2BCl, $LiBH_3(OMe)$),[120] 1,3-*syn* diol **236** was obtained as a single diastereomer (**Scheme 61**). The boron Lewis acid chelates to the

hydroxyl group and the ketone, allowing the molecule to adopt a half-chair conformation in **TS-** where hydride delivery is expected to occur from an axial approach.

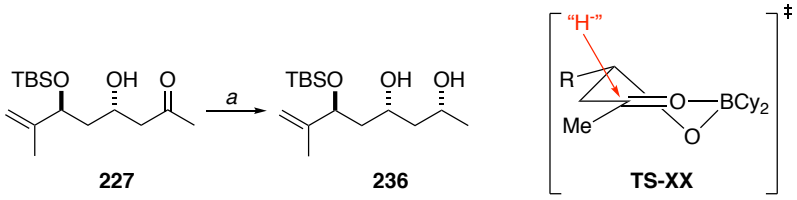

Reagents and conditions: (a) Cy_2BCl, Et_3N, THF, –78 °C, *then* $LiBH_3OMe$, –78 °C → 0 °C, 82%

Scheme 61: Narasaka reduction of aldol adduct **227**

In contrast, submitting aldol adduct **227** to an Evans-Tischenko reduction[121] (SmI_2, EtCHO) followed by ester cleavage (K_2CO_3, MeOH) furnished the 1,3-*anti* diol **237** with a *d.r.* of 10:1. The active catalytic species is believed to be a Sm(III) species **238** arising from a pinacol reaction between EtCHO and SmI_2. The free hydroxyl group then forms a hemiacetal with EtCHO and chelates to the Sm Lewis acid, leading to a highly organised transition state **TS-XXI** with all substituents in the equatorial position. This allows for an intramolecular delivery of hydride to account for the *anti* diastereoselectivity (**Scheme 62**).

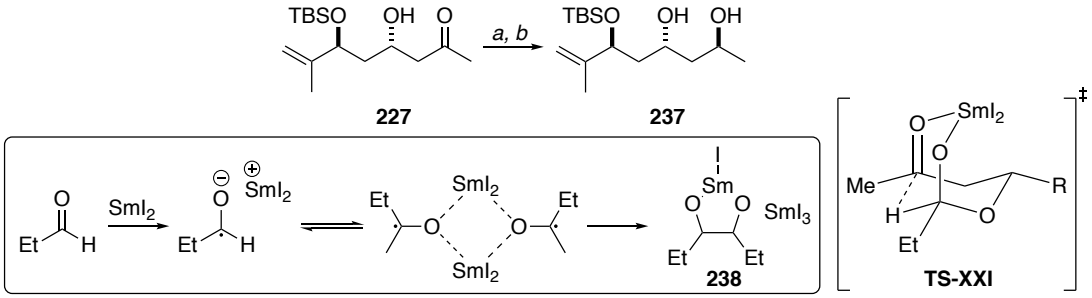

Reagents and conditions: (a) SmI_2, EtCHO, THF, rt; (b) K_2CO_3, MeOH, rt, 89% over two steps

Scheme 62: Evans-Tischenko reduction of aldol adduct **227** followed by acyl cleavage

By forming acetonides **239** and **240**, the relative configuration of diols **236** and **237** could be confirmed with the Rychnovsky method (**Scheme 63**).[122,123] 1,3-*syn* acetonides are known to take up a chair conformation with one of the acetal methyl groups axial and the other equatorial. These methyl groups are expected to have different ^{13}C NMR chemical shifts (*ca*. 20 ppm and 30 ppm respectively). In contrast, 1,3-*anti* acetonides adopt a twist-boat conformation where both acetal methyl groups are in quasi-identical environments, hence displaying similar ^{13}C chemical shifts (*ca*. 24 ppm). Inspection of the ^{13}C NMR of acetonides **239** and **240** indicated resonances that are characteristic of their respective *syn* and *anti* stereochemistry, thus validating the diastereoselective nature of the Narasaka reduction[119] and the Evans-Tischenko reduction.[121] Both 1,3-*syn* diol **237** and 1,3-*anti* diol **238** could also be *bis*-methylated (NaH, MeI)

uneventfully to give **241** and **242** respectively to set the stage for chain extension beyond C33 (**Scheme 63**).

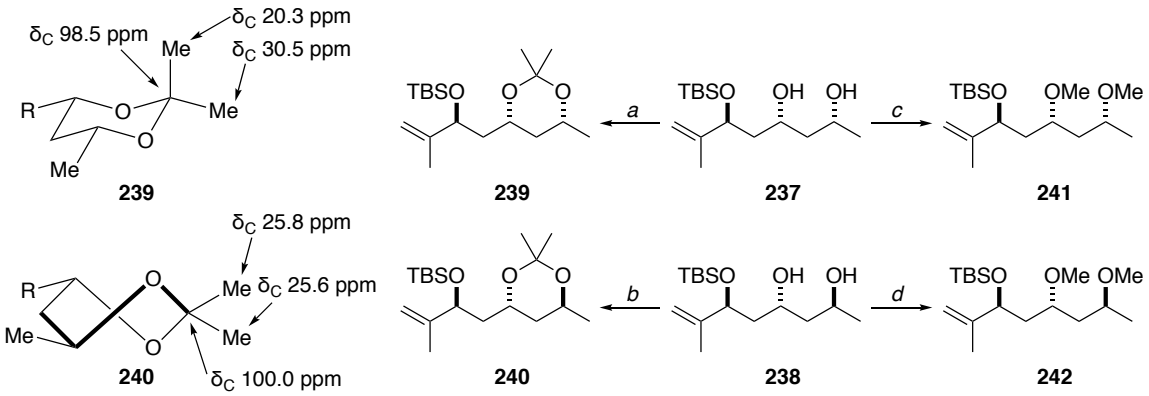

Reagents and conditions: (a) PPTS, $CMe_2(OMe)_2$, rt, 95%; (b) NaH, THF, 0 °C, *then* MeI, 0 °C → rt, 93%; (c) PPTS, $CMe_2(OMe)_2$, rt, 96%; (d) NaH, THF, 0 °C, *then* MeI, 0 °C → rt, 90%

Scheme 63: Formation of acetonides **239** and **240** and *bis*-methyl ethers **241** and **242**

It was envisaged that a hydroboration could be used to configure the final stereocentre in this fragment as well as provide a borane handle for a subsequent sp^2-sp^3 Suzuki coupling.[56] This is an attractive solution for many challenging natural product syntheses for its reliability. First discovered by Suzuki and Miyaura in 1986, this palladium-catalysed union of alkyl boranes with vinyl halides is hailed for its chemoselectivity and mildness, including tolerance of aqueous conditions. The alkyl borane partner can be readily accessed *via* hydroboration of an olefin and telescoped into the Suzuki coupling without isolation. This was successfully carried out in Danishefsky's synthesis[124] of epothilone A to generate intermediate **245** (*via* vinyl iodide **243** and olefin **244**) and Paterson's second-generation synthesis[125] of spirastrellolide A methyl ester involving fragment **248** (*via* vinyl iodide **247** and olefin **246**) (**Scheme 64**).

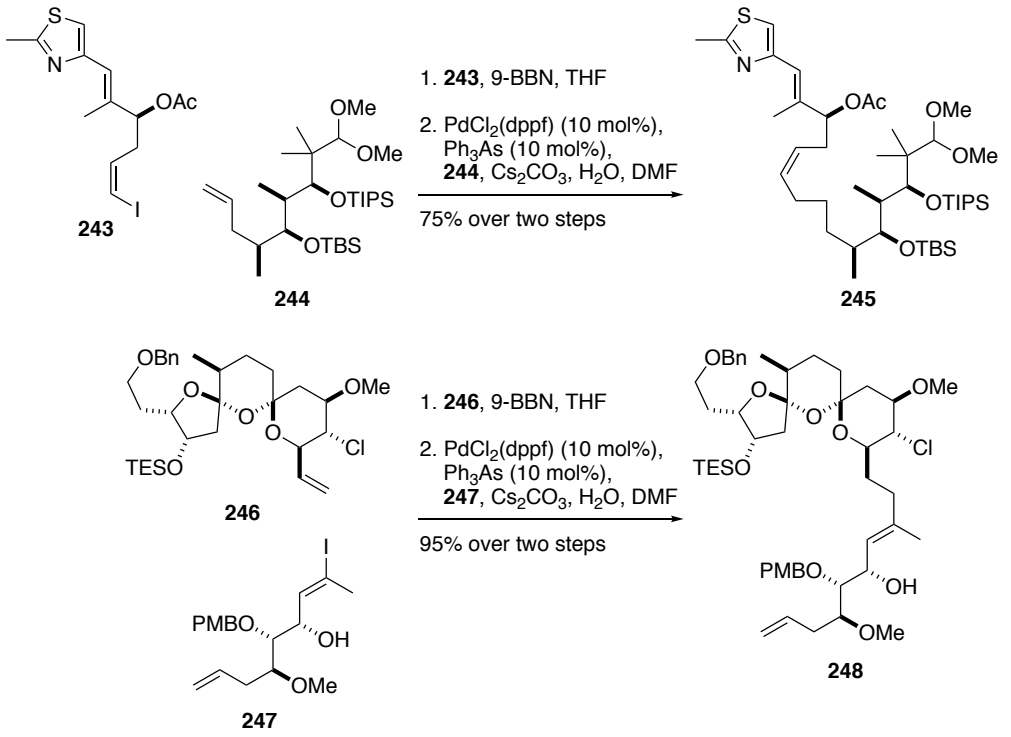

Scheme 64: Examples of a two-stage hydroboration-Suzuki coupling in total synthesis

The mechanism is thought to conform to the general catalytic cycle seen in palladium-catalysed cross couplings, involving the sequence of oxidative addition, transmetallation and reductive elimination (**Figure 41**). The Suzuki coupling is unique by requiring a base to activate the boron partner *via* a tetrahedral 'ate' complex, thus facilitating transmetallation. 9-BBN is an excellent choice of borane for the two-stage hydroboration-Suzuki coupling as its steric bulk enhances the regioselectivity of the hydroboration while the secondary alkyl ligands on boron transmetallate more slowly than the desired primary alkyl group.

Like all sp^2-sp^3 cross couplings, the sp^3 component is prone to β-hydride elimination (**Figure 41**). This can be overcome by employing the dppf ligand to accelerate the rate of reductive elimination relative to β-hydride elimination. The ligand's large bite angle also enforces a *cis* geometry around the sp^2 and sp^3 components, a geometrical requirement for the reductive elimination.

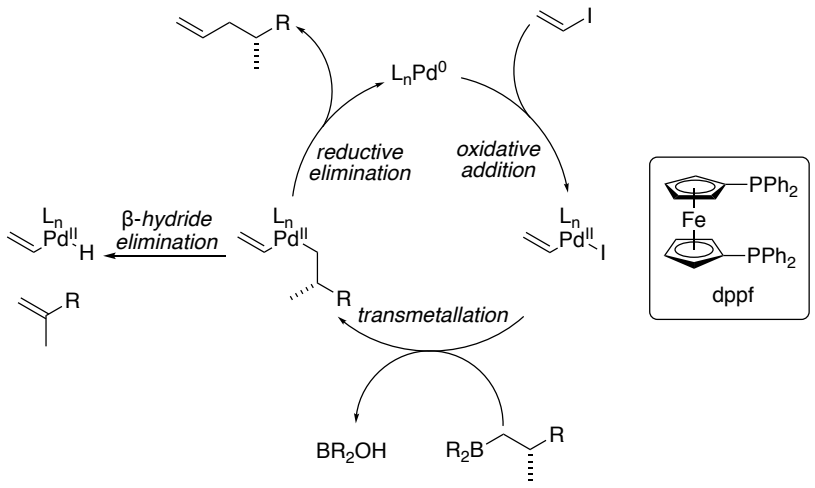

Figure 41: Mechanism of the Suzuki coupling

The hydroboration was first conducted on olefin **249** with 9-BBN as a model study, followed by oxidative workup of the borane intermediate **250** to verify the stereochemical outcome (**Scheme 65**). In the event, alcohol **251** was produced as a single diastereomer with the expected *anti* relative configuration and all spectroscopic data matched existing literature values.[126]

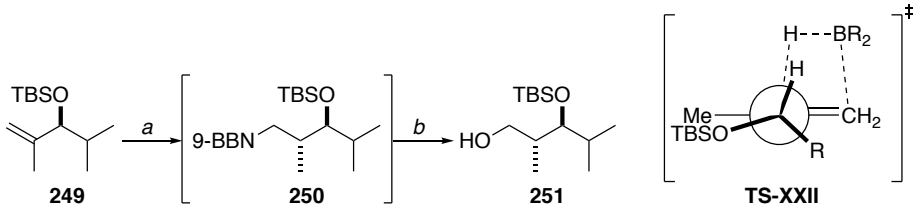

Reagents and conditions: (a) 9-BBN, THF, rt; (b) H_2O_2, NaOH, THF, 0 °C → rt, 63% over two steps

Scheme 65: Model hydroboration on TBS ether **249** with oxidative work-up

Kishi first suggested that the allylic chiral centre dictates the sense of stereoinduction by having the smallest group eclipse the olefin, thus biasing the reagent to approach *via* the medium group instead of the large group to minimise steric hindrance.[102] Additional computational work undertaken by Houk led to a revised model which takes into account further stereoelectronic parameters.[127] As the olefin becomes more electron deficient in the transition state **TS-XXII**, the molecule adopts a conformation where the C–O σ* bond of the TBS group is orthogonal to the C=C π bond to minimise further electron density withdrawal. The borane reagent then approaches from the less hindered face of the olefin, leading to the observed *anti* diastereoselectivity.

With confidence that the hydroboration result was reproducible, it was performed again on olefin **241** but this time telescoped into the Suzuki coupling with vinyl iodide (**Scheme 66**). Unfortunately, applying these conditions to **241** only resulted in 50% conversion to the desired

product **253** and any unreacted **241** could not be separated from **253** by chromatography. The hydroboration proved difficult to monitor by TLC due to the instability of borane **252** on silica. Presumably, the extended carbon chain in **241** adopts a conformation that presents extra steric bulk to the olefin, thus slowing down hydroboration. Although a β-hydride elimination pathway during the reaction would regenerate the starting material **241**, the use of the dppf ligand in this reaction should suppress this. Due to a lack of time, this reaction could not be fully investigated prior to the conclusion of this project.

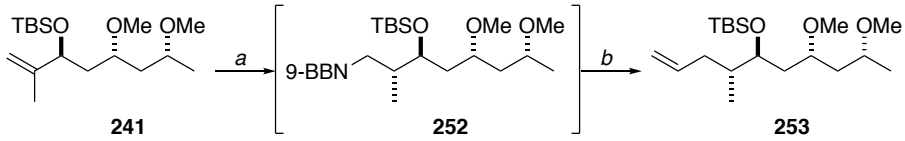

241 **252** **253**

Reagents and conditions: (a) 9-BBN, THF, rt; (b) $PdCl_2$(dppf), Ph_3As, CH_2=CHI, Cs_2CO_3, H_2O/DMF, rt, yield N.C.

Scheme 66: Two stage hydroboration-Suzuki coupling performed on olefin **241**

4.3 Conclusions

This study has led to the successful synthesis of several mid-stage to late-stage key intermediates for hemicalide, culminating in the synthesis of the advanced C1-C28 fragment ***ent*-99**.

Work on the C1-C15 fragment **101** has been complementary to MacGregor's established route[37] in both enantiomeric series and improvements have been made in several areas to enable a gram scale synthesis. This route features several highly diastereoselective key reactions which installs all but one stereocentre in the contiguous stereohexad. This work further demonstrates the synthetic utility of boron-mediated aldol reactions for their excellent and reliable levels of stereoinduction under mild conditions (**Scheme 67**).

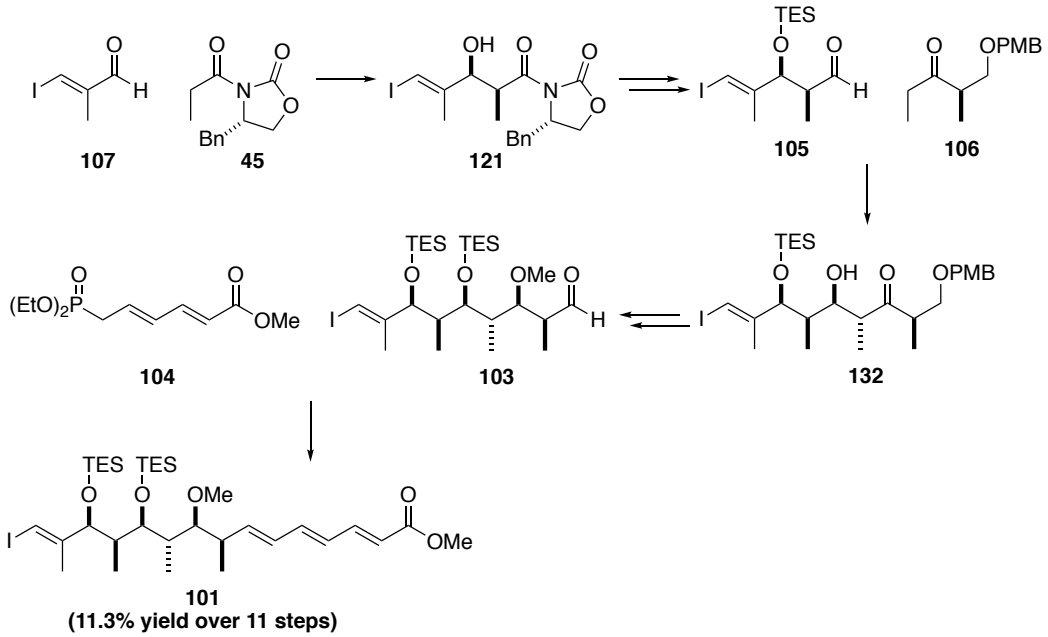

Scheme 67: Summary of the synthesis of C1-C15 intermediate **101** from building blocks **107**, **45** and **106**

For the C16-C28 fragment **102**, synthetic efforts have successfully accessed the final intermediate **102**. Modifications from MacGregor's established route[37] involve a change in choice of protecting group for the ketone in the aldol reaction, as well as other relevant downstream intermediates. The diastereoselectivity of the aldol reaction was also enhanced through the use of chiral ligands. Further improvements were also made in the dehydration and dihydroxylation reactions. A stereochemical reassignment of the proposed 18,19-*anti* relationship by Ardisson to 18,19-*syn* was successfully conducted by using diene **202** for NMR correlation studies (**Scheme 68**).[36] The Cossy group subsequently revisited their earlier work and concurred with our reassigned 18,19-*syn* relationship.[63]

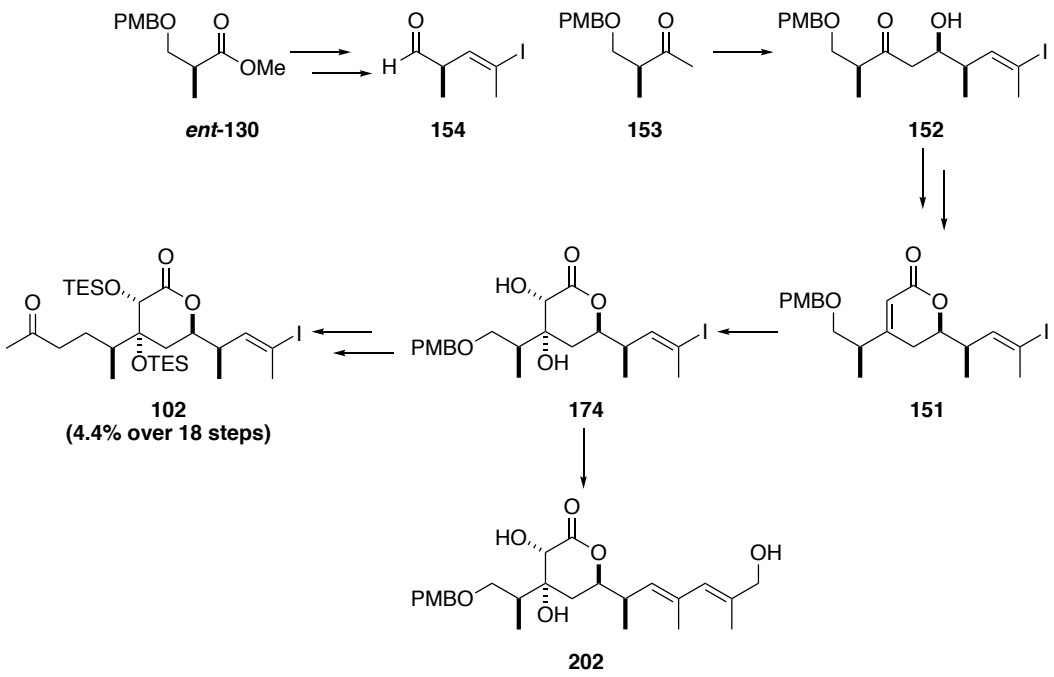

Scheme 68: Summary of the synthesis of C16-C28 intermediate **102** and diene **202** from building blocks ***ent*-130** and **153**

Fragment union strategies leading to the C1-C28 fragment ***ent*-100** have also been explored (**Scheme 69**). To maximise convergency, the C1-C15 fragment **101** was transformed into vinyl stannane **211** in a Wulff-Stille reaction, followed by a modified Stille coupling with C16-C28 vinyl iodide ***ent*-102**. In conjunction with co-worker Lam,[71] this led to the generation of two diastereomeric truncates, 13,18-*syn* **220** and 13,18-*anti* **221** in good yield. Further derivatisation and NMR correlation studies indicated that the 13,18-*syn* diastereomer **220** was an exceedingly good match for natural hemicalide, pointing towards the likely relative configuration between the two distal stereoclusters.[113] To date, the Cossy group has only worked in the 13,18-*anti* series without any rationalisation.

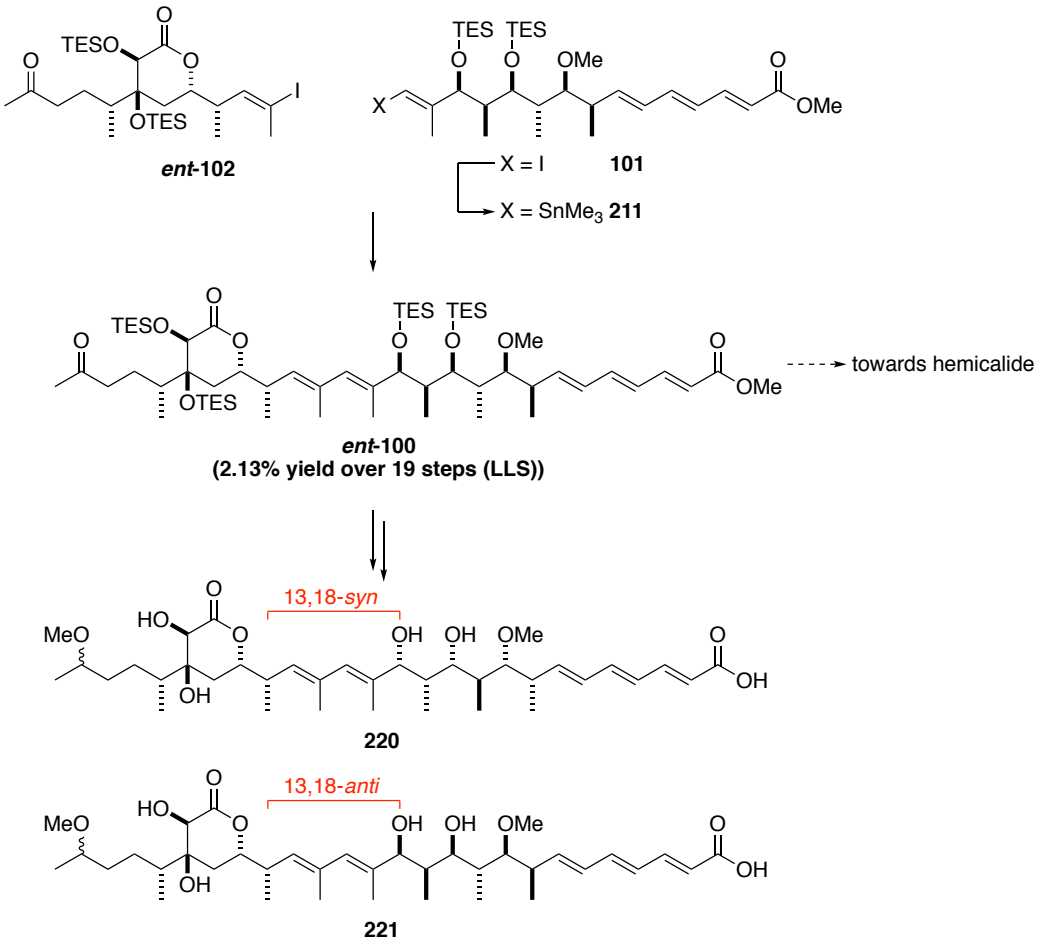

Scheme 69: Summary of the synthesis of 13,18-*anti* C1-C28 truncate ***ent*-100** and its derivatisation into **221** for NMR correlation studies alongside subunit **220**

To aid the computational work on the C27-C35 region of hemicalide, a library of fragments will be synthesised to help improve *ab initio* NMR predictions. This objective will allow more robust DP4 probabilities to be obtained regarding the most likely stereochemistry in this region. Currently, diastereoselective reactions to configure three of the four stereocentres in this region have been developed (**Scheme 70**). Studies into this region have also provided valuable insight for the planned late-stage fragment coupling *via* an aldol reaction and a hydroboration-Suzuki coupling.

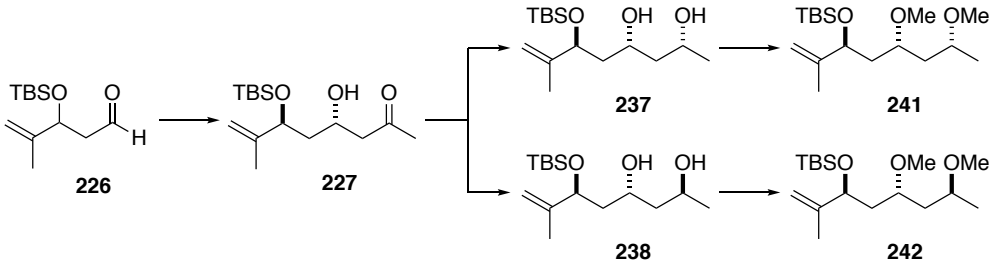

Scheme 70: Summary of the synthesis of two intermediates **241** and **242** towards a library of eight diastereomeric C26-C35 fragments

4.4 Future Work

Having developed a successful synthesis to access the C1-C28 methyl ketone subunit, attention should now be directed towards the C29-C46 section, featuring the α-hydroxylactone. Preliminary investigations into this region have been undertaken by Stockdale.[128]

The synthesis of the α-hydroxylactone begins with a reagent-controlled aldol reaction between ketone ***ent*-153** and aldehyde **254**, both obtained from the corresponding enantiomer of Roche ester in three steps, mediated by (+)-DIPCl. In the absence of chiral Ipc ligands, the reaction has been shown to proceed with a modest *d.r.* of 2:1. Following a TBS protection, intermediate **255** was further elaborated to the α,β-unsaturated δ-lactone **256** in an analogous fashion to the C16-C28 fragment. Configuring the C39 stereocentre remains a bottleneck in this route as most conjugate reduction strategies either deliver the undesired epimer or show no reactivity (**Scheme 71**).

Investigations into the reduction of the α,β-unsaturated lactone have now focused on a hydroxyl-directed hydrogenation. This can be achieved by removing the PMB group with DDQ and using Crabtree's catalyst[61] under an atmosphere of hydrogen gas. Intermediate **257** can then be further functionalised by a two step sequence of DMP-mediated oxidation[46] and a HWE olefination[91] with phosphonate **190** to reach the C46 terminus. A CBS reduction[112] using catalyst **258** can be conducted on enone **259** to configure C45 because of the large steric differentiation between the C46 methyl group and the C43-C44 olefin. A diastereoselective α-oxidation at C40 with the Davis oxaziridine[60] **260**, followed by *bis*-TES protection then affords intermediate **261**. Catalytic hydrogenation of the C43-C44 olefin should also effect concomitant benzyl deprotection before exposure to DMP to reveal aldehyde **262** as a key intermediate. A Takai olefination[129] would then generate vinyl iodide **263** in a single transformation but other olefination methods may also be explored at this stage (**Scheme 71**).

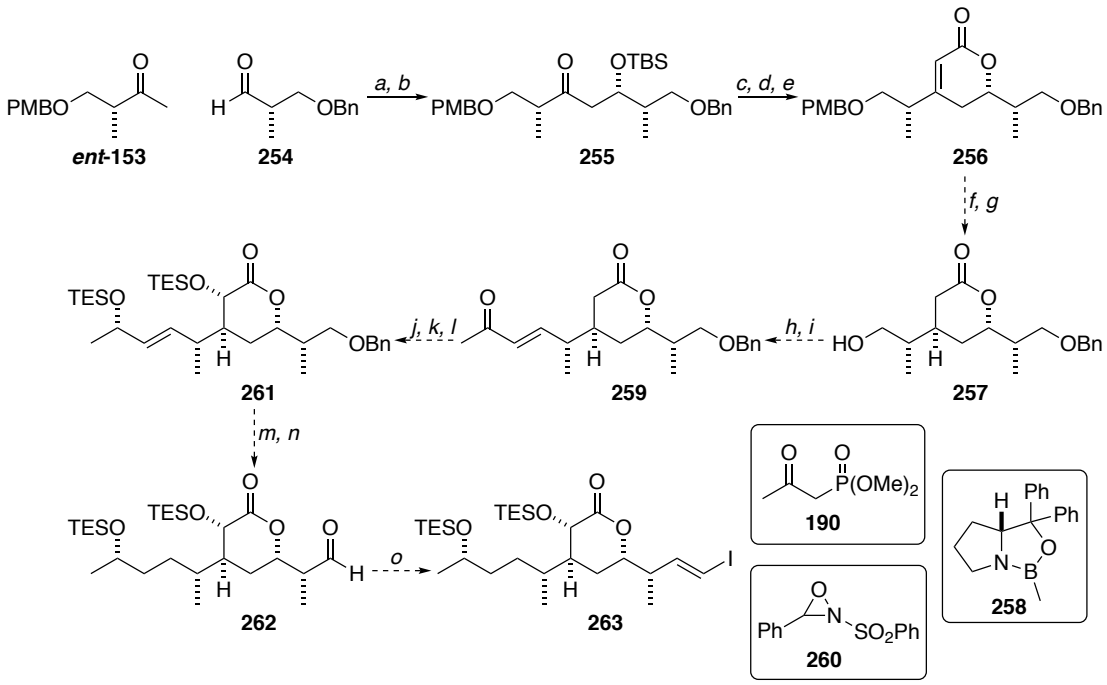

Reagents and conditions: (a) ***ent*-153**, (+)-DIPCl, Et_3N, Et_2O, 0 °C, *then* **250**, –78 °C → –20 °C, 79% (*d.r.* >20:1); (b) TBSOTf, 2,6-lutidine, CH_2Cl_2, –78 °C, 81%; (c) LDA, EtOAc, THF, –78 °C, 99%; (d) TsOH•□□□, MeOH, rt, 94%; (e) Ac_2O, DMAP, py, PhH, 125 °C, 90%; (f) DDQ, CH_2Cl_2/pH 7 buffer, 0 °C → rt; (g) H_2 (1 atm), $[Ir(COD)(PCy_3)(py)]PF_6$ (cat.), CH_2Cl_2, rt; (h) DMP, $NaHCO_3$, CH_2Cl_2, rt; (i) **190**, $Ba(OH)_2$, THF, rt, *then* **253**, 0 °C → rt; (j) BH_3•SMe_2, **254** (cat.), THF; (k) LiHMDS, **256**, THF, –78 °C; (l) TESOTf, 2,6-lutidine, CH_2Cl_2; –78 °C; (m) H_2 (1 atm), Pd/C, MeOH, rt; (n) DMP, $NaHCO_3$, CH_2Cl_2, rt; (o) CHI_3, $CrCl_2$, THF, 0 °C

Scheme 71: Planned synthesis of intermediate **259** by Stockdale

Synthetic studies into the flexible C27-C35 polyacetate region for computational input have currently paused at the penultimate *anti* hydroboration-Suzuki coupling stage. Further investigations will need to address the slow conversion of olefin **241** into borane **252**. Protocols for performing a *syn* hydroboration will also require exploration, including a rhodium-catalysed process[130] to yield **265**, or a hydroxyl-directed reaction with **266** leading to **268** (**Scheme 72**). Alternatively, the synthesis could be redesigned to allow for a lithium-halogen exchange with iodide **269**, followed by trapping with 9-BBN-OMe to access borane **252**. This modification would require C32 to be configured at an earlier stage.

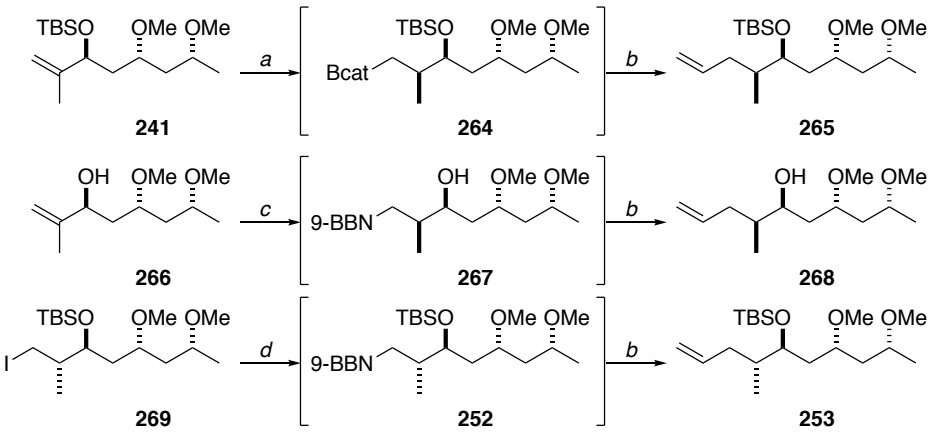

Reagents and conditions: (a) $Rh(PPh_3)_3Cl$, catecholborane, THF, rt; (b) $PdCl_2(dppf)$, Ph_3As, CH_2=CHI, Cs_2CO_3, H_2O/DMF, rt; (c) 9-BBN, THF, rt; (d) t-BuLi, THF, –78 °C, *then* 9-BBN-OMe, –78 °C

Scheme 72: Other methods for accessing *syn* and *anti* alkyl boranes

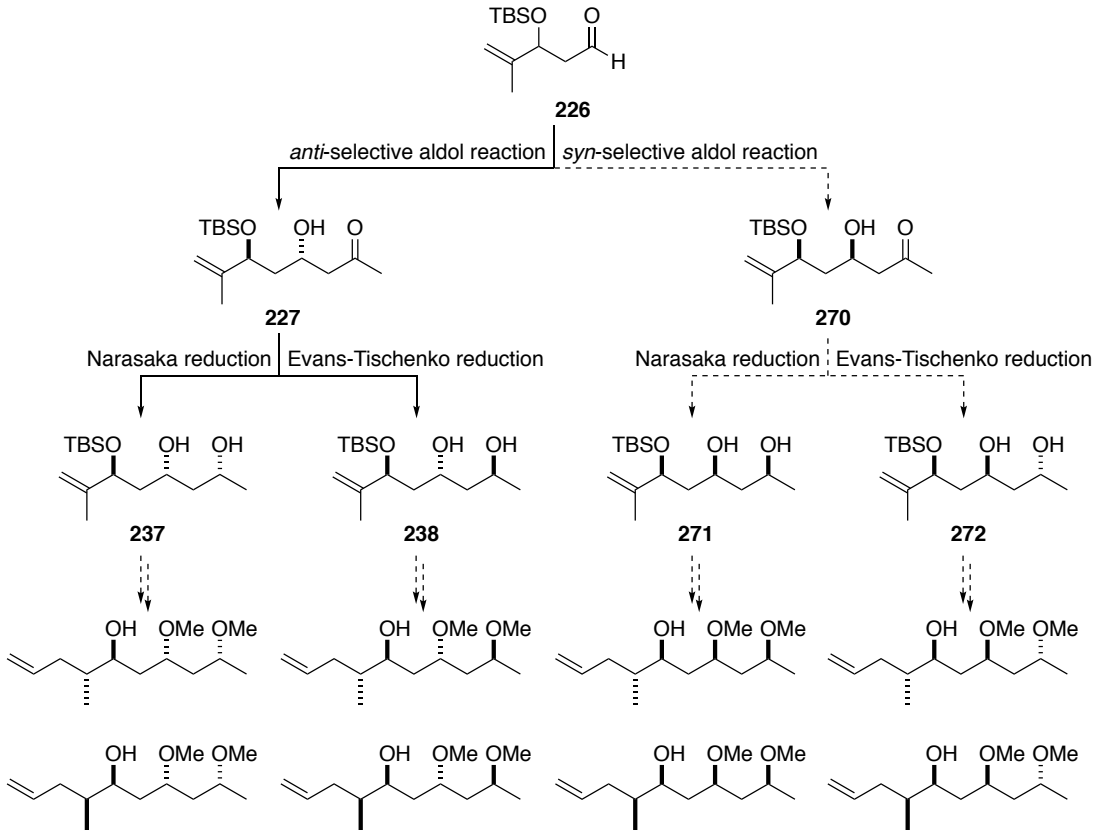

Scheme 73: Planned completion of the library of C26-C35 fragments

To synthesise a full library of fragments, a *syn*-selective aldol reaction of aldehyde **226** needs to be developed to complement the *anti*-selective Mukaiyama aldol. Subsequent elaboration of the *syn* aldol adduct **270** to the diols **271** and **272** will then be analogous to the established route in the *anti* series (**Scheme 73**). Having access to the complete set of fragments will be useful in reducing the number of possible diastereomers in this region. This will greatly simplify the

endgame for the total synthesis of hemicalide as the final bond constructions take place in this region.

The endgame strategy for hemicalide involves a telescoped hydroboration-Suzuki coupling of olefin **263** with the C34-C46 fragment **273** to arrive at fragment **274**. A selective deprotection of the primary TES ether at C29 followed by a mild oxidation will lead to aldehyde **275** which can then be coupled with the C1-C28 fragment ***ent*-99** in a boron-mediated aldol reaction. The final stereocentre can be set by a stereoselective reduction to give diol **276**. Finally, a *bis*-methylation and global deprotection will give one possible diastereomer of hemicalide **277** (**Scheme 74**).

Without any further stereochemical information about the C29-C46 region, several diastereomers of hemicalide will presumably have to be made in order to fully assign the relative configuration in the rest of the molecule. This can be achieved by using ***ent*-263** and ***ent*-273** during the hydroboration-Suzuki coupling step, as well as the complementary stereoselective methods for the hydroboration, boron-mediated aldol reaction and the subsequent reduction. A total of 16 diastereomers can be made in this fashion, representing a major synthetic effort. However, as computational efforts exponentially diminish in efficiency with increasing molecular size, total synthesis remains the most effective tool in validating a proposed structure.

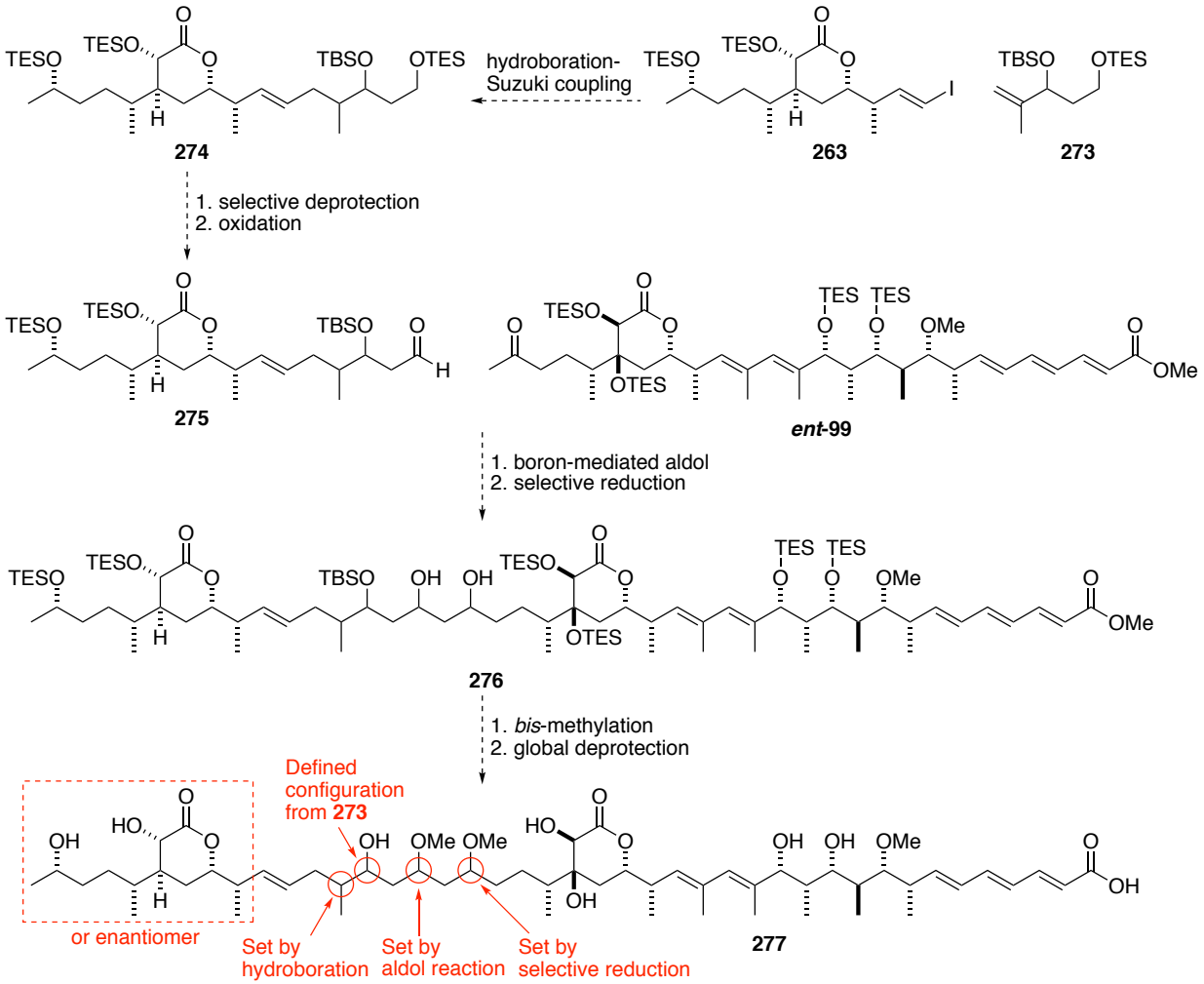

Scheme 74: Proposed endgame for the total synthesis of hemicalide

CHAPTER FIVE: EXPERIMENTAL

5.1 General Experimental Procedures

Reactions were carried out under an atmosphere of argon using oven dried glassware and standard techniques for handling air sensitive chemicals, unless the reaction contained aqueous reagents or unless otherwise stated.

Reagents were purified using standard laboratory procedures. Solvents used for extraction and chromatography were distilled. All solvents and reagents were distilled under an argon atmosphere. Where stated, solvents were degassed using the freeze–pump–thaw method. Benzene (PhH), cyclohexene, 1,5-cyclooctadiene, dichloromethane (CH_2Cl_2), diisopropylamine (i-Pr_2NH), acetonitrile (MeCN), *N*-methyl-2-pyrrolidone (NMP), oxalyl chloride ($COCl_2$), pyridine (py), toluene (PhMe), 2,6-lutidine, and triethylamine (Et_3N) were distilled from calcium hydride (CaH_2). Tetrahydrofuran (THF) and diethyl ether (Et_2O) were distilled from potassium and sodium wire/benzophenone ketyl radical respectively. Dimethyl sulfoxide (DMSO), *N,N*-dimethylformamide (DMF) and tributyltin chloride ($SnBu_3Cl$) were distilled from 4Å MS. Diisopropylethylamine (DIPEA) was first distilled from ninhydrin and then from CaH_2. DDQ was recrystallised from chloroform ($CHCl_3$), Proton Sponge® was recrystallised from methanol and NBS was recrystallised from water. Anhydrous barium hydroxide ($Ba(OH_2)$, lithium carbonate (Li_2CO_3) and lithium chloride (LiCl) were prepared by drying at 130 °C *in vacuo*. All other chemicals were used as received from the manufacturer unless otherwise stated.

Aqueous solutions of ammonium chloride (NH_4Cl), sodium bicarbonate ($NaHCO_3$), Rochelle's salt (Na/K tartrate), sodium thiosulfate ($Na_2S_2O_3$), sodium sulfite (Na_2SO_3) and brine (NaCl) were saturated.

Purification by flash column chromatography was carried out using Kieselgel 60 (230-400) mesh and a positive solvent pressure unless otherwise stated.

5.2 Analytical Procedures

TLC was carried out using Merck Kieselgel 60 F254 plates which were visualised using UV light (254 nm) and stained using potassium permanganate ($KMnO_4$) or phosphomolybdic acid/$Ce_2(SO_4)_3$ dips.

NMR spectra were recorded using the following machines: Bruker Avance BB500, Avance TCI-ATM 500 cryo and DRX400. ^1H NMR spectra were recorded at 298 K using an internal deuterium lock for $CDCl_3$ ($\delta_H = 7.26$). ^1H NMR data is presented as: chemical shift δ (in ppm, relative to TMS ($\delta_{TMS} = 0$), integration, multiplicity (s = singlet, d = doublet, t = triplet, q = quartet, qn = quintet, sx = sextet, m = multiplet, br = broad, obs = obscured) and coupling constants (*J* in Hz). Signals are assigned according to the numbering scheme for hemicalide (**Figure 1**) shown at the start of the data for that compound. Assignments were determined either on the basis of unambiguous chemical shift or coupling patterns, 2D NMR experiments, or by analogy to fully interpreted spectra for structurally related compounds. Protons of OH groups are missing in some spectra due to proton exchange. ^{13}C NMR spectra were recorded at 298 K with proton decoupling and an internal deuterium lock for $CDCl_3$ ($\delta_C = 77.0$) Data is listed by chemical shift (δ in ppm) relative to TMS ($\delta_{TMS} = 0$).

Fourier transform IR spectroscopy (FT-IR) was carried out using a Perkin-Elmer Spectrum One spectrometer and spectra were recorded as a thin film. Wavelengths of maximum absorption (ν_{max}) are reported in wavenumbers (cm^{-1}) and particularly broad (br) or weak (w) peaks are noted.

Optical rotations were measured using a Perkin-Elmer 241 polarimeter at the sodium D line (589 nm) and are reported as $[\alpha]_D^{20}$, concentration (*c* in g / 100 mL) and solvent.

High and low resolution mass spectra were recorded by the EPSRC Mass Spectrometry facility (Swansea, UK), using chemical ionisation (CI), electron impact (EI) or electron spray ionisation (ESI) techniques. The calculated and observed mass of the parent ion are quoted. High resolution values are calculated to 4 decimal places from the molecular formula.

5.3 Preparation of reagents used

Dibutylboron triflate (Bu_2BOTf)[132,133]

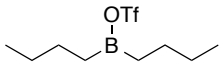

A two-neck flask was set up for distillation under reduced pressure and thoroughly dried. The setup was then carefully backfilled with argon and allowed to cool to rt. Tributylborane (16.3 mL, 66.63 mmol) was added to the two-neck flask, followed by a small portion of triflic acid (10 g, 66.63 mmol) with gentle warming to achieve a homogenous solution before adding the remaining triflic acid dropwise at rt to control the exothermic reaction. The reaction was left to stir for 45 min and distilled directly under reduced pressure (45 °C, 0.1 torr) to obtain Bu_2BOTf as a colourless oil (17.1 g, 61.3 mmol, 92%). This reagent is extremely moisture sensitive and was redistilled when any discolouration was observed.

Chlorodicyclohexylborane (Cy_2BCl)[134]

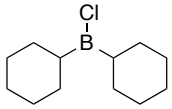

To a stirring solution of cyclohexene (40.0 mL, 400 mmol) in Et_2O (250 mL) at –10 °C was added dropwise $BH_2Cl{\bullet}SMe_2$ (20.6 ml, 200 mmol) over 30 min. The rate of addition was limited to control the rate of the highly exothermic reaction. The reaction mixture was allowed to warm to 0 °C and stirred for 1 h, then warmed to rt and stirred for a further 1 h. The solvent was removed by atmospheric distillation and then distillation under reduced pressure (95-97 °C, 0.3 torr) gave Cy_2BCl as a colourless liquid.

(–)-*B*-Chlorodiisopinocamphenylborane ((–)-Ipc_2BCl, (–)-DIPCl)[135]

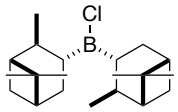

To a stirred solution of (+)-α-pinene (1.11 mL, 7.02 mmol) in Et_2O (1.88 mL) at –10 °C was added $BH_2Cl{\bullet}SMe_2$ (0.35 mL, 3.34 mmol). The mixture was stirred at 10 °C for 16 h to give a *ca.* 1.0 M solution of (–)-DIPCl.

9-Borabicyclo[3.3.1]nonane dimer (9-BBN)[136]

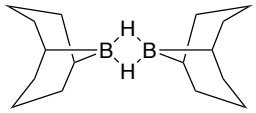

A three-neck flask equipped with a single-piece distillation apparatus, dropping funnel and thermometer was charged with BH_3•SMe_2 (15.3 mL, 153 mmol) and DME (50 mL). 1,5-cyclooctadiene (16.4 g, 152 mmol) was added *via* the dropping funnel over *ca*. 1 h, so as to maintain a steady reaction temperature of 50-60 °C. Following the addition, *ca*. 30 mL of the solution was distilled to reach a final distillation temperature of 85 °C, indicating the complete removal of SMe_2. Further DME was added to bring the total volumne to *ca*. 100 mL. The mixture was heated to effect dissolution of all solids and allowed to cool slowly to 0 °C. The supernatant was decanted, the product washed with ice-cold DME (100 mL) and dried *in vacuo* to provide 9-BBN dimer (13.2 g, 106 mmol, 70%) as large white needles.

Iodoxybenzoic acid (IBX)[137]

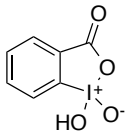

To a stirred solution of Oxone™ (181 g, 290 mmol) in water (650 mL) was added 2-iodobenzoic acid (50.0 g, 202 mmol) in one portion. The suspension was heated to 70 °C for 3 h, then cooled to –5 °C for 1.5 h. The solids were collected by filtration, washed with water (6 x 100 mL) and acetone (2 x 100 mL) and dried under vacuum for 12 h to afford IBX (39.8 g, 142 mmol, 70%) as a white powder.

Dess–Martin periodinane (DMP)[138]

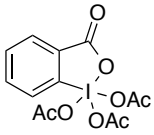

To a suspension of IBX (39.8 g, 142 mmol) in Ac_2O (160 mL) was added TsOH•H_2O (270 mg, 1.42 mmol) and the resulting mixture was heated to 85 °C for 2.5 h, then cooled to 0 °C for 1 h. The precipitate was collected by filtration, washed with Et_2O (5 x 30 mL) and dried under vacuum overnight to afford Dess–Martin periodinane (51.3 g, 121 mmol, 85%) as a white powder which was stored at 4 °C without appreciable deterioration.

4-Methoxybenzyl 2,2,2-trichloroacetimidate (PMBTCA)[131]

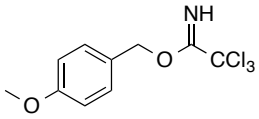

To a vigorously stirring solution of aq. KOH (50% w/v, 130 mL) at rt was added a solution of 4-methoxybenzyl alcohol (18.0 g, 130 mmol) in CH_2Cl_2 (130 mL) followed by NBu_4HSO_4 (4.4 g, 13.0 mmol). Cl_3CCN (14.3 mL, 143 mmol) was added dropwise over 20 min and the reaction left to stir for 1 h while warming to rt. Upon completion, the phases were separated and the aqueous layer extracted with Et_2O (3 x 80 mL). The combined organic extracts were washed with brine (50 mL), dried ($MgSO_4$), filtered and concentrated *in vacuo*. The crude product was purified by flash column chromatography (alumina, 5% EtOAc/PE 40-60) to give PMBTCA as a colourless oil (33.8 g, 120 mmol, 92%).

R_f: 0.50 (10% EtOAc/PE, alumina plate); **^{1}H NMR** (400 MHz, $CDCl_3$): δ 8.36 (1H, s, =NH), 7.37 (2H, d, *J* = 8.4 Hz, ArH), 6.91 (2H, d, *J* = 8.8 Hz, ArH), 5.28 (2H, s, OCH2Ar) 3.82 (3H, s, ArOMe).

Isopropylmagnesium chloride (i-PrMgCl)

To a suspension of Mg turnings (3.74 g, 154 mmol) and I_2 (1 crystal) in THF (70 mL) was added 2-chloropropane (12.8 mL, 140 mmol) dropwise to control the rate of the exothermic reaction. Upon complete addition, the reaction mixture was refluxed for a further 1 h before cooling to rt to give a dark grey solution of i-PrMgCl (*ca*. 2.0 M in THF).

Ethylmagnesium bromide (EtMgBr)

To a suspension of Mg turnings (5.70 g, 231 mmol) in Et_2O (70 mL) was added bromoethane (15.7 mL, 210 mmol) dropwise to control the rate of the exothermic reaction. Upon complete addition, the reaction mixture was refluxed for a further 1 h before cooling to rt to give a dark grey solution of EtMgBr (*ca*. 3.0 M in Et_2O).

Lithium diisopropylamide (LDA)

n-BuLi (1.6 M in hexanes, 1.70 mL, 2.72 mmo) was added to a solution of i-Pr_2NH (0.4 mL, 2.85 mmol) in THF (3.6 mL) at 0 ˚C. The reaction mixture was stirred for 10 min to give a solution of LDA (*ca*. 0.5 M in THF).

Samarium diiodide (SmI_2)[139,140]

A flask was charged with Sm (45.1 mg, 0.300 mmol), 1,2-diiodoethane (42.3 mg, 0.150 mmol) and THF (1.5 mL) at rt. The mixture was sonicated for 1 h to give a deep blue solution of SmI_2 (*ca.* 0.1 M in THF).

Stryker's reagent[105]

To a stirred suspension of $Cu(OAc)_2•H_2O$ (50 mg, 0.25 mmol) and PPh_3 (130 mg, 0.50 mmol) in degassed PhMe (9.3 mL) was added 1,1,3,3-tetramethyldisiloxane (0.70 mL, 3.78 mmol) at rt. The turquoise solution was stirred for 16 h at rt and the resulting blood red solution of Stryker's reagent was stored under an atmosphere of Ar at 4 °C. It was used as a *ca.* 0.025 M solution with respect to $Cu(OAc)_2•H_2O$.

5.4 Experimental Procedures for the C1-C15 Fragment

(*S*)-2-amino-3-phenylpropan-1-ol (109)

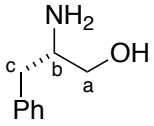

L−phenylalanine **108** (5.00 g, 30.3 mmol) was dissolved in THF (60 mL) and cooled to 0 °C before adding $LiAlH_4$ (2.30 g, 60.6 mmol) portionwise carefully while stirring. The reaction was warmed to rt for 1 h, then cooled to 0 °C again and successively quenched with H_2O (2.5 mL), NaOH (15%, 7.5 mL) and H_2O (7.5 mL) before warming to rt. The precipitate was removed by filtration and washed on the filter with Et_2O (3 x 20 mL). The combined organic portions were washed with brine (10 mL), dried ($MgSO_4$), filtered and concentrated *in vacuo*. The resulting yellow solid was recrystallised from EtOAc/n-hexane (9:1, two batches) to give the title compound as an off-white crystalline solid (3.44 g, 22.7 mmol, 75%). ***Ent*-109** was prepared in an analogous fashion from D−phenylalanine ***ent*-108** (24.0 g, 145 mmol) to give an off-white crystalline solid (16.2 g, 107 mmol, 74%).

^{1}H NMR (500 MHz, $CDCl_3$): δ_H 7.31 (2H, t, *J* = 7.4 Hz, ArH), 7.23 (1H, t, *J* = 7.4 Hz, ArH), 7.19 (2H, d, *J* = 7.2 Hz, ArH), 3.64 (1H, dd, *J* = 10.5, 3.9 Hz, Ha), 3.38 (1H, dd, *J* = 10.5, 7.2 Hz, Ha'), 3.12 (1H, dddd, *J* = 8.8, 7.2, 5.2, 3.9 Hz, Hb), 2.79 (1H, dd, *J* = 13.4, 5.1 Hz, Hc), 2.53 (1H, dd, *J* = 13.5, 8.6 Hz, Hc'); **^{13}C NMR** (125 MHz, $CDCl_3$): δ_C 138.8, 129.3, 128.7, 126.6, 66.5, 54.3, 41.1; **109** $[\alpha]_D^{20}$ = –20.2 (*c* 1.0, $CHCl_3$), ***ent*-109** $[\alpha]_D^{20}$ = +20.0 (*c* 1.0, $CHCl_3$).

Data in agreement with that reported by Evans.[74]

(*S*)-4-benzyloxazolidin-2-one (110)

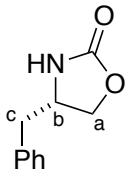

A suspension of aminoalcohol **109** (3.44 g, 22.7 mmol) and K_2CO_3 (314 mg, 2.27 mmol) in diethyl carbonate (5.50 mL, 45.4 mmol) was heated to 130 °C. EtOH was removed *via* distillation as the reaction progressed. After 3 h, the reaction was cooled to rt before diluting with CH_2Cl_2 (10 mL). The organic phase was washed sequentially with water (10 mL), $NaHCO_3$ (10 mL) and brine (10 mL), then dried ($MgSO_4$), filtered and concentrated in vacuo. The residue was

recrystallised from EtOAc/n-hexane (3:2, two batches) to give the title compound as a white crystalline solid (3.14 g, 17.7 mmol, 78%). ***Ent*-110** was prepared in an analogous fashion from ***ent*-109** (16.2 g, 107 mmol) to give a white crystalline solid (12.4 g, 70.0 mmol, 65%).

^{1}H NMR (400 MHz, $CDCl_3$): δ_H 7.34 (2H, m, ArH), 7.29 (1H, m, ArH), 7.18 (1H, m, ArH), 4.48 (1H, dd, *J* = 8.2, 8.2 Hz, Ha), 4.16 (1H, dd, *J* = 8.6, 5.6 Hz, Ha'), 4.09 (1H, m, Hb), 2.90 (1H, dd, *J* = 13.6, 6.0 Hz, Hc), 2.85 (1H, dd, *J* = 13.7, 7.8 Hz, Hc'); **110** $[\alpha]_D^{20}$ = –54.8 (*c* 1.0, $CHCl_3$), ***ent*-110** $[\alpha]_D^{20}$ = +54.1 (*c* 1.0, $CHCl_3$).

Data in agreement with that reported by Evans.[74]

(*S*)-4-benzyl-3-propionyloxazolidin-2-one (45)

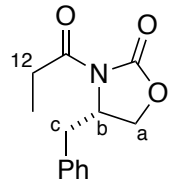

A solution of oxazolidinone **95** (3.14 g, 17.7 mmol) in THF (100 mL) was cooled to −78 °C and n-BuLi (1.6 M in hexanes, 11.6 mL, 18.6 mmol) was added dropwise. The resulting red-brown solution was stirred at −78 °C for 30 min and propionyl chloride (1.85 mL, 21.2 mmol) was added dropwise. After 2.5 h, the reaction was quenched with NH_4Cl (10 mL) and warmed to rt before diluting with CH_2Cl_2 (100 mL). The phases were separated and the organic phase was washed with NaOH (1 M, 50 mL). The combined aqueous phases were extracted with CH_2Cl_2 (2 x 50 mL) and the combined organic phases washed with brine (50 mL), dried ($MgSO_4$), filtered and concentrated *in vacuo*. The residue was recrystallised from Et_2O/n-hexane (1:1, two batches) to give the title compound as white needles (3.51 g, 15.0 mmol, 85%). ***Ent*-45** was prepared in an analogous fashion from ***ent*-110** (12.4 g, 70.0 mmol) to give a white crystalline solid (13.2 g, 56.7 mmol, 81%).

R_f: 0.45 (30% EtOAc/PE 40-60); **^{1}H NMR** (400 MHz, $CDCl_3$): δ_H 7.34 (2H, m, ArH), 7.29 (1H, m, ArH), 7.21 (2H, m, ArH), 4.71-4.64 (1H, m, Hb), 4.24-4.15 (2H, m, Ha), 3.31 (1H, d, *J* = 13.4, 3.2 Hz, Hc), 3.05-2.87 (2H, m, H12), 2.77 (1H, dd, *J* = 13.4, 9.6 Hz, Hc'), 1.21 (3H, t, *J* = 7.4 Hz, Me12); **45** $[\alpha]_D^{20}$ = +56.6 (*c* 1.0, $CHCl_3$), ***ent*-45** $[\alpha]_D^{20}$ = –56.2 (*c* 1.0, $CHCl_3$).

Data in agreement with that reported by Evans.[74]

(*E*)-3-Iodo-2-methylacrylic acid (113)

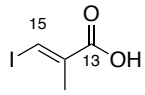

Sodium hydride (60 wt% in oil dispersion, 5.2 g, 130 mmol) was suspended in Et_2O and diethyl methylmalonate (16 mL, 92.8 mmol) was added over 30 min with vigorous stirring. Upon complete addition, the reaction mixture was heated to reflux for 1 h before adding CHI_3 (36.5 g, 92.8 mmol) in one portion while continuing to reflux overnight. The reaction mixture was then cooled to 0 °C, diluted with Et_2O (100 mL) and quenched with aq. HCl (3 M, 150 mL). The layers were separated and the aqueous layer extracted with Et_2O (3 x 60 mL). The combined organic extracts were dried ($MgSO_4$), filtered and concentrated *in vacuo* to afford a brown residue which was triturated with ice-cold pentanes (50 mL) before filtering through a short plug of Celite® to obtain a brown oil. The filtrate was concentrated *in vacuo* and taken up in EtOH (50 mL) before adding aq. KOH (13 g in 90 mL H_2O) and refluxed overnight. After cooling to rt, the reaction mixture was concentrated *in vacuo* to remove volatiles and the layers separated. The aqueous phase was diluted with aq. K_2CO_3 (1 M, 70 mL), washed with CH_2Cl_2 (2 x 30 mL), acidified with HCl (9 M, 50 mL) and extracted with CH_2Cl_2 (5 x 50 mL). The combined organic extracts were dried ($MgSO_4$), filtered and concentrated *in vacuo* to afford the title compound as a yellow oil (11.4 g, 53.8 mmol, 58%) which was used without further purification.

R_f: 0.10 (20% EtOAc/PE 40-60); **^{1}H NMR** (500 MHz, $CDCl_3$): δ_H 8.02 (1H, q, J = 1.2 Hz, H15), 2.06 (1H, d, J = 1.2 Hz, Me14); **^{13}C NMR** (125 MHz, $CDCl_3$): δ_C 169.0, 139.1, 101.9, 20.0; **FT-IR** (Thin film): ν_{max} 3500-2400 (br), 1688, 1595, 1412, 1300, 1235, 1109, 992, 917, 842, 729, 686.

Data in agreement with that reported by Baker.[76]

(*E*)-3-Iodo-2-methylprop-2-en-1-ol (114)

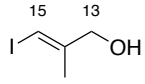

Carboxylic acid **60** (5 g, 23.6 mmol) was dissolved in Et_2O (100 mL) and cooled to 0 °C before adding $LiAlH_4$ (1.17 g, 30.7 mmol) portionwise carefully while stirring. The reaction was warmed to rt for 1 h, then cooled to 0 °C again and successively quenched with H_2O (1.5 mL), NaOH (15%, 1.5 mL) and H_2O (4.5 mL) before warming to rt. The precipitate was removed by filtration and washed on the filter with Et_2O (3 x 15 mL). The combined organic portions were

washed with brine (10 mL), dried ($MgSO_4$), filtered and concentrated *in vacuo* to afford the title compound as a pale yellow oil (3.69 g, 18.6 mmol, 79%) which was used without further purification.

R_f: 0.33 (20% EtOAc/PE 40-60); **^{1}H NMR** (400 MHz, $CDCl_3$): δ_H 6.29 (1H, q, *J* = 1.3 Hz, H15), 4.13 (2H, d, *J* = 1.3 Hz, H14), 1.85 (3H, s, Me14); **^{13}C NMR** (100 MHz, $CDCl_3$): δ_C 147.4, 77.5, 67.3, 21.5; **FT-IR** (Thin film): ν_{max} 3293 (br), 2917, 2851, 1623, 1445, 1377, 1276, 1253, 1147, 1069, 1012, 943, 775, 666.

Data in agreement with that reported by Baker.[76]

(*E*)-3-Iodo-2-methylacrylaldehyde (107)

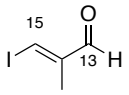

Method A (using MnO_2)

Activated manganese dioxide (2.23 g, 25.7 mmol) was added to a solution of allylic alcohol **62** (509 mg, 2.57 mmol) in CH_2Cl_2 (5 mL) at rt and stirred for 24 h. The reaction mixture was filtered through a short plug of Celite® and carefully concentrated *in vacuo* to give a solution of the title compound in CH_2Cl_2 (*ca*. 10 mL) which was used without further purification.

Method B (using aerobic oxidation)

To a solution of allylic alcohol **62** (3.97 g, 20.04 mmol) in MeCN (10 mL) was added copper (I) bromide (143.5 mg, 1.00 mmol), bipyridyl (156.2 mg, 1.00 mmol), TEMPO (156.3 mg, 1.00 mmol) and DMAP (122.2 mg, 2.00 mmol). The reaction flask was fitted with an O_2 balloon and evacuated to backfill the flask with O_2. The evacuation/backfill procedure was repeated two more times and the reaction left to stir for 5 h where it turned green-blue upon complete reaction. H_2O (10 mL) was added and the aqueous layer extracted with Et_2O (4 x 10 mL). The organic extracts were washed with brine (2 mL), dried ($MgSO_4$) and carefully concentrated *in vacuo* to give a solution of the title compound in Et_2O (*ca*. 20 mL) which was used without further purification.

R_f: 0.23 (5% EtOAc/PE 40-60); **^{1}H NMR** (400 MHz, $CDCl_3$): δ 9.50 (1H, s, H13), 7.79 (1H, q, *J* = 1.1 Hz, H15), 1.90 (3H, d, *J* = 1.1 Hz, Me14).

Data in agreement with that reported by Baker.[76]

(*S*)-4-Benzyl-3-((2*S*,3*S*,*E*)-3-hydroxy-5-iodo-2,4-dimethylpent-4-enoyl)oxazolidin-2-one (121)

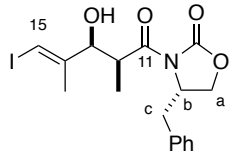

Method A (Evans conditions)

A flame-dried flask was charged with oxazolidinone **57** (3.90 g, 16.7 mmol) dissolved in CH_2Cl_2 (25 mL) and cooled to –78 °C before adding Bu_2BOTf (4.66 mL, 20.0 mmol) and DIPEA (4.95 mL, 28.4 mmol) dropwise. The reaction was warmed to –10 °C and stirred for 30 min before cooling to –78 °C again. A solution of aldehyde **107** (3.93 g, 20.00 mmol) in CH_2Cl_2 (20 mL) was added *via* cannula (2 x 2 mL wash) and left to stir at –78 °C for 3 h before transferring to a freezer for 16 h. The reaction was quenched with MeOH (10 mL), pH 7 buffer (20 mL) and the reaction stirred for 1 h while warming to rt. The reaction mixture was concentrated *in vacuo* and the residue was taken up in CH_2Cl_2 (25 mL). The phases were separated and the aqueous layer extracted with CH_2Cl_2 (3 x 25 mL). The combined organic extracts were washed with brine (5 mL), dried ($MgSO_4$), filtered and concentrated *in vacuo*. The crude product was azeotroped with MeOH (5 x 10 mL) before purifying by flash column chromatography (20% → 50% EtOAc/PE 40-60) to give the title compound as an off-white crystalline solid (5.74 g, 13.4 mmol, 80%, *d.r.* 20:1). ***Ent*-121** was prepared in an analogous fashion from ***ent*-45** (537 mg, 2.30 mmol) and aldehyde **107** (541 mg, 2.76 mmol) to give an off-white crystalline solid (781 mg, 1.82 mmol, 79%, *d.r.* 20:1).

Method B (Crimmins conditions)

A flame-dried flask was charged with oxazolidinone **45** (3.38 g, 14.5 mmol) dissolved in CH_2Cl_2 (120 mL) and cooled to 0 °C. $TiCl_4$ (1.68 mL, 15.3 mmol) was added dropwise and stirred for 10 min, during which time a yellow colour developed. DIPEA (2.72 mL, 16.0 mmol) was added dropwise, where the yellow reaction mixture turned wine-red, and stirred for 30 min. NMP (1.40 mL, 14.5 mmol) was added and stirred for 10 min before adding a solution of aldehyde **107** (3.14 g, 16.0 mmol) in CH_2Cl_2 (20 mL) *via* cannula (2 x 2 mL wash). The reaction was left to stir for another 3 h and quenched with half-saturated NH_4Cl. The phases were separated and the aqueous layer extracted with CH_2Cl_2 (3 x 25 mL). The combined organic extracts were washed with brine (5 mL), dried ($MgSO_4$), filtered and concentrated *in vacuo*. The crude product was purified by flash column chromatography (20% → 50% EtOAc/PE 40-60) to give the title compound as an off-white crystalline solid (5.74 g, 13.4 mmol, 80%, *d.r.* 10:1). ***Ent*-101** was prepared in an

analogous fashion from ***ent*-45** (3.22 g, 13.8 mmol) and aldehyde **101** (2.98 g, 15.2 mmol) to give an off-white crystalline solid (5.22 g, 12.1 mmol, 88%, *d.r.* 10:1).

R_f: 0.38 (30% EtOAc/PE 40-60); **^{1}H NMR** (400 MHz, $CDCl_3$): δ_H 7.35 (2H, t, *J* = 7.7 Hz, ArH), 7.30 (1H, t, *J* = 7.7 Hz, ArH), 7.22 (2H, d, *J* = 7.7 Hz, ArH), 6.42 (1H, s, H15), 4.70 (1H, ddt, *J* = 9.5, 7.6, 3.1 Hz, Hb), 4.51 (1H, m, H13), 4.25 (1H, dd, *J* = 9.1 Hz, 7.7 Hz, Ha), 4.21 (1H, dd, *J* = 9.2, 3.0 Hz, Ha'), 4.01 (1H, qd, *J* = 7.0, 3.6, Hz, H12), 3.36 (1H, d, *J* = 3.2 Hz, OH), 3.26 (1H, dd, *J* = 13.5, 3.4 Hz, Hc), 2.82 (1H, dd, *J* = 13.5, 9.3 Hz, Hc'), 1.82 (3H, d, *J* = 1.7 Hz, Me14), 1.20 (3H, d, *J* = 7.1 Hz, Me12); **^{13}C NMR** (125 MHz, $CDCl_3$): δ_C 176.4, 153.0, 146.0, 135.0, 129.4, 129.0, 127.5, 79.3, 75.3, 66.4, 55.3, 40.2, 37.7, 21.5, 10.5; **FT-IR** (Thin film): ν_{max} 3504 (br), 2920, 1774, 1698, 1455, 1380, 1290, 1209, 1110, 1079, 1050, 1005, 968, 923, 790, 762, 748, 702; **HRMS** (ES^+) Calc. for $C_{17}H_{20}INO_4H$ $[M+H]^+$ 430.0510, found 430.0510; **121 $[\alpha]_D^{20}$** = +32.0 (*c* 1.0, $CHCl_3$), ***ent*-121 $[\alpha]_D^{20}$** = –33.0 (*c* 1.0, $CHCl_3$).

Data in agreement with that reported by Evans.[141]

(2*S*,3*S*,*E*)-3-Hydroxy-5-iodo-*N*-methoxy-*N*,2,4-trimethylpent-4-enamide (125)

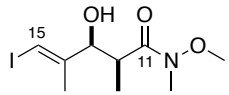

Pre-dried NHMeOMe•HCl (4.33 g, 44.4 mmol) was suspended in THF (60 mL) at 0 °C before adding $AlMe_3$ (2 M in PhMe, 22.2 mL, 44.4 mmol) dropwise. The reaction was warmed to rt and stirred for 1 h before cooling to 0 °C again. A solution of oxazolidinone **121** (6.35 g, 14.8 mmol) in THF (10 mL) was added to the reaction *via* cannula (2 x 2 mL wash) and left to stir overnight while warming to rt. The reaction mixture was cooled to 0 °C and carefully quenched with Rochelle's salt (50 mL), followed by vigorous stirring for 1 h while warming to rt. The phases were separated and the aqueous layer extracted with Et_2O (3 x 50 mL). The combined organic extracts were washed with brine (10 mL), dried (Na_2SO_4), filtered and concentrated *in vacuo*. The crude product was purified by flash column chromatography (30% → 50% EtOAc/PE 40-60) to give the title compound as a white crystalline solid (4.31 g, 13.8 mmol, 93%).

R_f: 0.28 (50% EtOAc/PE 40-60); **^{1}H NMR** (400 MHz, $CDCl_3$): δ_H 6.43 (1H, s, H15), 4.42 (1H, s, H13), 4.26 (1H, br s, OH), 3.73 (3H, s, OMe), 3.21 (3H, s, NMe), 3.14-3.05 (1H, m, H12), 1.79 (3H, s, Me14), 1.08 (3H, d, *J* = 7.2 Hz, Me12); **^{13}C NMR** (100 MHz, $CDCl_3$): δ_C 177.3, 145.2, 79.3, 75.3, 61.6, 36.3, 31.9, 21.8, 10.0; **FT-IR** (Thin film): ν_{max} 3417 (br), 2935, 1635, 1458,

1388, 1266, 1178, 992, 788; **HRMS** (ES^+) Calc. for $C_9H_{16}INO_3H$ $[M+H]^+$ 314.0248, found 314.0248; $[\alpha]_D^{20}$ = +4.5 (*c* 1.0, $CHCl_3$).

(2*S*,3*S*,*E*)-5-Iodo-*N*-methoxy-*N*,2,4-trimethyl-3-((triethylsilyl)oxy)pent-4-enamide (126)

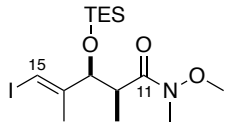

Alcohol **125** (2.02 g, 6.48 mmol) and imidazole (658 mg, 9.67 mmol) were dissolved in CH_2Cl_2 (35 mL) at rt and stirred until a clear homogenous solution was obtained, followed by the dropwise addition of TESCl (1.41 mL, 8.38 mmol). The reaction was stirred overnight and carefully quenched with NH_4Cl (25 mL). The phases were separated and the aqueous layer extracted with CH_2Cl_2 (3 x 30 mL). The combined organic extracts were washed with brine (5 mL), dried ($MgSO_4$), filtered and concentrated *in vacuo*. The crude product was purified by flash column chromatography (10% → 30% EtOAc/PE 40-60) to give the title compound as a colourless oil (2.60 g, 6.09 mmol, 94%).

R_f: 0.29 (30% EtOAc/PE 40-60); **^{1}H NMR** (400 MHz, $CDCl_3$): δ_H 6.17 (1H, s, H15), 4.32 (1H, d, *J* = 9.0 Hz, H13), 3.64 (3H, s, OMe), 3.18-3.07 (1H, m, H12), 3.12 (3H, s, NMe), 1.80 (3H, d, *J* = 0.9 Hz, Me14), 1.19 (3H, d, *J* = 6.8 Hz, Me12), 0.94 (9H, t, *J* = 8.0 Hz, $OSiCH_2\underline{CH_3}$), 0.58 (6H, q, *J* = 8.0 Hz, $OSi\underline{CH_2}CH_3$); **^{13}C NMR** (100 MHz, $CDCl_3$): δ_C 174.8, 148.4, 127.9, 78.9, 78.3, 61.2, 40.2, 31.7, 19.1, 13.9, 6.4, 4.2; **FT-IR** (Thin film): ν_{max} 2959, 2877, 1660, 1458, 1414, 1382, 1270, 1242, 1079, 996, 855, 728; **HRMS** (ES^+) Calc. for $C_{15}H_{30}INO_3SiH$ $[M+H]^+$ 428.1112, found 428.1110; $[\alpha]_D^{20}$ = –22.7 (*c* 1.0, $CHCl_3$).

(*S*)-4-benzyl-3-((2*R*,3*R*,*E*)-5-iodo-2,4-dimethyl-3-((triethylsilyl)oxy)pent-4-enoyl)oxazolidin-2-one (127)

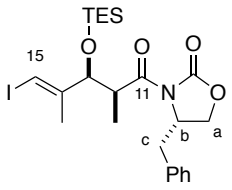

Alcohol **121** (5.50 g, 12.8 mmol) and imidazole (1.31 g, 19.2 mmol) were dissolved in CH_2Cl_2 (120 mL) at rt and stirred until a homogenous solution was obtained, followed by the dropwise addition of TESCl (2.58 mL, 15.4 mmol). The reaction was stirred overnight and quenched with NH_4Cl (30 mL). The phases were separated and the aqueous layer extracted with CH_2Cl_2 (3 x 30 mL). The combined organic extracts were washed with brine (20 mL), dried ($MgSO_4$), filtered

and concentrated *in vacuo*. The crude product was purified by flash column chromatography (10% → 30% EtOAc/PE 40-60) to give the title compound as a colourless oil (6.39 g, 11.8 mmol, 92%). ***Ent*-127** was prepared in an analogous fashion from ***ent*-121** (5.80 g, 13.5 mmol) to give a colourless oil (7.13 g, 13.1 mmol, 97%).

R_f: 0.26 (20% EtOAc/PE 40-60); **^{1}H NMR** (500 MHz, $CDCl_3$): δ_H 7.34 (2H, t, *J* = 7.3 Hz, ArH), 7.29 (1H, t, *J* = 7.3 Hz, ArH), 7.21 (2H, d, *J* = 7.0 Hz, ArH), 6.21 (1H, s, H15), 4.70 (1H, dq, *J* = 6.5, 3.1 Hz, Hb), 4.43 (1H, d, *J* = 7.4 Hz, H13), 4.20-4.15 (2H, m, Ha), 4.06 (1H, qn, *J* = 6.9, Hz, H12), 3.25 (1H, dd, *J* = 13.4, 3.3 Hz, Hc), 2.76 (1H, dd, *J* = 13.4, 9.7 Hz, Hc'), 1.80 (3H, d, *J* = 1.0 Hz, Me14), 1.23 (3H, d, *J* = 6.7 Hz, Me12), 0.93 (9H, t, *J* = 8.0 Hz, $OSiCH_2\underline{CH_3}$), 0.57 (6H, q, *J* = 7.8 Hz, $OSi\underline{CH_2}CH_3$); **^{13}C NMR** (125 MHz, $CDCl_3$): δ_C 174.6, 153.2, 149.0, 135.4, 129.6, 129.1, 127.5, 79.3, 78.4, 63.3, 55.9, 42.8, 37.9, 19.9, 13.1, 6.9, 4.8; **FT-IR** (Thin film): ν_{max} 2954, 2910, 2876, 1781, 1696, 1455, 1379, 1262, 1209, 1087, 1009, 967, 853, 745, 702; **HRMS** (ES^+) Calc. for $C_{23}H_{34}INO_4SiH$ $[M+H]^+$ 544.1375, found 544.1370; **127 $[\alpha]_D^{20}$** = +49.7 (*c* 1.0, $CHCl_3$), ***ent*-127 $[\alpha]_D^{20}$** = –47.2 (*c* 1.0, $CHCl_3$).

(2S,3R,E)-5-iodo-2,4-dimethyl-3-((triethylsilyl)oxy)pent-4-en-1-ol (128)

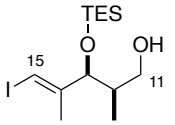

Oxazolidinone **127** (6.50 g, 12.0 mmol) was dissolved in Et_2O (120 mL) and cooled to –78 ˚C while stirring before adding $LiBH_4$ (4 M in Et_2O, 6.00 mL, 23.9 mmol) dropwise. The reaction was slowly warmed to 0 ˚C and stirred for 1 h. Upon complete reaction, the reaction mixture was quenched with NH_4Cl (40 mL). The layers were separated and the aqueous layer extracted with Et_2O (3 x 50 mL). The combined organic extracts were washed with brine (30 mL), dried (Na_2SO_4), filtered and concentrated *in vacuo*. The crude product was purified by flash column chromatography (10% → 30% EtOAc/PE 40-60) to give the title compound as a colourless oil (3.56 g, 9.60 mmol, 80%). ***Ent*-128** was prepared in an analogous fashion from ***ent*-127** (7.13 g, 13.1 mmol) to give a colourless oil (4.00 g, 10.8 mmol, 82%).

R_f: 0.19 (10% EtOAc/PE 40-60); **^{1}H NMR** (400 MHz, $CDCl_3$): δ_H 6.17 (1H, d, *J* = 1.0 Hz, H15), 4.21 (1H, d, *J* = 5.3 Hz, H13), 3.55-3.39 (2H, m, H11), 2.01 (1H, br s, OH), 1.88 (1H, m, H12), 1.77 (3H, s, Me14), 0.92 (9H, t, *J* = 8.3 Hz, $OSiCH_2\underline{CH_3}$), 0.84 (3H, d, J = 6.6 Hz, Me12), 0.56 (6H, q, *J* = 8.3 Hz, $OSi\underline{CH_2}CH_3$); **^{13}C NMR** (125 MHz, $CDCl_3$): δ_C 149.2, 78.7, 78.3, 65.5, 39.7,

21.2, 11.7, 6.9, 4.8; **FT-IR** (Thin film): ν_{max} 3353 (br), 2955, 2911, 2876, 1457, 1414, 1378, 1263, 1240, 1141, 1078, 1006, 828, 726; **HRMS** (ES^+) Calc. for $C_{13}H_{27}IO_2SiH$ $[M+H]^+$ 393.0717, found 393.0719; **128** $[\alpha]_D^{20}$ = –35.0 (*c* 1.0, $CHCl_3$), ***ent*-128** $[\alpha]_D^{20}$ = +38.2 (*c* 1.0, $CHCl_3$).

Data in agreement with that reported by Yokokawa.[142]

(2*R*,3*R*,*E*)-5-iodo-2,4-dimethyl-3-((triethylsilyl)oxy)pent-4-enal (105)

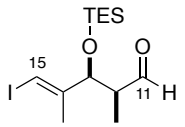

Method A (*via* Weinreb amide reduction)

Weinreb amide **126** (215 mg, 0.503 mmol) was dissolved in PhMe (2 mL) and cooled to –30 °C. DIBAL (1 M in hexanes, 755 µL, 0.755 mmol) was added dropwise and the reaction left to stir at –30 °C for 2 h. Upon complete reaction, the reaction was diluted with Et_2O (2 mL) and carefully quenched with ice-cold Rochelle's salt (2 mL) while stirring vigorously at 0 °C for 1 h. The phases were separated and the aqueous layer extracted with Et_2O (3 x 5 mL). The combined organic extracts were washed with Rochelle's salt (1 mL), brine (1 mL), dried ($MgSO_4$), filtered and concentrated *in vacuo*. The crude product was filtered through a short plug of silica to give the title compound as a colourless oil (130 mg, 0.352 mmol, 70%).

Method B (*via* Swern oxidation)

Anhydrous DMSO (1.56 mL, 22.0 mmol) was added to a stirred solution of $(COCl)_2$ (0.93 mL, 11.0 mmol) in CH_2Cl_2 (88 mL) at −78 °C. The solution was stirred at −78 °C for 20 min before adding a solution of alcohol **128** (3.25 g, 8.78 mmol) in CH_2Cl_2 (5 mL) *via* cannula (2 x 1 mL wash). The reaction mixture was stirred at −78 °C for 15 min, then Et_3N (6.12 mL, 43.9 mmol) was added dropwise and warmed up to –20 °C over 15 min. The reaction was quenched with NH_4Cl (20 mL) and warmed to rt. The layers were separated and the aqueous phase extracted with Et_2O (3 x 20 mL). The combined organic phases were washed with brine (20 mL), dried ($MgSO_4$), filtered and concentrated *in vacuo* to give the title compound as a yellow oil (3.20 g, 8.69 mmol, 99%) which was used immediately without further purification. ***Ent*-105** was prepared in an analogous fashion from ***ent*-128** (3.70 g, 9.99 mmol) to give a colourless oil (3.50 g, 9.49 mmol, 95%).

R_f: 0.49 (10% EtOAc/PE 40-60); **^{1}H NMR** (500 MHz, $CDCl_3$): δ_H 9.69 (1H, d, *J* = 1.4 Hz, H11), 6.29 (1H, s, H15), 4.58 (1H, d, *J* = 4.4 Hz, H13), 2.50 (1H, qdd, *J* = 6.8, 1.7, 5.1 Hz, H12), 1.79 (3H, d, *J* = 0.8 Hz, Me14), 1.06 (3H, d, *J* = 7.1 Hz, Me12), 0.93 (9H, t, *J* = 8.0 Hz, $OSiCH_2\underline{CH_3}$), 0.58 (6H, q, *J* = 8.1 Hz, $OSi\underline{CH_2}CH_3$); **^{13}C NMR** (125 MHz, $CDCl_3$): δ_C 203.8, 147.8, 79.5, 76.6, 50.6, 21.3, 8.4, 7.0, 5.0; **FT-IR** (Thin film): ν_{max} 2955, 2912, 2877, 1725, 1457, 1413, 1379, 1269, 1241, 1145, 1108, 1083, 1035, 1005, 976, 946, 929, 820, 783, 740, 727, 696; **HRMS** (ES^+) Calc. for $C_{13}H_{25}IO_2SiH$ $[M+H]^+$ 369.0741, found 369.0735; **105** $[\alpha]_D^{20}$ = –37.2 (*c* 1.0, $CHCl_3$), ***ent*-105** $[\alpha]_D^{20}$ = +42.2 (*c* 1.0, $CHCl_3$)

Data in agreement with that reported by Müller.[143]

Methyl (*R*)-3-((4-methoxybenzyl)oxy)-2-methylpropanoate (130)

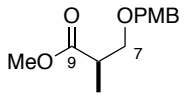

(*R*)-3-hydroxy-2-methylpropionate **(*R*)-40** (4.17 g, 35.3 mmol) was dissolved in CH_2Cl_2 (30 mL) at 0 °C. A solution of PMBTCA (11.98 g, 42.4 mmol) in CH_2Cl_2 (15 mL) was added, followed by PPTS (887 mg, 3.53 mmol). The reaction was warmed to rt and stirred for 5 h before carefully quenching with $NaHCO_3$ (50 mL). The phases were separated and the aqueous layer extracted with CH_2Cl_2 (3 x 50 mL). The combined organic extracts were dried ($MgSO_4$ and concentrated *in vacuo*. The crude product was triturated with ice-cold hexanes (ca. 30 mL) and filtered through a short plug of Celite®. The filtrate was concentrated *in vacuo* and purified by flash column chromatography (5% → 20% EtOAc/PE 40-60) to give the title compound as a colourless oil (7.15 g, 30.0 mmol, 85%). ***Ent*-130** was prepared in an analogous fashion from **(*S*)-40** (10.9 g, 92.6 mmol) to give a colourless oil (20.0 g, 89.1 mmol, 96%).

R_f: 0.30 (20% EtOAc/PE 40-60); **^{1}H NMR** (500 MHz, $CDCl_3$): δ_H 7.23 (2H, d, *J* = 8.7 Hz, ArH), 6.87 (2H, d, *J* = 8.8 Hz, ArH), 4.46 (1H, d, *J* = 11.8 Hz, $O\underline{CH_2}Ar$), 4.43 (1H, d, *J* = 11.8 Hz, $O\underline{CH_2}Ar$), 3.80 (3H, s, ArOMe), 3.69 (3H, s, OMe), 3.62 (1H, dd, *J* = 9.1, 7.3 Hz, H7a), 3.45 (1H, dd, *J* = 9.2, 5.9 Hz, H7b), 2.77 (1H, qnd, *J* = 7.1, 6.3 Hz, H8), 1.16 (3H, d, *J* = 7.1 Hz, Me8); **^{13}C NMR** (125 MHz, $CDCl_3$): δ_C 175.3, 159.2, 130.2, 129.2, 113.8, 72.7, 71.7, 55.2, 51.7, 40.1, 14.0; **FT-IR** (Thin film): ν_{max} 2951 (w), 1735, 1612, 1586 (w), 1512, 1459, 1363, 1302, 1244, 1199, 1173, 1085, 1033, 818, 759 (w), 710 (w); **HRMS** (ES^+) Calc. for $C_{13}H_{18}O_4NH_4$ $[M+NH_4]^+$ 256.1543, found 256.1539; **$[\alpha]_D^{20}$** = –5.1 (*c* 1.0, $CHCl_3$).

Data in agreement with that reported by Paterson.[41]

(*R*)-*N*-Methoxy-3-((4-methoxybenzyl)oxy)-*N*,2-dimethylpropanamide (131)

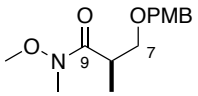

Ester **130** (8.41 g, 35.3 mmol) and pre-dried NHMeOMe•HCl (5.17 g, 53.0 mmol) were suspended in THF (80 mL) and cooled to –20 °C. i-PrMgCl (2.0 M in THF, 53.0 mL, 106 mmol) was added dropwise over 1 h while maintaining the reaction mixture temperature below –10 °C. The reaction mixture was stirred at –10 °C overnight before carefully quenching with NH_4Cl (100 mL). The reaction was warmed to rt with stirring before allowing the phases to separate and extracting the aqueous layer with EtOAc (3 x 100 mL). The combined organic extracts were washed with brine (30 mL), dried ($MgSO_4$), filtered and concentrated *in vacuo*. The crude product was purified by flash column chromatography (30% → 50% EtOAc/PE 40-60) to give the title compound as a colourless oil (8.33 g, 31.1 mmol, 88%).

R_f: 0.17 (30% EtOAc/PE 40-60); **^{1}H NMR** (400 MHz, $CDCl_3$): δ_H 7.23 (2H, d, *J* = 8.6 Hz, ArH), 6.86 (2H, d, *J* = 8.6 Hz, ArH), 4.48 (1H, d, *J* = 11.6 Hz, O$\underline{CH_2}$Ar), 4.41 (1H, d, *J* = 11.7 Hz, O$\underline{CH_2}$Ar), 3.80 (3H, s, ArOMe), 3.69 (3H, s, OMe), 3.68 (1H, t, *J* = 8.6 Hz, H7a), 3.39 (1H, dd, *J* = 8.9, 5.9 Hz, H7b), 3.32-3.22 (1H, m, H8), 3.20 (3H, s, NMe), 1.10 (3H, d, *J* = 7.0 Hz, Me8); **^{13}C NMR** (125 MHz, $CDCl_3$): δ_C 175.8, 159.0, 130.4, 129.0, 113.6, 72.8, 72.2, 61.4, 55.1, 35.7, 32.0, 14.1; **FT-IR** (Thin film): ν_{max} 2937 (w), 1655, 1613, 1586 (w), 1513, 1464, 1387, 1302, 1246, 1174, 1096, 1034, 993, 820, 758 (w); **HRMS** (ES^+) Calc. for $C_{14}H_{21}NO_4H$ $[M+H]^+$ 268.1543, found 268.1545; **$[\alpha]_D^{20}$** = –3.1 (*c* 1.0, $CHCl_3$).

Data in agreement with that reported by Paterson.[41]

(*R*)-1-((4-Methoxybenzyl)oxy)-2-methylpentan-3-one (106)

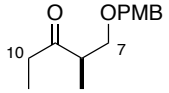

Weinreb amide **131** (12.5 g, 46.8 mmol) was dissolved in Et_2O (100 mL) and cooled to –78 °C. EtMgBr (3.0 M in Et_2O, 46.7 mL, 140 mmol) was added dropwise and the reaction stirred vigorously at –10 °C overnight before carefully quenching with NH_4Cl (100 mL). The reaction was warmed to rt with stirring before allowing the phases to separate and extracting the aqueous layer with EtOAc (3 x 100 mL). The combined organic extracts were washed with brine (30 mL),

dried ($MgSO_4$), filtered and concentrated *in vacuo*. The crude product was purified by flash column chromatography (15% → 50% EtOAc/PE 40-60) to give the title compound as a colourless oil (10.4 g, 44.0 mmol, 94%). ***Ent*-106** was prepared in an analogous fashion from ketone ***ent*-131** (5.10 g, 19.1 mmol) to give a colourless oil (4.11 g, 17.4 mmol, 91%).

R_f: 0.35 (20% EtOAc/PE 40-60); **^{1}H NMR** (400 MHz, $CDCl_3$): δ_H 7.21 (2H, d, *J* = 8.6 Hz, ArH), 6.87 (2H, d, *J* = 8.7 Hz, ArH), 4.43 (1H, d, *J* = 11.6 Hz, O$\underline{CH_2}$Ar), 4.39 (1H, d, *J* = 11.6 Hz, O$\underline{CH_2}$Ar), 3.80 (3H, s, ArOMe), 3.59 (1H, dd, *J* = 9.1, 7.8 Hz, H7a), 3.42 (1H, dd, *J* = 9.1, 5.5 Hz, H7b), 2.86 (1H, qnd, *J* = 7.2, 5.6 Hz, H8), 2.50 (2H, q, *J* = 7.3 Hz, H10), 1.06 (3H, d, *J* = 7.1 Hz, Me8), 1.04 (3H, t, *J* = 7.2 Hz, Me10); **^{13}C NMR** (100 MHz, $CDCl_3$): δ_C 213.1, 158.8, 129.9, 128.7, 113.3, 72.4, 71.7, 54.8, 45.8, 34.8, 13.2, 7.2; **FT-IR** (Thin film): ν_{max} 2973, 2938, 1712, 1612, 1586 (w), 1512, 1458, 1362, 1302, 1245, 1173, 1089, 1033, 952, 819, 758, (w), 709 (w); **HRMS** (ES^+) Calc. for $C_{14}H_{20}O_3H$ $[M+H]^+$ 254.1751, found 254.1747; **106 $[\alpha]_D^{20}$** = –20.8 (*c* 1.0, $CHCl_3$), ***ent*-106 $[\alpha]_D^{20}$** = +22.4 (*c* 1.0, $CHCl_3$).

Data in agreement with that reported by Paterson.[41]

(2*S*,4*S*,5*S*,6*S*,7*R*,*E*)-5-hydroxy-9-iodo-1-((4-methoxybenzyl)oxy)-2,4,6,8-tetramethyl-7-((triethylsilyl)oxy)non-8-en-3-one (132)

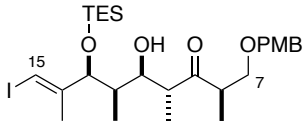

A flame-dried flask was charged with Cy_2BCl (2.00 mL, 11.4 mmol) in Et_2O (50 mL) at –10 ˚C before adding Et_3N (2.20 mL, 15.8 mmol) dropwise with stirring. A solution of ketone **106** (2.90 g, 12.3 mmol) in Et_2O (10 mL) was added *via* cannula (2 x 2 mL wash) and the reaction stirred at –10 ˚C for 1 h before cooling to –78 ˚C. A solution of aldehyde **105** (3.20 g, 8.69 mmol) in Et_2O (20 mL) was then added *via* cannula (2 x 2 mL wash) and the reaction stirred at –78 ˚C for 3 h before transferring to the freezer overnight. The reaction was quenched with MeOH (10 mL), pH 7 buffer (10 mL) and then warmed to rt. The phases were separated and the aqueous layer was extracted with Et_2O (3 x 40 mL). The combined organic extracts were concentrated *in vacuo* to *ca*. 40 mL and stirred over silica gel (*ca.* 20 g) for 1 h. The silica gel was removed by filtration, washed with EtOAc (3 x 30 mL) and the solvent removed *in vacuo*. The crude product was purified by flash column chromatography (15% → 40% EtOAc/PE 40-60) to give the title compound as a colourless oil (3.68 g, 6.08 mmol, 70%). ***Ent*-132** was prepared in an analogous

fashion from ketone ***ent*-106** (3.30 g, 14.0 mmol) and ***ent*-105** (3.68 g, 9.99 mmol) to give a colourless oil (4.26 g, 7.04 mmol, 74%).

R_f: 0.33 (20% EtOAc/PE 40-60); **^{1}H NMR** (500 MHz, $CDCl_3$): δ_H 7.22 (2H, d, *J* = 8.7 Hz, ArH), 6.88 (2H, d, *J* = 8.7 Hz, ArH), 6.07 (1H, s, H15), 4.42 (1H, d, *J* = 11.3 Hz, O$\underline{CH_2}$Ar), 4.37 (1H, d, *J* = 11.5 Hz, O$\underline{CH_2}$Ar), 4.16 (1H, d, *J* = 8.3 Hz, H13), 3.80 (3H, s, ArOMe), 3.65 (1H, t, *J* = 9.0 Hz, H7a), 3.59 (1H, ddd, *J* = 9.5, 4.0, 2.1 Hz, H11), 3.38 (1H, dd, *J* = 8.8, 4.6 Hz, H7b), 3.05 (1H, dqd, *J* = 9.2, 7.0, 4.8 Hz, H8), 2.86 (1H, d, *J* = 4.2 Hz, OH), 2.77 (1H, dq, *J* = 9.5, 7.1 Hz, H10), 1.76 (3H, d, *J* = 1.2 Hz, Me14), 1.72-1.67 (1H, m, H12), 1.02 (3H, d, *J* = 7.1 Hz, Me12), 0.96 (3H, d, *J* = 7.1 Hz, Me10), 0.93 (9H, t, *J* = 8.0 Hz, OSiCH$_2\underline{CH_3}$), 0.93 (3H, d, *J* = 7.0 Hz, Me8), 0.57 (6H, q, *J* = 8.0 Hz, OSi$\underline{CH_2}$CH$_3$); **^{13}C NMR** (125 MHz, $CDCl_3$): δ_C 217.3, 159.6, 149.2, 129.9, 129.8, 114.1, 80.6, 79.9, 73.4, 72.7, 72.5, 55.5, 51.2, 44.4, 38.1, 19.7, 14.5, 12.9, 8.4, 7.1, 5.0; **FT-IR** (Thin film): ν_{max} 3485 (br), 2957, 2877, 1711, 1614, 1514, 1459, 1376, 1303, 1248, 1174, 1066, 1037, 1006, 976, 865, 822, 744, 664; **HRMS** (ES^+) Calc. for $C_{27}H_{45}IO_5SiH$ $[M+H]^+$ 605.2154, found 605.2151; **132** $[\alpha]_D^{20}$ = –21.1 (*c* 1.0, $CHCl_3$), ***ent*-132** $[\alpha]_D^{20}$ = +23.0 (*c* 1.0, $CHCl_3$).

(2*S*,4*S*,5*S*,6*S*,7*R*,*E*)-9-iodo-1-((4-methoxybenzyl)oxy)-2,4,6,8-tetramethyl-5,7-bis((triethylsilyl)oxy)non-8-en-3-one (136)

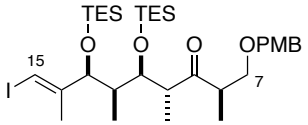

Alcohol **132** (1.70 g, 2.81 mmol) was dissolved in CH_2Cl_2 (28 mL) and cooled to –78 ˚C, followed by the sequential addition of 2,6-lutidine (0.479 mL, 4.07 mmol) and TESOTf (0.738 mL, 3.27 mmol). The reaction was stirred for 2 h before quenching with MeOH (4 mL) and $NaHCO_3$ (5 mL). The phases were separated and the aqueous layer extracted with CH_2Cl_2 (3 x 10 mL). The combined organic extracts were washed with brine (5 mL), dried (Na_2SO_4), filtered and concentrated *in vacuo*. The crude product was purified by flash column chromatography (5% → 10% EtOAc/PE 40-60) to give the title compound as a colourless oil (1.84 g, 2.56 mmol, 91%). ***Ent*-136** was prepared in an analogous fashion from ***ent*-132** (4.26 g, 7.04 mmol) to give a colourless oil (4.91 g, 6.83 mmol, 97%).

R_f: 0.32 (5% EtOAc/PE 40-60); **^{1}H NMR** (400 MHz, $CDCl_3$): δ_H 7.21 (2H, d, *J* = 8.6 Hz, ArH), 6.86 (2H, d, *J* = 8.7 Hz, ArH), 6.20 (1H, s, H15), 4.43 (1H, d, *J* = 11.5 Hz, O$\underline{CH_2}$Ar), 4.38 (1H, d, *J* = 11.6 Hz, O$\underline{CH_2}$Ar), 4.06 (1H, d, *J* = 8.7 Hz, H13), 3.80 (3H, s, ArOMe), 3.74 (1H, dd, *J* = 7.6,

1.8 Hz, H11), 3.59 (1H, dd, *J* = 9.1, 6.8 Hz, H7a), 3.45 (1H, dd, *J* = 9.1, 5.6 Hz, H7b), 2.94 (1H, qn, *J* = 7.2 Hz, H10), 2.87 (1H, sx, *J* = 6.6 Hz, H8), 1.78-1.72 (1H, m, H12), 1.71 (3H, d, *J* = 0.6 Hz, Me14), 1.05 (3H, d, *J* = 7.0 Hz, Me12), 0.96 (3H, d, *J* = 7.1 Hz, Me10), 0.95 (3H, d, *J* = 6.7 Hz, Me8), 0.94 (9H, t, *J* = 8.0 Hz, OSiCH$_2$<u>CH$_3$</u>), 0.93 (9H, t, *J* = 7.9 Hz, OSiCH$_2$<u>CH$_3$</u>), 0.56 (6H, q, *J* = 7.9 Hz, OSi<u>CH$_2$</u>CH$_3$), 0.55 (6H, q, *J* = 8.1 Hz, OSi<u>CH$_2$</u>CH$_3$); **^{13}C NMR** (125 MHz, $CDCl_3$): δ_C 214.4, 159.5, 150.0, 130.6, 129.5, 114.1, 80.8, 79.4, 73.4, 73.3, 72.1, 55.6, 50.7, 47.2, 40.4, 19.6, 13.9, 13.6, 10.5, 7.5, 7.2, 6.0; **FT-IR** (Thin film): ν_{max} 2956, 2911, 2877, 1713, 1615, 1514, 1459, 1409, 1379, 1248, 1173, 1067, 1039, 1004, 820, 736, 663; **HRMS** (ES^+) Calc. for $C_{33}H_{59}IO_5Si_2H$ $[M+H]^+$ 719.3018, found 719.3018; **136** $[\alpha]_D^{20}$ = –11.5 (*c* 1.0, $CHCl_3$), ***ent*-136** $[\alpha]_D^{20}$ = +12.0 (*c* 1.0, $CHCl_3$).

(2*S*,3*R*,4*R*,5*R*,6*S*,7*R*,*E*)-9-iodo-1-((4-methoxybenzyl)oxy)-2,4,6,8-tetramethyl-5,7-bis((triethylsilyl)oxy)non-8-en-3-ol (137)

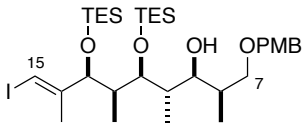

Ketone **136** (1.93 g, 2.69 mmol) was dissolved in CH_2Cl_2 (28 mL) and cooled to –78 ˚C. DIBAL (1 M in hexanes, 4.04 mL, 4.04 mmol) was added dropwise at this temperature and then warmed to –40 ˚C for 4 h. Upon complete reaction, the reaction was quenched with MeOH (5 mL) and warmed to rt. Rochelle's salt (10 mL) was added while stirring vigorously for 1 h. The phases were separated and the aqueous layer extracted with CH_2Cl_2 (3 x 10 mL). The combined organic extracts were washed with brine (10 mL), dried (Na_2SO_4), filtered and concentrated *in vacuo*. The crude product was purified by flash column chromatography (5% → 20% EtOAc/PE 40-60) to give the title compound as a colourless oil (1.60 g, 2.26 mmol, 84%, *d.r.* 20:1). ***Ent*-137** was prepared in an analogous fashion from ***ent*-136** (2.78 g, 3.87 mmol) to give a colourless oil (2.23 g, 3.17 mmol, 82%, *d.r.* 20:1).

R$_f$: 0.24 (10% EtOAc/PE 40-60); **^{1}H NMR** (500 MHz, $CDCl_3$): δ_H 7.25 (2H, d, *J* = 8.7 Hz, ArH), 6.88 (2H, d, *J* = 8.8 Hz, ArH), 6.17 (1H, s, H15), 4.44 (2H, br s, O<u>CH$_2$</u>Ar), 4.07 (1H, d, *J* = 7.6 Hz, H13), 3.81 (3H, s, ArOMe), 3.78 (1H, dd, *J* = 4.1, 3.0 Hz, H9), 3.62 (1H, d, *J* = 10.0 Hz, H11), 3.51 (1H, dd, *J* = 8.9, 6.3 Hz, H7a), 3.44 (1H, dd, *J* = 9.0, 5.1 Hz, H7b), 2.89 (1H, d, *J* = 2.1 Hz, H12), 1.94-1.83 (1H, m, H8), 1.81-1.73 (1H, m, H10), 1.78 (3H, s, Me14), 0.98 (9H, t, *J* = 7.9 Hz, OSiCH$_2$<u>CH$_3$</u>), 0.95 (3H, t, *J* = 7.8 Hz, Me12), 0.94 (9H, t, *J* = 7.8 Hz, OSiCH$_2$<u>CH$_3$</u>), 0.89 (3H, d, *J* = 7.0 Hz, Me10), 0.80 (3H, d, *J* = 7.0 Hz, Me8), 0.64 (6H, q, *J* = 7.6 Hz, OSi<u>CH$_2$</u>CH$_3$), 0.57 (6H, q, *J* = 8.1 Hz, OSi<u>CH$_2$</u>CH$_3$); **^{13}C NMR** (125 MHz, $CDCl_3$): δ_C 159.3,

150.0, 130.6, 129.4, 113.9, 80.2, 79.4, 74.8, 74.1, 74.0, 73.1, 55.4, 41.7, 40.5, 35.0, 20.1, 13.6, 11.2, 9.3, 7.2, 7.0, 5.7, 4.9; **FT-IR** (Thin film): ν_{max} 3500 (br), 2956, 2913, 2877, 1614, 1514, 1459, 1413, 1380, 1302, 1248, 1173, 1085, 1039, 1005, 865, 821, 738; **HRMS** (ES^+) Calc. for $C_{33}H_{61}IO_5Si_2H$ $[M+H]^+$ 721.3175, found 721.3174; **137** $[\alpha]_D^{20}$ = –9.4 (*c* 1.0, $CHCl_3$), ***ent*-137** $[\alpha]_D^{20}$ = +10.0 (*c* 1.0, $CHCl_3$).

Mosher ester analysis for alcohol 136

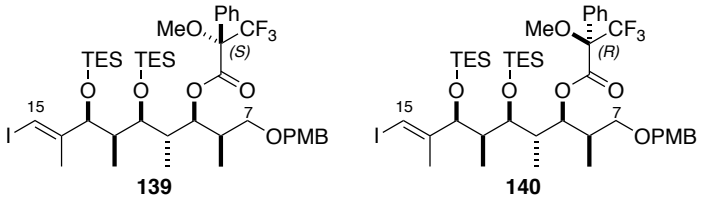

DCC (1 M in CH_2Cl_2, 3.47 µL, 34.7 µmol) was added in portion to a stirred solution of ***ent*-136** (5.0 mg, 6.94 µmol), (*S*)-α-methoxy-α-trifluoromethylphenylacetic acid (*S*-MTPA) (8.1 mg, 34.7 µmol) and DMAP (4.2 mg, 34.7 µmol) in CH_2Cl_2 (70 µL). The mixture was stirred for 24 h at rt, during which a white precipitate formed. The mixture was filtered through cotton wool and the filtrate reduced to dryness. Purification by flash chromatography (2% EtOAc/PE 40-60) afforded the product **(*S*)-MTPA ester 139** as a pale-yellow oil (3.4 mg, 4.16 µmol, 60%). The corresponding diastereomer was synthesised from ***ent*-16** (5.0 mg, 6.94 µmol) to afford the diastereomeric ester **(*R*)-MTPA ester 140** (5.5 mg, 5.82 µmol, 84%).

(*S*)-MTPA ester 139

R_f: 0.35 (5% EtOAc/PE 40-60); **^{1}H NMR** (400 MHz, $CDCl_3$): δ_H 7.55-7.48 (2H, m, ArH), 7.42-7.32 (3H, m, ArH), 7.19 (2H, d, *J* = 8.7 Hz, ArH), 6.86 (2H, d, *J* = 8.7 Hz, ArH), 6.10 (1H, s, H15), 5.65 (1H, dd, *J* = 4.3, 1.4 Hz, H9), 4.43 (1H, d, *J* = 2.4 Hz, H13), 4.37 (1H, d, *J* = 11.6 Hz, O$\underline{CH_2}$Ar), 4.34 (1H, d, *J* = 11.7 Hz, O$\underline{CH_2}$Ar), 3.81 (3H, s, ArOMe), 3.65 (1H, dd, *J* = 8.7, 3.3 Hz, H11), 3.48 (3H, s, OMe), 3.12-3.02 (2H, m, H7), 2.61-2.51 (1H, m, H8), 2.25-2.15 (1H, m, H10), 1.99-1.89 (1H, m, H12), 1.67 (3H, s, Me14), 1.06 (3H, d, *J* = 7.2 Hz, Me10), 0.97 (9H, t, *J* = 7.9 Hz, OSiCH$_2\underline{CH_3}$), 0.89 (9H, t, *J* = 8.0 Hz, OSiCH$_2\underline{CH_3}$), 0.82 (3H, d, *J* = 6.8 Hz, Me12), 0.81 (3H, d, *J* = 6.7 Hz, Me8), 0.64 (6H, q, *J* = 7.9 Hz, OSi$\underline{CH_2}$CH$_3$), 0.56-0.44 (6H, m, OSi$\underline{CH_2}$CH$_3$).

(*R*)-MTPA ester 140

R_f: 0.33 (5% EtOAc/PE 40-60); **^{1}H NMR** (400 MHz, $CDCl_3$): δ_H 7.55-7.49 (2H, m, ArH), 7.40-7.31 (3H, m, ArH), 7.19 (2H, d, *J* = 8.7 Hz, ArH), 6.85 (2H, d, *J* = 8.8 Hz, ArH), 6.11 (1H, s,

H15), 5.59 (1H, dd, *J* = 4.8, 1.6 Hz, H9), 4.44 (1H, d, *J* = 2.2 Hz, H13), 4.40 (1H, d, *J* = 11.6 Hz, O$\underline{CH_2}$Ar), 4.35 (1H, d, *J* = 11.5 Hz, O$\underline{CH_2}$Ar), 3.80 (3H, s, ArOMe), 3.61 (1H, dd, *J* = 8.7, 3.0 Hz, H11), 3.47 (3H, s, OMe), 3.14 (2H, d, *J* = 6.9 Hz, H7), 2.63-2.52 (1H, m, H8), 2.22-2.13 (1H, m, H10), 1.98-1.85 (1H, m, H12), 1.70 (3H, s, Me14), 0.96 (9H, t, *J* = 7.9 Hz, OSiCH$_2\underline{CH_3}$), 0.93 (9H, t, *J* = 7.9 Hz, OSiCH$_2\underline{CH_3}$), 0.90 (3H, d, *J* = 7.2 Hz, Me10), 0.85 (3H, d, *J* = 6.8 Hz, Me8), 0.76 (3H, d, *J* = 6.7 Hz, Me12), 0.62 (6H, q, *J* = 7.8 Hz, OSi$\underline{CH_2}$CH$_3$), 0.59-0.49 (6H, m, OSi$\underline{CH_2}$CH$_3$).

Proton	δ_H (*S*)-MTPA **139**	δ_H (*R*)-MTPA **140**	$\Delta\delta = \delta_S - \delta_R$
H12	1.94	1.92	+0.02
Me12	0.82	0.76	+0.06
H11	3.65	3.61	+0.04
H10	2.20	2.18	+0.02
Me10	1.06	0.89	+0.17
H8	2.56	2.58	–0.02
Me8	0.81	0.85	–0.04
H7a	3.10	3.14	–0.04
H7b	3.07	3.14	–0.07
ArCH$_{2a}$	4.37	4.40	–0.03
ArCH$_{2b}$	4.34	4.35	–0.01

Table 2: List of chemical shifts in MTPA esters **139** and **140** for Mosher ester analysis of **137**

(5*R*,6*S*,7*R*)-3,3,9,9-tetraethyl-5-((*E*)-1-iodoprop-1-en-2-yl)-7-((2*R*,3*R*,4*S*)-3-methoxy-5-((4-methoxybenzyl)oxy)-4-methylpentan-2-yl)-6-methyl-4,8-dioxa-3,9-disilaundecane (141)

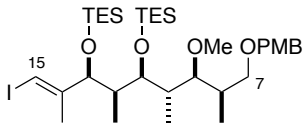

A flame-dried flask was charged with a suspension of Me_3OBF_4 (2.30 g, 15.5 mmol), Proton Sponge® (5.00 g, 23.3 mmol), activated 4 Å MS (*ca*. 6 g) in CH_2Cl_2 (16 mL). A solution of alcohol **137** (1.12 g, 1.55 mmol) in CH_2Cl_2 (2 mL) was added *via* cannula (2 x 1 mL wash) and the reaction left to stir for 7 h before quenching with $NaHCO_3$ (5 mL). The solids were removed by filtration and the layers were separated. The aqueous layer was extracted with Et_2O (3 x 10 mL) and the combined organic extracts were washed with citric acid (10% w/v, 3 x 5 mL), brine (10 mL), dried ($MgSO_4$), filtered and concentrated *in vacuo*. The crude product was purified by

flash column chromatography (2% → 10% EtOAc/PE 40-60) to give the title compound as a colourless oil (808 mg, 1.10 mmol, 71%). ***Ent*-141** was prepared in an analogous fashion from ***ent*-137** (4.00 g, 5.55 mmol) to give a colourless oil (2.94 g, 4.00 mmol, 72%).

R_f: 0.30 (4% EtOAc/PE 40-60); **^{1}H NMR** (500 MHz, $CDCl_3$): δ_H 7.26 (2H, d, *J* = 8.6 Hz, ArH), 6.87 (2H, d, *J* = 8.7 Hz, ArH), 6.12 (1H, s, H15), 4.43 (2H, br s, O$\underline{CH_2}$Ar), 4.20 (1H, d, *J* = 5.0 Hz, H13), 3.81 (3H, s, ArOMe), 3.62 (1H, dd, *J* = 6.4, 2.1 Hz, H11), 3.45 (1H, t, *J* = 8.6 Hz, H7a), 3.39 (1H, dd, *J* = 9.3, 2.0 Hz, H9), 3.33 (1H, dd, *J* = 9.0, 6.4 Hz, H7b), 3.30 (3H, s, OMe9), 2.01-2.00 (1H, m, H12), 1.99-1.98 (1H, m, H8), 1.95-1.91 (1H, m, H10) 1.72 (3H, d, *J* = 0.9 Hz, Me14), 0.97 (9H, t, *J* = 8.0 Hz, OSiCH$_2\underline{CH_3}$), 0.93 (9H, t, *J* = 8.0 Hz, OSiCH$_2\underline{CH_3}$), 0.88 (3H, d, *J* = 8.0 Hz, Me12), 0.87 (3H, d, *J* = 7.0 Hz, Me10), 0.84 (3H, d, *J* = 6.9 Hz, Me8), 0.62 (6H, q, *J* = 7.8 Hz, OSi$\underline{CH_2}$CH$_3$), 0.55 (6H, q, *J* = 7.9 Hz, OSi$\underline{CH_2}$CH$_3$); **^{13}C NMR** (125 MHz, $CDCl_3$): δ_C 159.5, 150.2, 130.9, 129.3, 113.9, 81.5, 78.8, 78.1, 77.0, 73.6, 72.7, 59.9, 55.5, 40.3, 39.0, 36.0, 21.1, 16.1, 11.0, 10.4, 7.4, 7.1, 5.9, 5.1; **FT-IR** (Thin film): ν_{max} 2955, 2910, 2877, 1613, 1514, 1458, 1377, 1246, 1079, 1006, 822, 738; **HRMS** (ES^+) Calc. for $C_{34}H_{63}IO_5Si_2H$ $[M+H]^+$ 735.3335, found 735.3331; **141 $[\alpha]_D^{20}$** = –15.7 (*c* 1.0, $CHCl_3$), ***ent*-141 $[\alpha]_D^{20}$** = +19.0 (*c* 1.0, $CHCl_3$).

(2*S*,3*R*,4*R*,5*R*,6*S*,7*R*,*E*)-9-iodo-3-methoxy-2,4,6,8-tetramethyl-5,7-bis((triethylsilyl)oxy)non-8-en-1-ol (144)

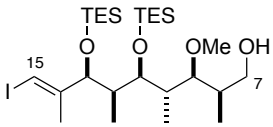

DDQ (375 mg, 1.65 mmol) was added to a solution of PMB ether **141** (808 mg, 1.10 mmol) in CH_2Cl_2/pH 7 buffer (9:1, 10 mL). After 1 h, the reaction was quenched with $NaHCO_3$ (2 mL). The phases were separated and the aqueous layer extracted with CH_2Cl_2 (3 x 5 mL). The combined organic phases were washed with brine (5 mL), dried ($MgSO_4$), filtered and concentrated *in vacuo*. The crude product was purified by flash column chromatography (50% PhMe/CH_2Cl_2 → 30% EtOAc/PE 40-60) to give the title compound as a colourless oil (510 mg, 0.846 mmol, 77%). ***Ent*-144** was prepared in an analogous fashion from ***ent*-141** (2.10 g, 2.86 mmol) to give a colourless oil (1.41 g, 2.29 mmol, 80%).

R_f: 0.17 (10% EtOAc/PE 40-60); **^{1}H NMR** (500 MHz, $CDCl_3$): δ_H 6.13 (1H, s, H15), 4.19 (1H, d, *J* = 5.0 Hz, H13), 3.67-3.60 (3H, m, H7a, H7b, H9), 3.38 (1H, dd, *J* = 8.9, 2.2 Hz, H11), 3.36 (3H, s, OMe9), 2.04-1.95 (2H, m, H8, H10), 1.94-1.86 (1H, m, H12), 1.74 (3H, s, Me14), 0.98 (9H, t,

J = 7.8 Hz, $OSiCH_2\underline{CH_3}$), 0.93 (9H, t, *J* = 9.1 Hz, $OSiCH_2\underline{CH_3}$), 0.91 (6H, d, *J* = 8.9 Hz, Me8, Me12), 0.88 (3H, d, *J* = 7.1 Hz, Me10), 0.63 (6H, q, *J* = 8.0 Hz, $OSi\underline{CH_2}CH_3$), 0.59-0.52 (6H, m, $OSi\underline{CH_2}CH_3$); **^{13}C NMR** (125 MHz, $CDCl_3$): δ_C 150.0, 8.9, 78.8, 78.2, 77.0, 67.0, 59.4, 40.3, 38.8, 37.9, 21.0, 15.8, 11.0, 10.7, 7.3, 7.0, 5.9, 5.0; **FT-IR** (Thin film): ν_{max} 3374 (br), 2958, 2910, 2877, 1458, 1377, 1239, 1138, 1077, 737; **HRMS** (ES^+) Calc. for $C_{26}H_{55}IO_4Si_2H$ $[M+H]^+$ 615.2756, found 615.2753; **144** $[\alpha]_D^{20}$ = –13.2 (*c* 1.0, $CHCl_3$), ***ent*-144** $[\alpha]_D^{20}$ = +8.7 (*c* 1.0, $CHCl_3$).

Methyl sorbate (142)

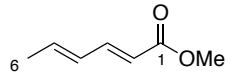

$SOCl_2$ (13.0 mL, 178 mmol) was added slowly to a solution of sorbic acid **54** (20.0 g, 178 mmol) in MeOH (200 mL) at 0 °C. The reaction was heated at reflux for 3 h, then cooled to rt before diluting with CH_2Cl_2 (200 mL). The solution was washed with $NaHCO_3$ (100 mL), dried ($MgSO_4$), filtered and concentrated *in vacuo*. The crude product was purified by distillation under reduced pressure (48 ˚C, 10 torr) to give the title compound as a colourless oil (21.3 g, 169 mmol, 95%).

R_f: 0.45 (10% EtOAc/PE 40-60); **^{1}H NMR** (500 MHz, $CDCl_3$): δ_H 7.26 (1H, dd, *J* = 15.4, 10.0 Hz, H3), 6.25-6.08 (2H, m, H4, H5), 5.78 (1H, d, *J* = 15.3 Hz, H2), 3.74 (3H, s, CO_2Me), 1.85 (3H, d, *J* = 5.7 Hz, H6).

Data in agreement with that reported by Law.[144]

methyl (2*E*,4*E*)-6-bromohexa-2,4-dienoate (143)

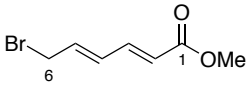

Methyl sorbate **142** (6 g, 47.5 mmol) and NBS (10.5 g, 59.4 mmol) were brought to reflux in PhH (100 mL). BzOOBz (75% w/w with water, 3.10 g, 2.50 mmol) was added in one portion and the reaction was maintained at this temperature for 4 h. After cooling to rt, the solvent was concentrated *in vacuo* and the residue was taken up in Et_2O (100 mL). The solution was washed with 10% NaOH until the washings were clear (5 x 20 mL) and then with H_2O (20 mL), dried ($MgSO_4$), filtered and concentrate *in vacuo*. The crude product was purified by flash column chromatography (5% EtOAc/PE 40-60) to give the title compound (3.56 g, 17.4 mmol, 37%).

R_f: 0.29 (10% EtOAc/PE 40-60); **^{1}H NMR** (500 MHz, $CDCl_3$): δ_H 7.26 (1H, dd, *J* = 15.2 Hz, 10.8 Hz, H3), 6.39 (1H, dd, *J* = 15.0 Hz, 11.0 Hz, H4), 6.27-6.21 (1H, m, H5), 5.94 (1H, d, *J* = 15.3 Hz, H2), 4.03 (2H, d, *J* = 7.5 Hz, H6), 3.75 (3H, s, CO_2Me); **^{13}C NMR** (125 MHz, $CDCl_3$): δ_C 167.0, 142.9, 136.8, 131.9, 122.8, 51.8, 31.3.

Data in agreement with that reported by Law.[144]

methyl (2*E*,4*E*)-6-(diethoxyphosphoryl)hexa-2,4-dienoate (104)

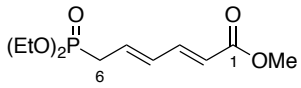

Allyl bromide **143** (3.56 g, 17.4 mmol) and triethyl phosphite (20.8 mL, 122 mmol) were heated to 120 °C for 1 h, then cooled to 50 °C. The excess triethyl phosphite was removed under reduced pressure (42 ˚C, 10 torr) to give the title compound as a yellow oil (4.29 g, 16.4 mmol, 94%).

R_f: 0.23 (EtOAc); **^{1}H NMR** (500 MHz, $CDCl_3$): δ_H 7.26 (1H, dd, *J* = 15.7 Hz, 10.8 Hz, H3), 6.33-6.27 (1H, m, H4), 6.09-6.01 (1H, m, H5), 5.85 (1H, dd, $^3J_{H,H}$ = 15.5 Hz, $^4J_{P,H}$ = 2.6 Hz, H2), 4.13-4.07 (4H, m, O$\underline{CH_2}CH_3$), 3.74 (3H, s, CO_2Me), 2.71 (2H, dd, $^1J_{P,H}$ = 23.1 Hz, $^3J_{H,H}$ = 7.7 Hz, H6), 1.31 (6H, t, *J* = 7.1 Hz, $OCH_2\underline{CH_3}$); **^{13}C NMR** (125 MHz, $CDCl_3$): δ_C 167.4 (1C, d, *J* = 1.4 Hz), 143.9 (1C, d, *J* = 4.8 Hz), 132.8 (1C, d, *J* = 14.7 Hz), 131.8 (1C, d, *J* = 12.5 Hz), 120.9 (1C, d, *J* = 4.3 Hz), 62.3 (1C, d, *J* = 6.7 Hz), 51.7 (1C, s), 31.4 (1C, d, *J* = 139.2 Hz), 16.6 (1C, d, *J* = 5.8 Hz).

Data in agreement with that reported by Cossy.[145]

(2*R*,3*S*,4*R*,5*R*,6*S*,7*R*,*E*)-9-iodo-3-methoxy-2,4,6,8-tetramethyl-5,7-bis((triethylsilyl)oxy)non-8-enal (103)

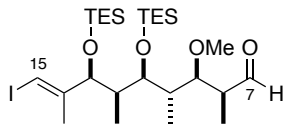

To a stirred suspension of alcohol **144** (520 mg, 0.846 mmol) and $NaHCO_3$ (284 mg, 3.38 mmol) in CH_2Cl_2 (8.5 mL) was added DMP (717 mg, 1.69 mmol). After 1 h, the reaction was diluted with CH_2Cl_2 (5 mL) and quenched with $NaHCO_3$ (3 mL) and $Na_2S_2O_3$ (3 mL) and stirring continued for another 30 min until a clear phase boundary was observed. The layers were separated and the aqueous phase extracted with CH_2Cl_2 (3 x 5 mL). The combined organic phases were washed with brine (2 mL), dried ($MgSO_4$), filtered and concentrated *in vacuo*. The crude

product was rapidly filtered through a short plug of silica, eluting with 20% Et_2O/PE 40-60 to give the title compound as a colourless oil (492 mg, 0.804 mmol, 95%). ***Ent*-103** was prepared in an analogous fashion from ***ent*-144** (400 mg, 0.651 mmol) to give a colourless oil (399 mg, 0.651 mmol, 99%).

R_f: 0.47 (10% EtOAc/PE 40-60); **^{1}H NMR** (500 MHz, $CDCl_3$): δ_H 9.84 (1H, s, H7), 6.14 (1H, s, H15), 4.13 (1H, d, *J* = 6.5 Hz, H13), 3.77 (1H, dd, *J* = 9.2, 1.7 Hz, H9), 3.74 (1H, dd, *J* = 4.7, 3.2 Hz, H11), 3.13 (3H, s, OMe9), 2.50-2.44 (1H, m, H8), 2.03-1.95 (1H, m, H10), 1.93-1.86 (1H, m, H12), 1.74 (3H, d, *J* = 1.0 Hz, Me14), 1.11 (3H, d, *J* = 7.1 Hz, Me8), 0.98 (9H, t, *J* = 7.9 Hz, $OSiCH_2\underline{CH_3}$), 0.95-0.90 (15H, m, $OSiCH_2\underline{CH_3}$, Me10, Me12), 0.65-0.53 (12H, m, $OSi\underline{CH_2}CH_3$ x2); **^{13}C NMR** (125 MHz, $CDCl_3$): δ_C 204.9, 149.9, 80.9, 79.3, 78.8, 74.5, 58.5, 49.2, 40.1, 39.8, 20.3, 14.8, 11.1, 7.3, 7.0, 6.8, 5.82, 5.0; **FT-IR** (Thin film): ν_{max} 2954, 2877, 1726, 1457, 1329; **HRMS** (ES^+) Calc. for $C_{26}H_{53}IO_4Si_2Na$ $[M+Na]^+$ 635.2419, found 635.2414; **103** $\boldsymbol{[\alpha]_D^{20}}$ = **–**12.5 (*c* 1.0, $CHCl_3$), ***ent*-103** $\boldsymbol{[\alpha]_D^{20}}$ = +14.0 (*c* 1.0, $CHCl_3$).

methyl (2*E*,4*E*,6*E*,8*S*,9*R*,10*R*,11*R*,12*S*,13*R*,14*E*)-15-iodo-9-methoxy-8,10,12,14-tetramethyl-11,13-bis((triethylsilyl)oxy)pentadeca-2,4,6,14-tetraenoate (101)

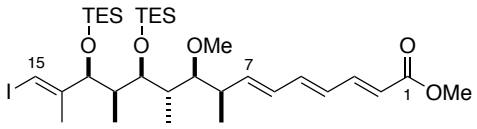

LDA (5.92 mL, 2.96 mmol, 0.5 M in THF) was added to a solution of phosphonate **104** (776 mg, 2.96 mmol) in THF (8.5 mL) at –78 °C to give a bright yellow-orange solution. The reaction was stirred for 30 min and then a solution of aldehyde **103** (492 mg, 0.804 mmol) in THF (1 mL) was added *via* cannula (2 x 0.5 mL wash). The reaction was stirred at –78 ˚C for 30 min, and then at –40 ˚C for 30 min before quenching with NH_4Cl (2 mL). The layers were separated and the aqueous phase extracted with Et_2O (3 x 3 mL). The combined organic phases were washed with brine (1 mL), dried ($MgSO_4$), filtered and concentrated *in vacuo*. The crude product was purified by flash column chromatography (5% EtOAc/PE 40-60) to give the title compound as a colourless oil (329 mg, 0.456 mmol, 70%). ***Ent*-101** was prepared in an analogous fashion from ***ent*-103** (399 mg, 0.651 mmol) to give a colourless oil (329 mg, 0.456 mmol, 70%).

R_f: 0.23 (20% EtOAc/PE 40-60); **^{1}H NMR** (500 MHz, $CDCl_3$): δ_H 7.32 (1H, d, *J* = 15.2, 11.2 Hz, H3), 6.55 (1H, d, *J* = 14.7, 10.8 Hz, H5), 6.26 (1H, d, *J* = 14.9, 11.3 Hz, H4), 6.17 (1H, d, *J* = 15.1, 10.9 Hz, H6), 6.13 (1H, s, H15), 5.92 (1H, d, *J* = 15.2, 8.0 Hz, H7), 5.86 (1H, d, *J* = 15.0

Hz, H2), 4.08 (1H, d, *J* = 7.5 Hz, H13), 3.74 (3H, s, CO_2Me), 3.63 (1H, t, *J* = 3.8 Hz, H9), 3.31 (3H, s, OMe9), 3.04 (1H, dd, *J* = 7.0, 5.0 Hz, H11), 2.47-2.37 (1H, m, H8), 2.02-1.92 (1H, m, H12), 1.90-1.83 (1H, m, H10), 1.73 (3H, d, *J* = 0.6 Hz, Me14), 1.05 (3H, d, *J* = 6.7 Hz, Me8), 0.98-0.89 (24H, m, Me10, Me12, $OSiCH_2\underline{CH_3}$ x2), 0.60-0.52 (12H, m, $OSi\underline{CH_2}CH_3$ x2); **^{13}C NMR** (125 MHz, $CDCl_3$): δ_C 167.7, 150.5, 145.1, 144.0, 141.3, 129.3, 128.5, 120.0, 87.0, 79.5, 78.8, 73.8, 60.3, 51.6, 41.0, 40.00, 39.97, 20.1, 15.0, 14.6, 10.9, 7.3, 7.0, 5.9, 4.9; **FT-IR** (Thin film): ν_{max} 2953, 2910, 2877, 1720, 1618, 1457, 1264, 1241, 1134, 1113, 1005, 727; **HRMS** (ES^+) Calc. for $C_{33}H_{61}IO_5Si_2H$ $[M+H]^+$ 721.3175, found 721.3176; **101** $\boldsymbol{[\alpha]_D^{20}}$ = −10.1 (*c* 1.0, $CHCl_3$), ***ent*-101** $\boldsymbol{[\alpha]_D^{20}}$ = +13.6 (*c* 1.0, $CHCl_3$).

5.5 Experimental Procedures for the C16-C28 Fragment

(*R*)-3-((4-Methoxybenzyl)oxy)-2-methylpropan-1-ol (155)

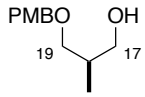

Ester ***ent*-130** (20.0 g, 89.1 mmol) was dissolved in THF (250 mL) and cooled to 0 °C before adding $LiAlH_4$ (3.89 g, 102.6 mmol) portionwise carefully while stirring. The reaction was warmed to rt for 3 h, then cooled to 0 °C again and carefully quenched with H_2O (4 mL), NaOH (4 mL) and H_2O (12 mL) successively. The precipitate was removed by filtration and washed on the filter with Et_2O (3 x 50 mL). The combined organic portions were washed with brine (30 mL), dried ($MgSO_4$), filtered and concentrated *in vacuo*. The crude product was purified by flash column chromatography (20% → 40% EtOAc/PE 40-60) to afford the title compound as a pale yellow oil (16.9 g, 80.4 mmol, 90%).

R_f: 0.25 (40% EtOAc/PE 40-60); **^{1}H NMR** (400 MHz, $CDCl_3$): δ_H 7.24 (2H, d, *J* = 8.5 Hz, ArH), 6.87 (2H, d, *J* = 8.7 Hz, ArH), 4.43 (2H, br s, O$\underline{CH_2}$Ar), 3.79 (3H, s, ArOMe), 3.62-3.53 (2H, m, H19), 3.52-3.45 (1H, m, H17a), 3.39 (1H, t, *J* = 8.6 Hz, H17b), 2.70 (1H, m, H18), 2.91-2.71 (1H, m, OH), 0.87 (3H, d, *J* = 7.1 Hz, Me18); **^{13}C NMR** (125 MHz, $CDCl_3$): δ_C 159.5, 130.4, 129.5, 114.0, 75.1, 73.2, 67.7, 55.5, 35.8, 13.8; **FT-IR** (Thin film): ν_{max} 3386 (br), 2872, 1612, 1586, 1512, 1463, 1362, 1302, 1244, 1173, 1085, 1033, 818, 757, 709; **HRMS** (ES^+) Calc. for $C_{12}H_{18}O_3Na$ $[M+Na]^+$ 233.1148, found 233.1149; $\mathbf{[\alpha]_D^{20}}$ = +14.6 (*c* 1.0, $CHCl_3$).

Data in agreement with that reported by Kalesse.[146]

(*S*)-3-((4-Methoxybenzyl)oxy)-2-methylpropanal (156)

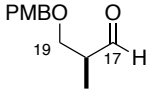

DMSO (7.3 mL, 103 mmol) was added dropwise to a stirring solution of $(COCl)_2$ (4.4 mL, 51.7 mmol) in CH_2Cl_2 (120 mL) at –78 °C and stirred for 15 min. A solution of alcohol **155** (8.7 g, 4.76 mmol) in CH_2Cl_2 (10 mL) was added dropwise to the reaction mixture *via* cannula (2 x 5 mL wash) at –78 °C and stirred for 15 min. Et_3N (28.8 mL, 207 mmol) was added dropwise and the reaction stirred for another 45 min before quenching with NH_4Cl (30 mL) while warming to 0 °C. The layers were separated and the organic layer was washed with H_2O (20 mL), brine (20

mL), dried (Na_2SO_4), filtered and concentrated *in vacuo* to give a solution of the title compound in CH_2Cl_2 (*ca*. 20 mL) and used without further purification.

R_f: 0.25 (40% EtOAc/PE 40-60); **^{1}H NMR** (400 MHz, $CDCl_3$): δ_H 9.71 (1H, d, *J* = 1.5 Hz, H17), 7.24 (2H, d, *J* = 8.8 Hz, ArH), 6.88 (2H, d, *J* = 8.8 Hz, ArH), 4.46 (2H, br s, O$\underline{CH_2}$Ar), 3.81 (3H, s, ArOMe), 3.65 (1H, dd, *J* = 9.3, 6.8 Hz, H19a), 3.60 (1H, dd, *J* = 9.3, 4.9 Hz, H19b), 2.61-2.69 (1H, m, H18), 1.12 (3H, d, *J* = 7.3 Hz, Me18).

Data in agreement with that reported by Kalesse.[146]

(*R*)-1-(((4,4-Dibromo-2-methylbut-3-en-1-yl)oxy)methyl)-4-methoxybenzene (157)

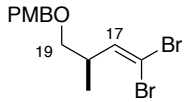

To a stirring solution of CBr_4 (27.4 g, 82.8 mmol) in CH_2Cl_2 (150 mL) at 0 °C was added PPh_3 (43.4 g, 166 mmol) and stirred for 30 min. A solution of aldehyde **156** (assumed 8.6 g, 41.4 mmol) in CH_2Cl_2 (20 mL) was added to the reaction mixture at 0 °C *via* cannula (2 x 10 mL wash). The reaction mixture was stirred at –78 °C for 30 min, then at 0 °C for 30 min before quenching with NH_4Cl (50 mL) and warmed up to rt. The layers were separated and the aqueous layer extracted with CH_2Cl_2 (3 x 50 mL). The combined organic extracts were washed with brine (5 mL), dried ($MgSO_4$), filtered and concentrated *in vacuo*. The crude product was purified by flash column chromatography (5% → 20% EtOAc/PE 40-60) to afford the title compound as a colourless oil (11.6 g, 31.9 mmol, 77% over two steps).

R_f: 0.29 (5% EtOAc/PE 40-60); **^{1}H NMR** (400 MHz, $CDCl_3$): δ_H 7.25 (2H, d, *J* = 8.5 Hz, ArH), 6.88 (2H, d, *J* = 8.5 Hz, ArH), 6.30 (1H, d, *J* = 9.0 Hz, H17), 4.46 (1H, d, *J* = 12.0 Hz, O$\underline{CH_2}$Ar), 4.43 (1H, d, *J* = 11.9 Hz, O$\underline{CH_2}$Ar), 3.81 (3H, s, ArOMe), 3.36 (1H, dd, *J* = 9.0, 6.3 Hz, H19a), 3.33 (1H, dd, *J* = 8.7, 5.6 Hz, H19b), 2.82-2.72 (1H, m, H18), 1.05 (3H, d, *J* = 6.8 Hz, Me18); **^{13}C NMR** (100 MHz, $CDCl_3$): δ_C 158.5, 140.6, 130.0, 128.4, 113.0, 88.0, 72.0, 71.9, 54.5, 38.0, 15.1; $[\alpha]_D^{20}$ = –15.6 (*c* 1.0, $CHCl_3$).

Data in agreement with that reported by Smith.[147]

(*R*)-1-Methoxy-4-(((2-methylpent-3-yn-1-yl)oxy)methyl)benzene (158)

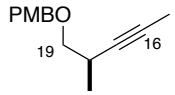

To a solution of vinyl dibromide **157** (12.5 g, 34.3 mmol) in THF (200 mL) at –78 °C was added n-BuLi (1.6 M in hexanes, 42.9 mL, 68.7 mmol) over 10 min. The reaction mixture was stirred for 1 h before adding MeI (6.4 mL, 103 mmol) and stirred for another 30 min. The reaction was quenched with NH_4Cl (50 mL) while warming to rt and the layers separated. The aqueous layer was extracted with Et_2O (3 x 50 mL). The combined organic extracts were washed with brine (20 mL), dried ($MgSO_4$), filtered and concentrated *in vacuo*. The crude product was purified by flash column chromatography (5% → 20% EtOAc/PE 40-60) to afford the title compound as a colourless oil (6.90 g, 31.6 mmol, 92%).

R_f: 0.37 (5% EtOAc/PE 40-60); **^{1}H NMR** (400 MHz, $CDCl_3$): δ_H 7.27 (2H, d, *J* = 8.7 Hz, ArH), 6.88 (2H, d, *J* = 8.7 Hz, ArH), 4.51 (1H, d, *J* = 11.8 Hz, O$\underline{CH_2}$Ar), 4.47 (1H, d, *J* = 11.9 Hz, O$\underline{CH_2}$Ar), 3.81 (3H, s, ArOMe), 3.45 (1H, dd, *J* = 9.1, 6.1 Hz, H19a), 3.29 (1H, dd, *J* = 9.0, 7.5 Hz, H19b), 2.70-2.65 (1H, m, H18), 1.79 (3H, d, *J* = 2.4 Hz, Me16), 1.16 (3H, d, *J* = 6.9 Hz, Me18); **^{13}C NMR** (100 MHz, $CDCl_3$): δ_C 159.1, 130.4, 129.1, 113.7, 81.1, 76.3, 74.0, 72.5, 55.2, 26.6, 18.0, 3.5; **FT-IR** (Thin film): ν_{max} 2858, 1612, 1512, 1457, 1358, 1302, 1245, 1173, 1087, 1035, 819; **HRMS** (ES^+) Calc. for $C_{14}H_{18}O_2H$ $[M+H]^+$ 219.1380, found 219.1381; $\mathbf{[\alpha]_D^{20}}$ = +2.3 (*c* 1.0, $CHCl_3$).

Data in agreement with that reported by Smith.[147]

(*R*,*E*)-1-(((4-Iodo-2-methylpent-3-en-1-yl)oxy)methyl)-4-methoxybenzene (159)

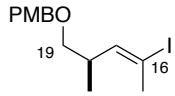

The following reaction was carried out in darkness due to the light sensitivity of the Schwartz reagent $Cp_2Zr(H)Cl$.

DIBAL (1 M in hexanes, 63.2 mL, 63.2 mmol) was added to a suspension of Cp_2ZrCl_2 (18.5 g, 63.2 mmol) in THF (90 mL) at 0 °C and stirred for 30 min. A solution of alkyne **158** (6.90 g, 31.6 mmol) in THF (80 mL) was added to the reaction mixture *via* cannula (2 x 5 mL wash) before warming to rt and left to stir for 7 h. The reaction was cooled to –78 °C, followed by adding a solution of I_2 (24.0 g, 94.8 mmol) in THF (90 mL) *via* cannula. After 10 min, the reaction was

quenched with HCl (1 M, 50 mL) and warmed to rt. The reaction mixture was diluted with Et_2O (50 mL) and the layers separated. The aqueous layer was extracted with Et_2O (3 x 50 mL) and the combined organic extracts washed with $Na_2S_2O_3$ (2 x 50 mL), brine (20 mL), dried ($MgSO_4$), filtered and concentrated *in vacuo*. The crude product was purified by flash column chromatography (5% → 20% EtOAc/PE 40-60) to afford the title compound as a yellow oil (8.28 g, 0.357 mmol, 76%).

R_f: 0.37 (5% EtOAc/PE 40-60); **^{1}H NMR** (400 MHz, $CDCl_3$): δ_H 7.23 (2H, d, *J* = 8.7 Hz, ArH), 6.87 (2H, d, *J* = 8.8 Hz, ArH), 5.98 (1H, dq, *J* = 9.5, 1.4 Hz, H17), 4.46 (2H, br s, O$\underline{CH_2}$Ar), 3.79 (3H, s, ArOMe), 3.29 (2H, dd, *J* = 6.7, 2.8 Hz, H19), 2.74-2.65 (1H, m, H18), 2.38 (3H, d, *J* = 1.6 Hz, Me16), 0.97 (3H, d, *J* = 6.8 Hz, Me18); **^{13}C NMR** (125 MHz, $CDCl_3$): δ_C 159.2, 143.9, 130.5, 129.2, 113.8, 94.5, 73.9, 72.7, 55.3, 36.2, 28.0, 17.0; **FT-IR** (Thin film): ν_{max} 2960, 2852, 1612, 1586, 1512, 1456, 1358, 1302, 1246, 1172, 1091, 1036, 819, 757; **HRMS** (ES^+) Calc. for $C_{14}H_{19}IO_2NH_4$ $[M+NH_4]^+$ 364.0768, found 364.0770; $\mathbf{[\alpha]_D^{20}}$ = +10.8 (*c* 1.0, $CHCl_3$).

Data in agreement with that reported by Smith.[147]

(*R*,*E*)-4-iodo-2-methylpent-3-en-1-ol (169)

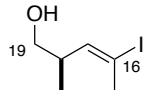

To a stirred solution of the PMB ether **159** (4.99 g, 14.4 mmol) in CH_2Cl_2/pH 7 buffer (9:1, 140 mL) at 0 °C was added DDQ (4.93 g, 21.7 mmol). The reaction mixture was warmed to rt and stirred for 2 h before being quenched with $NaHCO_3$ (50 mL) and diluted with H_2O (30 mL). The layers were separated and the aqueous layer extracted with CH_2Cl_2 (3 x 50 mL). The combined organic extracts were washed with brine (30 mL), dried ($MgSO_4$), filtered and concentrated *in vacuo*. The crude product was purified by flash column chromatography (5% → 40% Et_2O/PE 30-40) to afford the title compound as a colourless oil (2.94 g, 13.0 mmol, 90%).

R_f: 0.25 (20% Et_2O/PE 30-40); **^{1}H NMR** (400 MHz, $CDCl_3$): δ_H 5.95 (1H, dq, *J* = 9.7, 1.4 Hz, H17), 3.43 (1H, dd, *J* = 10.8, 5.9 Hz, H19a), 3.38 (1H, dd, *J* = 10.7, 7.5 Hz, H19b), 2.65-2.57 (1H, m, H18), 2.39 (3H, d, *J* = 2.0 Hz, Me16), 0.94 (3H, d, *J* = 7.0 Hz, Me18); **^{13}C NMR** (125 MHz, $CDCl_3$): δ_C 114.4, 95.4, 66.9, 38.5, 28.1, 16.4; **FT-IR** (Thin film): ν_{max} 3335, 2960, 2925, 2871, 1636, 1602, 1429, 1377, 1258, 1117, 1076, 1030, 996, 977, 936, 906, 857; **HRMS** (ES^+) Calc. for $C_6H_{11}IOH$ $[M–H]^+$ 224.9771, found 224.9776; $\mathbf{[\alpha]_D^{20}}$ = +32.5 (*c* 1.0, $CHCl_3$).

Data in agreement with that reported by Commeiras.[148]

(*R*,*E*)-4-Iodo-2-methylpent-3-enal (154)

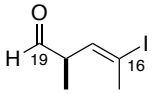

A slurry of DMP (810 mg, 1.91 mmol) and $NaHCO_3$ (160 mg, 1.91 mmol) in CH_2Cl_2 (15 mL) was stirred at rt for 10 min before cooling to 0 °C. A solution of alcohol **160** (354 mg, 0.956 mmol) in CH_2Cl_2 (1 mL) was added *via* cannula (2 x 0.5 mL wash) and the reaction warmed to rt. Upon complete reaction, the reaction was cooled to 0 °C and quenched with $Na_2S_2O_3$ (3 mL) and $NaHCO_3$ (3 mL) and stirred vigorously for 30 min while warming to rt. The layers were separated and the aqueous layer was extracted with CH_2Cl_2 (3 x 10 mL). The combined organic extracts were washed with brine (2 mL), dried (Na_2SO_4), filtered and carefully concentrated *in vacuo* to give the title compound. This solution was kept at 0 °C when left idle and was used without further purification.

R_f: 0.27 (10% Et_2O/PE 30-40); **^{1}H NMR** (400 MHz, $CDCl_3$): δ_H 9.51 (1H, d, J = 1.7 Hz, H19), 6.06 (1H, dq, J = 9.2, 1.3 Hz, H17), 3.30-3.24 (1H, m, H18), 2.45 (3H, d, J = 1.5 Hz, Me18), 1.20 (3H, d, J = 7.0 Hz, Me16).

Data in agreement with that reported by Meiries.[148]

(*R*)-1-((4-Methoxybenzyl)oxy)-2-methylpentan-3-one (153)

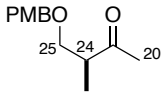

Weinreb amide ***ent*-131** (4.10 g, 15.3 mmol) was dissolved in Et_2O (150 mL) and cooled to –78 °C. MeMgBr (3.0 M in Et_2O, 15.3 mL, 46.0 mmo) was added dropwise and the reaction stirred vigorously at –10 °C overnight before carefully quenching with NH_4Cl (50 mL). The reaction was warmed to rt with stirring before allowing the phases to separate and extracting the aqueous layer with EtOAc (3 x 30 mL). The combined organic extracts were washed with brine (30 mL), dried ($MgSO_4$), filtered and concentrated *in vacuo*. The crude product was purified by flash column chromatography (10% → 20% EtOAc/PE 40-60) to give the title compound as a colourless oil (3.13 g, 14.1 mmol, 92%).

R_f: 0.35 (20% EtOAc/PE 40-60); **^{1}H NMR** (400 MHz, $CDCl_3$): δ_H 7.23 (1H, d, *J* = 8.7 Hz, ArH), 6.87 (1H, d, *J* = 8.7 Hz, ArH), 4.44 (1H, d, *J* = 11.7 Hz, OCH2Ar), 4.41 (1H, d, *J* = 11.7 Hz, OCH2Ar), 3.80 (3H, s, ArOMe), 3.59 (1H, dd, *J* = 9.2, 7.6 Hz, H25a), 3.45 (1H, dd, *J* = 9.3, 5.5 Hz, H25b), 2.89-2.78 (1H, m, H24), 2.17 (3H, s, H20), 1.08 (3H, d, *J* = 7.1 Hz, Me24); **$[\alpha]_D^{20}$** = +14.8 (*c* 1.0, $CHCl_3$).

Data in agreement with that reported by Paterson.[41]

(2*S*,5*R*,6*R*,*E*)-5-hydroxy-8-iodo-1-((4-methoxybenzyl)oxy)-2,6-dimethylnon-7-en-3-one (152)

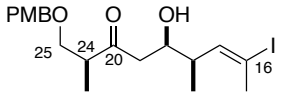

A solution of ketone **153** (642 mg, 3.08 mmol) in Et_2O (5 mL) was added *via* cannula (2 x 2 mL wash) to a stirred solution of (–)-Ipc_2BCl (1.0 M in Et_2O, 2.83 mL, 2.83 mmol) and NEt_3 (0.57 mL, 4.11 mmol) at 0 °C. The resulting yellow suspension was stirred for 1 h at 0 °C then cooled to −78 °C. A solution of aldehyde **154** (575 mg, 2.57 mmol) in Et_2O (5 mL) was dried over activated 4 Å MS and added to the reaction mixture *via* cannula (2 x 1 mL wash). After 3 h, the reaction mixture was transferred to a freezer and left for a further 16 h. The reaction was then quenched with MeOH (5 mL) and pH 7 buffer (5 mL) and H_2O_2 (30% aq., 5 mL). The mixture was warmed to rt, stirred for 1 h and the layers separated. The aqueous layer was extracted with EtOAc (5 x 10 mL) and the combined organic phases washed with water (5 mL), brine (5 mL), dried (Na_2SO_4), filtered and concentrated *in vacuo*. The resulting residue was purified by flash column chromatography (20% → 50% EtOAc/PE 40-60) to give the title compound as a colourless oil (807 mg, 1.80 mmol, 70% over two steps) as a single diastereomer.

R_f: 0.24 (20% EtOAc/PE 40-60); **^{1}H NMR** (500 MHz, $CDCl_3$): δ_H 7.21 (2H, d, *J* = 8.8 Hz, ArH), 6.88 (2H, d, *J* = 8.7 Hz, ArH), 5.96 (1H, dq, *J* = 10.2, 1.6 Hz, H17), 4.43 (1H, d, *J* = 11.8 Hz, O$\underline{CH_2}$Ar), 4.40 (1H, d, *J* = 11.6 Hz, O$\underline{CH_2}$Ar), 3.84-3.78 (1H, m, H19), 3.83 (3H, s, ArOMe), 3.57 (1H, dd, *J* = 9.0, 8.4 Hz, H25a), 3.45 (1H, dd, *J* = 9.0, 5.0 Hz, H25b), 3.15 (1H, d, *J* = 4.1 Hz, OH), 2.92-2.85 (1H, m, H24), 2.72 (1H, dd, *J* = 17.4, 2.5 Hz, H20a), 2.49 (1H, dd, *J* = 17.5, 9.5 Hz, H20b), 2.46 (1H, dd, *J* = 10.1, 7.2 Hz, H18), 2.38 (3H, d, *J* = 1.6 Hz, Me16), 1.05 (3H, d, *J* = 7.1 Hz, Me24), 1.02 (3H, d, *J* = 6.8 Hz, Me18); **^{13}C NMR** (125 MHz, $CDCl_3$): δ_C 215.0, 160.0, 143.4, 130.0, 129.7, 114.2, 95.1, 73.4, 72.2, 71.1, 55.6, 47.0, 46.9, 41.3, 28.4, 16.5, 14.5, 13.5; **FT-IR** (Thin film): ν_{max} 3485 (br), 2933, 1707, 1613, 1514, 1462, 1376, 1203, 1248, 1174,

1091, 1034, 821; **HRMS** (ES^+) Calc. for $C_{19}H_{27}IO_4NH_4$ $[M+NH_4]^+$ 464.1292, found 464.1282; $[\alpha]_D^{20}$ = +46.6 (*c* 1.0, $CHCl_3$).

Mosher ester analysis for aldol adduct 152

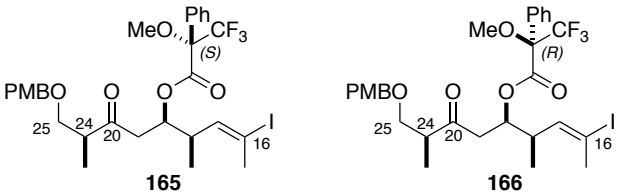

DCC (1 M in CH_2Cl_2, 89.6 μL, 896 μmol) was added in portion to a stirred solution of ***ent*-16** (5.0 mg, 11.2 μmol), (*S*)-α-methoxy-α-trifluoromethylphenylacetic acid (*S*-MTPA) (21.0 mg, 89.6 μmol) and DMAP (11.0 mg, 89.6 μmol) in CH_2Cl_2 (50 μL). The mixture was stirred for 24 h at rt, during which a white precipitate formed. The mixture was filtered through cotton wool and the filtrate reduced to dryness. Purification by flash chromatography (10% → 20% EtOAc/PE 40-60) afforded the product **(*S*)-MTPA ester 165** as a pale-yellow oil (3.7 mg, 5.59 μmol, 50%). The corresponding diastereomer was synthesised from ***ent*-16** (5.0 mg, 11.2 μmol) to afford the diastereomeric ester **(*R*)-MTPA ester 166** (5.6 mg, 8.45 μmol, 75%).

(*S*)-MTPA ester 165

R_f: 0.26 (20% EtOAc/PE 40-60); **^{1}H NMR** (500 MHz, $CDCl_3$): δ_H 7.52-7.46 (2H, m, ArH), 7.42-7.37 (3H, m, ArH), 7.20 (2H, d, *J* = 8.7 Hz, ArH), 6.87 (2H, d, *J* = 8.8 Hz, ArH), 5.87 (1H, dq, *J* = 10.3, 1.4 Hz, H17), 5.42 (1H, q, *J* = 5.8 Hz, H19), 4.41 (1H, d, *J* = 11.4 Hz, O$\underline{CH_2}$Ar), 4.37 (1H, d, *J* = 11.6 Hz, O$\underline{CH_2}$Ar), 3.80 (3H, s, ArOMe), 3.52 (1H, t, *J* = 8.7 Hz, H25a), 3.49 (3H, s, OMe), 3.44 (1H, dd, *J* = 9.0, 5.1 Hz, H25b), 2.84-2.76 (4H, m, H18, H20a, H20b, H24), 2.32 (3H, d, *J* = 1.5 Hz, Me16), 0.99 (3H, d, *J* = 7.0 Hz, Me24), 0.87 (3H, d, *J* = 6.7 Hz, Me18).

(*R*)-MTPA ester 166

R_f: 0.26 (20% EtOAc/PE 40-60); **^{1}H NMR** (500 MHz, $CDCl_3$): δ_H 7.19 (2H, d, *J* = 8.8 Hz, ArH), 6.88 (2H, d, *J* = 8.7 Hz, ArH), 5.98 (1H, dq, *J* = 9.8, 1.4 Hz, H17), 5.42 (1H, dt, *J* = 6.9, 5.2 Hz, H19), 4.40 (1H, d, *J* = 11.6 Hz, O$\underline{CH_2}$Ar), 4.37 (1H, d, *J* = 11.7 Hz, O$\underline{CH_2}$Ar), 3.81 (3H, s, ArOMe), 3.57 (1H, m, H25a), 3.49 (3H, s, OMe), 3.41 (1H, dd, *J* = 9.0, 5.1 Hz, H25b), 2.92-2.86 (1H, m, H24), 2.85 (1H, dd, *J* = 18.1, 7.0 Hz, H20a), 2.49 (1H, dd, *J* = 18.1, 5.5 Hz, H20b), 2.80-2.74 (1H, m, H18), 2.40 (3H, d, *J* = 1.5 Hz, Me16), 0.94 (3H, d, *J* = 7.1 Hz, Me24), 0.92 (3H, d, *J* = 6.9 Hz, Me18).

Proton	δ_H (*S*)-MTPA **165**	δ_H (*R*)-MTPA **166**	$\Delta\delta = \delta_S - \delta_R$
H25a	3.55	3.49	+0.06
H25b	3.46	3.41	+0.05
H24	N.A.[a]	2.88	N.A.
Me24	0.99	0.94	+0.05
H20a	N.A.[a]	2.85	N.A.
H20b	N.A.[a]	2.75	N.A.
H18	N.A.[a]	2.76	N.A.
Me18	0.87	0.92	–0.05
H17	5.87	5.98	–0.11
Me16	2.32	2.40	–0.08

[a] obscured in a 4H multiplet

Table 3: List of chemical shifts in MTPA esters **165** and **166** for Mosher ester analysis of **152**

(2*S*,5*R*,6*R*,*E*)-5-((*tert*-butyldimethylsilyl)oxy)-8-iodo-1-((4-methoxybenzyl)oxy)-2,6-dimethylnon-7-en-3-one (167)

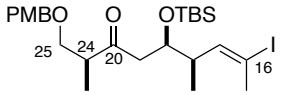

To a stirred solution of alcohol **152** (980 mg, 2.20 mmol) in CH_2Cl_2 (20 mL) at −78 °C was added 2,6-lutidine (0.38 mL, 3.29 mmol) and TBSOTf (0.61 mL, 2.64 mmol). After 30 min the reaction was quenched with MeOH (5 mL) and $NaHCO_3$ (5 mL). The aqueous layer was extracted with CH_2Cl_2 (3 x 10 mL) and the organics dried (Na_2SO_4), filtered and concentrated *in vacuo*. The residue was purified by flash column chromatography (5-20% EtOAc/PE 40-60) to give the title compound as a colourless oil (1.18 g, 2.10 mmol, 95%).

R_f: 0.17 (5% EtOAc/PE 40-60); **^{1}H NMR** (500 MHz, $CDCl_3$): δ_H 7.21 (2H, d, *J* = 8.6 Hz, ArH), 6.87 (2H, dq *J* = 8.6 Hz, ArH), 6.03 (1H, dq, *J* = 9.8, 1.4 Hz, H17), 4.43 (1H, d, *J* = 11.6 Hz, O$\underline{CH_2}$Ar), 4.39 (1H, d, *J* = 11.7 Hz, O$\underline{CH_2}$Ar), 4.13 (1H, td, *J* = 6.0, 4.0 Hz, H19), 3.80 (3H, s, ArOMe), 3.57 (1H, dd, *J* = 9.0, 7.7 Hz, H25a), 3.44 (1H, dd, *J* = 9.1, 5.4 Hz, H25b), 2.80 (1H, qnd, *J* = 7.2, 5.4 Hz, H24), 2.72 (1H, dd, *J* = 17.7, 6.2 Hz, H20a), 2.49 (1H, dd, *J* = 17.7, 5.7 Hz, H20b), 2.53-2.46 (1H, m, H18), 2.39 (3H, d, *J* = 1.4 Hz, Me16), 1.05 (3H, d, *J* = 7.0 Hz, Me24), 0.90 (3H, d, *J* = 6.8 Hz, Me18), 0.86 (9H, s, OSi$\underline{t\text{-}Bu}Me_2$), 0.07 (3H, s, OSit-Bu$\underline{Me_2}$), –0.02 (3H, s, OSit-Bu$\underline{Me_2}$); **^{13}C NMR** (125 MHz, $CDCl_3$): δ_C 211.4, 159.6, 144.9, 130.4, 129.6, 114.1, 94.6, 73.3, 72.2, 70.9, 55.6, 48.0, 47.5, 41.1, 28.3, 26.2, 18.4, 14.5, 13.5, –4.2, –4.5; **FT-IR** (Thin film): ν_{max} 2933, 2856, 1714, 1613, 1514, 1462, 1376, 1302, 1249, 1173, 1097, 1037, 836, 777; **HRMS**

(ES$^+$) Calc. for $C_{25}H_{41}IO_4SiNH_4$ $[M+NH_4]^+$ 578.2157, found 578.2143; $[\alpha]_D^{20}$ = +52.3 (*c* 1.0, $CHCl_3$).

ethyl (5*R*,6*R*,*E*)-5-((*tert*-butyldimethylsilyl)oxy)-3-hydroxy-8-iodo-3-((*S*)-1-((4-methoxybenzyl)oxy)propan-2-yl)-6-methylnon-7-enoate (168)

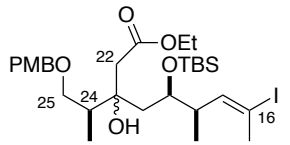

To a stirred solution of i-Pr_2NH (3.00 mL, 21.4 mmol) in THF (4 mL) at 0 °C was added n-BuLi (11.7 mL, 18.7 mmol, 1.6 M in hexanes). The resulting pale yellow solution was stirred at 0 °C for 15 min then cooled to −78 °C. Ethyl acetate (1.74 mL, 17.8 mmol) was added dropwise. The reaction mixture was stirred at −78 °C for 1 h to give a *ca.* 0.9 M solution of the derived lithium enolate.

A solution of ketone **167** (1.00 g, 1.78 mmol) in THF (10 mL) was cooled to −78 °C before adding the above lithium enolate solution (0.9 M in THF, 9.89 mL, 8.90 mmol). The reaction was quenched after 1.5 h with $NaHCO_3$ (10 mL) and warmed to rt. The mixture was diluted with Et_2O (20 mL) and the aqueous layer extracted with Et_2O (3 x 20 mL). The organic phases were dried (Na_2SO_4), filtered and concentrated *in vacuo*. The residue was purified by flash column chromatography (10% EtOAc/PE 40-60) to give the title compound as a colourless oil (1.12 g, 1.72 mmol, 97%) as a mixture of diastereomers (*d.r.* 5:1).

Major isomer: $\mathbf{R_f}$: 0.16 (5% EtOAc/PE 40-60); **^{1}H NMR** (500 MHz, $CDCl_3$): δ_H 7.24 (2H, d, *J* = 8.7 Hz, Ar*H*), 6.88 (2H, d, *J* = 8.8 Hz, Ar*H*), 6.18 (1H, dq, *J* = 9.5, 1.5 Hz, H17), 4.44 (1H, d, *J* = 11.6 Hz, O$\underline{CH_2}$Ar), 4.40 (1H, d, *J* = 11.5 Hz, O$\underline{CH_2}$Ar), 4.12 (2H, q, *J* = 7.3 Hz, O$\underline{CH_2}CH_3$), 3.99-3.95 (1H, m, H19), 3.97 (1H, s, OH), 3.81 (3H, s, ArOMe), 3.60 (1H, dd, J = 9.2, 5.0 Hz, H25a), 3.39 (1H, dd, *J* = 9.3, 6.4 Hz, H25b), 2.74-2.66 (1H, m, H24), 2.58 (1H, d, *J* = 15.3 Hz, H22a), 2.53 (1H, d, *J* = 15.3 Hz, H22b), 2.38 (3H, d, *J* = 1.4 Hz, Me16), 2.12-2.03 (1H, m, H18), 1.79 (1H, dd, *J* = 15.0, 5.8 Hz, H20a), 1.68 (1H, dd, *J* = 14.9, 5.9 Hz, H20$_b$), 1.24 (3H, t, *J* = 7.1 Hz, $OCH_2\underline{CH_3}$) 1.00 (3H, d, *J* = 7.0 Hz, Me24), 0.93 (3H, d, *J* = 7.0 Hz, Me18), 0.89 (9H, s, OSi$\underline{t\text{-}Bu}Me_2$), 0.08 (3H, s, OSit-Bu$\underline{Me_2}$), 0.07 (3H, s, OSit-Bu$\underline{Me_2}$); **^{13}C NMR** (125 MHz, $CDCl_3$): δ_C 172.3, 159.2, 144.7, 130.4, 129.3, 113.8, 93.8, 74.3, 73.0, 72.1, 72.0, 60.6, 55.3, 42.1, 41.1, 40.8, 39.3, 28.1, 26.0, 18.1, 14.2, 14.1, 12.9, –4.1, –4.3; **HRMS** (ES$^+$) Calc. for $C_{29}H_{49}IO_6SiH$ $[M+H]^+$ 649.2416, found 649.2407.

(6*R*)-4-hydroxy-6-((*R*,*E*)-4-iodopent-3-en-2-yl)-4-((*S*)-1-((4-methoxybenzyl)oxy)propan-2-yl)tetrahydro-2*H*-pyran-2-one (169)

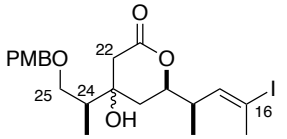

Method A

A solution of ester **168** (1.12 g, 1.72 mmol) in THF (5 mL) was cooled to 0 °C before slowly adding HF•py (1.5 mL). The reaction mixture was allowed to warm to rt and stirred for 3 h. The reaction mixture was transferred to an ice-cold $NaHCO_3$ (20 mL) portionwise and stirred until effervescence ceased. The layers were separated and the aqueous layer extracted with EtOAc (3 x 30 mL). The combined organic phases were dried ($MgSO_4$), filtered and concentrated *in vacuo*. The residue was purified by flash column chromatography (30% → 50% EtOAc/PE 40-60) to give the title compound as a colourless oil (713 mg, 1.46 mmol, 85%) as a mixture of diastereomers (*d.r.* 5:1).

Method B

TsOH•H_2O (140 mg, 0.74 mmol) was added to a solution of ester **168** (1.20 g, 1.85 mmol) in MeOH (20 mL) at rt and stirred for 16 h. The reaction was quenched with $NaHCO_3$ (5 mL) and concentrated *in vacuo* before partitioning between EtOAc (20 mL) and H_2O (10 mL). The phases were separated and the aqueous phase extracted with EtOAc (3 x 10 mL). The organic phases were dried ($MgSO_4$), filtered and concentrated *in vacuo*. The residue was purified by flash column chromatography (30% → 50% EtOAc/PE 40-60) to give the title compound as a colourless oil (750 mg, 1.54 mmol, 83%) as a mixture of diastereomers (*d.r.* 5:1).

Major isomer: $\mathbf{R_f}$: 0.32 (40% EtOAc/PE 40-60); **^{1}H NMR** (500 MHz, $CDCl_3$): δ_H 7.23 (2H, d, *J* = 8.7 Hz, ArH), 6.90 (2H, d, *J* = 8.7 Hz, ArH), 5.98 (1H, dq, *J* = 10.0, 1.5 Hz, H17), 4.48 (1H, d, *J* = 11.5 Hz, O$\underline{CH_2}$Ar), 4.41 (1H, d, *J* = 11.5 Hz, O$\underline{CH_2}$Ar), 3.88 (1H, ddd, *J* = 11.4, 7.2, 4.5 Hz, H19), 3.87 (1H, s, O*H*), 3.82 (3H, s, ArOMe), 3.70 (1H, dd, *J* = 9.6, 3.4 Hz, H25a), 3.44 (1H, dd, *J* = 9.8, 5.1 Hz, H25b), 2.75-2.65 (1H, m, H18), 2.58 (2H, s, H22), 2.38 (3H, d, *J* = 1.6 Hz, Me16), 2.00 (1H, dd, *J* = 14.6, 4.5 Hz, H20a), 1.85-1.77 (1H, m, H24), 1.68 (1H, dd, *J* = 14.5, 11.1 Hz, H20b), 1.09 (3H, d, *J* = 6.7 Hz, Me18), 1.04 (3H, d, *J* = 7.0 Hz, Me24); **^{13}C NMR** (125 MHz, $CDCl_3$): δ_C 171.4, 159.7, 141.2, 129.7, 129.1, 114.1, 96.0, 79.1, 73.6, 73.5, 72.1, 55.4, 42.6, 40.9, 40.4, 37.3, 28.3, 16.1, 12.7; **HRMS** (ES^+) Calc. for $C_{21}H_{29}IO_5NH_4$ $[M+NH_4]^+$ 506.1398, found 506.1386.

(*R*)-6-((*R*,*E*)-4-iodopent-3-en-2-yl)-4-((*R*)-1-((4-methoxybenzyl)oxy)propan-2-yl)-5,6-dihydro-2*H*-pyran-2-one (151)

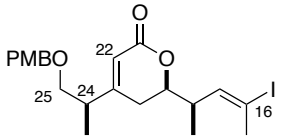

To a stirred solution of lactone **169** (480 mg, 0.983 mmol) in Ac_2O/pyr/PhH (1:5:5, 11 mL) was added DMAP (100 mg, 0.983 mmol). The reaction mixture was heated to reflux for 16 h then cooled to rt, diluted with CH_2Cl_2 (3 mL) and carefully quenched with $NaHCO_3$ (3 mL). The layers were separated and the aqueous layer extracted with CH_2Cl_2 (3 x 5 mL). The combined organic phases were dried (Na_2SO_4), filtered and concentrated *in vacuo*. The residue was purified by flash column chromatography (30% → 50% EtOAc/PE 40-60) to give the title compound as a pale yellow oil (384 mg, 0.816 mmol, 83%).

R_f: 0.15 (20% EtOAc/PE 40-60); **^{1}H NMR** (500 MHz, $CDCl_3$): δ_H 7.22 (2H, d, *J* = 8.7 Hz, ArH), 6.89 (2H, d, *J* = 8.7 Hz, ArH), 5.97 (1H, dq, *J* = 10.1, 1.4 Hz, H17), 5.82 (1H, s, H22), 4.44 (1H, d, *J* = 11.6 Hz, O$\underline{CH_2}$Ar), 4.39 (1H, d, *J* = 11.6 Hz, O$\underline{CH_2}$Ar), 4.06 (1H, ddd, *J* = 11.0, 6.8, 4.4 Hz, H19), 3.81 (3H, s, ArOMe), 3.45 (1H, dd, *J* = 9.4, 5.6 Hz, H25a), 3.41 (1H, dd, *J* = 9.4, 7.6 Hz, H25b), 2.76-2.66 (1H, m, H18), 2.66-2.54 (1H, m, H24), 2.40 (3H, d, *J* = 1.6 Hz, Me16), 2.26 (1H, dd, *J* = 17.6, 4.6 Hz, H20a), 2.19 (1H, dd, *J* = 17.6, 11.4, 1.4 Hz, H20b), 1.10 (3H, d, *J* = 7.0 Hz, Me24), 1.09 (3H, d, *J* = 7.0 Hz, Me18); **^{13}C NMR** (125 MHz, $CDCl_3$): δ_C 165.2, 163.2, 159.5, 141.2, 130.0, 129.5, 115.7, 114.1, 96.0, 80.0, 73.1, 72.6, 55.5, 40.4, 39.9, 29.7, 28.3, 16.2, 15.7; **FT-IR** (Thin film): ν_{max} 2964, 2932, 2870, 1715, 1637, 1612, 1586, 1513, 1457, 1380, 1359, 1302, 1248, 1208, 1173, 1091, 1034, 868, 820, 733, 666; **HRMS** (ES^+) Calc. for $C_{21}H_{27}IO_4NH_4$ $[M+NH_4]^+$ 488.1292, found 488.1283; **$[\alpha]_D^{20}$** = +82.5 (*c* 0.67, $CHCl_3$).

(3*S*,4*R*,6*R*)-3,4-dihydroxy-6-((*R*,*E*)-4-iodopent-3-en-2-yl)-4-((*S*)-1-((4-methoxybenzyl)oxy)propan-2-yl)tetrahydro-2*H*-pyran-2-one (174)

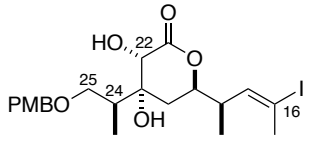

To a stirred solution of enoate **151** (160 mg, 0.340 mmol) in THF/t-BuOH/H_2O (1:1:1, 0.6 mL) was added citric acid (130 mg, 0.680 mmol), K_2OsO_4•$2H_2O$ (2.5 mg, 6.8 μmol) and NMO (50 wt% in H_2O, 49 μL, 0.238 mmol). The reaction mixture was stirred for 5 h then quenched with Na_2SO_3 (0.5 mL) and $NaHCO_3$ (0.5 mL). The layers were separated and the aqueous layer extracted with EtOAc (3 x 3 mL). The organic phases were dried (Na_2SO_4), filtered and

concentrated *in vacuo*. The residue was purified by flash column chromatography (20% → 50% EtOAc/PE 40-60) to give the title compound as a colourless oil (94.3 mg, 0.187 mmol, 55%, 85% brsm) as a single diastereomer. The stereochemistry was confirmed by the diagonostic nOe interaction of H20b and H22.

R_f: 0.43 (50% EtOAc/PE 40-60); **^{1}H NMR** (500 MHz, $CDCl_3$): δ_H 7.23 (2H, d, *J* = 8.8 Hz, ArH), 6.88 (2H, d, *J* = 8.7 Hz, ArH), 6.02 (1H, dq, *J* = 10.0, 1.5 Hz, H17), 4.50 (1H, ddd, *J* = 11.5, 6.6, 3.7 Hz, H19), 4.44 (2H, s, O$\underline{CH_2}$Ar), 4.19 (1H, d, *J* = 1.2 Hz, H22), 3.92 (1H, d, J = 1.9 Hz, OH22), 3.81 (3H, s, ArOMe), 3.68 (1H, dd, *J* = 9.7, 8.4 Hz, H25a), 3.57 (1H, br s, OH21), 3.50 (1H, dd, *J* = 9.7, 4.2 Hz, H25b), 2.71-2.61 (1H, m, H18), 2.38 (3H, d, *J* = 1.5 Hz, Me16), 2.22-2.12 (1H, m, H24), 1.85 (1H, dd, *J* = 14.2, 3.7 Hz, H20a), 1.76 (1H, ddd, *J* = 14.5, 11.1, 1.9 Hz, H20b), 1.06 (3H, d, *J* = 6.7 Hz, Me18), 0.98 (3H, d, *J* = 7.1 Hz, Me24); **^{13}C NMR** (125 MHz, $CDCl_3$): δ_C 174.8, 159.5, 141.0, 129.7, 129.6, 114.1, 96.1, 80.3, 74.4, 73.3, 73.0, 71.8, 55.4, 40.3, 40.1, 33.6, 28.3, 15.9, 12.2; **FT-IR** (Thin film): ν_{max} 3441 (br), 2963, 2933, 2862, 1731, 1637, 1613, 1586, 1514, 1461, 1302, 1218, 1174, 1100, 1033, 821, 760, 669; **HRMS** (ES^+) Calc. for $C_{21}H_{29}IO_6NH_4$ $[M+NH_4]^+$ 522.1347, found 522.1339; $\mathbf{[\alpha]_D^{20}}$ **=** –9.4 (*c* 0.67, $CHCl_3$).

(3*S*,4*R*,6*R*)-6-((*R*,*E*)-4-iodopent-3-en-2-yl)-4-((*S*)-1-((4-methoxybenzyl)oxy)propan-2-yl)-3,4-bis((triethylsilyl)oxy)tetrahydro-2*H*-pyran-2-one (187)

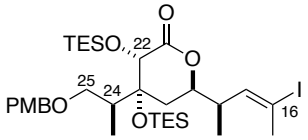

A solution of diol **174** (170 mg, 0.337 mmol) in CH_2Cl_2 (3 mL) was cooled to 0 °C and 2,6-lutidine (0.31 mL, 2.70 mmol) and TESOTf (0.38 mL, 1.69 mmol) were added sequentially. The reaction mixture was stirred at 0 °C for 24 h then quenched with $NaHCO_3$ (1 mL). The layers were separated and the aqueous layer extracted with CH_2Cl_2 (3 x 5 mL). The combined organic phases were dried ($MgSO_4$), filtered and concentrated *in vacuo*. The residue was purified by flash column chromatography (5% → 10% EtOAc/PE 40-60) to give the title compound as a colourless oil (218 mg, 0.297 mmol, 88%).

R_f: 0.44 (10% EtOAc/PE 40-60); **^{1}H NMR** (500 MHz, $CDCl_3$): δ_H 7.21 (2H, d, *J* = 8.6 Hz, ArH), 6.89 (2H, d, *J* = 8.6 Hz, ArH), 6.00 (1H, dq, *J* = 10.0, 1.3 Hz, H17), 4.41 (1H, d, *J* = 11.6 Hz, O$\underline{CH_2}$Ar), 4.38 (1H, d, *J* = 11.6 Hz, O$\underline{CH_2}$Ar), 4.37-4.30 (1H, m, H19), 4.22 (1H, s, H22), 3.81 (3H, s, ArOMe), 3.32 (1H, dd, *J* = 9.5, 4.9 Hz, H25a), 3.23 (1H, dd, *J* = 9.5, 5.4 Hz, H25b), 2.69-2.59 (1H, m, H18), 2.35 (3H, d, *J* = 1.5 Hz, Me16), 2.36-2.28 (1H, m, H24), 1.80 (1H, dd, *J* =

14.2, 3.5 Hz, H20a), 1.60 (1H, dd, *J* = 14.0, 11.8 Hz, H20b), 1.03 (3H, d, *J* = 6.8 Hz, Me18), 0.99 (3H, d, *J* = 7.0 Hz, Me24), 0.94 (9H, t, *J* = 8.0 Hz, $OSiCH_2\underline{CH_3}$), 0.94 (9H, t, *J* = 8.0 Hz, $OSiCH_2\underline{CH_3}$), 0.90 (12H, m, $OSi\underline{CH_2}CH_3$); **^{13}C NMR** (125 MHz, $CDCl_3$): δ_C 172.7, 159.5, 141.4, 130.1, 129.7, 114.0, 96.0, 79.6, 78.8, 74.1, 73.5, 71.8, 55.4, 40.1, 37.7, 33.0, 28.3, 16.1, 11.9, 7.4, 7.2, 6.7, 5.3; **FT-IR** (Thin film): ν_{max} 2955, 2912, 2876, 1751, 1612, 1514, 1458, 1379, 1302, 1248, 1145, 1082, 1010, 978, 831, 731; **HRMS** (ES^+) Calc. for $C_{33}H_{57}IO_6Si_2H$ $[M+H]^+$ 733.2811, found 733.2808; $\mathbf{[\alpha]_D^{20}}$ = +18.6 (*c* 1.0, $CHCl_3$).

(3*S*,4*R*,6*R*)-4-((*S*)-1-hydroxypropan-2-yl)-6-((*R*,*E*)-4-iodopent-3-en-2-yl)-3,4-bis((triethylsilyl)oxy)tetrahydro-2*H*-pyran-2-one (188)

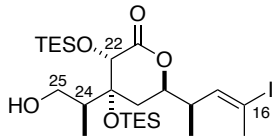

To an emulsion of PMB ether **187** (190 mg, 0.260 mmol) in CH_2Cl_2/pH 7 buffer (9:1, 2 mL) at 0 °C was added DDQ (118 mg, 0.520 mmol). The resulting green suspension was stirred for 2 h then quenched with $NaHCO_3$ (2 mL). The layers were separated and the aqueous layer extracted with CH_2Cl_2 (3 x 10 mL). The combined organic phases were washed with brine (5 mL), dried (Na_2SO_4), filtered and concentrated *in vacuo*. The residue was purified by flash column chromatography (10% → 20% EtOAc/PE 40-60) to give the title compound as a colourless oil (125 mg, 0.208 mmol, 80%).

R_f: 0.14 (10% EtOAc/PE 40-60); **^{1}H NMR** (500 MHz, $CDCl_3$): δ_H 6.00 (1H, dq, *J* = 9.7, 1.5 Hz, H17), 4.36 (1H, ddd, *J* = 11.6, 6.6, 3.5 Hz, H19), 4.29 (1H, s, H22), 3.63-3.51 (2H, m, H25), 2.71-2.61 (1H, m, H18), 2.41 (3H, d, *J* = 1.5 Hz, Me16), 2.31-2.22 (1H, m, H24), 1.85 (1H, dd, *J* = 14.1, 3.6 Hz, H20a), 1.57 (1H, dd, *J* = 14.0, 11.8 Hz, H20b), 1.06 (3H, d, *J* = 6.8 Hz, Me18), 1.02-0.97 (12H, m, Me24, $OSiCH_2\underline{CH_3}$), 0.92 (9H, t, *J* = 7.9 Hz, $OSiCH_2\underline{CH_3}$), 0.84-0.72 (6H, m, $OSi\underline{CH_2}CH_3$), 0.72-0.58 (6H, m, $OSi\underline{CH_2}CH_3$); **^{13}C NMR** (125 MHz, $CDCl_3$): δ_C 172.5, 141.3, 95.9, 79.5, 79.7, 74.2, 64.6, 40.3, 39.6, 33.3, 28.4, 16.2, 11.4, 7.4, 7.3, 6.7, 5.4; **FT-IR** (Thin film): ν_{max} 3477 (br), 2955, 2876, 1731, 1638, 1458, 1416, 1380, 1239, 1161, 1044, 1008, 977, 832, 730; **HRMS** (ES^+) Calc. for $C_{25}H_{49}IO_5Si_2H$ $[M+H]^+$ 613.2236, found 613.2228; $\mathbf{[\alpha]_D^{20}}$ = +14.8 (*c* 1.0, $CHCl_3$).

(*R*)-2-((3*S*,4*R*,6*R*)-6-((*R*,*E*)-4-iodopent-3-en-2-yl)-2-oxo-3,4-bis((triethylsilyl)oxy)tetrahydro-2*H*-pyran-4-yl)propanal (1989)

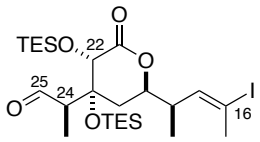

DMP (125 mg, 294 μmol) and $NaHCO_3$ (49.4 mg, 588 μmol) were added to a stirred solution of alcohol **188** (60.0 mg, 98.0 μmol) in CH_2Cl_2 (1 mL) at 0 °C then warmed to rt. After 1 h, the reaction was quenched with $Na_2S_2O_3$ (1 mL) and $NaHCO_3$ (1 mL) at 0 °C and stirred for 10 min at rt. The layers were separated and the aqueous layer extracted with CH_2Cl_2 (3 x 5 mL). The combined organic phases were dried ($MgSO_4$), filtered and concentrated *in vacuo* to give the title compound as a colourless oil which was used immediately without further purification.

R_f: 0.43 (10% EtOAc/PE 40-60); **^{1}H NMR** (500 MHz, $CDCl_3$): δ_H 9.69 (1H, d, *J* = 1.0 Hz, H25), 5.98 (1H, dq, *J* = 9.9, 1.5 Hz, H17), 4.44 (1H, s, H22), 4.34 (1H, ddd, *J* = 11.3, 7.2, 4.0 Hz, H19), 3.00 (1H, dq, *J* = 7.5, 0.9 Hz, H24), 2.71-2.61 (1H, m, H18), 2.40 (3H, d, *J* = 1.5 Hz, Me16), 1.86 (1H, dd, *J* = 14.0, 4.0 Hz, H20a), 1.76 (1H, dd, *J* = 14.0, 11.5 Hz, H20b), 1.22 (3H, d, *J* = 7.6 Hz, Me24), 1.07 (3H, d, *J* = 6.7 Hz, Me18), 0.97 (9H, t, *J* = 7.9 Hz, $OSiCH_2\underline{CH_3}$), 0.93 (9H, t, *J* = 7.9 Hz, $OSiCH_2\underline{CH_3}$), 0.79-0.69 (6H, m, $OSi\underline{CH_2}CH_3$), 0.69-0.59 (6H, m, $OSi\underline{CH_2}CH_3$); **^{13}C NMR** (125 MHz, $CDCl_3$): δ_C 202.3, 171.6, 141.0, 96.2, 79.1, 77.7, 73.7, 50.7, 40.4, 33.9, 29.8, 28.3, 16.2, 7.3, 7.1, 6.7, 5.2; **FT-IR** (Thin film): ν_{max} 2953, 2877, 1755, 1722, 1457, 1379, 1240, 1147, 1010, 975, 830, 730; **HRMS** (ES^+) Calc. for $C_{25}H_{47}IO_5Si_2H$ $[M+H]^+$ 611.2079, found 611.2070; **$[\alpha]_D^{20}$** = +14.5 (*c* 0.4, $CHCl_3$).

(3*S*,4*R*,6*R*)-6-((*R*,*E*)-4-iodopent-3-en-2-yl)-4-((*S*,*E*)-5-oxohex-3-en-2-yl)-3,4-bis((triethylsilyl)oxy)tetrahydro-2*H*-pyran-2-one (191)

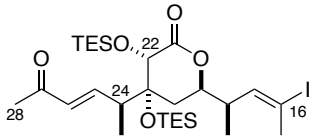

Dimethyl (2-oxopropyl)phosphonate **190** (67.7 μL, 490 μmol) was added to a stirred suspension of oven-dried $Ba(OH)_2$ (50.3 mg, 294 μmol) in THF (0.5 mL) at rt. After 30 min, the reaction mixture was cooled to 0 °C and a solution of aldehyde **189** (60.0 mg, 98.0 μmol) in THF/H_2O (40:1, 0.5 mL) added *via* cannula (0.5 mL wash). The reaction mixture was warmed to rt and after 16 h, the reaction was quenched with NH_4Cl (1 mL) and diluted with CH_2Cl_2 (5 mL). The layers were separated and the aqueous layer extracted with CH_2Cl_2 (3 x 10 mL). The combined organic phases were dried ($MgSO_4$), filtered and concentrated *in vacuo*. The residue was purified by flash column chromatography (10% → 20% EtOAc/PE 40-60) to give the title compound as a colourless oil (51.0 mg, 78.4 μmol, 80% over two steps).

R_f: 0.20 (10% EtOAc/PE 40-60); **^{1}H NMR** (500 MHz, $CDCl_3$): δ_H 6.65 (1H, dd, *J* = 15.8, 8.3 Hz, H25), 6.23 (1H, d, *J* = 15.8 Hz, H26), 5.97 (1H, dq, *J* = 10.0, 1.4 Hz, H17), 4.35 (1H, ddd, *J* = 11.3, 6.9, 3.4 Hz, H19), 3.98 (1H, s, H22), 3.02-2.93 (1H, m, H18), 2.69-2.59 (1H, m, H24), 2.41 (3H, d, *J* = 1.4 Hz, Me16), 2.26 (3H, s, H28), 1.89 (1H, dd, *J* = 13.9, 3.4 Hz, H20a), 1.76 (1H, dd, *J* = 13.9, 11.6 Hz, H20b), 1.10 (3H, d, *J* = 7.0 Hz, Me24), 1.07 (3H, d, *J* = 6.7 Hz, Me18), 1.00 (9H, t, *J* = 7.8 Hz, $OSiCH_2\underline{CH_3}$), 0.93 (9H, t, *J* = 7.9 Hz, $OSiCH_2\underline{CH_3}$), 0.83-0.74 (6H, m, $OSi\underline{CH_2}CH_3$), 0.74-0.60 (6H, m, $OSi\underline{CH_2}CH_3$); **^{13}C NMR** (125 MHz, $CDCl_3$): δ_C 197.6, 171.8, 146.4, 141.0, 132.1, 96.2, 79.3, 78.8, 74.4, 41.5, 40.3, 32.6, 28.4, 28.2, 16.3, 13.4, 7.4, 7.3, 6.7, 5.6; **FT-IR** (Thin film): ν_{max} 2956, 2877, 1751, 1679, 1626, 1458, 1380, 1238, 1143, 1059, 1006, 978, 826, 730; **HRMS** (ES^+) Calc. for $C_{28}H_{51}IO_5Si_2H$ $[M+H]^+$ 651.2392, found 651.2406; **$[\alpha]_D^{20}$ =** –2.0 (*c* 0.20, $CHCl_3$).

(3*S*,4*R*,6*R*)-6-((*R*,*E*)-4-iodopent-3-en-2-yl)-4-((*S*)-5-oxohexan-2-yl)-3,4-bis((triethylsilyl)oxy)tetrahydro-2*H*-pyran-2-one (102)

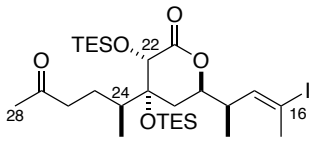

To a solution of enone **191**(45 mg, 69 μmol) in degassed PhMe (100 μL) at rt was added a solution of Stryker's reagent (2.73 mL, 1.0 eq wrt Cu, 69 μmol). The reaction mixture was stirred for 2 h and then diluted with hexanes (2 mL) and stirred vigorously with exposure to air. The resulting suspension was filtered through a plug of silica gel, eluting with 10% EtOAc/PE 40-60. The solvent was removed *in vacuo* and the resulting residue purified by flash column chromatography (5% → 20% EtOAc/PE 40-60) to give the title compound as a colourless oil (30 mg, 46 μmol, 67%).

R_f: 0.27 (10% EtOAc-Pet. Ether; **^{1}H NMR** (400 MHz, $CDCl_3$): δ_H 5.98 (1H, dq, *J* = 10.1, 1.4 Hz, H17), 4.34 (1H, ddd, *J* = 11.6, 7.0, 3.6 Hz, H19), 4.22 (1H, s, H22), 2.69-2.52 (2H, m, H18, H26a), 2.37-2.27 (1H, m, H26b), 2.41 (3H, d, *J* = 1.5 Hz, Me16), 2.17 (3H, s, H28), 2.02-1.92 (1H, m, H24), 1.78 (1H, dd, *J* = 13.9, 3.5 Hz, H20a), 1.43 (1H, dd, *J* = 13.8, 11.7 Hz, H20b), 1.66-1.56 (1H, m, H25a), 1.27-1.17 (1H, m, H25b), 1.06 (3H, d, *J* = 6.7 Hz, Me18), 0.98 (9H, t, *J* = 7.9 Hz, $OSiCH_2\underline{CH_3}$), 0.91 (9H, t, *J* = 7.9 Hz, $OSiCH_2\underline{CH_3}$), 0.90 (3H, d, *J* = 7.0 Hz, Me24), 0.80-0.70 (6H, m, $OSi\underline{CH_2}CH_3$), 0.68-0.58 (6H, m, $OSi\underline{CH_2}CH_3$); **^{13}C NMR** (100 MHz, $CDCl_3$): δ_C 208.2, 172.5, 141.2, 95.9, 79.8, 79.5, 73.2, 42.4, 40.4, 37.0, 32.1, 30.2, 28.4, 25.7, 16.3, 13.0, 7.4, 7.2, 6.8, 5.3; **FT-IR** (Thin film): ν_{max} 2957, 2877, 1751, 1718, 1459, 1380, 1259, 1157, 1091,

1014, 912, 829, 728; **HRMS** (ES^+) Calc. for $C_{28}H_{53}IO_5Si_2H$ $[M+H]^+$ 653.2549, found 653.2542; $\mathbf{[\alpha]_D^{20}}$ = +2.2 (*c* 0.50, $CHCl_3$)

5.6 Experimental Procedures for the C1-C28 Fragment

Methyl (2*E*,4*E*,6*E*,8*S*,9*R*,10*S*,11*S*,12*S*,13*R*,14*E*)-11,13-dihydroxy-15-iodo-9-methoxy-8,10,12,14-tetramethylpentadeca-2,4,6,14-tetraenoate (195)

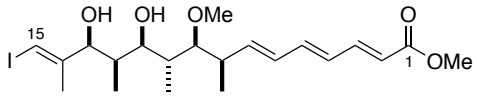

A solution of HF•py/py was prepared by the addition of HF•py (100 µL) to a solution of py (200 µL) in THF (1 mL) at 0 °C and stirred for 30 min at rt before use.

To a stirring solution of silyl ether **101** (4 mg, 5.5 µmol) in THF (200 uL) at 0 °C was added a solution of HF•py/py (200 µL). The reaction mixture was stirred for 5 h at rt before diluting with THF (1 mL) and quenched with $NaHCO_3$ (1 mL). The layers were separated and the aqueous phase extracted with Et_2O (3 x 2 mL) and the combined organic extracts were washed with $NaHCO_3$ (0.5 mL), dried (Na_2SO_4) and concentrated *in vacuo*. The crude product was purified by flash column chromatography (10% → 20% EtOAc/PE 40-60) to give the title compound as a colourless oil (2 mg, 4.06 µmol, 75%).

R_f: 0.23 (20% EtOAc/PE 40-60); **^{1}H NMR** (500 MHz, $CDCl_3$): δ_H 7.41 (1H, dd, *J* = 15.1, 11.3 Hz, H3), 6.71 (1H, dd, *J* = 15.0, 10.8 Hz, H5), 6.34 (1H, dd, *J* = 15.0, 11.3 Hz, H4), 6.31 (1H, s, H15), 6.20 (1H, dd, *J* = 15.2, 10.8 Hz, H6), 5.91 (1H, dd, *J* = 15.2, 0.9 Hz, H7), 5.90 (1H, d, *J* = 15.3 Hz, H2), 4.13 (1H, d, *J* = 8.0 Hz, H13), 3.73 (3H, s, CO_2Me), 3.38 (1H, dd, *J* = 9.3, 2.2 Hz, H11), 3.37 (1H, s, H9a), 3.27 (1H, dd, *J* = 7.7, 3.7 Hz, H9), 2.50 (1H, m, H8), 1.96 (1H, m, H10), 1.75 (1H, m, H12), 1.67 (3H, d, *J* = 0.9 Hz, Me14), 1.08 (3H, d, *J* = 6.7 Hz, Me8), 0.93 (3H, d, *J* = 6.8 Hz, Me12), 0.83 (3H, d, *J* = 7.1 Hz, Me10); **^{13}C NMR** (125 MHz, $CDCl_3$): δ_C 169.4, 150.2, 146.7, 144.5, 143.2, 130.7, 129.6, 120.4, 87.1, 80.7, 79.4, 74.1, 59.0, 52.0, 41.9, 40.3, 38.9, 19.5, 17.9, 12.1, 7.8; **FT-IR** (Thin film): ν_{max} 3387 (br), 2919, 2850, 1717, 1616, 1458, 1378, 1260, 1089, 1008, 973, 797, 703, 661; **HRMS** (ES^+) Calc. for $C_{21}H_{33}IO_5H$ $[M+H]^+$ 493.1445, found 493.1439; $\mathbf{[\alpha]_D^{20}}$ = +37.0 (*c* 0.1, $CHCl_3$).

Atom	^{1}H NMR							^{13}C NMR		
	Natural	Mult.	*J* (Hz)	**195**	Mult.	*J* (Hz)	Δ	Natural	**195**	Δ
1	N.A.			N.A.			N.A.	174.1	169.4	-4.7
2	5.90	d	15.3	5.90	d	15.3	0	127.6	120.4	-7.2
3	7.10	dd	15,1, 11.1	7.41	dd	15.1, 11.3	0.31	142.7	146.7	4.0
4	6.27	dd	15.0, 11.0	6.34	dd	15.0, 11.3	0.07	130.7	129.6	-1.1
5	6.45	dd	15.0, 10.7	6.71	dd	15.0, 10.8	0.26	139.8	143.2	3.4
6	6.17	dd	15.3, 10.7	6.20	dd	15.2, 10.8	0.03	130.9	130.7	-0.2
7	5.87	dd	15.1, 8.7	5.91	dd	15.2, 0.9	0.04	142.8	144.5	1.7
8	2.53	m		2.50	m		-0.03	41.5	41.9	0.4
Me8	1.07	d	6.7	1.08	d	6.7	0.01	17.2	17.9	0.7
9	3.27	dd	6.7, 4.6	3.27	dd	7.7, 3.7	0	88.3	87.1	-1.2
OMe9	3.38	s		3.37	s		-0.01	59.6	59	-0.6
10	2.02-1.22	m		1.96	m		N.A.	40.1	40.3	0.2
Me10	0.85	d	7.0	0.83	d	7.1	-0.02	13	12.1	-0.9
11	3.57	dd	9.6, 2.0	3.38	dd	9.3, 2.2	-0.19	75.5	74.1	-1.4
12	2.02-1.22	m		1.75	m		N.A.	38.5	38.9	0.4
Me12	0.93	d	No J value	0.93	d	6.8	0	7.6	7.8	0.2
13	3.99	d	7.3	4.13	d	8.0	0.14	82.1	80.7	-1.4
14	N.A.			N.A.			N.A.	137.4	150.2	12.8
Me14	1.69	s		1.67	d	0.9	-0.02	14	19.5	5.5
15	5.95	s		6.31	s		0.36	131.7	79.4	-52.3

Table 10: NMR correlation table of diol **195** against natural hemicalide

(*E*)-2-methyl-3-(tributylstannyl)prop-2-en-1-ol (201)

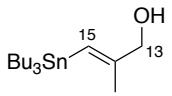

NaH (60 wt% in oil dispersion, 101 mg, 2.53 mmol) was washed with hexane (2 × 3 mL), suspended in Et_2O (3 mL) and cooled to 0 °C. A solution of vinyl iodide **114** (100 mg, 0.505 mmol) in Et_2O (2 mL) was added *via* cannula (2 x 1 mL wash) and the mixture was stirred at rt for 30 min before being cooled to −78 °C. $SnBu_3Cl$ (205 µL, 0.758 mmol) was added followed by dropwise addition of t-BuLi (1.7 M in pentanes, 2.10 mL, 2.53 mmol). The reaction mixture was stirred for 15 minutes before quenching with NH_4Cl (5 mL) and warmed to rt. The layers were separated and the aqueous phase extracted with Et_2O (4 × 5 mL), the combined organic extracts

were dried (Na_2SO_4), filtered and concentrated *in vacuo*. Purification by flash column chromatography (Et_3N washed silica gel, 5% → 20% EtOAc/PE 40-60) gave the title compound as a colourless oil (109 mg, 0.303 mmol, 60%).

R_f: 0.18 (5% EtOAc/PE 40-60); **^{1}H NMR** (400 MHz, $CDCl_3$): δ_H 5.80 (1H, s, H15), 4.08 (2H, s, H13), 1.78 (3H, s, Me14), 1.49 (6H, m, $SnBu_3$), 1.31 (6H, m, $SnBu_3$), 0.94-0.87 (15H, m, $SnBu_3$); **^{13}C NMR** (100 MHz, $CDCl_3$): δ_C 152.8, 120.3, 68.5, 28.8, 27.0, 13.3, 9.7; **FT-IR** (Thin film): ν_{max} 3267 (br), 2956, 2922, 2872, 2856, 1620, 1464, 1376, 1292, 1133, 1072, 1009, 961, 863, 840, 796; **HRMS** (ES^+) calc. for $C_{16}H_{34}OSn–C_4H_9$ $[M–Bu]^+$ 297.0948, found 297.0946.

(3*S*,4*R*,6*R*)-3,4-dihydroxy-6-((*R*,3*E*,5*E*)-7-hydroxy-4,6-dimethylhepta-3,5-dien-2-yl)-4-((*S*)-1-((4-methoxybenzyl)oxy)propan-2-yl)tetrahydro-2*H*-pyran-2-one (202)

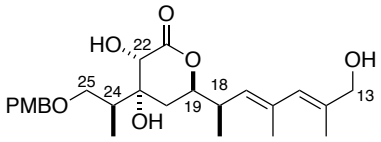

A solution of $Pd(PPh_3)_4$ (5.5 mg, 4.8 μmol), CuTC (9.0 mg, 47.6 μmol) and $[NBu_4][Ph_2PO_2]$ (21.9 mg, 47.6 μmol) was prepared in degassed DMF (0.2 mL) and cooled to 0 °C. A degassed solution of vinyl iodide **174** (12.0 mg, 23.8 μmol) and vinyl stannane **201** (9.0 mg, 25.0 μmol) in DMF (0.2 mL) was added via cannula (2 x 0.1 mL wash) and the reaction mixture was stirred at 0 °C in the dark for 2 h. H_2O (2 mL) and Et_2O (2 mL) were added and the layers were separated. The aqueous phase was extracted with Et_2O (3 x 5 mL) and the combined organic extracts were washed with water (2 x 4 mL) dried (Na_2SO_4), concentrated *in vacuo* and purified by flash column chromatography (30% → 50% EtOAc/PE 40-60) to give the title compound as a colourless oil (7.9 mg, 17.7 μmol, 74%).

R_f: 0.20 (50% EtOAc/PE 40-60); **^{1}H NMR** (500 MHz, d_4-MeOD): δ_H 7.25 (2H, d, *J* = 8.7 Hz, ArH), 6.89 (2H, d, *J* = 8.7 Hz, ArH), 5.87 (1H, s, H15), 5.10 (1H, d, *J* = 10.2 Hz, H17), 4.42 (1H, d, J = 11.4 Hz, O$\underline{CH_2}$Ar), 4.41 (1H, ddd, *J* = 11.6, 7.7, 3.7 Hz, H19), 4.39 (1H, d, J = 11.4 Hz, O$\underline{CH_2}$Ar), 4.23 (1H, s, H22), 3.96 (2H, s, H13) 3.78 (3H, s, ArOMe), 3.50 (1H, dd, *J* = 9.8, 5.6 Hz, H25a), 3.47 (1H, dd, *J* = 9.7, 5.1 Hz, H25b), 2.75-2.66 (1H, m, H18), 2.31-2.23 (1H, m, H24), 1.94 (1H, dd, *J* = 14.5, 3.8 Hz, H20a), 1.79 (1H, d, *J* = 14.5, 11.9 Hz, H20b), 1.75 (3H, s, Me14), 1.71 (1H, s, Me16), 1.07 (3H, d, *J* = 6.6 Hz, H18), 1.00 (3H, d, *J* = 7.1 Hz, Me24); **^{13}C NMR** (125 MHz, d_4-MeOD): δ_C 176.6, 160.8, 136.5, 135.2, 131.6, 131.1, 130.6, 129.6, 114.8, 82.6, 75.4, 74.0, 73.2, 73.0, 69.0, 55.7, 40.0, 39.2, 33.9, 17.6, 17.1, 15.5, 11.9; **FT-IR** (Thin film): ν_{max}

3444 (br), 2933, 1730, 1613, 1514, 1455, 1380, 1247, 1174, 1103, 1033, 819; **HRMS** (ES^+) calc. for $C_{25}H_{36}O_7Na$ $[M+Na]^+$ 471.2353, found 471.2348; $[\alpha]_D^{20}$ = +8.0 (*c* 0.20, $CHCl_3$).

Atom	^{1}H NMR							^{13}C NMR		
	Natural	Mult.	*J* (Hz)	**202**	Mult.	*J* (Hz)	Δ	Natural	**202**	Δ
13	3.99	d	7.3	3.96	s		-0.03	82.1	69	-13.1
14	N.A.			N.A.			N.A.	137.4	136.5	-0.9
Me14	1.69	s		1.75	s		0.06	14	15.5	1.5
15	5.95	s		5.87	s		-0.08	131.7	129.6	-2.1
16	N.A.			N.A.			N.A.	135.4	135.2	-0.2
Me16	1.82	s		1.71	s		-0.11	17.9	17.6	-0.3
17	5.16	d	9.8	5.10	d	10.2	-0.06	131.6	131.1	-0.5
18	2.81	m		2.70	m		-0.11	39.3	39.2	-0.1
Me18	1.10	d	6.7	1.07	d	6.6	-0.03	17.2	17.1	-0.1
19	4.42	ddd	11.3, 7.5, 3.5	4.41	ddd	11.6, 7.7, 3.7	-0.01	82.8	82.6	-0.2
20a	2.02-1.22	m		1.94	dd	14.5, 13.8	N.A.	32.2	33.9	1.7
20b	2.02-1.22	m		1.79	dd	14.5, 11.9	N.A.	76.4	75.4	
21	N.A.			N.A.			N.A.	72.5	73.2	-1.0
22	4.27	s		4.23	s		-0.04	177	176.6	0.7
23	N.A.			N.A.			N.A.	39.3	40	-0.4
24	2.02-1.22	m		2.27	m		N.A.	13.1	11.9	0.7
Me24	0.96	d	6.7	1.00	d	7.1	0.04	13.1	11.9	-1.2
25a	2.02-1.22	m		3.50	dd	9.8, 5.6	N.A.	28.0	73.0	45.0
25b	1.00	m		3.47	dd	9.7, 5.1	N.A.			

Table 11: NMR correlation table of diene **202** against natural hemicalide

(2*S*,3*R*,4*R*,5*R*,6*S*,7*R*,*E*)-3-methoxy-2,4,6,8-tetramethyl-9-(tributylstannyl)-5,7-bis((triethylsilyl)oxy)non-8-en-1-ol (203)

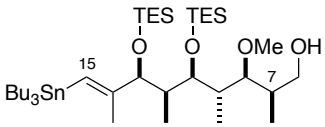

NaH (60 wt% in oil dispersion, 17.9 mg, 447 μmol) was washed with hexane (2 × 1 mL) and cooled to 0 °C. A solution of vinyl iodide **144** (55.0 mg, 89.5 μmol) in Et_2O (0.5 mL) was added *via* cannula (1 x 0.5 mL wash) and the mixture was stirred at rt for 30 min before being cooled to

−78 °C. $SnBu_3Cl$ (194 µL, 716 µmol) was added followed by dropwise addition of t-BuLi (1.6 M in pentanes, 560 µL, 895 µmol). The reaction mixture was stirred for 15 minutes before quenching with pH 7 buffer (1 mL) and immediately warmed to rt. The layers were separated and the aqueous phase extracted with Et_2O (4 × 1 mL), the combined organic extracts were dried (Na_2SO_4), filtered and concentrated *in vacuo*. Purification by flash column chromatography (Et_3N washed silica gel, 0% → 5% EtOAc/PE 40-60) gave the title compound as a colourless oil (42.9 mg, 55.1 µmol, 62%) contaminated with proto-destannylated **204**. ***Ent*-203** was prepared in an analogous fashion from ***ent*-144** (27 mg, 43.9 µmol) as a colourless oil (*ca*. 15.0 mg, 25.7 µmol, 59%) contaminated with ***ent*-204**.

R_f: 0.21 (10% EtOAc/PE 40-60); **^{1}H NMR** (500 MHz, $CDCl_3$): δ_H 5.78 (1H, s, H15), 4.08 (1H, d, *J* = 4.9 Hz, H13), 3.67-3.60 (3H, m, H7a, H7b, H9), 3.48 (1H, dd, *J* = 8.0, 2.0 Hz, H11), 3.36 (3H, s, OMe9), 2.11-2.02 (1H, m, H8), 2.00-1.90 (2H, m, H12), 1.69 (3H, s, Me14), 1.54-1.44 (6H, m, $SnBu_3$), 1.37-1.26 (6H, m, $SnBu_3$) 1.01-0.84 (42H, m, $OSiCH_2\underline{CH_3}$ x2, Me8, Me10, Me12, $SnBu_3$ x2) 0.63 (6H, q, *J* = 7.7 Hz, $OSi\underline{CH_2}CH_3$), 0.60-0.53 (6H, m, $OSi\underline{CH_2}CH_3$); **^{13}C NMR** (125 MHz, $CDCl_3$): δ_C 155.4, 123.6, 83.1, 80.1, 78.0, 67.7, 58.8, 40.2, 38.2, 37.6, 29.4, 27.5, 20.9, 15.9, 13.8, 10.9, 10.8, 10.1, 7.4, 7.2, 5.9, 5.2; **FT-IR** (Thin film): ν_{max} 3444 (br), 2933, 1730, 1613, 1514, 1455, 1380, 1247, 1174, 1103, 1033, 819; **HRMS** (ES^+) Calc. for $C_{38}H_{82}O_4Si_2SnH$ $[M+H]^+$ 779.4859, found 779.4861; **203 $[\alpha]_D^{20}$** = +8.0 (*c* 0.20, $CHCl_3$), ***ent*-203 $[\alpha]_D^{20}$** = –6.8 (*c* 0.20, $CHCl_3$).

(3*S*,4*R*,6*R*)-6-((2*R*,3*E*,5*E*,7*S*,8*R*,9*S*,10*S*,11*S*,12*R*)-13-hydroxy-11-methoxy-4,6,8,10,12-pentamethyl-7,9-bis((triethylsilyl)oxy)trideca-3,5-dien-2-yl)-4-((*S*)-5-oxohexan-2-yl)-3,4-bis((triethylsilyl)oxy)tetrahydro-2*H*-pyran-2-one (207)

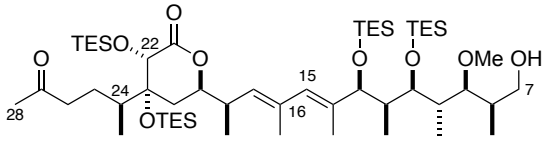

A solution of $Pd(PPh_3)_4$ (8.1 mg, 4.8 µmol), CuTC (13.4 mg, 70.5 µmol) and $[NBu_4][Ph_2PO_2]$ (32.4 mg, 70.5 µmol) was prepared in degassed DMF (100 µL) and cooled to 0 °C. A degassed solution of vinyl iodide **102** (23.0 mg, 35.2 µmol) and vinyl stannane **203** (27.4 mg, 35.2 µmol) in DMF (100 µL) was added via cannula (2 x 100 µL wash) and the reaction mixture was stirred at 0 °C in the dark for 2 h. H_2O (2 mL) and Et_2O (2 mL) were added and the layers were separated. The aqueous phase was extracted with Et_2O (3 x 2 mL) and the combined organic extracts were washed with water (2 x 2 mL) dried (Na_2SO_4), concentrated *in vacuo* and purified by flash

column chromatography (30% → 50% EtOAc/PE 40-60) to give the title compound as a colourless oil (27.8 mg, 27.5 μmol, 78%).

R_f: 0.10 (10% EtOAc/PE 40-60); **^{1}H NMR** (500 MHz, $CDCl_3$): δ_H 5.80 (1H, s, H15), 5.00 (1H, d, *J* = 9.8 Hz, H17), 4.33 (1H, ddd, *J* = 11.2, 7.7, 3.2 Hz, H19), 4.23 (1H, s, H22), 3.96 (1H, d, *J* = 5.9 Hz, H13), 3.69 (1H, dd, *J* = 5.4, 3.1 Hz, H11), 3.66-3.58 (2H, m, H7a, H7b), 3.39 (1H, dd, *J* = 8.3, 2.3 Hz, H9), 3.36-3.33 (1H, obs m, OH), 3.34 (3H, s, OMe9), 2.65 (1H, m, H18), 2.56 (1H, ddd, *J* = 17.3, 11.6, 5.2 Hz, H26a), 2.31 (1H, ddd, *J* = 17.5, 11.2, 4.1 Hz, H26b), 2.15 (3H, s, H28), 2.07-1.89 (4H, m, H8, H10, H12, H24), 1.87 (1H, dd, *J* = 13.9, 3.4 Hz, H20a), 1.74 (3H, s, Me16), 1.66 (3H, s, Me14), 1.60 (1H, m, H25a), 1.46 (1H, dd, *J* = 13.4, 11.4 Hz, H20b), 1.19 (1H, m, H25b), 1.08 (3H, d, *J* = 6.6 Hz, Me18), 1.01-0.85 (48H, m, Me8, Me10, Me12, Me24, $OSiCH_2\underline{CH_3}$ x4), 0.78-0.69 (6H, m, $OSi\underline{CH_2}CH_3$), 0.67-0.53 (18H, m, $OSi\underline{CH_2}CH_3$ x3); **^{13}C NMR** (125 MHz, $CDCl_3$): δ_C 208.3, 172.8, 137.4, 133.8, 130.2, 130.1, 83.1, 80.8, 79.9, 79.8, 73.2, 67.3, 59.0, 58.9, 42.4, 50.1, 39.4, 38.1, 37.7, 37.0, 32.8, 30.2, 25.8, 17.6, 17.2, 15.2, 14.3, 12.8, 11.02, 11.00, 7.35, 7.33, 7.22, 7.09, 6.75, 5.89, 5.33, 5.14; **FT-IR** (Thin film): ν_{max} 3478 (br), 2959, 2913, 2877, 1751, 1720, 1459, 1411, 1376, 1239, 1147, 1080, 1008, 964, 902, 830, 737; **HRMS** (ES^+) Calc. for $C_{54}H_{108}O_9Si_4H$ $[M+H]^+$ 1013.7143, found 1013.7143; $\mathbf{[\alpha]_D^{20}}$ = +11.6 (*c* 0.5, $CHCl_3$).

(3*S*,4*R*,6*R*)-6-((2*R*,3*E*,5*E*,7*R*,8*S*,9*R*,10*R*,11*R*,12*S*)-13-hydroxy-11-methoxy-4,6,8,10,12-pentamethyl-7,9-bis((triethylsilyl)oxy)trideca-3,5-dien-2-yl)-4-((*S*)-5-oxohexan-2-yl)-3,4-bis((triethylsilyl)oxy)tetrahydro-2*H*-pyran-2-one (208)

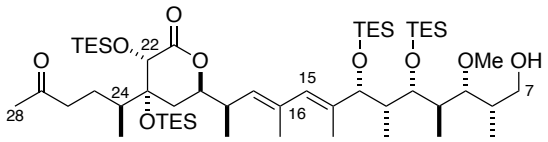

A solution of $Pd(PPh_3)_4$ (6.0 mg, 5.1 μmol), CuTC (9.8 mg, 51.4 μmol) and $[NBu_4][Ph_2PO_2]$ (23.6 mg, 51.4 μmol) was prepared in degassed DMF (100 μL) and cooled to 0 °C. A degassed solution of vinyl iodide **102** (13.0 mg, 25.7 μmol) and vinyl stannane ***ent*-203** (15.0 mg, 25.7 μmol) in DMF (100 μL) was added via cannula (1 x 100 μL wash) and the reaction mixture was stirred at 0 °C in the dark for 2 h. H_2O (1 mL) and Et_2O (1 mL) were added and the layers were separated. The aqueous phase was extracted with Et_2O (3 x 1 mL) and the combined organic extracts were washed with water (2 x 1 mL) dried (Na_2SO_4), concentrated *in vacuo* and purified by flash column chromatography (10% EtOAc/PE 40-60) to give the title compound as a colourless oil (19.3 mg, 19.0 μmol, 74%).

R_f: 0.10 (10% EtOAc/PE 40-60); **^{1}H NMR** (500 MHz, $CDCl_3$): δ_H 5.82 (1H, s, H15), 4.99 (1H, d, *J* = 9.4 Hz, H17), 4.33 (1H, ddd, *J* = 11.3, 7.7, 3.5 Hz, H19), 4.23 (1H, s, H22), 3.99 (1H, d, *J* = 5.4 Hz, H13), 3.68 (1H, dd, *J* = 5.9, 2.8 Hz, H11), 3.64-3.59 (2H, m, H7a, H7b), 3.43-3.38 (1H, m, H9), 3.35 (3H, s, OMe9), 2.66 (1H, m, H18), 2.57 (1H, ddd, *J* = 17.5, 11.5, 5.3 Hz, H26a), 2.31 (1H, ddd, *J* = 17.4, 11.1, 4.0 Hz, H26b), 2.15 (3H, s, H28), 2.10-1.89 (4H, m, H8, H10, H12, H24), 1.87 (1H, dd, *J* = 14.0, 3.2 Hz, H20a), 1.74 (3H, s, Me16), 1.65 (3H, s, Me14), 1.63-1.54 (1H, m, H25a), 1.46 (1H, dd, *J* = 13.8, 12.0 Hz, H20b), 1.18 (1H, m, H25b), 1.09 (3H, d, *J* = 6.8 Hz, Me18), 1.00-0.85 (48H, m, Me8, Me10, Me12, Me24 and $OSiCH_2\underline{CH_3}$ x4), 0.81-0.69 (6H, m, $OSi\underline{CH_2}CH_3$), 0.69-0.53 (18H, m, $OSi\underline{CH_2}CH_3$ x3); **^{13}C NMR** (125 MHz, $CDCl_3$): δ_C 208.3, 172.9, 137.5, 133.8, 129.82, 129.78, 82.9, 80.9, 79.8, 79.5, 76.9, 73.2, 67.2, 59.0, 42.5, 40.1, 39.0, 38.0, 37.7, 37.1, 32.7, 30.2, 25.8, 17.7, 17.1, 15.4, 14.6, 12.8, 11.0, 10.9, 7.4, 7.3, 7.2, 7.1, 6.8, 5.9, 5.3, 5.2; **FT-IR** (Thin film): ν_{max} 3671 (br), 2955, 2912, 2878, 1752, 1721, 1459, 1414, 1379, 1237, 1154, 1094, 1007, 826, 737; **HRMS** (ES^+) Calc. for $C_{54}H_{108}O_9Si_4H$ $[M+H]^+$ 1013.7143, found 1013.7143; $\mathbf{[\alpha]_D^{20}}$ = +8.5 (*c* 1.0, $CHCl_3$).

methyl (2*E*,4*E*,6*E*,8*S*,9*R*,10*R*,11*R*,12*S*,13*R*,14*E*)-9-methoxy-8,10,12,14-tetramethyl-11,13-bis((triethylsilyl)oxy)-15-(trimethylstannyl)pentadeca-2,4,6,14-tetraenoate (211)

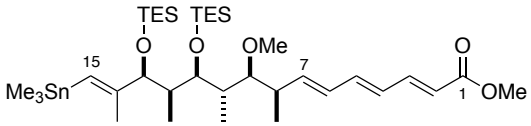

A flask was charged with $Pd(PPh_3)_2Cl_2$ (15.0 mg, 20.8 μmol), Li_2CO_3 (76.8 mg, 1.04 mmol), vinyl iodide **101** (150 mg, 208 μmol) and $(Me_3Sn)_2$ (216 μL, 1.04 mmol) in THF (7 mL) and heated to 40 ˚C for 1 h. Upon complete reaction, the reaction mixture was cooled to rt, filtered through Celite® and concentrated *in vacuo*. The crude product was purified by flash column chromatography (0 → 2% EtOAc/PE 40-60) to give the title compound as a colourless oil (111 mg, 0.146 mmol, 70%). ***Ent*-211** was prepared in an analogous fashion from ***ent*-101** (255 mg, 354 μmol) to give a colourless oil (329 mg, 456 μmol, 70%).

R_f: 0.35 (10% EtOAc/PE 40-60); **^{1}H NMR** (500 MHz, $CDCl_3$): δ_H 7.31 (1H, d, *J* = 15.1, 11.6 Hz, H3), 6.53 (1H, d, *J* = 14.8, 10.5 Hz, H5), 6.23 (1H, d, *J* = 14.9, 11.3 Hz, H4), 6.13 (1H, d, *J* = 15.4, 10.6 Hz, H6), 5.97 (1H, d, *J* = 15.2, 7.5 Hz, H7), 5.85 (1H, d, *J* = 15.1 Hz, H2), 5.75 (1H, s, H15), 3.95 (1H, d, *J* = 7.3 Hz, H13), 3.74 (3H, s, CO_2Me), 3.73 (1H, t, *J* = 3.8 Hz, H9), 3.30 (3H, s, OMe9), 3.08 (1H, dd, *J* = 7.3, 4.2 Hz, H11), 2.52-2.44 (1H, m, H8), 1.97-1.86 (2H, m, H12, H10), 1.70 (3H, s, Me14), 1.04 (3H, d, *J* = 6.9 Hz, Me8), 0.98-0.89 (24H, m, Me10, Me12, $OSiCH_2\underline{CH_3}$ x2), 0.61-0.53 (12H, m, $OSi\underline{CH_2}CH_3$ x2), 0.16 (9H, s, $SnMe_3$); **^{13}C NMR** (125 MHz,

$CDCl_3$): δ_C 167.6, 155.9, 145.0, 144.6, 144.2, 128.7, 128.2, 125.9, 119.7, 86.7, 81.9, 74.2, 60.0, 51.5, 40.9, 39.6, 39.5, 19.2, 14.9, 14.1, 11.0, 7.2, 7.0, 5.8, 5.0, -9.1; **FT-IR** (Thin film): ν_{max} 2953, 2877, 2913, 1721, 1618, 1458, 1261, 1241, 1133, 1097, 1005, 726; **HRMS** (ES^+) Calc. for $C_{36}H_{70}O_5Si_2SnH$ $[M+H]^+$ 759.3863, found 759.3859; **211** $[\alpha]_D^{20}$ = –12.4 (*c* 0.88, $CHCl_3$), ***ent*-211** $[\alpha]_D^{20}$ = +12.0 (*c* 1.0, $CHCl_3$).

methyl (2*E*,4*E*,6*E*,8*R*,9*S*,10*S*,11*S*,12*R*,13*S*,14*E*,16*E*,18*R*)-9-methoxy-8,10,12,14,16-pentamethyl-18-((2*R*,4*R*,5*S*)-6-oxo-4-((*S*)-5-oxohexan-2-yl)-4,5-bis((triethylsilyl)oxy)tetrahydro-2*H*-pyran-2-yl)-11,13-bis((triethylsilyl)oxy)nonadeca-2,4,6,14,16-pentaenoate (99)

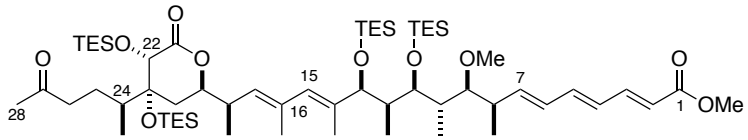

To a stirred suspension of alcohol **207** (20 mg, 19.7 μmol) and $NaHCO_3$ (16.6 mg, 197 μmol) in CH_2Cl_2 (200 μL) was added Dess–Martin periodinane (25.1 mg, 59.2 μmol). After 1 h, the reaction was diluted with CH_2Cl_2 (1 mL) and quenched with $NaHCO_3$ (1 mL) and $Na_2S_2O_3$ (1 mL) and stirring continued for another 30 min until a clear phase boundary was observed. The layers were separated and the aqueous phase extracted with CH_2Cl_2 (3 x 1 mL). The combined organic phases were dried ($MgSO_4$), filtered and concentrated *in vacuo*. The crude product was rapidly filtered through a short plug of silica, eluting with 20% Et_2O/PE 40-60 and used without further purification.

LDA (237 μL, 118 μmol, 0.5 M in THF) was added to a solution of phosphonate **104** (31.0 mg, 118 μmol) in THF (100 μL) at –78 °C to give a bright yellow-orange solution. The reaction was stirred for 30 min and then a solution of the crude aldehyde in THF (100 μL) was added *via* cannula (1 x 100 μL wash). The reaction was stirred at –78 ˚C for 30 min, and then at –40 ˚C for 30 min before quenching with NH_4Cl (1 mL). The layers were separated and the aqueous phase extracted with Et_2O (3 x 1 mL). The combined organic phases were dried ($MgSO_4$), filtered and concentrated *in vacuo*. The crude product was purified by flash column chromatography (5% EtOAc/PE 40-60) to give the title compound as a colourless oil (329 mg, 0.456 mmol, 52%).

R_f: 0.45 (25% EtOAc/PE 40-60); **^{1}H NMR** (500 MHz, $CDCl_3$): δ 7.30 (1H, dd, *J* = 15.4, 11.4 Hz, H3), 6.52 (1H, dd, *J* = 14.8, 10.7 Hz, H5), 6.21 (1H, dd, *J* = 15.0, 11.2 Hz, H4), 6.13 (1H, dd, *J* = 15.0, 10.3 Hz, H6), 5.98 (1H, dd, *J* = 15.1, 7.3 Hz, H7), 5.85 (1H, d, *J* = 15.2 Hz, H2), 5.77 (1H,

s, H15), 5.02 (1H, d, *J* = 9.8 Hz, H17), 4.32 (1H, ddd, *J* = 11.3, 8.3, 3.3 Hz, H19), 4.24 (1H, s, H22), 3.89 (1H, d, *J* = 7.6 Hz, H13), 3.74 (3H, s, CO_2Me), 3.76-3.73 (1H, obs m, H11), 3.28 (3H, s, OMe9), 3.07 (1H, dd, *J* = 7.6, 3.9 Hz, H9), 2.65 (1H, m, H18), 2.56 (1H, ddd, *J* = 17.4, 11.7, 5.5 Hz, H26a), 2.49 (1H, m , H8), 2.30 (1H, ddd, *J* = 17.3, 11.3, 3.9 Hz, H26b), 2.15 (3H, s, H28), 2.00-1.93 (2H, m, H12, H24), 1.93-1.87 (2H, m, H10, H20a), 1.74 (3H, s, Me16), 1.66 (3H, s, Me14), 1.60-1.55 (1H, obs m, H25a), 1.45 (1H, dd, *J* = 13.7, 11.8 Hz, H20b), 1.17 (1H, dd, *J* = 12.3, 4.7 Hz, H25b), 1.09 (3H, d, *J* = 6.5 Hz, Me18), 1.04 (3H, d, *J* = 7.0 Hz, Me8), 1.00-0.87 (42H, m, Me10, Me12, $OSiCH_2\underline{CH_3}$ x4), 0.86 (3H, d, *J* = 6.9 Hz, Me24), 0.81-0.67 (6H, m, $OSi\underline{CH_2}CH_3$), 0.67-0.52 (18H, m, $OSi\underline{CH_2}CH_3$ x3); **^{13}C NMR** (125 MHz, $CDCl_3$): δ 208.2, 172.8, 167.8, 145.1, 144.7, 141.4, 137.8, 133.5, 130.5, 130.2, 128.9, 128.3, 119.9, 86.8, 80.84, 80.79, 79.8, 74.1, 73.2, 60.1, 51.6, 42.5, 41.1, 39.7, 39.5, 38.3, 37.0, 33.1, 30.2, 25.8, 17.7, 17.4, 14.8, 14.1, 13.8, 12.8, 11.2, 7.35, 7.34, 7.2, 7.1, 6.8, 5.8, 5.3, 5.1; **FT-IR** (Thin film): ν_{max} 2954, 2877, 1747, 1720, 1618, 1457, 1414, 1378, 1260, 1143, 1093, 1005, 802, 725; **HRMS** (ES^+) Calc. for $C_{61}H_{114}O_{10}Si_4H$ $[M+H]^+$ 1119.7562, found 1119.7571; $[\alpha]_D^{20}$ = +5.3 (*c* 0.15, $CHCl_3$).

methyl (2*E*,4*E*,6*E*,8*R*,9*S*,10*S*,11*S*,12*R*,13*S*,14*E*,16*E*,18*S*)-9-methoxy-8,10,12,14,16-pentamethyl-18-((2*S*,4*S*,5*R*)-6-oxo-4-((*R*)-5-oxohexan-2-yl)-4,5-bis((triethylsilyl)oxy)tetrahydro-2*H*-pyran-2-yl)-11,13-bis((triethylsilyl)oxy)nonadeca-2,4,6,14,16-pentaenoate (*ent*-100)

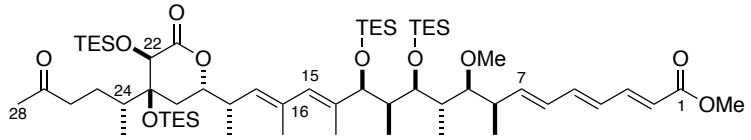

Method A

Ester **100** was prepared in an analogous fashion to **99** from **208** (15.0 mg, 14.8 μmol) to give a colourless oil (9.1 mg, 8.1 μmol, 55%).

Method B

A solution of $Pd(PPh_3)_4$ (34.3 mg, 29.2 μmol) and CuTC (55.7 mg, 292 μmol) was prepared in degassed DMF (1 mL) and cooled to 0 °C. A degassed solution of vinyl iodide ***ent*-102** (95 mg, 146 μmol) and vinyl stannane **211** (111 mg, 146 μmol) in DMF (1 mL) was added *via* cannula (2 x 0.1 mL wash) and the reaction mixture was stirred at 0 °C in the dark for 5 h. H_2O (10 mL) and Et_2O (10 mL) were added and the layers were separated. The aqueous phase was extracted with Et_2O (3 x 10 mL) and the combined organic extracts were washed with water (2 x 4 mL) dried

(Na_2SO_4), concentrated in vacuo and purified by flash column chromatography (2% → 10% EtOAc/PE 40-60) to give the title compound as a colourless oil (114 mg, 102 µmol, 70%).

R_f: 0.20 (10% EtOAc/PE 40-60); **^{1}H NMR** (500 MHz, $CDCl_3$): δ_H 7.30 (1H, dd, *J* = 15.3, 11.4 Hz, H3), 6.53 (1H, dd, *J* = 14.9, 10.6 Hz, H5), 6.22 (1H, dd, *J* = 15.0, 11.3 Hz, H4), 6.13 (1H, dd, *J* = 15.3, 10.8 Hz, H6), 6.00 (1H, dd, *J* = 15.4, 7.3 Hz, H7), 5.85 (1H, d, *J* = 15.4 Hz, H2), 5.82 (1H, s, H15), 5.00 (1H, d, *J* = 9.4 Hz, H17), 4.31 (1H, ddd, *J* = 11.5, 8.0, 3.2 Hz, H19), 4.23 (1H, s, H22), 3.92 (1H, d, *J* = 6.8 Hz, H13), 3.74 (3H, s, CO_2Me), 3.73 (1H, dd, *J* = 7.7, 3.8 Hz, H11), 3.27 (3H, s, OMe9), 3.10 (1H, dd, *J* = 7.8, 3.6 Hz, H9), 2.64 (1H, m, H18), 2.55 (1H, ddd, *J* = 17.1, 11.3, 5.1 Hz, H26a), 2.49 (1H, m , H8), 2.30 (1H, ddd, *J* = 17.2, 11.3, 4.1 Hz, H26b), 2.14 (3H, s, H28), 2.00-1.89 (3H, m, H10, H12, H24), 1.86 (1H, dd, *J* = 14.2, 3.3 Hz, H20a), 1.76 (3H, s, Me16), 1.65 (3H, s, Me14), 1.60-1.55 (1H, obs m, H25a), 1.45 (1H, dd, *J* = 13.6, 11.9 Hz, H20b), 1.16 (1H, dd, *J* = 12.3, 5.0 Hz, H25b), 1.10 (3H, d, *J* = 6.6 Hz, Me18), 1.03 (3H, d, *J* = 6.6 Hz, Me8), 1.00-0.87 (42H, m, Me10, Me12, $OSiCH_2\underline{CH_3}$ x4), 0.85 (3H, d, *J* = 6.9 Hz, Me24), 0.80-0.68 (6H, m, $OSi\underline{CH_2}CH_3$), 0.68-0.53 (18H, m, $OSi\underline{CH_2}CH_3$ x3); **^{13}C NMR** (125 MHz, $CDCl_3$): δ_C 208.1, 172.8, 167.8, 145.1, 144.9, 141.4, 137.7, 133.8, 130.38, 130.37, 128.8, 128.3, 119.8, 86.5, 80.8, 80.4, 79.8, 75.0, 73.2, 60.0, 51.6, 42.5, 40.7, 39.7, 39.5, 38.2, 37.0, 33.0, 30.2, 25.8, 17.6, 17.2, 15.2, 14.0, 13.8, 12.8, 11.1, 7.35, 7.34, 7.2, 7.1, 6.8, 5.9, 5.3, 5.2; **FT-IR** (Thin film): ν_{max} 2952, 2877, 1752, 1720, 1618, 1463, 1378, 1241, 1147, 1006, 831, 727; **HRMS** (ES^+) Calc. for $C_{61}H_{114}O_{10}Si_4NH_4$ $[M+NH_4]^+$ 1136.7827, found 1136.7823; $[\alpha]_D^{20}$ = –16.2 (*c* 0.13, $CHCl_3$).

methyl (2*E*,4*E*,6*E*,8*R*,9*S*,10*S*,11*S*,12*R*,13*S*,14*E*,16*E*,18*S*)-18-((2*S*,4*S*,5*R*)-4-((2*R*)-5-hydroxyhexan-2-yl)-6-oxo-4,5-bis((triethylsilyl)oxy)tetrahydro-2*H*-pyran-2-yl)-9-methoxy-8,10,12,14,16-pentamethyl-11,13-bis((triethylsilyl)oxy)nonadeca-2,4,6,14,16-pentaenoate (214)

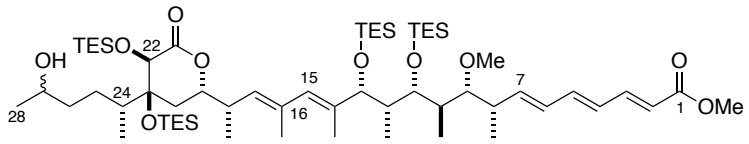

$NaBH_4$ (6.8 mg, 179 µmol) was added to a stirring solution of ketone ***ent*-100** (40.0 mg, 35.7 µmol) in MeOH (1 mL) at 0 °C. The reaction was stirred at 0 °C for 30 min before quenching with a solution of NH_4Cl (1 mL) and diluting with Et_2O (3 mL). The layers were separated, and the aqueous phase was extracted with Et_2O (3 x 1 mL). The combined organic phases were dried ($MgSO_4$) and concentrated *in vacuo*. Purification by flash column chromatography (5%

EtOAc/PE 40-60) afforded the title compound as a colourless oil (36.8 mg, 32.8 μmol, 92%) as a 3:2 epimeric mixture at C27.

R_f 0.14 (10% EtOAc/PE 40-60); **^{1}H NMR** (500 MHz, $CDCl_3$): δ_H 7.30 (1H, dd, *J* = 15.4, 11.1 Hz, H3), 6.53 (1H, dd, *J* = 15.0, 10.5 Hz, H5), 6.22 (1H, dd, *J* = 14.9, 11.2 Hz, H4), 6.13 (1H, dd, *J* = 14.9, 10.6 Hz, H6), 6.00 (1H, dd, *J* = 15.0, 7.2 Hz, H7), 5.85 (1H, d, *J* = 15.2 Hz, H2), 5.82 (1H, s, H15), 5.02 (1H, d, *J* = 8.5 Hz, H17), 4.34 (1H, ddd, J = 11.3, 7.5, 3.0 Hz, H19), 4.23 (1H, s, H22; minor epimer 4.21, s), 3.92 (d, *J* = 6.9 Hz, H13), 3.80-3.70 (5H, m, H11, H27, CO_2Me), 3.27 (3H, s, OMe9), 3.10 (dd, *J* = 7.7, 3.7 Hz, H9), 2.67 (1H, m, H18), 2.49 (1H, m, H8), 2.02-1.92 (2H, m, H12, H24), 1.92-1.83 (2H, m, H10, H20a), 1.76 (3H, s, Me16), 1.65 (3H, s, Me14), 1.60-1.38 (3H, m, H20b, H25a, H26a), 1.28 (1H, m, H26b), 1.19 (3H, d, *J* = 6.4 Hz, H28; minor epimer 1.21, d *J* = 6.5 Hz), 1.09 (3H, d, *J* = 6.7 Hz, Me18), 1.04 (3H, d, *J* = 6.7 Hz, Me8), 1.01-0.81 (47H, m, Me10, Me12, Me24, H25b, $OSiCH_2\underline{CH_3}$ x4), 0.80-0.72 (6H, m, $OSi\underline{CH_2}CH_3$), 0.68-0.53 (18H, m, $OSi\underline{CH_2}CH_3$ x3); **^{13}C NMR** (125 MHz, $CDCl_3$): δ_C 173.0, 167.8, 145.1, 144.8, 141.4, 137.7, 133.9, 130.4, 130.3, 128.8, 128.3, 119.9, 86.5, 80.8 (minor 80.9), 80.4, 79.9, 75.0, 73.2 (minor 73.2), 68.5 (minor 68.9), 60.0, 51.6, 40.7, 39.7, 39.5, 38.0, 38.0, 37.5, 32.6, 28.3 (minor 28.9), 23.9 (minor 24.2), 17.6, 17.2, 15.2, 14.0, 13.8, 13.0 (minor 12.9), 7.4, 7.3, 7.1, 6.8, 5.7, 5.4, 5.2; **FT-IR** (Thin film): ν_{max} 3502 (br), 2955, 2932, 2877, 1748, 1721, 1618, 1458, 1241, 1147, 1115, 1006, 728; **HRMS** (ES+) Calc. for $C_{61}H_{116}O_{10}Si_4NH_4$ $[M+NH_4]^+$ 1138.7984, found 1138.7993; **$[\alpha]_D^{20}$** –11.1 (*c* 0.18, $CHCl_3$).

methyl (2*E*,4*E*,6*E*,8*R*,9*S*,10*S*,11*S*,12*R*,13*S*,14*E*,16*E*,18*S*)-9-methoxy-18-((2*S*,4*S*,5*R*)-4-((2*R*)-5-methoxyhexan-2-yl)-6-oxo-4,5-bis((triethylsilyl)oxy)tetrahydro-2*H*-pyran-2-yl)-8,10,12,14,16-pentamethyl-11,13-bis((triethylsilyl)oxy)nonadeca-2,4,6,14,16-pentaenoate (215)

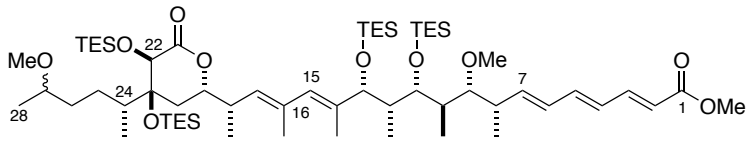

A solution of alcohol **22a** (37 mg, 33.0 μmol) in CH_2Cl_2 (200 μL) was added to a suspension of Me_3OBF_4 (48.5 mg, 143 μmol), Proton Sponge® (106 mg, 494 μmol) and crushed 4 Å molecular sieves (*ca*. 28 mg) in CH_2Cl_2 (200 μL). The resulting suspension was stirred for 3 h at rt before quenching with $NaHCO_3$ (1 mL). The layers were separated and the aqueous phase was extracted with CH_2Cl_2 (3 x 1 mL). The combined organic extracts were dried ($MgSO_4$) and concentrated *in vacuo*. Purification by flash column chromatography (5% EtOAc/PE 40-60) afforded methyl ether **24** as a colourless oil (25.6 mg, 22.4 μmol, 68%).

R_f 0.21 (10% EtOAc/PE 40-60); **^{1}H NMR** (500 MHz, $CDCl_3$): δ_H 7.30 (1H, dd, *J* = 15.0, 11.1 Hz, H3), 6.53 (1H, dd, *J* = 14.8, 10.5 Hz, H5), 6.22 (1H, dd, *J* = 14.8, 11.4 Hz, H4), 6.13 (1H, dd, *J* = 15.3, 10.6 Hz, H6), 5.99 (1H, dd, *J* = 15.2, 7.2 Hz, H7; minor epimer 6.00, dd, *J* = 15.4, 7.2 Hz), 5.84 (1H, d, *J* = 15.2 Hz, H2), 5.82 (1H, s, H15), 5.02 (1H, dq, *J* = 9.6, 1.7 Hz, H17), 4.35 (1H, ddd, *J* = 11.2, 7.7, 3.4 Hz, H19), 4.21 (1H, s, H22), 3.93 (1H, d, *J* = 7.2 Hz, H13), 3.74-3.71 (4H, m, H11, CO_2Me), 3.29 (3H, s, OMe27; minor epimer 3.30, s), 3.27 (3H, s, OMe9), 3.27-3.20 (1H, m, H27), 3.10 (1H, m, H9), 2.68 (1H, m, H18), 2.49 (1H, m, H8), 2.00-1.92 (2H, m, H12, H24), 1.94-1.86 (2H, m, H10, H20a), 1.76 (3H, s, Me16), 1.66 (3H, s, Me14), 1.57-1.51 (1H, m, H26a), 1.45-1.36 (2H, m, H20b, H25a), 1.13 (3H, d, *J* = 5.7 Hz, H28; minor epimer 1.12, d, *J* = 6.0 Hz), 1.09 (3H, d, *J* = 6.7 Hz, Me18), 1.04 (3H, d, *J* = 6.7 Hz, Me8), 1.01-0.86 (46H, m, Me10, Me12, Me24, H25b, $OSiCH_2\underline{CH_3}$ x4), 0.80-0.74 (6H, m, $OSi\underline{CH_2}CH_3$), 0.68-0.53 (18H, m, $OSi\underline{CH_2}CH_3$ x3); **^{13}C NMR** (125 MHz, $CDCl_3$): δ_C 173.0, 167.8, 145.0, 144.9 (minor 144.8), 141.4, 137.6, 133.9, 130.4 (minor 130.4), 130.3, 128.8, 128.3, 119.9, 86.5 (minor 86.5), 80.9 (minor 80.8), 80.4 (minor 80.4), 79.9 (minor 79.9), 73.2, 59.9, 56.1, 51.6, 40.7 (minor 40.6), 39.7 (minor 39.7), 39.5, 38.0, 37.6, 35.5, 34.5, 32.7 (minor 32.6), 29.9, 28.4, 27.6, 19.2, 17.6, 17.2, 15.2 (minor 15.2), 14.0, 13.8 (minor 13.8), 12.9 (minor 12.9), 11.1, 7.4, 7.3, 7.1, 6.8, 5.9, 5.4 (minor 5.4), 5.2, 5.0; **FT-IR** (Thin film): ν_{max} 2954, 2876, 1749, 1720, 1617, 1458, 1378, 1260, 1239, 1145, 1089, 1005, 973, 803, 725; **HRMS** (ES^+) Calc. for $C_{62}H_{118}O_{10}Si_4H$ $[M+H]^+$ 1135.7875, found 1135.7880; **$[\alpha]_D^{20}$** –8.2 (*c* 0.17, $CHCl_3$).

methyl (2*E*,4*E*,6*E*,8*R*,9*S*,10*R*,11*R*,12*R*,13*S*,14*E*,16*E*,18*S*)-18-((2*S*,4*S*,5*R*)-4,5-dihydroxy-4-((2*R*)-5-methoxyhexan-2-yl)-6-oxotetrahydro-2*H*-pyran-2-yl)-11,13-dihydroxy-9-methoxy-8,10,12,14,16-pentamethylnonadeca-2,4,6,14,16-pentaenoate (219)

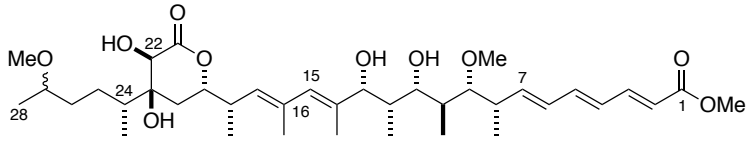

To a solution of TES ether **215** (10 mg, 8.8 μmol) in THF was added a solution of TASF (12.2 mg, 44.1 μmol) in DMF (300 μL) at 0 °C. The light pink solution was stirred at 0 °C for 30 min, before quenching with NH_4Cl (1 mL) and diluting with EtOAc (1 mL). The aqueous phase was extracted with EtOAc (5 × 0.5 mL), dried ($MgSO_4$), concentrated *in vacuo* and the crude immediately redissolved in THF (300 □L) and stirred at 0 °C. A solution of HF•py/py (1:3, 300 μL) was added and the solution was stirred at 0 °C for 3 h. The reaction was quenched by slow addition of sat. $NaHCO_3$ (1 mL), the layers separated and the aqueous phase extracted with EtOAc (5 × 1 mL). The combined organic phases were dried ($MgSO_4$), filtered and concentrated

in vacuo. Purification by flash column chromatography (80% EtOAc/PE 40-60) afforded the title compound as a colourless oil (4.0 mg, 5.89 μmol, 67% over two steps).

R_f 0.39 (80% EtOAc/PE 40-60); **^{1}H NMR** (500 MHz, $CDCl_3$): δ_H 7.31 (1H, dd, *J* = 15.4, 11.3 Hz, H3), 6.61 (1H, dd, *J* = 14.8, 10.6 Hz, H5), 6.33 (1H, dd, *J* = 14.6, 11.5 Hz, H4), 6.21 (1H, dd, *J* = 15.3, 10.7 Hz, H6), 5.99 (1H, dd, *J* = 15.3, 8.8 Hz, H7), 5.95 (1H, s, H15), 5.90 (1H, d, *J* = 15.4 Hz, H2), 5.15 (1H, d, *J* = 9.6, H17), 4.42 (1H, ddd, *J* = 11.4, 7.4, 3.9 Hz, H19), 4.24 (1H, s, H22), 3.99 (1H, d, *J* = 7.4 Hz, H13), 3.72 (3H, s, CO_2Me) 3.55 (1H, d, *J* = 9.6 Hz, H11), 3.38 (3H, s, OMe9), 3.33 (1H, m, H27), 3.31 (3H, s, OMe27), 3.28 (1H, dd, *J* = 6.6, 4.4 Hz, H9), 2.78 (1H, m, H18), 2.58 (1H, m, H8), 2.00-1.89 (3H, m, H10, H20a, H24), 1.84-1.75 (4H, m, H12, Me16), 1.73-1.64 (4H, m, Me14, H20b), 1.62-1.43 (3H, m, H25a, H26a, H26b), 1.13 (3H, d, *J* = 6.1 Hz, H28), 1.12 (3H, d, *J* = 6.8 Hz, Me18), 1.08 (3H, d, *J* = 6.7 Hz, Me8), 0.97-0.90 (7H, m, Me12, Me24, H25b), 0.85 (3H, d, *J* = 7.1 Hz, Me10); **^{13}C NMR** (125 MHz, $CDCl_3$): δ_C 176.9, 169.3, 146.6, 145.1, 143.0, 137.4, 135.3, 131.6, 131.3, 130.5, 129.4, 120.5, 88.1, 82.7, 82.0, 78.5 (minor 78.2), 76.3, 75.7, 72.5, 59.5, 56.2 (minor 56.3), 52.0, 41.5, 40.0, 39.2, 39.2 (minor 39.1), 38.4, 35.8 (minor 36.1), 32.1, 28.7, 19.3 (minor 19.4), 17.9, 17.1, 17.0 (minor 17.1), 14.1, 13.0, 13.0, 7.5; **FT-IR** (Thin film): ν_{max} 3394 (br), 2960, 2935, 1719, 1615, 1456, 1437, 1379, 1304, 1232, 1137, 1105, 1008, 971; **HRMS** (ES^+) Calc. for $C_{38}H_{62}O_{10}NH_4$ $[M+NH_4]^+$ 696.4681, found 696.4682; **$[\alpha]_D^{20}$** –16.5 (*c* 0.33, $CHCl_3$).

(2*E*,4*E*,6*E*,8*R*,9*S*,10*R*,11*R*,12*R*,13*S*,14*E*,16*E*,18*S*)-18-((2*S*,4*S*,5*R*)-4,5-dihydroxy-4-((2*R*)-5-methoxyhexan-2-yl)-6-oxotetrahydro-2*H*-pyran-2-yl)-11,13-dihydroxy-9-methoxy-8,10,12,14,16-pentamethylnonadeca-2,4,6,14,16-pentaenoic acid (221)

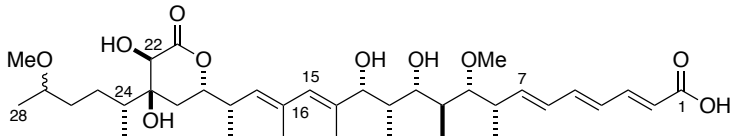

$Ba(OH)_2$•$8H_2O$ (4.7 mg, 14.8 μmol) was added to a stirred solution of tetraol **219** (2.0 mg, 2.95 μmol) in methanol (70 μL). The resulting pale-yellow suspension was stirred at rt for 24 h before quenching with 1 M HCl (1 mL) and partitioning with EtOAc (1 mL). The aqueous phase was extracted with EtOAc (5 × 0.5 mL), dried (Na_2SO_4), concentrated *in vacuo* and purified by flash column chromatography (1% AcOH in 10% MeOH/CH_2Cl_2) to the title compound as an amorphous white solid (0.98 mg, 1.48 μmol, 50%).

R_f 0.30 (10% MeOH/CH_2Cl_2); **^{1}H NMR** (500 MHz, d_4-MeOD): δ_H 7.26 (1H, dd, *J* = 14.9, 11.4 Hz, H3), 6.57 (1H, dd, *J* = 14.4, 10.4 Hz, H5), 6.32 (1H, dd, *J* = 14.7, 11.5 Hz, H4), 6.21 (1H, dd,

J = 15.1, 10.6 Hz, H6), 5.96 (1H, dd, *J* = 15.0, 8.7 Hz, H7), 5.86 (1H, d, *J* = 15.2 Hz, H2), 5.95 (1H, s, H15), 5.15 (1H, d, *J* = 10.0, H17), 4.42 (1H, ddd, *J* = 11.3, 7.3, 3.7 Hz, H19), 4.24 (1H, s, H22), 4.00 (1H, d, *J* = 7.0 Hz, H13), 3.61 (1H, dd, *J* = 9.5, 1.5 Hz, H11), 3.39 (3H, s, OMe9), 3.31 (3H, s, OMe27), 3.34-3.30 (1H, m, H27), 3.28 (1H, dd, *J* = 6.4, 4.4 Hz, H9), 2.79 (1H, m, H18), 2.56 (1H, m, H8), 2.00-1.91 (3H, m, H10, H20a, H24a), 1.83-1.77 (4H, m, H12, Me16), 1.73-1.66 (4H, m, Me14, H20b), 1.62-1.41 (3H, m, H25a, H26a, H26b), 1.13 (3H, d, *J* = 6.1 Hz, H28), 1.12 (3H, d, *J* = 7.0 Hz, Me18), 1.08 (3H, d, *J* = 6.4 Hz, Me8), 0.95-0.90 (7H, m, Me12, Me24, H25b), 0.85 (3H, d, *J* = 7.1 Hz, Me10); **^{13}C NMR** (125 MHz, d_4-MeOD): δ_C 177.0, 174.9 (br), 142.6, 142.1, 139.4, 137.4, 135.4, 131.3, 131.2, 130.9, 130.8, 128.1 (br), 88.7, 82.8, 81.9, 78.5 (minor 78.2), 76.3, 76.1, 72.5, 59.8, 56.2 (minor 56.3), 41.4, 40.0, 39.2 (minor 39.1), 39.2 (minor 39.1), 38.3, 35.8 (minor 36.1), 32.1, 28.7 (minor 28.6), 19.3 (minor 19.4), 17.9, 17.1, 16.8, 14.3, 13.1, 13.0 (minor 13.0), 7.3; **FT-IR** (Thin film): ν_{max} 3654 (br), 2957, 2925, 1723, 1697, 1684, 1615, 1458, 1379, 1258, 1232, 1155, 1092, 1010, 667; **HRMS** (ES^+) Calc. for $C_{37}H_{60}O_{10}Na$ $[M+Na]^+$ 687.4073, found 687.4079; $\mathbf{[\alpha]_D^{20}}$ +23.0 (*c* 0.1, $CHCl_3$).

Atom	^{1}H NMR											^{13}C NMR				
	Natural	Mult.	*J* (Hz)	**220**	Mult.	*J* (Hz)	Δ	**221**	Mult.	*J* (Hz)	Δ	Natural	**220**	Δ	**221**	Δ
1	N.A.			N.A.				N.A.				174.1		0.0	174.9	0.8
2	5.90	d	15.3	5.89	d	15.4	-0.01	5.86	d	15.2	-0.04	127.6	128.2	0.6	128.1	0.5
3	7.10	dd	15,1, 11.1	7.13	dd	15.3, 11.1	0.03	7.26	dd	14.9, 11.4	0.16	142.7	143.2	0.5	142.1	-0.6
4	6.27	dd	15.0, 11.0	6.27	dd	14.9, 11.2	0.00	6.32	dd	14.7, 11.5	0.05	130.7	130.8	0.1	130.8	0.1
5	6.45	dd	15.0, 10.7	6.47	dd	14.6, 10.7	0.02	6.57	dd	14.4, 10.4	0.12	139.8	140.1	0.3	139.4	-0.4
6	6.17	dd	15.3, 10.7	6.18	dd	15.0, 10.7	0.01	6.21	dd	15.1, 10.6	0.04	130.9	130.5	-0.4	130.9	0.0
7	5.87	dd	15.1, 8.7	5.89	dd	15.0, 8.8	0.02	5.96	d	15.0, 8.7	0.09	142.8	143	0.2	142.6	-0.2
8	2.53	m		2.54	m		-0.01	2.56	m		0.01	41.5	41.5	0.0	41.4	-0.1
Me8	1.07	d	6.7	1.07	d	6.7	0.00	1.08	d	6.4	0.01	17.2	17.2	0.0	16.8	-0.4
9	3.27	dd	6.7, 4.6	3.28	dd	6.4, 4.5	0.01	3.28	dd	6.4, 4.4	0.01	88.3	88.3	0.0	88.7	0.4
OMe9	3.38	s		3.39	s		0.00	3.39	s		0.00	59.6	59.6	0.0	59.8	0.2
10	2.02-1.22	m		1.98	m		0.00	1.98	m		0.00	40.1	40.1	0.0	40.0	-0.1
Me10	0.85	d	7.0	0.85	d	7.1	0.00	0.85	d	7.1	0.00	13.0	13.1	0.1	13.0	0.0
11	3.57	dd	9.6, 2.0	3.57	dd	9.8, 2.0	0.00	3.61	dd	9.5, 1.5	0.04	75.5	75.5	0.0	76.1	0.6
12	2.02-1.22	m		1.80	m		0.00	1.81	m		0.00	38.5	38.5	0.0	38.3	-0.2
Me12	0.93	d	No J value	0.93	d	6.7	0.00	0.92	d	7.0	-0.01	7.6	7.5	-0.1	7.3	-0.3
13	3.99	d	7.3	3.99	d	7.2	0.00	4.00	d	7.0	0.01	82.1	82.1	0.0	81.9	-0.2
14	N.A.			N.A.				N.A.				137.4	137.3	-0.1	137.4	0.0
Me14	1.69	s		1.68	s		-0.01	1.68	s		-0.01	14.0	13.9	-0.1	14.3	0.3
15	5.95	s		5.95	s		0.00	5.96	s		0.00	131.7	131.7	0.0	131.3	-0.4
16	N.A.			N.A.				N.A.				135.4	135.4	0.0	135.4	0.0

Me16	1.82	s		1.82	s		0.00	1.80	s		-0.02	17.9	17.8	-0.1	17.9	0.0
17	5.16	d	9.8	5.16	d	9.6	0.00	5.15	d	10.0	-0.01	131.6	131.6	0.0	131.2	-0.4
18	2.81	m		2.81	m		0.00	2.79	m		-0.02	39.3	39.2	-0.1	39.2	-0.1
Me18	1.10	d	6.7	1.10	d	6.7	0.00	1.12	d	7.0	0.02	17.2	17.2	0.0	17.1	-0.1
19	4.42	ddd	11.3, 7.5, 3.5	4.42	ddd	11.1, 7.3, 3.5	0.00	4.42	ddd	11.3, 7.3, 3.7	0.00	82.8	82.8	0.0	82.8	0.0
20a	2.02-1.22	m		1.97	m		0.00	1.95	m		0.00	32.2	32.1	-0.1	32.1	-0.1
20b	2.02-1.22	m		1.67	m		0.00	1.65	m		0.00					
21	N.A.			N.A.				N.A.				76.4	76.4	0.0	76.3	-0.1
22	4.27	s		4.26	s		-0.01	4.24	s		-0.03	72.5	72.5	0.0	72.5	0.0
23	N.A.			N.A.			-0.01	N.A.				177.0	177	0.0	177.0	0.0
24	2.02-1.22	m		1.93	m		0.00	1.93	m		0.00	39.3	39.2	-0.1	39.2	-0.1
Me24	0.96	d	6.7	0.95	d	6.8	-0.01	0.94	d	7.0	-0.02	13.1	13.1	0.0	13.1	0.0
25a	2.02-1.22	m		1.57	m		0.00	1.57	m		0.00	28.0	28.7	0.7	28.7	0.7
25b	1.00	m		0.96	m		-0.04	0.97	m		-0.03					
26a	2.02-1.22	m		1.50	m		0.00	1.54	m		0.00	40.8	35.9	-4.9	35.8	-5.0
26b	2.02-1.22	m		1.44	m		0.00	1.47	m		0.00					
27	3.33	m		3.31	m		-0.02	3.32	m		-0.01	79.1	78.5	-0.6	78.5	-0.6
OMe27	3.33	s		3.32	s		-0.01	3.31	s		-0.02	56.5	56.3	-0.2	56.2	-0.3
28	2.02-1.22	m		1.12	d	6.0	0.00	1.13	d	6.1	0.00	40.8	19.3	-21.5	19.3	-21.5

Table 12: NMR correlation table of 13,18-*syn* acid **220**[71] and 13,18-*anti* salt **221** against natural hemicalide

sodium (2*E*,4*E*,6*E*,8*R*,9*S*,10*R*,11*R*,12*R*,13*S*,14*E*,16*E*,18*S*)-18-((2*S*,4*S*,5*R*)-4,5-dihydroxy-4-((2*R*)-5-methoxyhexan-2-yl)-6-oxotetrahydro-2*H*-pyran-2-yl)-11,13-dihydroxy-9-methoxy-8,10,12,14,16-pentamethylnonadeca-2,4,6,14,16-pentaenoate (223)

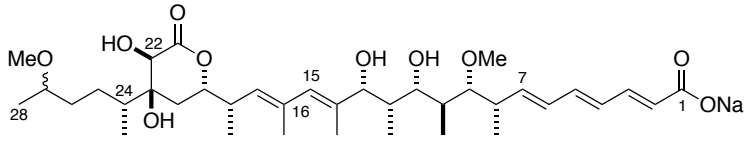

In a 5 mm NMR tube, Na_2CO_3 (*ca.* 5 mg) was added to a solution of the free acid **221** in d_4-MeOD (500 μL). The mixture was vigorously shaken for *ca.* 30 seconds to afford the title compound as a solution in d_4-MeOD.

^{1}H NMR (500 MHz, d_4-MeOD): δ_H 7.02 (1H, dd, *J* = 15.3, 11.2 Hz, H3), 6.43 (1H, dd, *J* = 14.8, 10.6 Hz, H5), 6.25 (1H, dd, *J* = 14.9, 10.6 Hz, H4), 6.16 (1H, dd, *J* = 15.2, 10.7 Hz, H6), 5.91 (1H, d, *J* = 15.3 Hz, H2), 5.85 (1H, dd, *J* = 15.2, 8.6 Hz, H7), 5.96 (1H, s, H15), 5.15 (1H, d, *J* = 9.8, H17), 4.42 (1H, ddd, *J* = 11.4, 7.3, 4.0 Hz, H19), 4.25 (1H, s, H22), 4.02 (1H, d, *J* = 6.6 Hz, H13), 3.61 (1H, dd, *J* = 9.5, 1.8 Hz, H11), 3.39 (3H, s, OMe9), 3.33 (1H, m, H27), 3.31 (3H, s, OMe27), 3.26 (1H, dd, *J* = 5.6, 4.8 Hz, H9), 2.80 (1H, m, H18), 2.53 (1H, m, H8), 2.00-1.91 (3H, m, H10, H20a, H24a), 1.83-1.77 (4H, m, H12, Me16), 1.73-1.64 (4H, m, Me14, H20b), 1.62-1.43 (3H, m, H25a, H26a, H26b), 1.13 (3H, d, *J* = 6.1 Hz, H28), 1.11 (3H, d, *J* = 6.6 Hz, Me18), 1.07 (3H, d, *J* = 6.7 Hz, Me8), 0.96-0.89 (7H, m, Me12, Me24, H25b), 0.85 (3H, d, *J* = 7.0 Hz, Me10); **^{13}C NMR** (125 MHz, d_4-MeOD): δ_C 177.0, 175.9, 161.5 (CO_3^{2-}), 142.0, 141.0, 138.7, 137.4, 135.3, 131.2, 131.2, 131.0, 131.0, 129.7, 88.7 (minor 88.8), 82.8 (minor 82.8), 81.9, 78.5, 76.4 (minor 76.3), 76.2, 72.5, 59.8 (minor 59.8), 56.2 (minor 56.3), 41.4, 40.1, 39.2, 39.2 (minor 39.1), 38.3, 35.9 (minor 36.1), 32.1, 28.7 (minor 28.6), 19.3 (minor 19.4), 17.9, 17.1, 16.8 (minor 16.7), 14.3 (minor 14.3), 13.1, 13.1, 7.3.

Atom	^{1}H NMR											^{13}C NMR				
	Natural	Mult.	*J* (Hz)	**222**	Mult.	*J* (Hz)	Δ	**223**	Mult.	*J* (Hz)	Δ	Natural	**222**	Δ	**223**	Δ
1	N.A.			N.A.				N.A.				174.1	175.9	1.8	175.9	1.8
2	5.90	d	15.3	5.90	d	15.4	0.00	5.91	d	15.3	0.01	127.6	129.7	2.1	129.7	2.1
3	7.10	dd	15,1, 11.1	7.02	dd	15.3, 11.3	-0.08	7.02	dd	15.3, 11.2	-0.08	142.7	142	-0.7	141	-1.7
4	6.27	dd	15.0, 11.0	6.24	dd	15.1, 11.2	-0.03	6.25	dd	14.9, 10.6	-0.02	130.7	131	0.3	131	0.3
5	6.45	dd	15.0, 10.7	6.41	dd	15.0, 10.8	-0.04	6.43	dd	14.8, 10.6	-0.02	139.8	138.6	-1.2	138.7	-1.1
6	6.17	dd	15.3, 10.7	6.16	dd	15.2, 10.8	-0.01	6.16	dd	15.2, 10.7	-0.01	130.9	131.1	0.2	131	0.1
7	5.87	dd	15.1, 8.7	5.83	dd	15.2, 8.8	-0.04	5.85	d	15.2, 8.6	-0.02	142.8	141	-1.8	142	-0.8
8	2.53	m		2.53	m		-0.02	2.53	m		-0.02	41.5	41.5	0.0	41.4	-0.1
Me8	1.07	d	6.7	1.07	d	6.7	0.00	1.07	d	6.7	0.00	17.2	17.2	0.0	16.8	-0.4
9	3.27	dd	6.7, 4.6	3.27	dd	6.3, 4.6	0.00	3.26	dd	5.6, 4.8	-0.01	88.3	88.5	0.2	88.7	0.4
OMe9	3.38	s		3.39	s		0.00	3.39	s		0.00	59.6	59.6	0.0	59.8	0.2
10	2.02-1.22	m		1.98	m		0.00	1.98	m		0.00	40.1	40.1	0.0	40.1	0.0
Me10	0.85	d	7.0	0.85	d	7.0	0.00	0.85	d	7.0	0.00	13.0	13.1	0.1	13.1	0.1
11	3.57	dd	9.6, 2.0	3.59	dd	9.6, 2.2	0.02	3.61	dd	9.5, 1.8	0.04	75.5	75.7	0.2	76.2	0.7
12	2.02-1.22	m		1.80	m		0.00	1.82	m		0.00	38.5	38.4	-0.1	38.3	-0.2
Me12	0.93	d	No J value	0.92	d	6.8	-0.01	0.91	d	6.9	-0.02	7.6	7.5	-0.1	7.3	-0.3
13	3.99	d	7.3	4.00	d	7.3	0.01	4.02	d	6.6	0.03	82.1	82	-0.1	81.9	-0.2
14	N.A.			N.A.				N.A.				137.4	137.4	0.0	137.4	0.0
Me14	1.69	s		1.69	s		0.00	1.69	s		0.00	14.0	14	0.0	14.3	0.3
15	5.95	S		5.95	s		0.00	5.96	s		0.01	131.7	131.6	-0.1	131.2	-0.5

16	N.A.			N.A.				N.A.				135.4	135.5	0.1	135.3	-0.1
Me16	1.82	s		1.82	s		0.00	1.8	s		-0.02	17.9	17.9	0.0	17.9	0.0
17	5.16	d	9.8	5.15	d	9.9	-0.01	5.15	d	9.8	-0.01	131.6	131.5	-0.1	131.2	-0.4
18	2.81	m		2.81	m		0.00	2.8	m		-0.01	39.3	39.2	-0.1	39.2	-0.1
Me18	1.10	d	6.7	1.10	d	6.7	0.00	1.11	d	6.6	0.01	17.2	17.1	-0.1	17.1	-0.1
19	4.42	ddd	11.3, 7.5, 3.5	4.42	ddd	11.4, 7.6, 3.9	0.00	4.42	ddd	11.4, 7.3, 4.0	0.00	82.8	83	0.2	82.8	0.0
20a	2.02-1.22	m		1.97	m		0.00	1.95	m		0.00	32.2	32.1	-0.1	32.1	-0.1
20b	2.02-1.22	m		1.68	m		0.00	1.67	m		0.00					
21	N.A.			N.A.				N.A.				76.4	76.4	0.0	76.4	0.0
22	4.27	s		4.26	s		-0.01	4.25	s		-0.02	72.5	72.5	0.0	72.5	0.0
23	N.A.			N.A.				N.A.				177.0	177	0.0	177	0.0
24	2.02-1.22	m		1.94	m		0.00	1.94	m		0.00	39.3	39.2	-0.1	39.2	-0.1
Me24	0.96	d	6.7	0.95	d	6.9	-0.01	0.94	d	6.9	-0.02	13.1	13.1	0.0	13.1	0.0
25a	2.02-1.22	m		1.57	m		0.00	1.56	m		0.00	28.0	28.7	0.7	28.7	0.7
25b	1.00	m		0.96	m		-0.04	0.97	m		-0.03					
26a	2.02-1.22	m		1.51	m		0.00	1.53	m		0.00	40.8	35.9	-4.9	35.9	-4.9
26b	2.02-1.22	m		1.43	m		0.00	1.46	m		0.00					
27	3.33	m		3.32	m		-0.01	3.33	m		0.00	79.1	78.6	-0.5	78.5	-0.6
OMe27	3.33	s		3.31	s		-0.02	3.31	s		-0.02	56.5	56.3	-0.2	56.2	-0.3
28	2.02-1.22	m		1.13	d	6.2	0.00	1.13	d	6.1	0.00	40.8	19.3	-21.5	19.3	-21.5

Table 13: NMR correlation table of 13,18-*syn* salt **222**[71] and 13,18-*anti* salt **223** against natural hemicalide

5.7 Experimental Procedures for the C27-C35 Fragment

(±)-ethyl 3-hydroxy-4-methylpent-4-enoate (224)

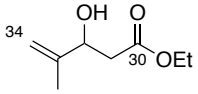

To a stirred solution of i-Pr_2NH (14.6, 102.5 mmol) in THF (85 mL) at 0 ˚C was added n-BuLi (72.3 mL, 86.7 mmol, 1.2 M in hexanes). The resulting pale yellow solution was stirred at 0 ˚C for 15 min then cooled to −78 ˚C. Ethyl acetate (10.0 mL, 102.5 mmol) was added dropwise. The reaction mixture was stirred at −78 ˚C for 1 h before adding methacrolein (6.5 mL, 78.8 mmol) and stirring continued for another 2 h. The reaction was quenched after 1.5 h with NH_4Cl (30 mL) and warmed to rt. The mixture was diluted with Et_2O (30 mL) and the layers were separated. The aqueous layer was extracted with Et_2O (3 x 50 mL) and the combined organic extracts were washed with brine (20 mL), dried ($MgSO_4$), filtered and concentrated *in vacuo*. The residue was purified by flash column chromatography (10% Et_2O/PE 30-40) to give ester **19** as a colourless oil (11.6 g, 73.3 mmol, 93%).

R_f 0.40 (10% EtOAc/PE 40-60); **^{1}H NMR** (500 MHz, $CDCl_3$): δ_H 5.03 (1H, s, H34a), 4.88 (1H, s, H34b), 4.47 (1H, ddd, *J* = 8.3, 4.1, 4.1 Hz, H32), 4.18 (2H, q, *J* = 7.0 Hz, O$\underline{CH_2}CH_3$), 2.92 (1H, d, *J* = 4.0 Hz, OH), 2.59 (1H, dd, *J* = 16.2, 4.1 Hz, H31a), 2.54 (1H, dd, *J* = 16.1, 8.5 Hz, H31b), 1.76 (3H, s, Me33), 1.28 (3H, t, *J* = 7.3 Hz, $OCH_2\underline{CH_3}$); **^{13}C NMR** (125 MHz, $CDCl_3$): δ_C 172.8, 145.6, 111.6, 71.7, 61.0, 40.2, 18.4, 14.3.

Data in agreement with that presented by Yamashita.[149]

(±)-ethyl 3-((*tert*-butyldimethylsilyl)oxy)-4-methylpent-4-enoate (225)

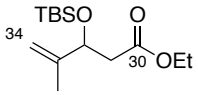

Alcohol **224** (2.00 g, 12.6 mmol), Et3N (2.65 mL, 19.0 mmol) and DMAP (2.32 g, 19.0 mmol) were dissolved in CH_2Cl_2 (120 mL) at rt and stirred until a clear homogenous solution was obtained, followed by the addition of TBSCl (2.29 g, 15.2 mmol). The reaction was stirred for 3 h and carefully quenched with NH_4Cl (30 mL). The layers were separated and the aqueous layer extracted with CH_2Cl_2 (3 x 30 mL). The combined organic extracts were washed with brine (15 mL), dried ($MgSO_4$), filtered and concentrated *in vacuo*. The crude

product was purified by flash column chromatography (5% Et_2O/PE 30-40) to give the title compound as a colourless oil (3.02 g, 11.1 mmol, 88%).

R_f 0.58 (10% EtOAc/PE 40-60); **^{1}H NMR** (500 MHz, $CDCl_3$): δ_H 4.95 (1H, s, H34a), 4.79 (1H, s, H34b), 4.55 (1H, dd, *J* = 8.9, 4.4 Hz, H32), 4.11 (2H, m, O$\underline{CH_2}CH_3$), 2.53 (1H, dd, *J* = 14.3, 8.8 Hz, H31a), 2.41 (1H, dd, *J* = 14.1, 4.5 Hz, H31b), 1.71 (3H, s, Me33), 1.26 (1H, dd, *J* = 7.2, 7.2 Hz, $OCH_2\underline{CH_3}$), 0.86 (9H, s, OSi$\underline{t\text{-}Bu}Me_2$), 0.04 (3H, s, OSit-Bu$\underline{Me_2}$), 0.01 (3H, s, OSit-Bu$\underline{Me_2}$); **^{13}C NMR** (125 MHz, $CDCl_3$): δ_C 171.6, 146.8, 111.7, 74.0, 60.5, 42.7, 25.8, 18.2, 17.1, 14.3, –4.7, –5.2; **HRMS** (ES^+) Calc. for $C_{14}H_{28}O_3SiH$ $[M+H]^+$ 273.1886, found 273.1890.

Data in agreement with that presented by Romo.[150]

(±)-3-((*tert*-butyldimethylsilyl)oxy)-4-methylpent-4-enal (226)

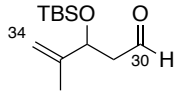

Ester **225** (1.80 g, 6.61 mmol) was dissolved in CH_2Cl_2 (33 mL) and cooled to –78 ˚C. DIBAL (7.28 mL, 1 M in hexanes, 7.28 mmol) was added dropwise at this temperature and stirring continued for 1 h. Upon complete reaction, the reaction was quenched with MeOH (10 mL) and warmed to rt. Rochelle's salt (30 mL) was added while stirring vigorously for 2 h. The layers were separated and the aqueous layer extracted with CH_2Cl_2 (3 x 20 mL). The combined organic extracts were dried ($MgSO_4$), filtered and concentrated *in vacuo*. The crude product was purified by flash column chromatography (5% Et_2O/PE 30-40) to give the title compound as a colourless oil (1.40 g, 6.13 mmol, 93%).

R_f 0.57 (10% EtOAc/PE 40-60); **^{1}H NMR** (500 MHz, $CDCl_3$): δ_H 9.76 (1H, dd, *J* = 2.9, 2.3 Hz, H30), 5.00 (1H, s, H34a), 4.85 (1H, s, H34b), 4.57 (1H, dd, *J* = 7.8, 4.3 Hz, H32), 2.64 (1H, ddd, *J* = 15.5, 7.8, 3.0 Hz, H31a), 2.46 (1H, ddd, *J* = 15.5, 4.4, 2.2 Hz, H31b), 1.71 (3H, s, Me33), 0.87 (9H, s, OSi$\underline{t\text{-}Bu}Me_2$), 0.06 (3H, s, OSit-Bu$\underline{Me_2}$), 0.03 (3H, s, OSit-Bu$\underline{Me_2}$); **^{13}C NMR** (125 MHz, $CDCl_3$): δ_C 202.0, 146.3, 111.8, 72.3, 49.9, 25.8, 18.2, 17.6,–4.6, –5.1.

Data in agreement with that presented by Romo.[150]

(±)-(4*S*,6*S*)-6-((*tert*-butyldimethylsilyl)oxy)-4-hydroxy-7-methyloct-7-en-2-one (227)

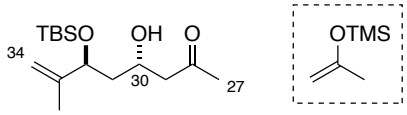

A flame-dried flask was charged with Et_2O (90 mL) and Et_3N (13.5 mL, 97.2 mmol) then cooled to 0 ˚C. TMSOTf (16.0 mL, 88.3) was added dropwise over 10 min and stirring continued for 30 min, during which time a red-brown oily precipitate formed. The red-brown phase was discarded and the remaining ethereal phase washed with $NaHCO_3$ (40 mL). The aqueous phase was extracted with Et_2O (2 x 20 mL) and the combined ethereal extracts dried (Na_2SO_4), filtered, and concentrated *in vacuo* to *ca*. 20 mL. The crude product was fractionally distilled through a 150 mm Vigreux column to afford the silyl enol ether as a colourless oil (9.78 g, 75.0 mmol, 85%).

Aldehyde **226** (1.40 g, 6.13 mmol) and silyl enol ether (2.79 mL, 18.4 mmol) were dissolved in CH_2Cl_2 (61 mL) and cooled to –78 ˚C. BF_3•Et_2O (1.13 mL, 9.19 mmol) was added dropwise and the reaction stirred for 20 min before quenching with $NaHCO_3$ (30 mL). The layers were separated and the aqueous layer was extracted with CH_2Cl_2 (3 x 20 mL). The combined organic extracts were dried (Na_2SO_4), filtered and concentrated *in vacuo*. The crude product was purified by flash column chromatography (10% Et_2O/PE 30-40) to give the title compound as a colourless oil (1.37 g, 4.78 mmol, 78%, *d.r.* 5:1).

Major isomer: **R_f** 0.30 (10% EtOAc/PE 40-60); **^{1}H NMR** (500 MHz, $CDCl_3$): δ_H 5.00 (1H, m, H34a), 4.85 (1H, m, H34b), 4.34 (1H, m, H32), 4.24 (1H, m, H30), 3.45 (1H, d, *J* = 2.4 Hz, OH), 2.60 (1H, dd, *J* = 17.0, 8.0 Hz, H29a), 2.54 (1H, dd, *J* = 16.9, 4.4 Hz, H29b), 2.17 (3H, s, H27), 1.69 (3H, s, Me33), 1.61 (2H, m, H31), 0.90 (6H, s, OSi<u>t-Bu</u>Me_2), 0.083 (3H, s, OSit-Bu<u>Me_2</u>), 0.032 (3H, s, OSit-Bu<u>Me_2</u>); **^{13}C NMR** (125 MHz, $CDCl_3$): δ_C 209.2, 146.8, 111.1, 74.0, 64.7, 50.8, 41.8, 30.9, 26.0, 25.9, 18.4, –4.7, –5.2; **FT-IR** (Thin film): ν_{max} 3524 (br), 2956, 2929, 2858, 1712, 1472, 1361, 1251, 1163, 1079, 1004, 961, 898, 836, 776, 667; **HRMS** (ES^+) Calc. for $C_{15}H_{30}O_3SiH$ $[M+H]^+$ 287.2043, found 287.2043.

(±)-(2*R*,4*R*,6*S*)-6-((*tert*-butyldimethylsilyl)oxy)-7-methyloct-7-ene-2,4-diol (236)

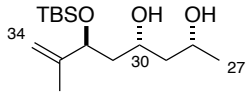

MeOH (535 μL, 13.2 mmol) was added to $LiBH_4$ (3.00 mL, 4M in THF, 12.0) in THF (9 mL) at 0 ˚C and stirred at rt for 1.5 h. The resulting solution of $LiBH_3OMe$ (*ca.* 1 M in THF) was used immediately.

A flame-dried flask was charged with Cy_2BCl (386 μL, 2.20 mmol), Et_3N (408 μL, 2.93 mmol) in THF (10 mL) at 0 °C. A solution of ketone **227** (210 mg, 0.733 mmol) in THF (1 mL) was added *via* cannula (2 x 1 mL wash) and the reaction mixture stirred for 30 min before cooling to –78 ˚C. $LiBH_3OMe$ (5.86 mL, 1 M in THF, 5.86 mmol) was added and stirring continued at –78 ˚C for 1 h and allowed to warm slowly to 0 ˚C over 4 h. The reaction was quenched with pH 7 buffer (3 mL), MeOH (3 mL) and H_2O_2 (30% aq. 1 mL) and stirred at rt for 1 h. The reaction was partitioned between H_2O (5 mL) and Et_2O (10 mL) and the layers were separated. The aqueous layer was extracted with Et_2O (3 x 10 mL) and the combined organic extracts were dried (Na_2SO_4), filtered and concentrated *in vacuo*. The crude product was purified by flash column chromatography (10% EtOAc/PE 40-60) to give the title compound as a colourless oil (173 mg, 0.601 mmol, 82%, *d.r.* 5:1).

Major isomer: $\mathbf{R_f}$ 0.18 (20% EtOAc/PE 40-60); **^{1}H NMR** (500 MHz, $CDCl_3$): δ_H 5.05 (1H, s, H34a), 4.91 (1H, s, H34b), 4.35 (1H, dd, *J* = 4.6, 4.6, Hz, H32), 4.10-4.00 (2H, m, H30, H28), 1.70-1.65 (2H, m, H31), 1.67 (3H, s, Me33), 1.57-1.52 (1H, m, H29a), 1.42 (1H, ddd, *J* = 14.1, 2.4, 2.4, Hz, H29b), 1.16 (3H, d, *J* = 6.4 Hz, H27), 0.90 (9H, s, OSi<u>t-Bu</u>Me_2), 0.09 (3H, s, OSit-Bu<u>Me_2</u>), 0.04 (3H, s, OSit-Bu<u>Me_2</u>); **^{13}C NMR** (125 MHz, $CDCl_3$): δ_C 145.9, 111.5, 75.0, 70.0, 68.6, 45.4, 41.6, 25.9, 23.9, 19.0, 18.3, –4.8, –5.3; **FT-IR** (Thin film): ν_{max} 3348 (br), 2930, 2857, 1452, 1407, 1320, 1251, 1137, 1071, 1004, 965, 897, 836, 776; **HRMS** (ES^+) Calc. for $C_{15}H_{32}O_3SiH$ $[M+H]^+$ 289.2199, found 289.2202.

(±)-*tert*-butyldimethyl(((*S*)-3-methyl-1-((4*R*,6*R*)-2,2,6-trimethyl-1,3-dioxan-4-yl)but-3-en-2-yl)oxy)silane (239)

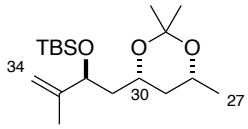

To a solution of diol **237** (10 mg, 34.7 μmol) in 2,2-dimethoxypropane (500 μL) was added PPTS (1 crystal) at rt. The reaction mixture was stirred for 16 h and then concentrated *in vacuo*. The residue was purified by flash column chromatography flash column chromatography (5% Et_2O/PE 30-40) to give the title compound as a colourless oil (10.8 mg, 33.0 μmol, 95%, *d.r.* 5:1).

Major isomer: $\mathbf{R_f}$ 0.67 (10% EtOAc/PE 40-60); **^{1}H NMR** (500 MHz, $CDCl_3$): δ_H 4.88 (1H, s, H34a), 4.73 (1H, s, H34b), 4.25 (1H, dd, *J* = 9.3, 3.3 Hz, H32), 4.01-3.94 (2H, m, H30, H28), 1.67 (3H, s, Me33), 1.58-1.48 (2H, m, H31), 1,48-1.6 (1H, m, H29a), 1.44 (3H, s Me), 1.39 (3H, s, Me), 1.15 (3H, d, *J* = 6.1 Hz, H27), 1.13-1.07 (1H, m, H29b), 0.89 (9H, s, OSit-BuMe$_2$), 0.04 (3H, s, OSit-BuMe$_2$), 0.00 (3H, s, OSit-BuMe$_2$); **^{13}C NMR** (125 MHz, $CDCl_3$): δ_C 148.5, 110.8, 98.5, 72.6, 65.4, 65.2, 44.3, 39.5, 30.5, 26.0, 24.3, 22.4, 20.3, 17.1, –4.4, –4.9.

(±)-*tert*-butyl(((3*S*,5*R*,7*R*)-5,7-dimethoxy-2-methyloct-1-en-3-yl)oxy)dimethylsilane (241)

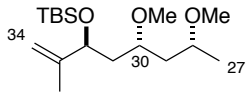

NaH (528 mg, 60 wt% suspension in mineral oil, 13.2 mmol) was suspended in THF (10 mL) cooled to 0 °C. A solution of diol **236** (380 mg, 1.32 mmol) in THF (1 mL) was added *via* cannula (2 x 1 mL wash) and the reaction mixture stirred for 30 min before adding MeI (820 μL, 13.2 mmol). The reaction was stirred at rt for 1 h before quenching with NH_4Cl (10 mL). The mixture was diluted with Et_2O (10 mL) and the layers were separated. The aqueous layer was extracted with Et_2O (3 x 5 mL) and the combined organic extracts were dried ($MgSO_4$), filtered and concentrated *in vacuo*. The crude product was purified by flash column chromatography (5% Et_2O/PE 30-40) to give the title compound as a colourless oil (389 mg, 1.23 mmol, 93%, *d.r.* 5:1).

Major isomer: $\mathbf{R_f}$ 0.72 (10% EtOAc/PE 40-60); **^{1}H NMR** (500 MHz, $CDCl_3$): δ_H 4.89 (1H, m, H34a), 4.75 (1H, m, H34b), 4.21 (1H, dd, *J* = 6.3, 6.3, Hz, H32), 3.45 (1H, m, H30), 3.40 (1H, m, H28), 3.33 (3H, s, OMe), 3.31 (3H, s, OMe), 1.69 (3H, s, Me33), 1.59 (4H, m, H31a, H31b, H29a, H29b), 1.14 (3H, d, *J* = 6.3 Hz, H27), 0.89 (9H, s, OSit-BuMe$_2$), 0.06 (3H, s,

OSit-Bu<u>Me$_2$</u>), 0.00 (3H, s, OSit-Bu<u>Me$_2$</u>); **^{13}C NMR** (125 MHz, $CDCl_3$): δ_C 148.2, 111.0, 75.0, 74.1, 73.6, 56.4, 56.1, 42.3, 41.7, 26.0, 19.6, 18.3, 17.1, –4.4, –5.0; **FT-IR** (Thin film): ν_{max} 2960, 2930, 1470, 1375, 1251, 1085, 897, 835, 775; **HRMS** (ES^+) Calc. for $C_{17}H_{36}O_3SiH$ $[M+H]^+$ 317.2512, found 317.2513.

(±)-(2*S*,4*R*,6*S*)-6-((*tert*-butyldimethylsilyl)oxy)-7-methyloct-7-ene-2,4-diol (238)

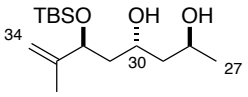

A solution of EtCHO (457 µL, 6.28 mmol) in THF (7 mL) was cooled to 0 ˚C and SmI_2 (1.05 mL, 0.1 M in THF, 0.105 mmol) was added dropwise. The reaction mixture was stirred for 10 min before cooling to –20 ˚C, A solution of ketone **227** (300 mg, 1.05 mmol) in THF (1 mL) was added *via* cannula (2 x 1 mL wash) at this temperature and stirring was continued for 2 h. The reaction was quenched with $NaHCO_3$ (4 mL) and the layers were separated. The aqueous layer was extracted with Et_2O (3 x 5 mL) and the combined organic extracts were dried (Na_2SO_4), filtered and concentrated *in vacuo*.

The crude product was suspended in MeOH (7 mL) and K_2CO_3 (290 mg, 2.10 mmol) was added. The reaction mixture was stirred for 5 h and quenched with NH_4Cl (2 mL). The solution was extracted with CH_2Cl_2 (4 x 5 mL) and the combined organic extracts were dried (Na_2SO_4), filtered and concentrated *in vacuo*. The crude product was purified by flash column chromatography flash column chromatography (10% EtOAc/PE 40-60) to give the title compound as a colourless oil (270 mg, 0.935 mmol, 89% over two steps, *d.r.* 5:1).

Major isomer: **R_f** 0.18 (20% EtOAc/PE 40-60); **^{1}H NMR** (500 MHz, $CDCl_3$): δ_H 5.07 (1H, s, H34a), 4.92 (1H, s, H34b), 4.37 (1H, dd, *J* = 4.4, 4.4 Hz, H32), 4.18 (1H, m, H30), 4.12 (1H, m, H28), 3.74 (1H, s, OH), 2.95 (1H, s, OH), 1.81 (1H, ddd, *J* = 14.4, 10.1, 4.4 Hz, H31a), 1.64 (1H, ddd, *J* = 14.4, 4.8, 2.0 Hz, H31b), 1.67 (3H, s, Me33), 1.65 (1H, ddd, *J* = 14.4, 4.7, 1.9 HX), 1.56 (2H, ddd, *J* = 7.0, 4.3, 2.6 Hz, H29); **^{13}C NMR** (125 MHz, $CDCl_3$): δ_C 145.8, 111.5, 75.1, 66.6, 65.3, 44.6, 40.6, 25.9, 23.6, 19.2, 18.3, –4.8, –5.3; **FT-IR** (Thin film): ν_{max} 3351 (br), 2953, 2930, 2859, 1463, 1374, 1252, 1072, 1004, 967, 938, 836, 776, 668; **HRMS** (ES^+) Calc. for $C_{15}H_{32}O_3SiH$ $[M+H]^+$ 289.2199, found 289.2202.

(±)-*tert*-butyldimethyl(((*S*)-3-methyl-1-((4*R*,6*S*)-2,2,6-trimethyl-1,3-dioxan-4-yl)but-3-en-2-yl)oxy)silane (240)

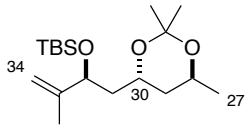

To a solution of diol **240** (10 mg, 34.7 μmol) in 2,2-dimethoxypropane (500 μL) was added PPTS (1 crystal) at rt. The reaction mixture was stirred for 16 h and then concentrated *in vacuo*. The residue was purified by flash column chromatography flash column chromatography (5% Et_2O/PE 30-40) to give the title compound as a colourless oil (10.9 mg, 33.3 μmol, 96%, *d.r.* 5:1).

Major isomer: $\mathbf{R_f}$ 0.67 (10% EtOAc/PE 40-60); **^{1}H NMR** (500 MHz, $CDCl_3$): δ_H 4.88 (1H, s, H34a), 4.74 (1H, s, H34b), 4.20 (1H, dd, *J* = 6.3, 6.3 Hz, H32), 4.00-3.88 (2H, m, H30, H28), 1.68 (3H, s, Me33), 1.62 (2H, dd, *J* = 6.3, 6.3 Hz, H31), 1.60-1.55 (2H, m, H29), 1.36 (3H, s, Me), 1.35 (3H, s, Me), 1.18 (3H, d, *J* = 6.3 Hz, H27), 0.88 (9H, s, OSi<u>t-Bu</u>Me_2), 0.05 (3H, s, OSit-Bu<u>Me_2</u>), 0.00 (3H, s, OSit-Bu<u>Me_2</u>); **^{13}C NMR** (125 MHz, $CDCl_3$): δ_C 148.3, 111.1, 100.0, 73.5, 63.5, 62.9, 43.9, 40.4, 26.0, 25.8, 25.6, 18.3, 16.9, –4.4, –4.9.

(±)-*tert*-butyl(((3*S*,5*R*,7*S*)-5,7-dimethoxy-2-methyloct-1-en-3-yl)oxy)dimethylsilane (242)

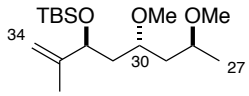

NaH (332 mg, 60 wt% suspension in mineral oil, 8.32 mmol) was suspended in THF (2 mL) cooled to 0 °C. A solution of diol **238** (120 mg, 0.416 mmol) in THF (1 mL) was added *via* cannula (2 x 0.5 mL wash) and the reaction mixture stirred for 30 min before adding MeI (518 μL, 8.32 mmol). The reaction was stirred at rt for 1 h before quenching with NH_4Cl (2 mL). The mixture was diluted with Et_2O (2 mL) and the layers were separated. The aqueous layer was extracted with Et_2O (3 x 1 mL) and the combined organic extracts were dried ($MgSO_4$), filtered and concentrated *in vacuo*. The crude product was purified by flash column chromatography (5% Et_2O/PE 30-40) to give the title compound as a colourless oil (118 mg, 0.374 mmol, 90%, *d.r.* 5:1).

Major isomer: $\mathbf{R_f}$ 0.72 (10% EtOAc/PE 40-60); **^{1}H NMR** (500 MHz, $CDCl_3$): δ_H 4.90 (1H, m, H34a), 4.74 (1H, m, H34b), 4.23 (1H, dd, *J* = 8.8, 3.7 Hz, H32), 3.47 (1H, m, H30), 3.36 (1H, m, H28), 3.31 (3H, s, OMe), 3.30 (3H, s, OMe), 1.89 (1H, ddd, *J* = 14.0, 7.4, 5.3 Hz, H29a), 1.63 (1H, ddd, *J* = 14.0, 8.8, 3.8 Hz, H31a), 1.55 (1H, ddd, *J* = 14.0, 8.6, 3.7 Hz, H31b), 1.37

(1H, ddd, *J* = 14.1, 7.0, 5.4 Hz, H29b), 1.15 (3H, d, *J* = 6.1 Hz, H27), 0.89 (9H, s, OSit-BuMe$_2$), 0.06 (3H, s, OSit-BuMe$_2$), 0.00 (3H, s, OSit-BuMe$_2$); **^{13}C NMR** (125 MHz, $CDCl_3$): δ_C 148.4, 110.8, 74.8, 74.1, 73.4, 56.2, 55.8, 42.1, 40.6, 26.0, 19.5, 18.3, 17.2, –4.4, –5.0; **FT-IR** (Thin film): ν_{max} 2974, 2928, 1452, 1381, 1251, 1066, 897, 836, 775, 667; **HRMS** (ES^+) Calc. for $C_{17}H_{36}O_3SiH$ $[M+H]^+$ 317.2512, found 317.2510.

CHAPTER SIX: SELECTED SPECTRA

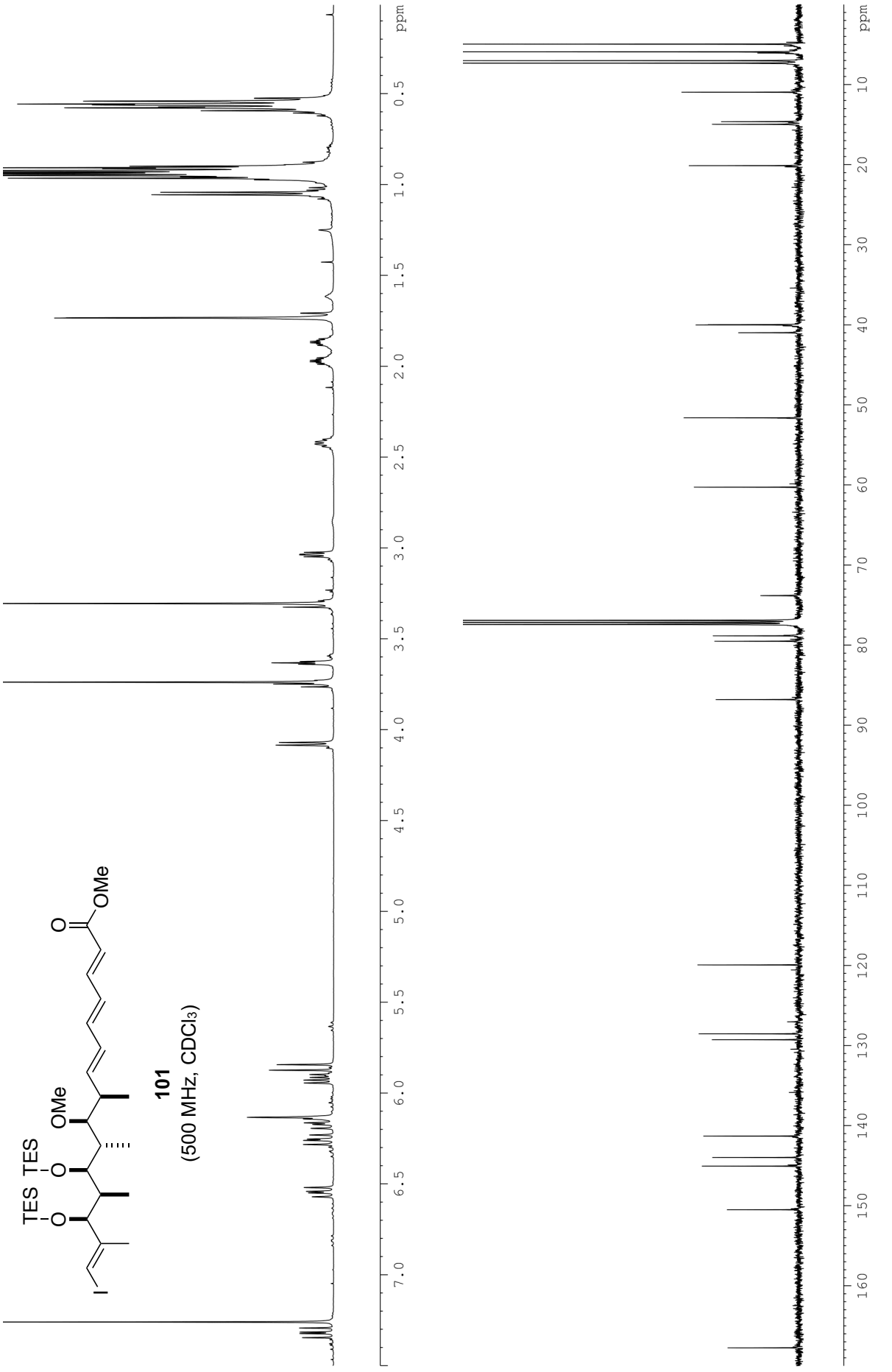
TES
TES
OMe
OMe
I
101
(500 MHz, CDCl3)
ppm
ppm

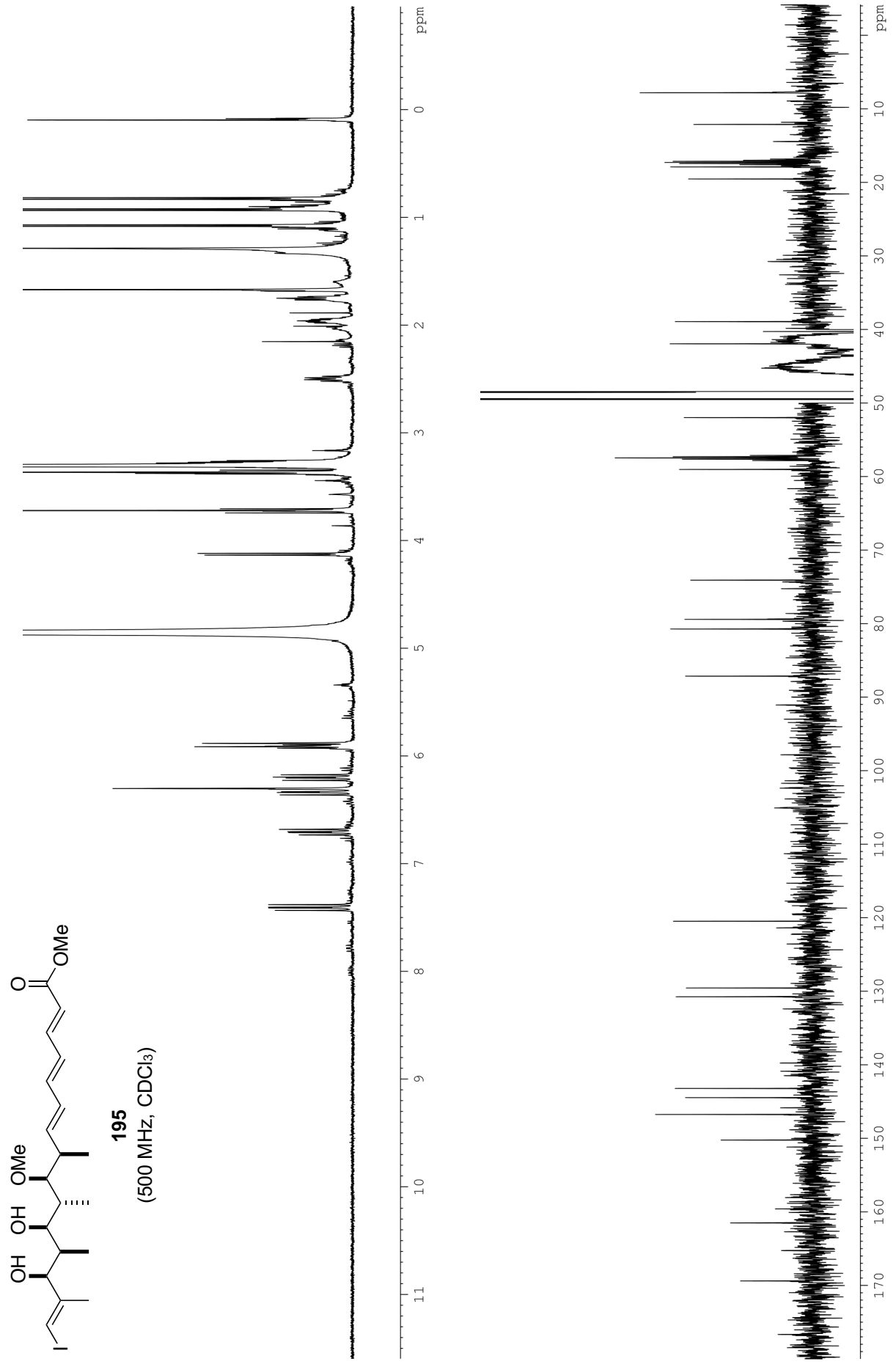
OMe
O
OMe
OH
OH
I
195
(500 MHz, CDCl3)
ppm
ppm

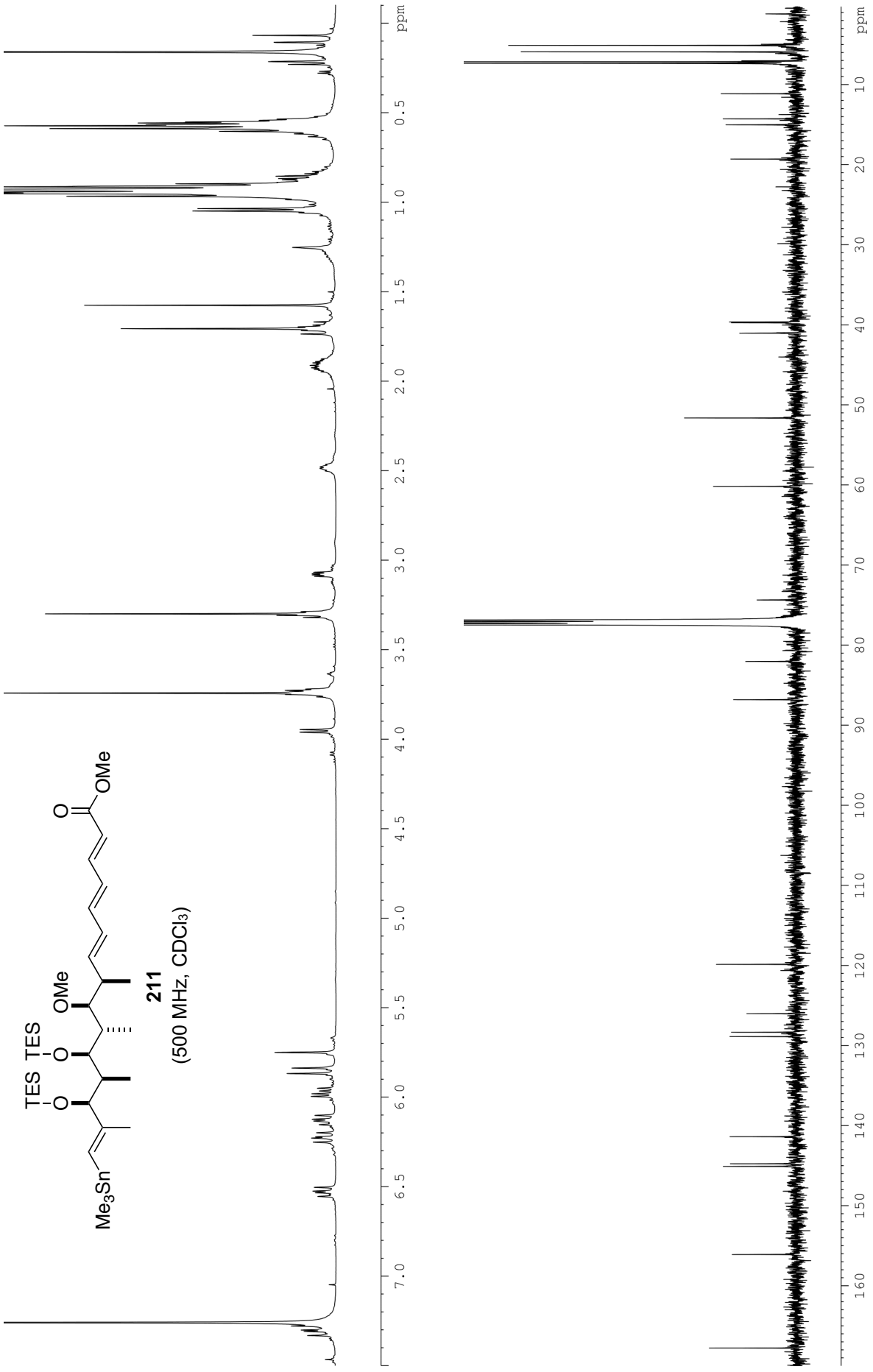
TES TES
O
O
OMe
O
OMe
Me3Sn
211
(500 MHz, CDCl3)
ppm
ppm

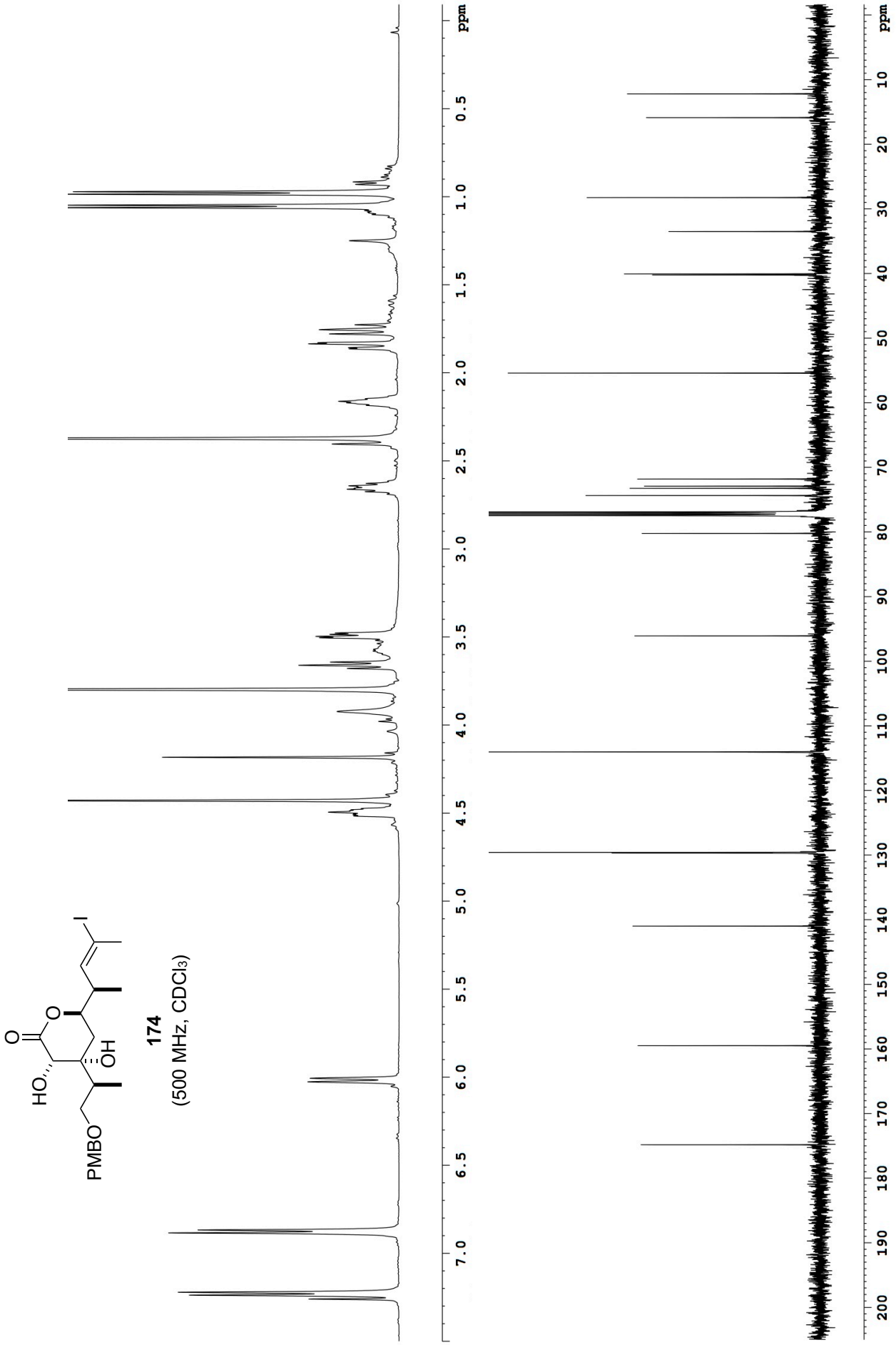
O
O
HO
OH
PMBO
I
174
(500 MHz, CDCl3)
ppm
7.0
6.5
6.0
5.5
5.0
4.5
4.0
3.5
3.0
2.5
2.0
1.5
1.0
0.5
ppm
200
190
180
170
160
150
140
130
120
110
100
90
80
70
60
50
40
30
20
10

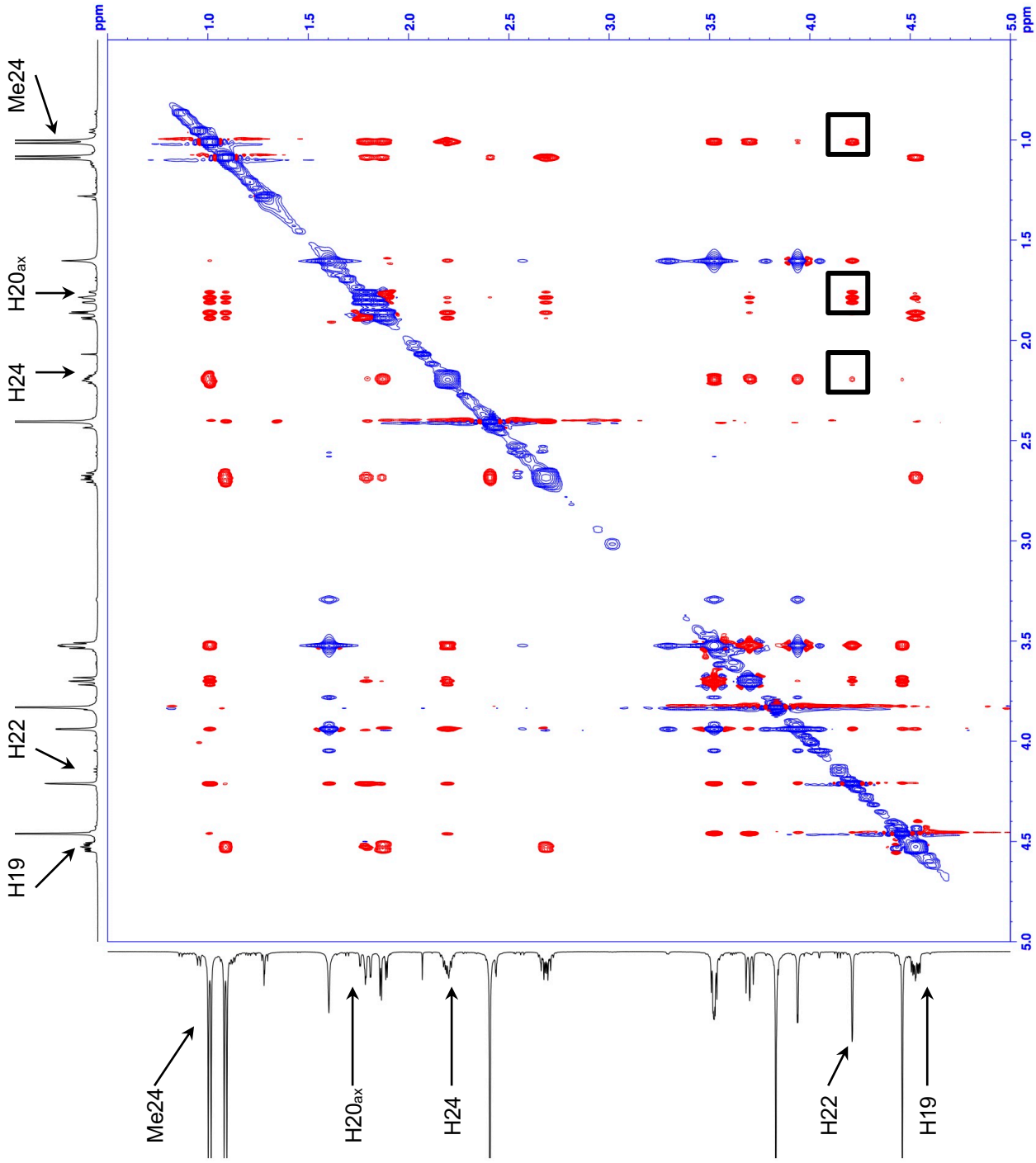

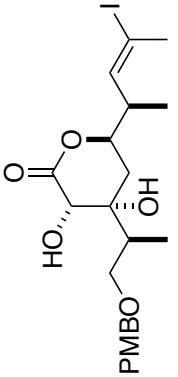

174

(500 MHz, $CDCl_3$)

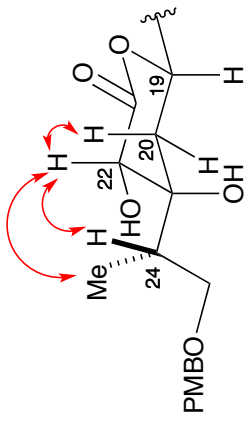

The NOE correlation between H22 and $H20_{ax}$ together with the *trans* coupling of $H20_{ax}$ and H19 (^3J = 11.1 Hz) suggest that H-22 is also *trans* to H-19, thus confirming the relative stereochemistry of the molecule as shown above.

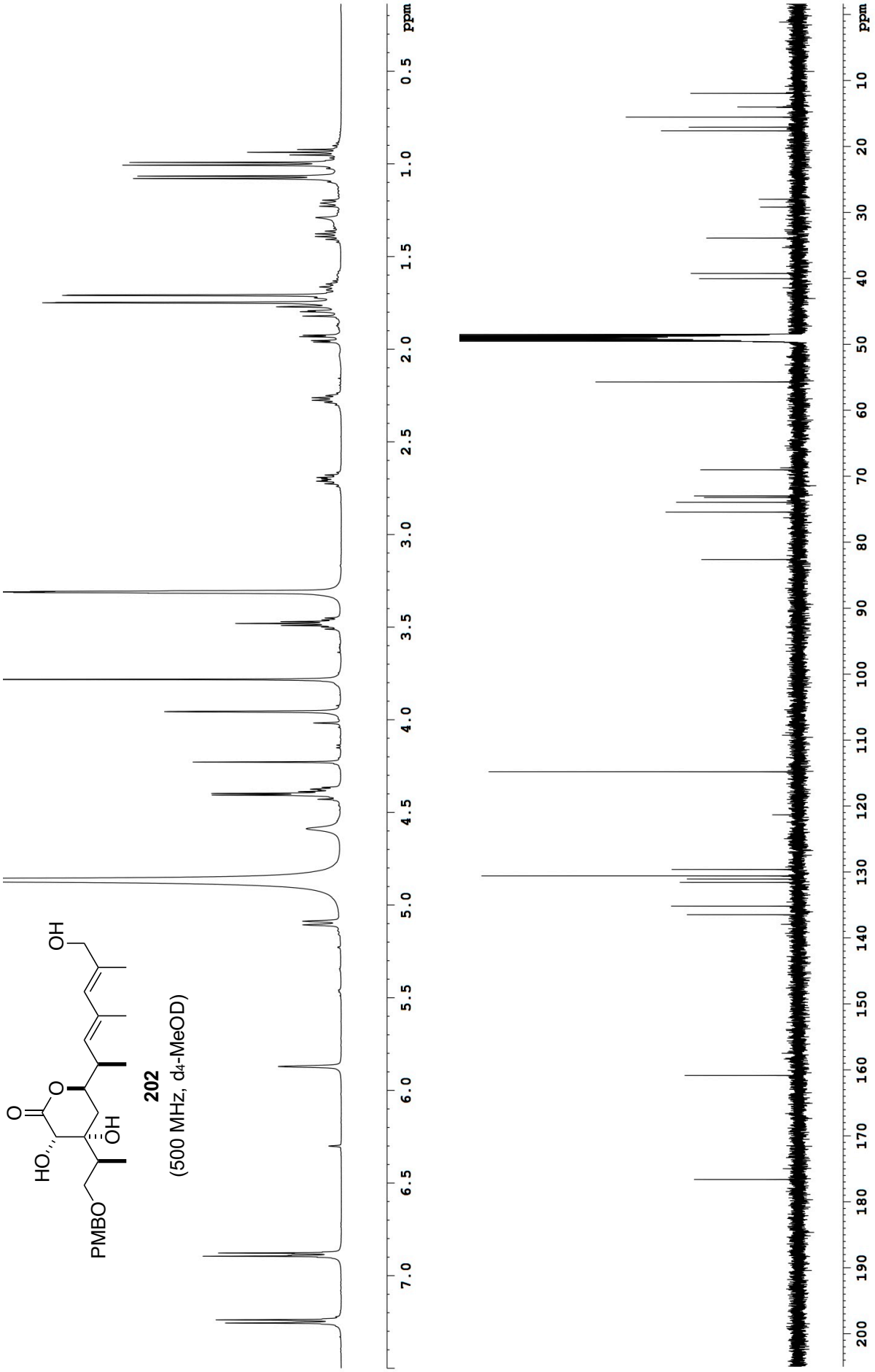
OH
O
O
HO
OH
PMBO
202
(500 MHz, d4-MeOD)
ppm
0.5
1.0
1.5
2.0
2.5
3.0
3.5
4.0
4.5
5.0
5.5
6.0
6.5
7.0
ppm
10
20
30
40
50
60
70
80
90
100
110
120
130
140
150
160
170
180
190
200

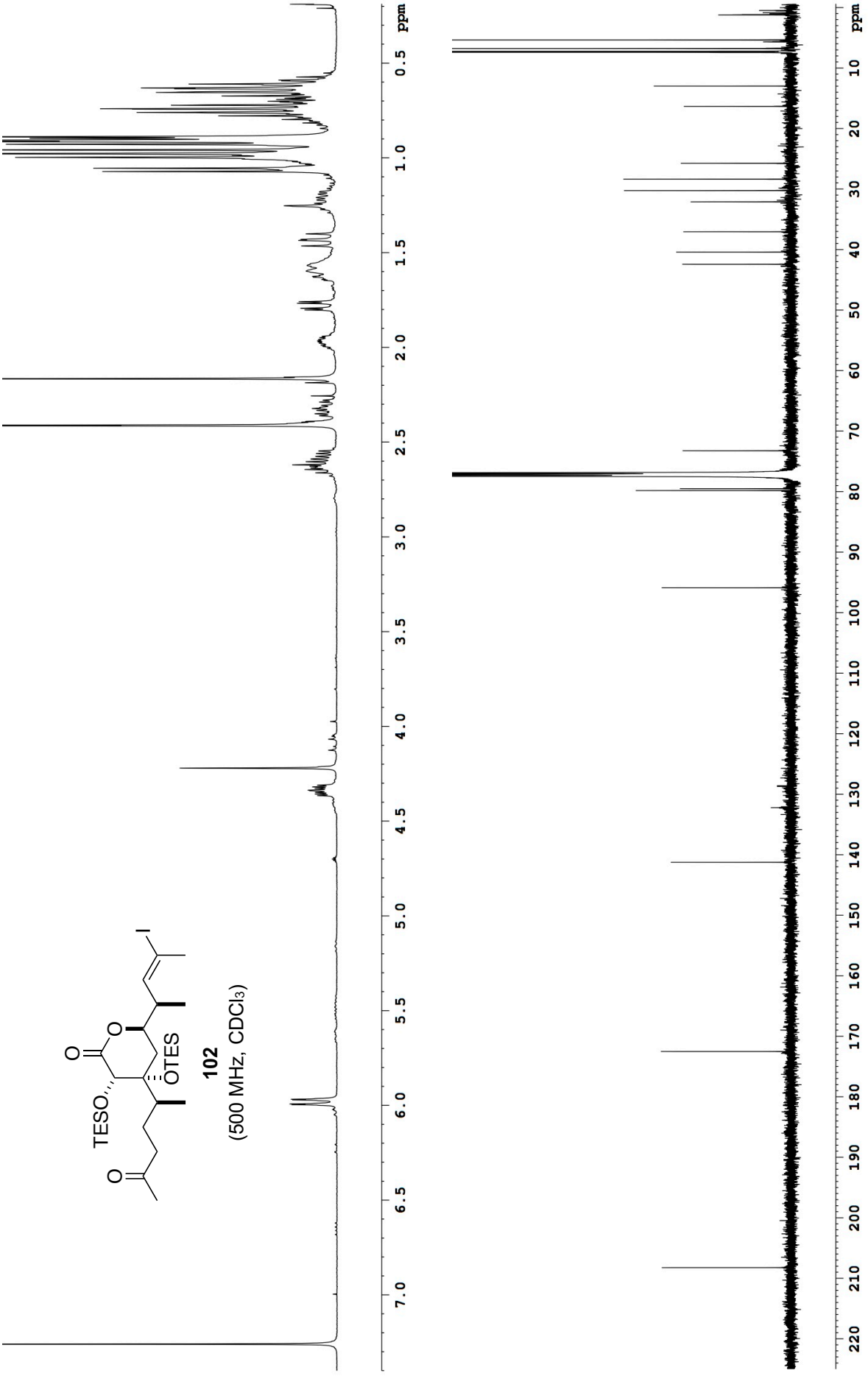
TESO
OTES
O
O
O
O
I
102
(500 MHz, CDCl3)
ppm
0.5
1.0
1.5
2.0
2.5
3.0
3.5
4.0
4.5
5.0
5.5
6.0
6.5
7.0
ppm
10
20
30
40
50
60
70
80
90
100
110
120
130
140
150
160
170
180
190
200
210
220

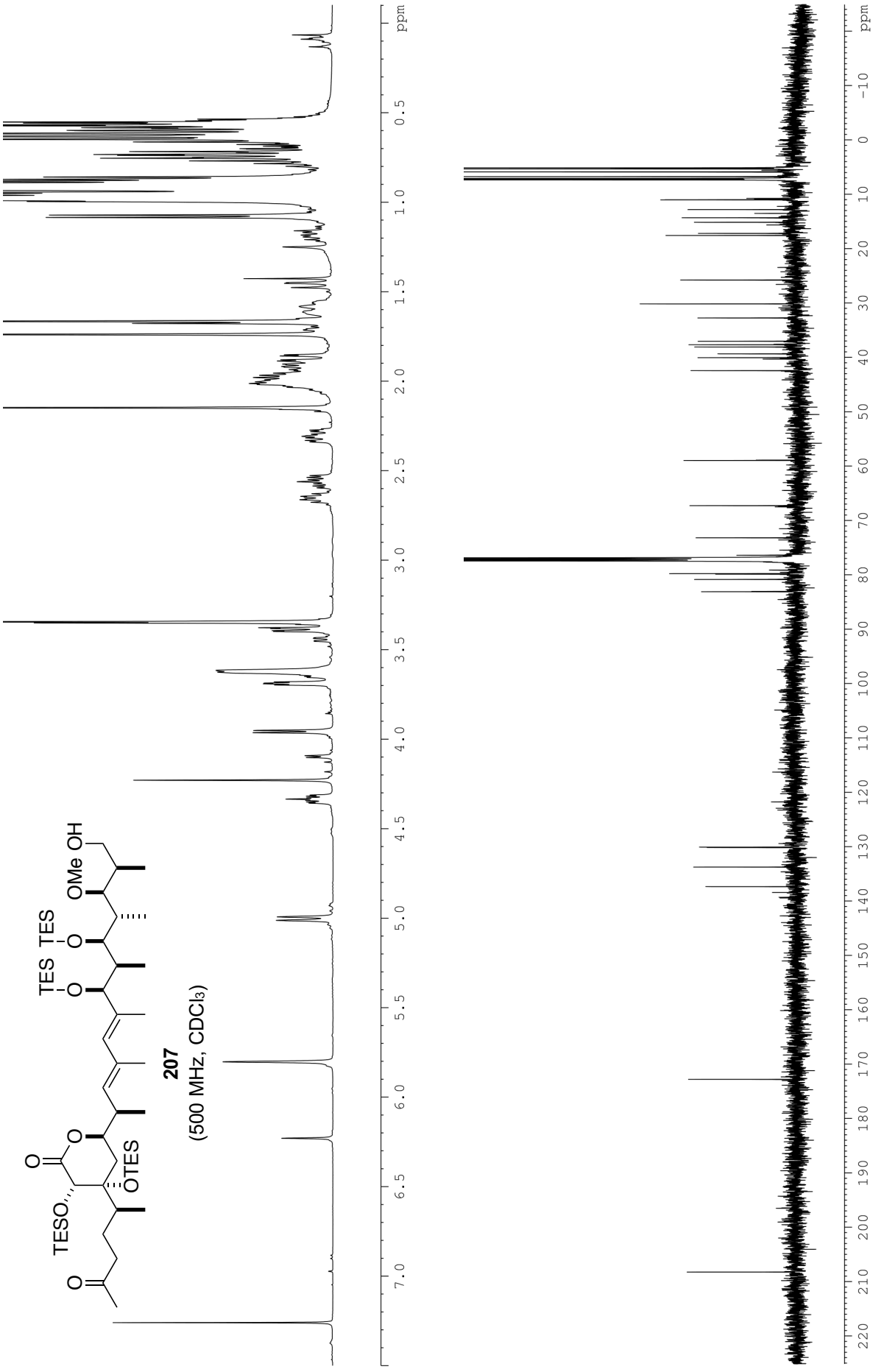
TES TES
OMe OH
TESO
OTES
207
(500 MHz, CDCl3)
ppm
ppm

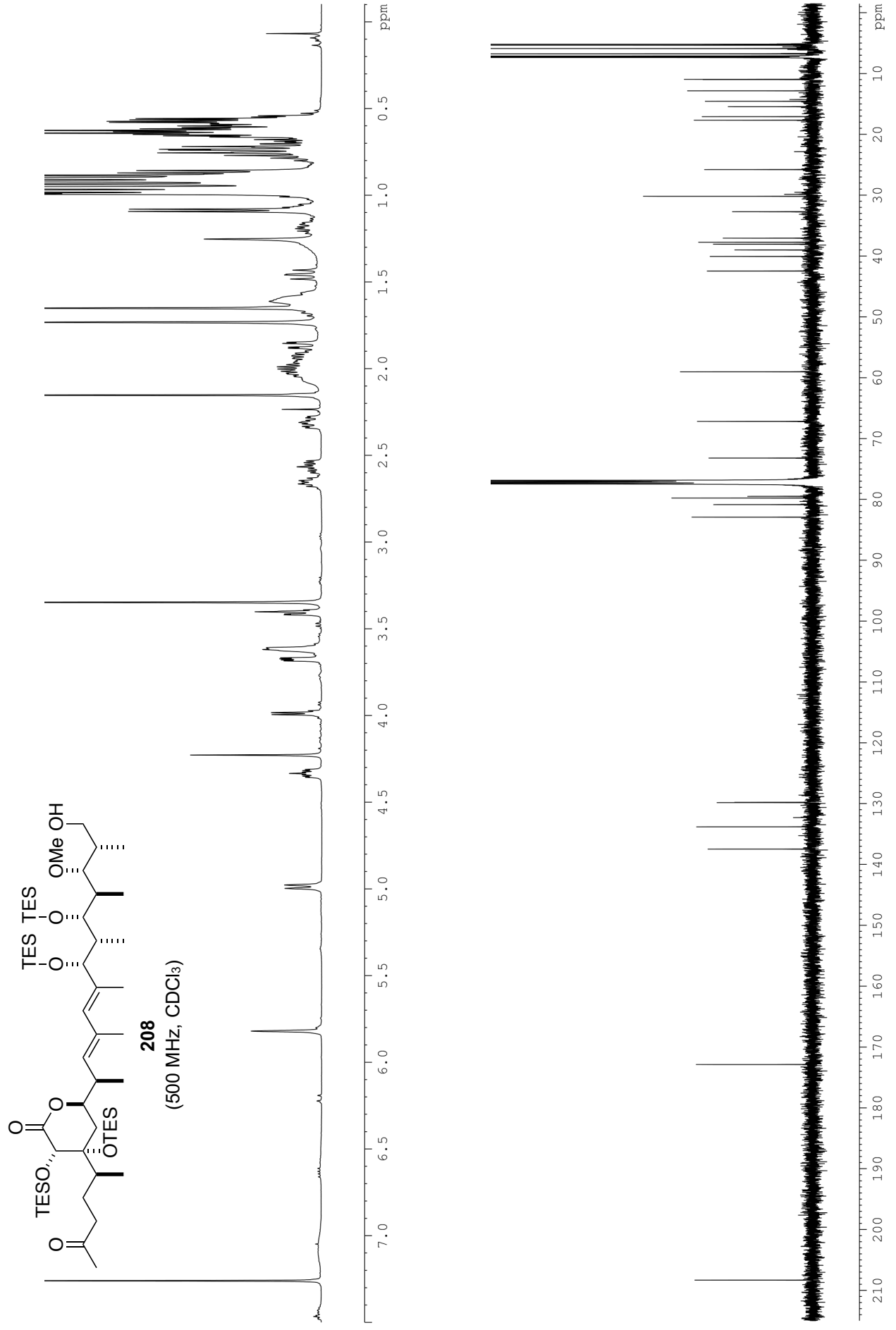
TES TES
OMe OH
TESO
OTES
O
O
O
O
O
O
208
(500 MHz, CDCl3)
ppm
0.5
1.0
1.5
2.0
2.5
3.0
3.5
4.0
4.5
5.0
5.5
6.0
6.5
7.0
ppm
10
20
30
40
50
60
70
80
90
100
110
120
130
140
150
160
170
180
190
200
210

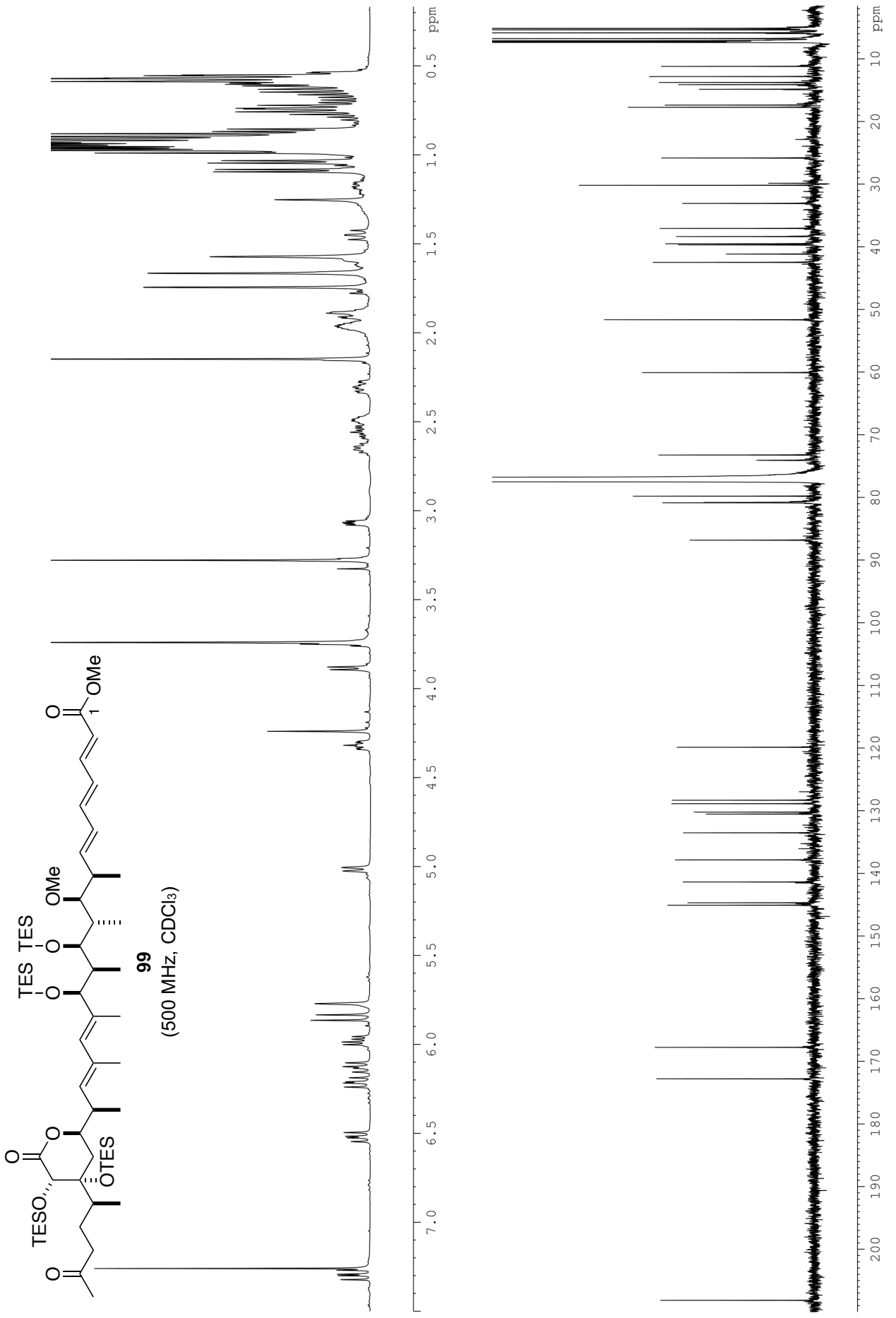
TES TES
OMe
OMe
OTES
TESO
O
O
O
O
O
O
O
1
99
(500 MHz, CDCl3)
ppm
0.5
1.0
1.5
2.0
2.5
3.0
3.5
4.0
4.5
5.0
5.5
6.0
6.5
7.0
ppm
10
20
30
40
50
60
70
80
90
100
110
120
130
140
150
160
170
180
190
200

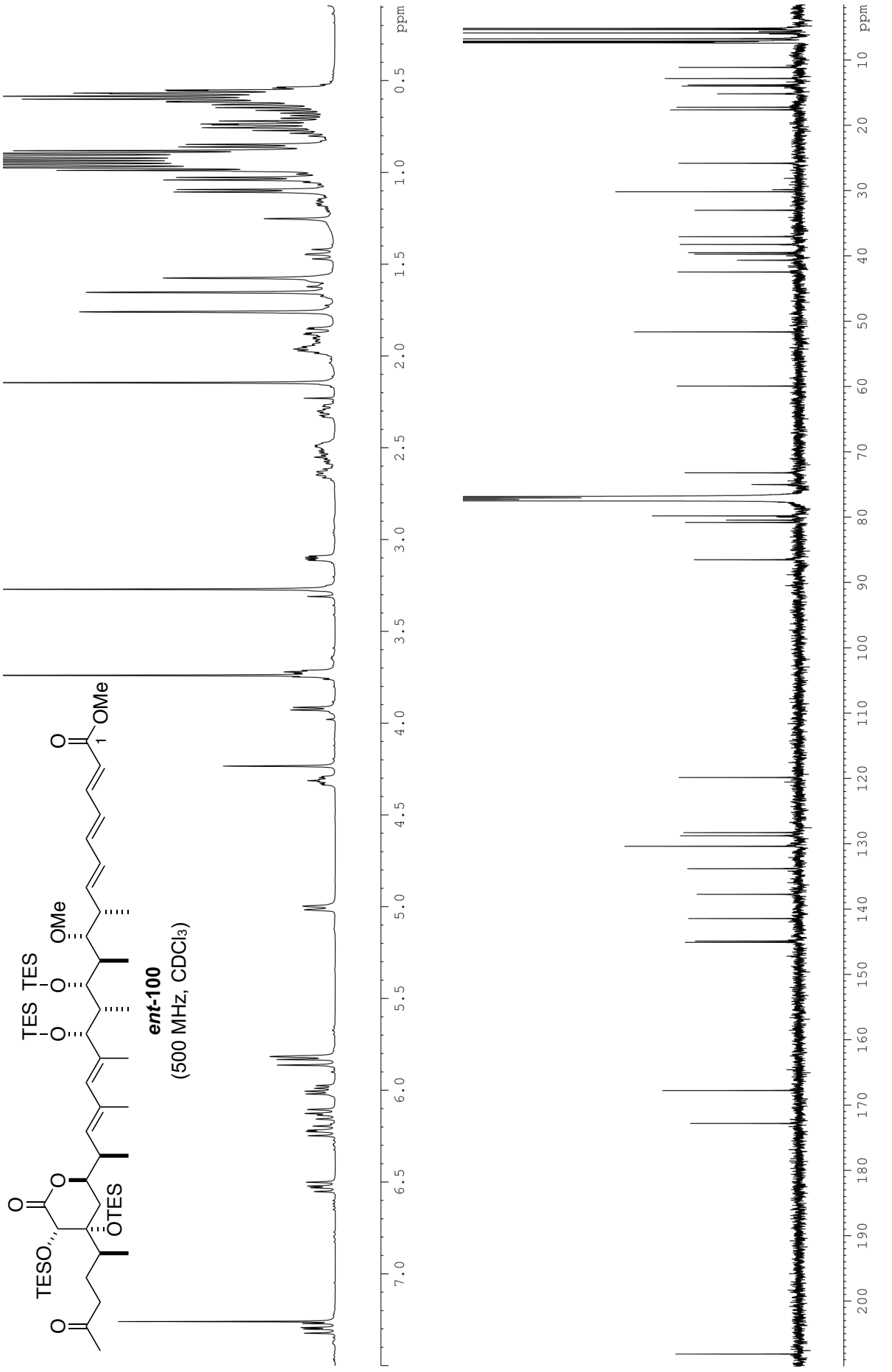
TESO
OTES
TES TES
OMe
OMe
***ent*-100**
(500 MHz, $CDCl_3$)
ppm
ppm

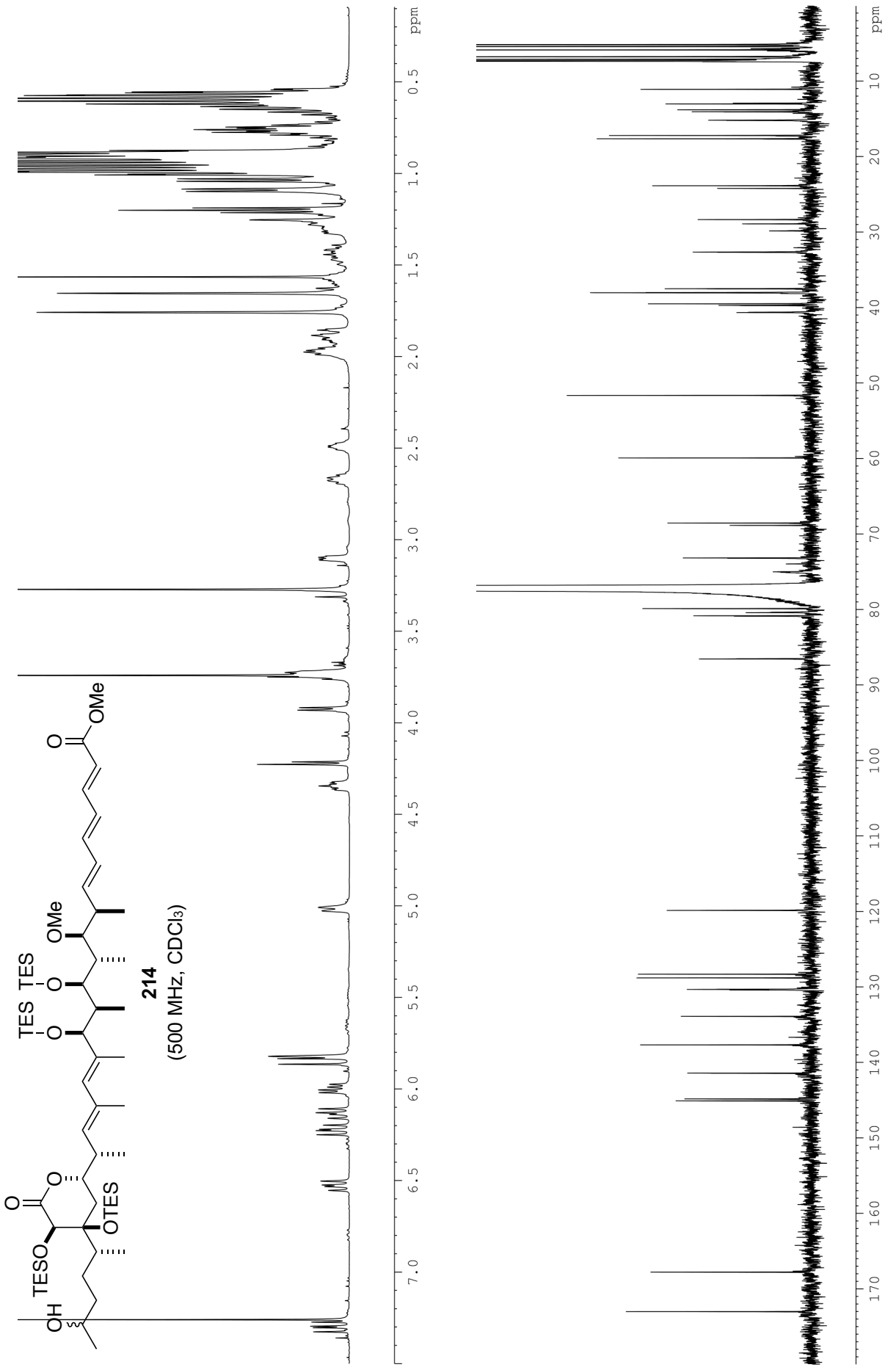
TES TES
OMe
OMe
TESO
OTES
OH
214
(500 MHz, CDCl3)
ppm
ppm

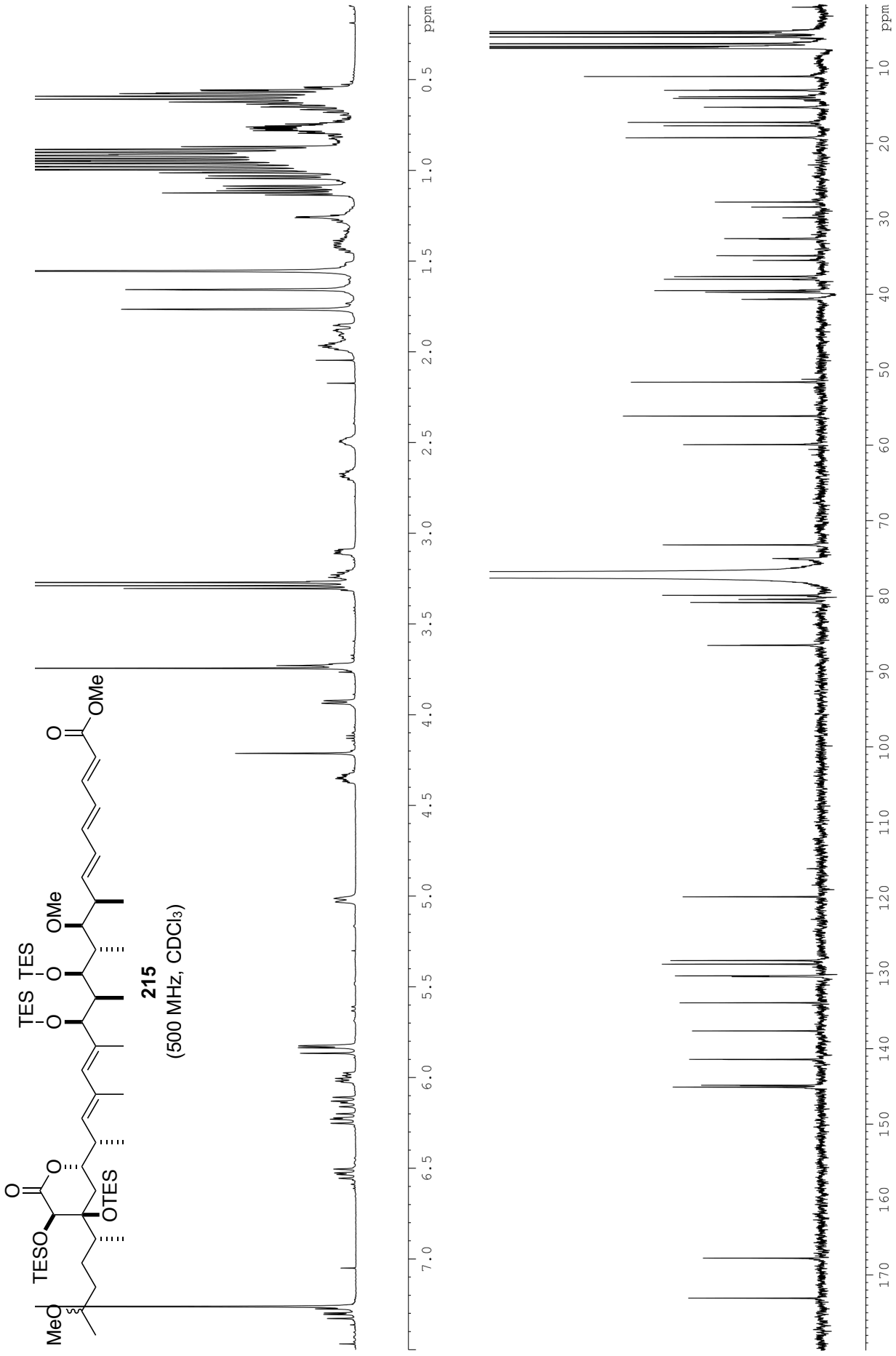
MeO
TESO
OTES
O
O
O
TES
TES
O
O
OMe
O
OMe
215
(500 MHz, CDCl3)
ppm
0.5
1.0
1.5
2.0
2.5
3.0
3.5
4.0
4.5
5.0
5.5
6.0
6.5
7.0
ppm
10
20
30
40
50
60
70
80
90
100
110
120
130
140
150
160
170

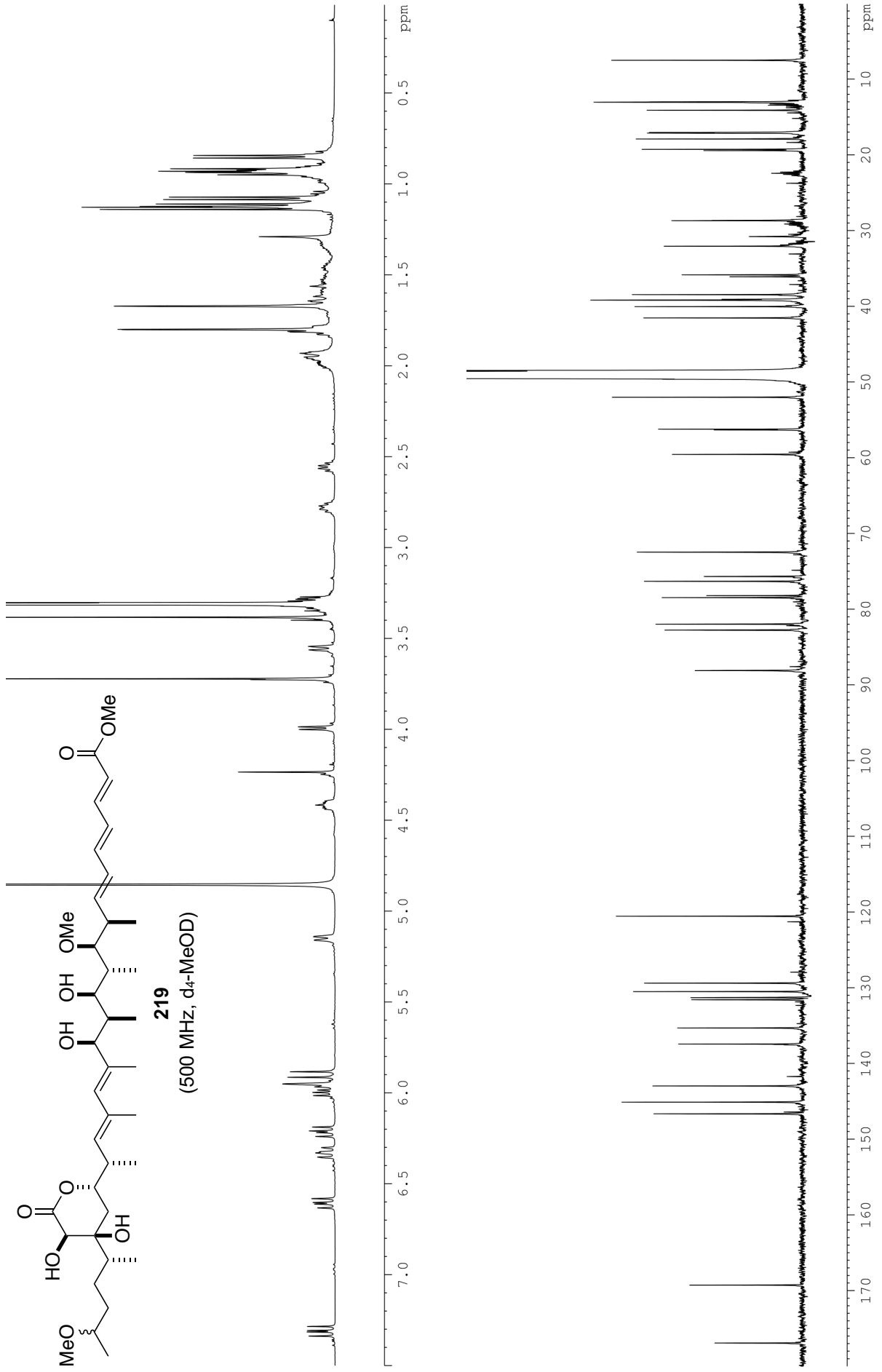
MeO
HO
OH
OH
OH
OMe
OMe
O
219
(500 MHz, d4-MeOD)
ppm
ppm

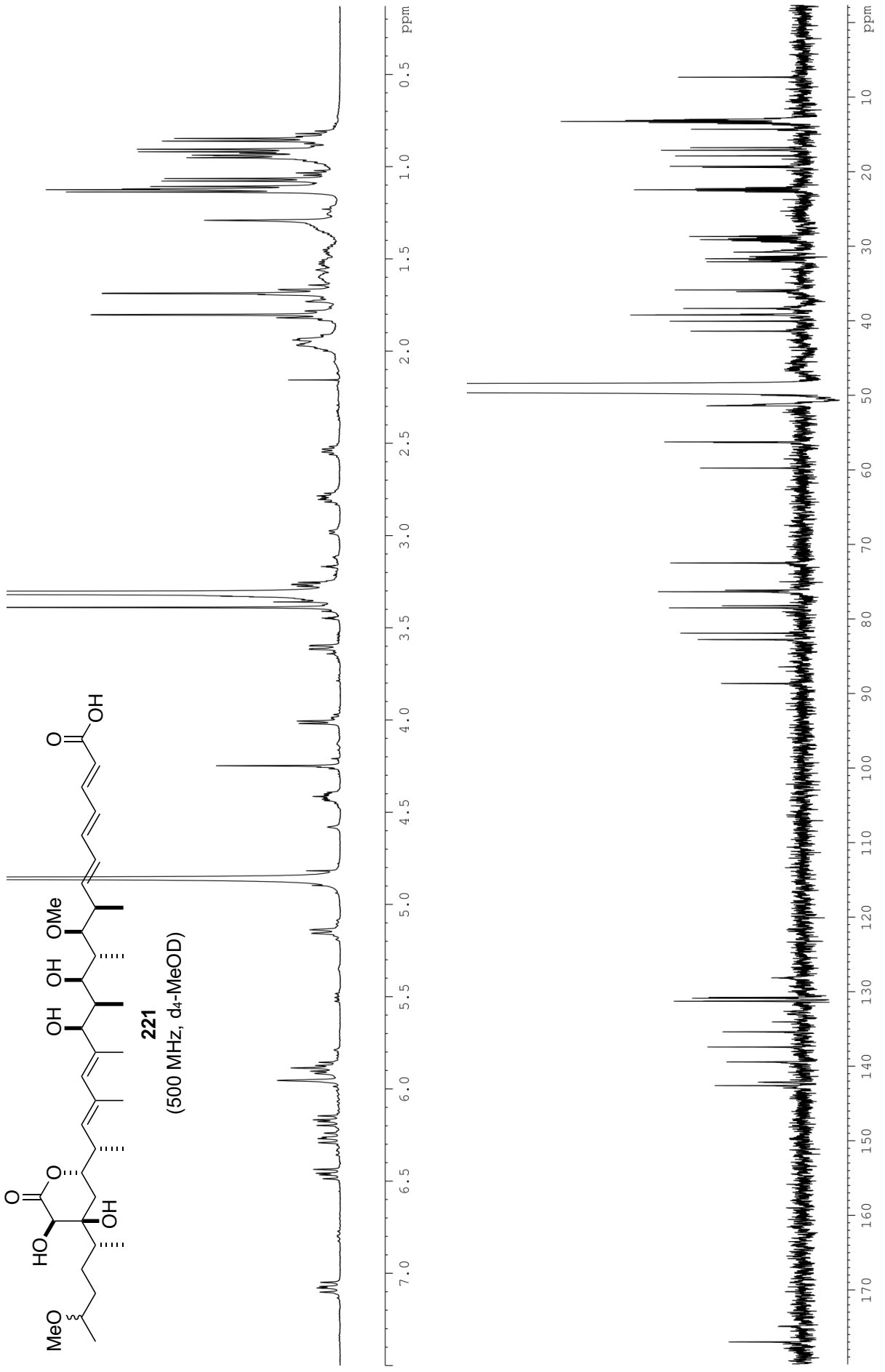

221
(500 MHz, d_4-MeOD)

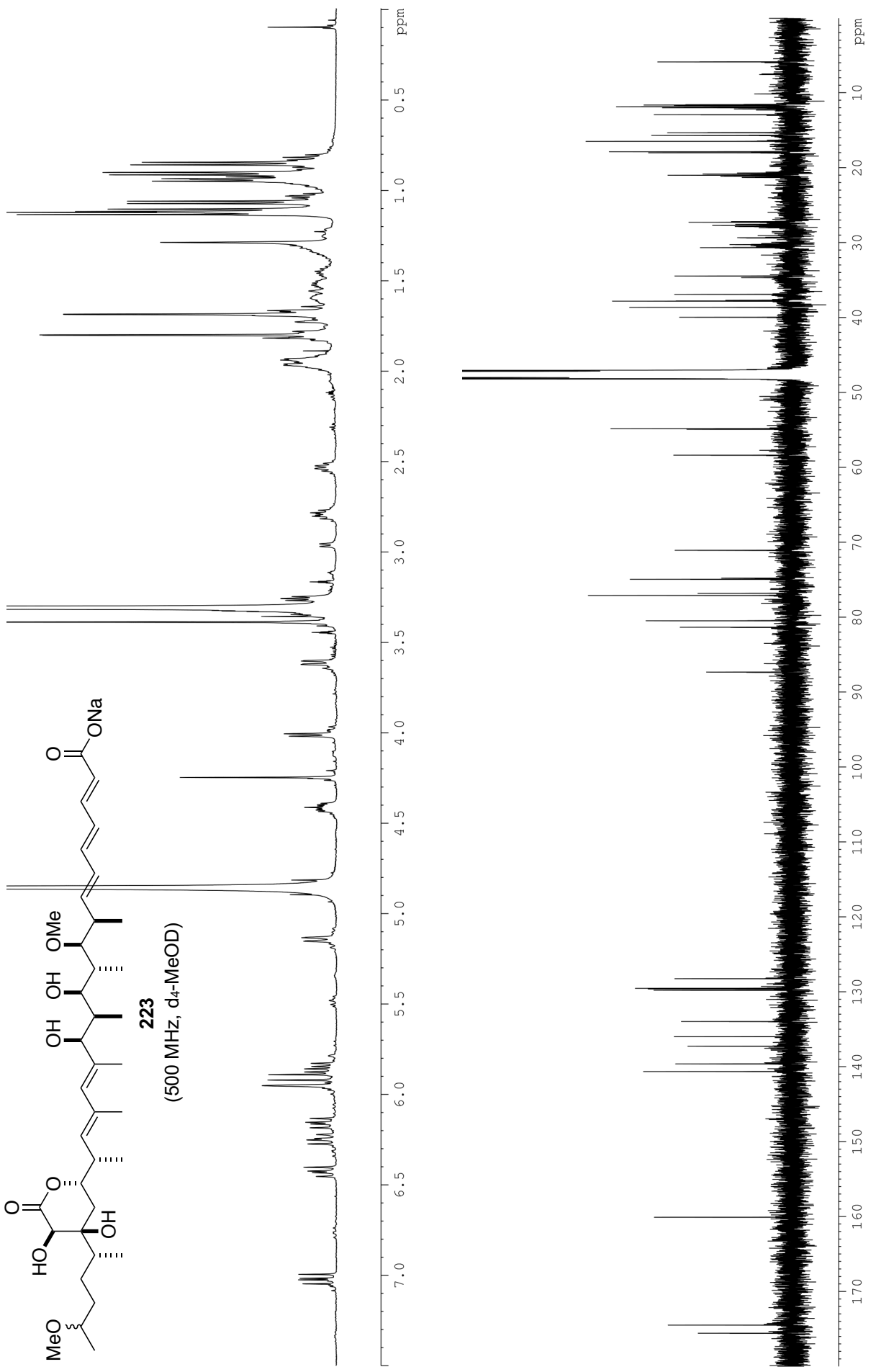
MeO
HO
OH
OH
OH
OMe
ONa
223
(500 MHz, d4-MeOD)
ppm
ppm

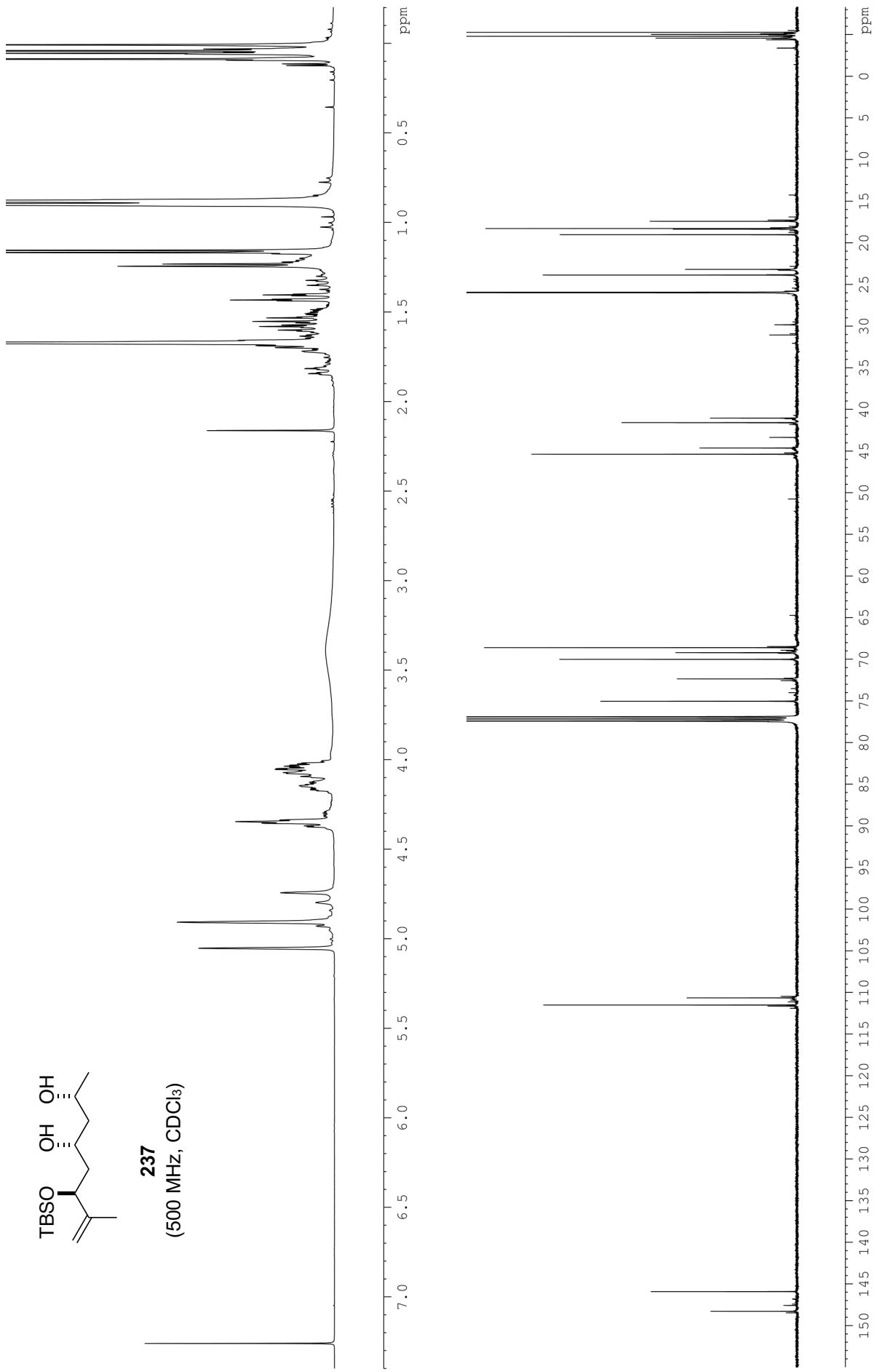
TBSO
OH
OH
237
(500 MHz, CDCl3)
ppm
ppm

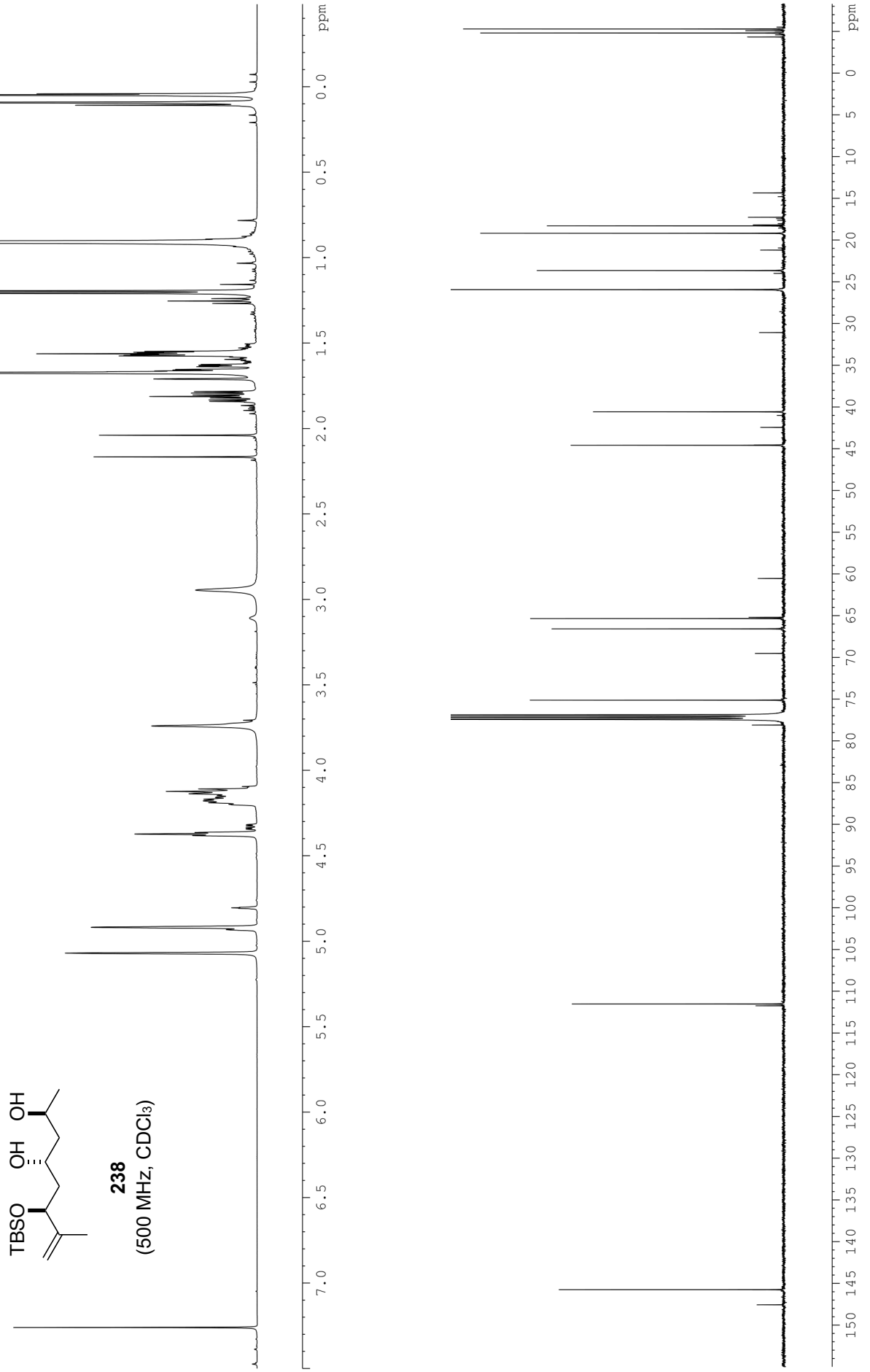
TBSO
OH
OH
238
(500 MHz, CDCl3)
ppm
ppm

CHAPTER SEVEN: REFERENCES

[1] Carletti, I.; Massiot, G.; Debitus, C. Polyketide Molecules As Anticancer Agents. US2012252889 (A1), 2012.

[2] Masamune, S.; Ali, S. A.; Snitman, D. L.; Garvey, D. S. *Angew. Chemie Int. Ed.* **1980**, *19*, 557–558.

[3] Dias, D. A.; Urban, S.; Roessner, U. *Metabolites* **2012**, *2*, 303–336.

[4] Newman, D. J.; Cragg, G. M. *J. Nat. Prod.* **2012**, *75*, 311–335.

[5] Martins, A.; Vieira, H.; Gaspar, H.; Santos, S. *Mar. Drugs* **2014**, *12*, 1066–1101.

[6] Koehn, F. E.; Carter, G. T. *Nat. Rev. Drug Discov.* **2005**, *4*, 206–220.

[7] Cragg, G. M.; Boyd, M. R.; Khanna, R.; Kneller, R.; Mays, T. D.; Mazan, K. D.; Newman, D. J.; Sausville, E. a. *Pure Appl. Chem.* **1999**, *77*, 1923–1942.

[8] Skropeta, D. *Nat. Prod. Rep.* **2008**, *25*, 989–1216.

[9] Haefner, B. *Drug Discov. Today* **2003**, *8*, 536–544.

[10] Newman, D. J.; Cragg, G. M. *J. Nat. Prod.* **2004**, *67*, 1216–1238.

[11] Paterson, I.; Anderson, E. A. *Science.* **2005**, *310*, 451–453.

[12] Wilson, R. M.; Danishefsky, S. J. *Chem. Soc. Rev.* **2007**, *36*, 1207–1226.

[13] Mayer, A. M. S.; Glaser, K. B.; Cuevas, C.; Jacobs, R. S.; Kem, W.; Little, R. D.; McIntosh, J. M.; Newman, D. J.; Potts, B. C.; Shuster, D. E. *Trends Pharmacol. Sci.* **2010**, *31*, 255–265.

[14] Bhalla, K. N. *Oncogene* **2003**, *22*, 9075–9086.

[15] Kingston, D. G. I. *J. Nat. Prod.* **2009**, *72*, 507–515.

[16] Van Vuuren, R. J.; Visagie, M. H.; Theron, A. E.; Joubert, A. M. *Cancer Chemother. Pharmacol.* **2015**, *76*, 1101–1112.

[17] Nicolaou, K. C.; Snyder, S. A. *Angew. Chemie - Int. Ed.* **2005**, *44*, 1012–1044.

[18] Alcock, L. J.; Norris, M. D.; Perkins, M. V. *Org. Biomol. Chem.* **2018**, 1351–1358.

[19] Paterson, I.; Davies, R. D. M.; Marquez, R. *Angew. Chemie - Int. Ed.* **2001**, *40*, 603–607.

[20] Trost, B. M.; Gunzner, J. L.; Dirat, O.; Rhee, Y. H. *J. Am. Chem. Soc.* **2002**, *124*, 10396–10415.

[21] Paterson, I.; Paquet, T. *Org. Lett.* **2010**, *12*, 2158–2161.

[22] Bifulco, G.; Dambruoso, P.; Gomez-Paloma, L.; Riccio, R. *Chem. Rev.* **2007**, *107*, 3744–3779.

[23] Rychnovsky, S. D. *Org. Lett.* **2006**, *8*, 2895–2898.

[24] Saielli, G.; Bagno, A. *Org. Lett.* **2009**, *11*, 1409–1412.

[25] Nicolaou, K. C.; Frederick, M. O. *Angew. Chemie - Int. Ed.* **2007**, *46*, 5278–5282.

[26] Smith, S. G.; Goodman, J. M. *J. Am. Chem. Soc.* **2010**, *132*, 12946–12959.

[27] Smith, S. G.; Goodman, J. M. *J. Org. Chem.* **2009**, *74*, 4597–4607.

[28] Paterson, I.; Dalby, S. M.; Roberts, J. C.; Naylor, G. J.; Guzmán, E. A.; Isbrucker, R.; Pitts, T. P.; Linley, P.; Divlianska, D.; Reed, J. K.; et al. *Angew. Chemie - Int. Ed.* **2011**, *50*, 3219–3223.

[29] Guchhait, S.; Chatterjee, S.; Ampapathi, R. S.; Goswami, R. K. *J. Org. Chem.* **2017**, *82*, 2414–2435.

[30] Wu, J.; Lorenzo, P.; Zhong, S.; Ali, M.; Butts, C. P.; Myers, E. L.; Aggarwal, V. K. *Nature* **2017**, *547*, 436–440.

[31] Bootwicha, T.; Feilner, J. M.; Myers, E. L.; Aggarwal, V. K. *Nat. Chem.* **2017**, *9*, 896–902.

[32] Fleury, E.; Lannou, M. I.; Bistri, O.; Sautel, F.; Massiot, G.; Pancrazi, A.; Ardisson, J. *J. Org. Chem.* **2009**, *74*, 7034–7045.

[33] Fleury, E.; Sorin, G.; Prost, E.; Pancrazi, A.; Sautel, F.; Massiot, G.; Lannou, M. I.; Ardisson, J. *J. Org. Chem.* **2013**, *78*, 855–864.

[34] Lafontaine, J. A.; Provencal, D. P.; Gardelli, C.; Leahy, J. W. *J. Org. Chem.* **2003**, *68*, 4215–4234.

[35] Sorin, G.; Fleury, E.; Tran, C.; Prost, E.; Molinier, N.; Sautel, F.; Massiot, G.; Specklin, S.; Meyer, C.; Cossy, J.; et al. *Org. Lett.* **2013**, *15*, 4734–4737.

[36] MacGregor, C. I.; Han, B. Y.; Goodman, J. M.; Paterson, I. *Chem. Commun.* **2016**, *52*, 4632–4635.

[37] MacGregor, C. I. Studies Towards the Structural Elucidation and Total Synthesis of Hemicalide, University of Cambridge, 2015.

[38] Specklin, S.; Boissonnat, G.; Lecourt, C.; Sorin, G.; Lannou, M. I.; Ardisson, J.; Sautel, F.; Massiot, G.; Meyer, C.; Cossy, J. *Org. Lett.* **2015**, *17*, 2446–2449.

[39] Mancuso, A. J.; Swern, D. *Synthesis.* **1981**, *3*, 165–185.

[40] Paterson, I. *Synthesis.* **1998**, *1998*, 639–652.

[41] Paterson, I.; Florence, G. J.; Gerlach, K.; Scott, J. P.; Sereinig, N. *J. Am. Chem. Soc.* **2001**, *123*, 9535–9544.

[42] Evans, D. A.; Bartroli, J.; Shih, T. L. *J. Am. Chem. Soc.* **1981**, *103*, 2127–2129.

[43] Basha, A.; Lipton, M.; Weinreb, S. M. *Tetrahedron Lett.* **1977**, *18*, 4171–4172.

[44] Nahm, S.; Weinreb, S. M. *Tetrahedron Lett.* **1981**, *22*, 3815–3818.

[45] Oishi, T.; Nakata, T. *Acc. Chem. Res.* **1984**, *17*, 338–344.

[46] Dess, D. B.; Martin, J. C. *J. Org. Chem.* **1983**, *48*, 4155–4156.

[47] Wadsworth, W. S.; Emmons, W. D. *J. Am. Chem. Soc.* **1961**, *83*, 1733–1738.

[48] Mitsunobu, O. *Synthesis.* **1981**, *1*, 1–28.

[49] Garber, S. B.; Kingsbury, J. S.; Gray, B. L.; Hoveyda, A. H. *J. Am. Chem. Soc.* **2000**, *122*, 8168–8179.

[50] Arbusow, B. A. *Pure Appl. Chem*. **1964**, *9*, 307–335.

[51] Dias, L. C.; Giacomini, R. *Tetrahedron Lett.* **1998**, *39*, 5343–5346.

[52] Narayanan, B. A.; Bunnelle, W. H. *Tetrahedron Lett.* **1987**, *28*, 6261–6264.

[53] Peterson, D. J. *J. Org. Chem.* **1968**, *33*, 780–784.

[54] Evans, D. A.; Urpi, F.; Somers, T. C.; Stephen Clark, J.; Bilodeau, M. T. *J. Am. Chem. Soc.* **1990**, *112*, 8215–8216.

[55] Molander, G. A.; Harris, C. R. *Chem. Rev.* **1996**, *96*, 307–338.

[56] Miyaura, N.; Yamada, K.; Suzuki, A. *Tet. Lett.* **1979**, No. 36, 3437–3440.

[57] Hafner, A.; Duthaler, R. O.; Marti, R.; Rihs, G.; Rothe-streit, P.; Schwarzenbach, F. *J. Am. Chem. Soc.* **1992**, *114*, 2321–2336.

[58] Scholl, M.; Trnka, T. M.; Morgan, J. P.; Grubbs, R. H. *Tetrahedron Lett.* **1999**, *40*, 2247–2250.

[59] Sakai, M.; Hayashi, H.; Miyaura, N. *Organometallics* **1997**, *16*, 4229–4231.

[60] Davis, F. A.; Haque, M. S.; Ulatowski, T. G.; Towson, J. C. *J. Org. Chem.* **1986**, *51*, 2402–2404.

[61] Davis, M. W.; Crabtree, R. H. *J. Org. Chem.* **1986**, *51*, 2655–2661.

[62] De Gussem, E.; Herrebout, W.; Specklin, S.; Meyer, C.; Cossy, J.; Bultinck, P. *Chem. - A Eur. J.* **2014**, *20*, 17385–17394.

[63] Lecourt, C.; Boinapally, S.; Dhambri, S.; Boissonnat, G.; Meyer, C.; Cossy, J.; Sautel, F.; Massiot, G.; Ardisson, J.; Sorin, G.; et al. *J. Org. Chem.* **2016**, *81*, 12275–12290.

[64] Erkkilä, A.; Pihko, P. M. *J. Org. Chem.* **2006**, *71*, 2538–2541.

[65] Trost, B. M.; Herndon, J. W. *J. Am. Chem. Soc.* **1984**, *106*, 6835–6837.

[66] Corey, E. J.; Yu, C. M.; Kim, S. S. *J. Am. Chem. Soc.* **1989**, *111*, 5495–5496.

[67] Clavier, H.; Nolan, S. P. *Chem. - A Eur. J.* **2007**, *13*, 8029–8036.

[68] Dupau, P.; Epple, R.; Thomas, A. A.; Fokin, V. V.; Sharpless, K. B. *Adv. Synth. Catal.* **2002**, *344*, 421–433.

[69] Paterson, I.; Maltas, P.; Anderson, E. A. *Pure Appl. Chem.* **2013**, *85*, 1133–1147.

[70] Stille, B. J. K. **1986**, *25*, 508–524.

[71] Lam, N. Unpublished Ph.D. Thesis, University of Cambridge.

[72] Paton, R. S.; Goodman, J. M. *J. Org. Chem.* **2008**, *73*, 1253–1263.

[73] Paterson, I.; Cowden, C. J.; Woodrow, M. D. *Tetrahedron Lett.* **1998**, *39*, 6037–6040.

[74] Evans, D. A.; Weber, A. E. *J. Am. Chem. Soc.* **1986**, *108*, 6757–6761.

[75] Paterson, I.; Ng, K. K. H.; Williams, S.; Millican, D. C.; Dalby, S. M. *Angew. Chemie - Int. Ed.* **2014**, *53*, 2692–2695.

[76] Baker, R.; Castro, J. L. *J. Chem. Soc. Perkin Trans. 1* **1990**, *0*, 47–65.

[77] Hoover, J. M.; Stahl, S. S. *J. Am. Chem. Soc.* **2011**, *133*, 16901–16910.

[78] Hoover, J. M.; Ryland, B. L.; Stahl, S. S. *J. Am. Chem. Soc.* **2013**, *135*, 2357–2367.

[79] Evans, D. A.; Takacs, J. M.; Mcgee, L. R.; Ennis, M. D.; Mathre, D. J.; Bartroli, J. *Pure Appl. Chem.* **1981**, *53*, 1109–1127.

[80] Heathcock, C. H.; Pirrung, M. C.; Sohn, J. E. *J. Org. Chem.* **1979**, *44*, 4294–4299.

[81] Dale, J. A.; Mosher, H. S. *J. Am. Chem. Soc.* **1973**, *95*, 512–519.

[82] Sullivan, G. R.; Dale, J. A.; Mosher, H. S. *J. Org. Chem.* **1973**, *38*, 2143–2147.

[83] Hoye, T. R.; Jeffrey, C. S.; Shao, F. *Nat. Protoc.* **2007**, *2*, 2451–2458.

[84] Crimmins, M. T.; King, B. W.; Tabet, E. A.; Chaudhary, K. *J. Org. Chem.* **2001**, *66*, 894–902.

[85] Crimmins, M. T.; She, J. *Synlett*. **2004**, 8, 1371–1374.

[86] Goodman, J. M.; Paterson, I. *Tetrahedron Lett.* **1992**, *33*, 7223–7226.

[87] Anh, N. T.; Eisentein, O. *Nouv. J. Chem.* **1077**, *1*, 61.

[88] Roush, W. R. *J. Org. Chem.* **1991**, *56*, 4151–4157.

[89] Evans, D. A.; Allison, B. D.; Yang, M. G.; Masse, C. E. *J. Am. Chem. Soc.* **2001**, *123*, 10840–10852.

[90] Neises, B.; Steglich, W. *Angew. Chemie Int. Ed. English* **1978**, *17*, 522–524.

[91] Paterson, I.; Yeung, K.-S.; Smaill, J. B. *Synlett*. **1993**, *10*, 774–776.

[92] Corey, E. J.; Fuchs, P. L. *Tetrahedron Lett.* **1972**, No. 36, 3769–3772.

[93] Hart, D. W.; Schwartz, J. *J. Am. Chem. Soc.* **1974**, *96*, 8115–8116.

[94] Hart, D. W.; Blackburn, T. F.; Schwartz, J. *J. Am. Chem. Soc.* **1975**, *97*, 679–680.

[95] Nicolaou, K. C.; Li, Y.; Sugita, K.; Monenschein, H.; Guntupalli, P.; Mitchell, H. J.; Fylaktakidou, K. C.; Vourloumis, D.; Giannakakou, P.; O'Brate, A. *J. Am. Chem. Soc.* **2003**, *125*, 15443–15454.

[96] Paterson, I.; Gibson, L. J.; Kan, S. B. J. *Org. Lett.* **2010**, *12*, 5530–5533.

[97] Paterson, I.; Goodman, J. M.; Anne Lister, M.; Schumann, R. C.; McClure, C. K.; Norcross, R. D. *Tetrahedron* **1990**, *46*, 4663–4684.

[98] Atkins, G. M.; Burgess, E. M. *J. Am. Chem. Soc.* **1968**, *90*, 4744–4745.

[99] Ohmori, K.; Nishiyama, S.; Yamamura, S. *Tetrahedron Lett.* **1995**, *36*, 6519–6522.

[100] Bataille, C. J. R.; Donohoe, T. J. *Chem. Soc. Rev.* **2011**, *40*, 114–128.

[101] Bhaket, P.; Stauffer, C. S.; Datta, A. *J. Org. Chem.* **2004**, *69*, 8594–8601.

[102] Paddon-Row, M. N.; Rondan, N. G.; Houk, K. N. *J. Am. Chem. Soc.* **1982**, *104*, 7162–7166.

[103] Vedejs, E.; McClure, C. K. *J. Am. Chem. Soc.* **1986**, *108*, 1094–1096.

[104] Mahoney, W. S.; Brestensky, D. M.; Stryker, J. M. *J. Am. Chem. Soc.* **1988**, *110*, 291–293.

[105] Lee, D. W.; Yun, J. *Tetrahedron Lett.* **2004**, *45*, 5415–5417.

[106] Wulff, W. D.; Peterson, G. A.; Bauta, W. E.; Chan, K. S.; Faron, K. L.; Gilbertson, S. R.; Kaesler, R. W.; Yang, D. C.; Murray, C. K. *J. Org. Chem.* **1986**, *51*, 277–279.

[107] Mee, S. P. H.; Lee, V.; Baldwin, J. E. *Chem. - A Eur. J.* **2005**, *11*, 3294–3308.

[108] Fürstner, A.; Funel, J. A.; Tremblay, M.; Bouchez, L. C.; Nevado, C.; Waser, M.; Ackerstaff, J.; Stimson, C. C. *Chem. Commun.* **2008**, No. 25, 2873–2875.

[109] Gagnepain, J.; Moulin, E.; Fürstner, A. *Chem. - A Eur. J.* **2011**, *17*, 6964–6972.

[110] Renata, H.; Zhou, Q.; Baran, P. S. *Science.* **2013**, No. January, 59–63.

[111] Heck, K. F.; Nolley, J. P. *J. Org. Chem.* **1972**, *37*, 2320–2322.

[112] Corey, E. J.; Bakshi, R. K.; Shibata, S. *J. Am. Chem. Soc.* **1987**, *109*, 5551–5553.

[113] Han, B. Y.; Lam, N. Y. S.; MacGregor, C. I.; Goodman, J. M.; Paterson, I. *Chem. Commun.* **2018**, *54*, 3247–3250.

[114] Martin, V. S.; Woodard, S. S.; Katsuki, T.; Yamada, Y.; Ikeda, M.; Sharpless, K. B. *J. Am. Chem. Soc.* **1981**, *103*, 6237–6240.

[115] Katsuki, T.; Sharpless, K. B. *J. Am. Chem. Soc.* **1980**, *102*, 5974–5976.

[116] Mukaiyama, T.; Banno, K.; Narasaka, K. *J. Am. Chem. Soc.* **1974**, *96*, 7503–7509.

[117] Evans, D. A.; Duffy, J. L.; Dart, M. J. *Tetrahedron Lett.* **1994**, *35*, 8537–8540.

[118] Tang, Y.; Yang, J. H.; Liu, J.; Wang, C. C.; Lv, M. C.; Wu, Y. B.; Yu, X. L.; Ko, C.; Hsung, R. P. *Heterocycles* **2012**, *86*, 565–598.

[119] Narasaka, K.; Pai, F.-C. *Tetrahedron* **1984**, *40*, 2233–2238.

[120] Mickel, S. J.; Sedelmeier, G. H.; Niederer, D.; Schuerch, F.; Grimler, D.; Koch, G.; Daeffler, R.; Osmani, A.; Hirni, A.; Schaer, K.; et al. *Org. Process Res. Dev.* **2004**, *8*, 101–106.

[121] Evans, D. A.; Hoveyda, A. H. *J. Am. Chem. Soc.* **1990**, *112*, 6447–6449.

[122] Rychnovsky, S. D.; Skalitzky, D. J. *Tetrahedron Lett.* **1990**, *31*, 945–948.

[123] Evans, D. A.; Rieger, D. L.; Gage, J. R. *Tetrahedron Lett.* **1990**, *31*, 7099–7100.

[124] Balog, A.; Meng, D.; Kamenecka, T.; Bertinato, P.; Su, D.; Sorensen, E. J.; Danishefsky, S. J. **1996**, *7*, 2801–2803.

[125] Paterson, I.; Maltas, P.; Dalby, S. M.; Lim, J. H.; Anderson, E. A. *Angew. Chemie - Int.*

Ed. **2012**, *51*, 2749–2753.

[126] Roush, W. R.; Bannister, T. D.; Wendt, M. D.; Jablonowski, J. A.; Scheidt, K. A. *J. Org. Chem.* **2002**, *67*, 4275–4283.

[127] Houk, K. N.; Rondan, N. G.; Wu, Y. D.; Metz, J. T.; Paddon-Row, M. N. *Tetrahedron* **1984**, *40*, 2257–2274.

[128] Stockdale, T. Unpublished Ph.D. Thesis, University of Cambridge.

[129] Takai, K.; Nitta, K.; Utimoto, K. *J. Am. Chem. Soc.* **1986**, *108*, 7408–7410.

[130] Evans, D. A.; Fu, G. C. *J. Am. Chem. Soc.* **1991**, *113*, 4042–4043.

[131] Patil, V. J. *Tetrahedron Lett.* **1996**, *37*, 1481–1484.

[132] Mukaiyama, T.; Inoue, T. *Chem. Lett.* **1976**, *5*, 559–562.

[133] Inoue, T.; Mukaiyama, T. *Bull. Chem. Soc. Jpn.* **1980**, *53*, 174–178.

[134] Herbert, C. B.; Ravindran, N.; Surendra, U. K. *J. Org. Chem.* **1979**, *44*, 2417–2422.

[135] Moeder, C. W.; Sowa, J. R. *J. Phys. Org. Chem.* **2004**, *17*, 317–324.

[136] Soderquist, J. A.; Negron, A. *Org. Synth.* **1972**, *70*, 169.

[137] Frigerio, M.; Santagostino, M.; Sputore, S. *J. Org. Chem.* **1999**, *64*, 4537–4538.

[138] Ireland, R. E.; Liu, L. *J. Org. Chem.* **1993**, *58*, 2899.

[139] Girard, P.; Namy, J. L.; Kagan, B. *J. Am. Chem. Soc.* **1980**, *102*, 2693–2698.

[140] Concellón, J. M.; Rodríguez-Solla, H.; Bardales, E.; Huerta, M. *European J. Org. Chem.* **2003**, No. 9, 1775–1778.

[141] Evans, D. A.; Nagorny, P.; McRae, K. J.; Reynolds, D. J.; Sonntag, L. S.; Vounatsos, F.; Xu, R. *Angew. Chemie - Int. Ed.* **2007**, *46*, 537–540.

[142] Yokokawa, F.; Fujiwara, H.; Shioiri, T. *Tetrahedron* **2000**, *56*, 1759–1775.

[143] Müller, S.; Mayer, T.; Sasse, F.; Maier, M. E. *Org. Lett.* **2011**, *13*, 3940–3943.

[144] Law, K. R.; McErlean, C. S. P. *Chem. - A Eur. J.* **2013**, *19*, 15852–15855.

[145] Amans, D.; Bellosta, V.; Cossy, J. *Angew. Chemie - Int. Ed.* **2006**, *45*, 5870–5874.

[146] Janssen, D.; Albert, D.; Jansen, R.; Müller, R.; Kalesse, M. *Angew. Chemie - Int. Ed.* **2007**, *46*, 4898–4901.

[147] Smith, A. B.; Lee, D. *J. Am. Chem. Soc.* **2007**, *129*, 10957–10962.

[148] Meiries, S.; Bartoli, A.; Decostanzi, M.; Parrain, J. L.; Commeiras, L. *Org. Biomol. Chem.* **2013**, *11*, 4882–4890.

[149] Yamashita, S.; Iso, K.; Kitajima, K.; Himuro, M.; Hirama, M. *J. Org. Chem.* **2011**, *76*, 2408–2425.

[150] Andrew Mitchell, T.; Romo, D. *J. Org. Chem.* **2007**, *72*, 9053–9059.